

REPUBLIC OF CAMEROON

THE UNIVERSITY OF YAOUNDE I

FACULTY OF SCIENCE

POSTGRADUATE SCHOOL OF
SCIENCES, TECHNOLOGY AND
GEOSCIENCES

DOCTORATE RESEARCH UNIT
FOR GEOSCIENCES AND
APPLICATIONS



REPUBLIQUE DU CAMEROUN

UNIVERSITE DE YAOUNDE I

FACULTE DES SCIENCES

CENTRE DE RECHERCHE ET DE
FORMATION DOCTORALE EN
SCIENCES, TECHNOLOGIE ET
GEOSCIENCES

UNITE DE RECHERCHE ET DE
FORMATION DOCTORALE EN
GEOSCIENCES ET APPLICATIONS

DEPARTMENT OF EARTH SCIENCES
DEPARTEMENT DES SCIENCES DE LA TERRE

LABORATORY OF GEOSCIENCES OF SUPERFICIAL
FORMATIONS AND APPLICATIONS
*LABORATOIRE DE GEOSCIENCES DES FORMATIONS
SUPERFICIELLES ET APPLICATIONS*

LACUSTRINE SEDIMENTS FROM THREE REGIONS OF CAMEROON
(YAOUNDE DIZANGUE AND NGAOUNDERE): SEDIMENTOLOGICAL AND
PETROLOGICAL CHARACTERIZATION FOR A PALEOENVIRONMENTAL
RECONSTRUCTION

Thesis submitted for the degree of **Philosophiae Doctor (PhD)**
in Earth Sciences

Option : Mining Geology and Petroleum Resources

By

EKOA BESSA Armel Zacharie

Reg. Number: 10X0515

Msc in Earth Sciences

In front of the jury composed of :

MEMBERS

Ngueutchoua Gabriel

Associate Professor

University of Yaoundé I, Cameroon

Onana Vincent Laurent

Associate Professor

University of Yaoundé I, Cameroon

Nguetsop Victor François

Professor

University of dschang , cameroon

PRESIDENT

Nzenti Jean Paul

Professor

University of Yaoundé I,
Cameroon

Ndjigui Paul-Désiré Professor
University of Yaoundé I,
Cameroon

John S. Armstrong-Altrin

Investigator B

Institute of Marine Sciences and
Limnology, Mexico

2021



UNIVERSITE DE YAOUNDE I
FACULTE DES SCIENCES
CENTRE DE RECHERCHE
ET FORMATION DOCTORALE
EN SCIENCES, TECHNOLOGIES
ET GEOSCIENCES



THE UNIVERSITY OF YAOUNDE I
FACULTY OF SCIENCE
POSTGRADUATE SCHOOL
IN SCIENCES, TECHNOLOGY
AND GEOSCIENCES

DEPARTEMENT DES SCIENCES DE LA TERRE
DEPARTMENT OF EARTH SCIENCES

UNITE DE FORMATION ET DE RECHERCHE DOCTORALE
EN GEOSCIENCES ET APPLICATIONS

CERTIFICATE OF CORRECTION OF DOCTORATE/PhD THESIS

Laboratory: Geosciences of Superficial Formations and Applications
Option: Mining Geology and Petroleum Resources

Names and surnames of applicant: EKO A BESSA Armel Zacharie

Registration number : 10X0515

Title of the thesis: "lacustrine sediments from three regions of Cameroon (Yaoundé Dizangué and Ngaoundéré): sedimentological and petrological characterization for a paleoenvironmental reconstruction"

Date of defense: Monday, 18th July 2021.

We, the members of the jury, have read the document presented to us and certify that the applicant has made all the corrections in accordance with the observations made during the examination.

In witness whereof, the present **Certificate of Correction** is delivered to him, to serve and be worth what is right.

President of the Jury

Members

*...dedicated to my beloved father recalled to the Kingdom of
Heaven in 1992.*

Acknowledgements

This thesis is the result of many years of research, marked by the contribution of several actors. It was carried out mainly at the Department of Earth Sciences of the University of Yaounde I.

I thank **God almighty** first and foremost for the gift of life, good health, knowledge and wisdom he provided to me.

I thank Pr. Ndjigui Paul-Désiré for initiating me into research and adopting me as a son. I thank him immensely for his meticulous corrections of this thesis and for the advisory and fatherly role he played in my life all these years.

I sincerely thank the administrative authorities of the University of Yaounde I, in particular the Rector of the University of Yaounde I, the Dean of the Faculty of Science, the Director of the Postgraduate School of Sciences, Technology and Geosciences and the Head of the Department of Earth Sciences, for the wonderful welcome and assistance in this University.

I would like to thank my co-supervisor, Pr. John S. Armstrong-Altrin for his confidence in me. Although several thousand kilometres away, he believed in me and gave me a good grounding in sedimentology. He was always there for me when I needed him.

My thanks equally go to Pr. Onana Vincent Laurent, for his support during the period of misguidance. He knows how to put me back on the rail and never got tired despite my failures, respecting his advice as a brother, friend and educator; thank you prof.

I also thank Dr. Bineli Betsi Thierry, Mrs. Tebogo Kelepile, Kouadio Nelly, Serwalo Mokgosi, Trust Manyiwa and Mothusi Madiba; Prs. Kofane Timoleon and Tabi Conrad and their research teams from Botswana International University of Sciences and Technology.

I would like to extend my sincere thanks to the people who helped me and contributed to the development of this brief and to the success of these wonderful academic years. Specialy Pr. Bilong Paul, my master supervisor, other lecturers in the said department such as: Prs. Ndam Ngoupayou, Nkoumbou, Yongue Fouateu, Nzenti, Tchouankoue, Temdjim, Ganno, Yene Atangana, Abossolo Angue, Drs. Ngo Bidjeck, Mouafo, Temga, Tehna, Ngo Belnoun, Metang, Bekoa, Lamilen Billa, Tchakounté, Tchaptchet and all my classmates for their academic and moral support.

I also want to thank my sedimentologist team include Prs. Ngueutchoua Gabriel, Ekomane Emile, Ngos Simon; Drs. Eyong John Taken, Bessong Moise, Mbesse Cecile, Ntsama Jacqueline, Bisse Salomon, Bokanda Eric, N'nganga Alexandrine; the researchers Edgenge Elvine, Chougong Durane, Janpou Annick, Kankeu Romaric, Evina Stéphane, Tsanga Duviol and the new commers.

My profound gratitude equally goes to my wonderful elders, colleagues and friends, Drs. Elisé Sababa, Tessontsap Teutsong and Tobias Sprafke who helped me immensely in the last three years of my study. Friend in need are really friends in deed.

I thank Mss Eyenga Marie Dorine, the secretary of the the Department of Earth Sciences for his cordial support.

I also thank my laboratory mates for their unceasing encouragements and the good atmosphere they produced, they will recognize each other, it is about -in no particular order: *Julio, Energizer, Mamy Nyanga, Gaele, La diasporat, Totancine, Mr le ministre, teacher henriette, Sidonie, Bois blanc, Etchamàkà, Sam man, Lucky luke, Arnaud, Le joel, La star, Yvess, plastini, Jonas, l'Européenne, Motakakuma, Le kok, Sonia la sœur, Audrey, la magia, Le chercheur Binam* and many cadets.

My immense thanks go to my family, especially to my mom, Bessa Nicole, who sacrificed her life to raise her kids ; my brother and sisters Bessa Nadège, Bessa Claude, Bessa Flavie, Bessa Cathérine and Bessa Kelly Dorcas ; the Bokono families (Celestin, Marie, francklin, Christelle, Yolande, Fortune and fils) ; the Assoa family ; my son Bessa Ryad ; my nephews and nieces Aimé, Ange, Samantha, Daniel, Divine, Simelia, Obo, junior, Claude, Nicole, Thérésia and Rusia ; Binong Madelaine, Amba family and Wamba Yves.

I thank all my friends especially Ngono Arsene, Manguelle Gabriel, Nwagoum Steve, Fongoum Audrey, Coco Armelle, Noula Ines, Talla Mbé, Kembiet Kloran, Mballa Clémence, Essomba Aloïs, Alene Walessa, Ongbasouek Bibiche, Madiesse, the twins Lisa and Ines, Simon Nkolo, Eto'o sheryl, Sahatem Blandine, Ambassa Bela, Bachiru, Bayiha joel, Belinga Cedric, Molo Marc, Abodo Belibi and Ngah Yeme for their endless encouragements.

I thank Mr. Talla, the regent chief of Dibi village who facilitated my field work in the Adamawa Region especially regarding administrative procedures and logistics.

I thank the African-German Network of Excellence in Science (AGNES) for granting a Mobility Grant in 2019; the Grant was generously sponsored by German Federal Ministry of Education and Research and supported by the Alexander von Humboldt Foundation.

To all those who helped me in one way or the other whose names have not been mentioned, I say 'thank you'.

Summary

DEDICACE
Acknowledgements	i
List of Figures	iv
List of Table	viii
List of abbreviations	ix
Abstract.....	x
Résumé.....	xii
General introduction	1
Part one: Background	6
Chapter I: Natural setting.....	7
Chapter II: Litterature review	38
Chapter III: Material and methods	58
Part two: Results and interpretations.....	70
Chapter IV: Sedimentological characteristics of lake deposits.....	71
Chapter V: Petrological and environmental aspects of lake sediments.....	90
Chapter VI: Dating and paleoenvironmental reconstruction.....	128
Part three: Discussions	167
Chapter VII: Synthesis and discussion	168
Conclusions and suggestions for further studies	195
References	199
Table of contents.....	220

List of Figures

Figure I.1. Location of Cameroon and the different sites studied: a) Administrative map of Cameroon; b) Lake Simbock; c) Lake Ossa and d) Lake Ngaoundaba.....	9
Figure I.2. Climate map of Cameroon (Anonymous, 2010).....	11
Figure I.3. Ombrothermal curves of Yaounde town (1935- 2019), according to Bagnouls and Gausson (1957).	12
Figure I.4. Ombrothermal curves of the town of Dizangue.....	13
Figure I.5. Ombrothermal curves of the city of Ngaoundere.....	14
Figure I.6. Natural hydrological regimes of Cameroon.....	15
Figure I.7. Location of Lake Simbock in the sub-catchment of the Mefou.....	16
Figure I.8. Sanaga catchment with its great lakes including Ossa and Ngaoundaba lakes	18
Figure I.9. Vegetation distribution of Cameroon).....	19
Figure I.10. Vegetation around Lake Simbock	21
Figure I.11. Vegetation around Lake Ossa	22
Figure I.12. Vegetation around Lake Ngaoundaba	23
Figure I.13. Distribution of relief in Cameroon	24
Figure I.14. Relief of the Yaoundé area	25
Figure I.15. Relief around Lake Ossa.....	26
Figure I.16. Relief around Lake Ngaoundaba.....	27
Figure I.17. Soil distributions in Cameroon)	29
Figure I.18. Geological map of Cameroon	32
Figure I.19. Geological map of the south-western part of the Yaoundé	34
Figure I.20. Geological map of Dizangue and Lake Ossa).....	35
Figure I.21. Geological map of the Ngaoundaba area.....	36
Figure II.1. Different shapes of lakes	43
Figure II.2. Evolution of a lake	44
Figure II.3. Some core drills	46
Figure III.1. Sampling procedure used in the lakes.....	59
Figure III.2. Exemple of some collected cores	60
Figure III.3. Location map and samples location of: a) studied lakes in Cameroon b) Ossa lakes Complex in Dizanguè; c) Simbock Lake in Yaoundé and d) Ngaoundaba Lake in Ngaoundéré.....	61
Figure IV.1. Evolution of Simbock Lake with time.....	72
Figure IV.2. Simbock Lake sediments in the ternary textural diagram.....	73

Figure IV.3. Macroscopic organization of core sediments from the Simbock Lake	74
Figure IV.3. The Ossa Lakes Complex	76
Figure IV.4. Ossa lakes Complex sediments in the ternary textural diagram (Shepard, 1954)77	
Figure IV.5. Macroscopic organization of core sediments from the Ossa lake Complex.....	78
Figure IV.6. The Ngaoundaba Crater Lake	79
Figure IV.7. Ngaoundaba crater Lake sediments in the ternary textural diagram	80
Figure IV.8. Macroscopic organization of core sediments from the Ngaoundaba Crater Lake:	81
Figures IV.9. SEM images of quartz grain surfaces and shapes from the Ossa lake Complex;	82
Figures IV.10. SEM images of quartz grain surfaces and shapes from the Ngaoundaba crater Lake.....	84
Figure IV.11. Vertical distribution of OM concentrations in sediments from Simbock Lake .	86
Figure IV.12. Vertical distribution of OM concentrations in sediments from Ossa lakes Complex	87
Figure IV.13. Vertical distribution of OM concentrations in sediments from Ngaoundaba Lake.....	88
Figure V.1. X-ray diffraction spectra for Simbock Lake bulk sediments: a) NR core and b) EB core.....	92
Figure V.2. X-ray diffraction spectra of the finest grain-sized fractions for after specific treatments	93
Figure V.3. FT-IR spectra of the sediments from the Simbock Lake: a) core NR and b) core EB	95
Figure V.4. X-ray diffraction spectra for sediments from Ossa lakes Complex.....	97
Figure V.5. Scanning electron microscope and SEM-EDS spectrum for sediments from the Ossa lakes Complex.....	98
Figure V.6. X-ray diffraction spectra for sediments from Ngaoundaba Crater lake.....	100
Figure V.7. Scanning electron microscope and SEM-EDS spectrum for grains from the Ngaoundaba Lake	101
Figure V.8. Binary diagrams of selected major elements in Simbock Lake sediments	104
Figure V.9. REE patterns of Simbock Lake sediments	106
Table V.5. REE concentrations (ppm) of the sediments Simbock Lake	107
Figure V.10. Hacker diagram of Al ₂ O ₃ versus major oxides showing the distribution of Ossa lake Complex samples	110
Table V.7. Trace elements (ppm) in sediments from the Ossa lakes Complex	112
Figure V.11. REE patterns of the lacustrine sediments.....	114

Figure V.12. Hacker diagram of SiO ₂ versus some major oxides showing different sources of sediment from Ngaoundaba crate Lake	115
Figure VI.1. Sketch showing a variety of possible sources of errors, which can influence bulk sediment radiocarbon dates in sub-tropical lakes	130
Figure VI.3. Lithology, radiocarbon ages and age models of OW4 and LO cores from Ossa lakes Complex	133
Figure VI.4. Lithology, radiocarbon ages and age models of T2 and AZ cores from Tizon and Ngaoundaba lakes	134
Figure VI.5. Specific diversity (in %) of the dominant genera along the Simbock sedimentary column.....	138
Figure VI.6. Variation in relative abundance of dominant species.....	139
Figure VI.7. Schematic representation of the characteristic groups of axes 1 and 2 of the CFA	141
Figure VI.8. Variation in relative abundance of habitat indicator ecological groupsh	143
Figure VI.9. Specific diversity (in %) of the dominant genera along the Ossa sedimentary column.....	144
Figure VI.10. Variation in relative abundance of dominant species (> 5 % at least in a sample) as a function of depth along the Ossa sedimentary column.....	145
Figure VI.11. Schematic representation of the characteristic groups of axes 1 and 2 of the CFA.....	148
Figure VI.12. Variation in relative abundance of habitat indicator of ecological groups (tycho + planktonic, benthic, epiphytic, aerophilic), trophic (eutrophic and oligotrophic), pH (alkaliphilic, acidophilic, indifferent) and hydrological phases along the Ossa core as a function of depth.	149
Figure VI.13. Specific diversity (%) of dominant genera along the Ngaoundaba sedimentary column.....	152
Figure VI.14. Variation in relative abundance of dominant species (> 5 % at least in one sample) as a function of depth along the Ngaoundaba sedimentary column.....	154
Figure VI.15. Schematic representation of the characteristic groups of axes 1 and 2 of the CFA.....	156
Figure VI.16. Variation in relative abundance of habitat indicator ecological groups (tycho + planktonic, benthic, epiphytic, aerophilic), trophic (eutrophic and oligotrophic) and pH (alkaliphile, acidophilic, indifferent) along the Ngaoundaba core as a function of depth.....	157
Figure VI.17. Distribution of species recorded in the sequence of : a) NR core from Simbock Lake (Yaoundé, South-Cameroon) ; b) LO core from Ossa lakes Complex (Dizangué, South-West, Cameroon) and c) AZ core from Ngaoundaba Lake (Adamawa, North-Cameroon).....	162
Figure VII.1. Geochemical classification of lacustrine sediments based on: a) log (SiO ₂ /Al ₂ O ₃) versus log (Na ₂ O/K ₂ O) diagram (Pettijohn et al., 1972) and b) log (SiO ₂ /Al ₂ O ₃) versus log (Fe ₂ O ₃ /K ₂ O) diagram (after Herron, 1988).....	170

Figure VII.2. a) ICV versus CIA diagram (Nesbitt and Young, 1984; Cox et al. 1995) showing maturity of sediments and b) Th/Sc vs. Zr/Sc bivariate plot (after McLennan et al., 1993) for samples from studied lakes showing possible sorting effects and recycling sediments.....	172
Figure VII.3. Ternary diagram A-CN-K (Nesbitt and Young, 1982, 1984) to infer the intensity of weathering for the samples from Simbock, Ossa Complex and Ngaoundaba lakes. Oxides A (Al_2O_3), CN ($\text{CaO} + \text{Na}_2\text{O}$), and K (K_2O) are plotted as molar proportions; (1) weathering trend for Upper Archean crust; (2) K-metasomatism	175
Figure VII.4. Major and trace element provenance diagrams.....	180
Figure VII.5. Tectonic diagrams for the samples from Simbock, Ossa Complex and Ngaoundaba lakes).....	181
Figure VII.6. Comparison between Lake Ossa (South-West Cameroon), Paurosa Marsh (West Gabo), Lake Barombi Mbo (West Cameroon) and Bambili (West Cameroon): regional synthesis.....	190
Figure VII.7. Plots of: a) V versus Al_2O_3 ; b) P_2O_5 versus Al_2O_3 and c) Sr/Cu versus Ga/Rb ratios in the studied lakes for paleoenvironmental reconstructions.....	192
Figure VII.8. Comparison between Lake Ngaoundaba (North Cameroon), Lake Gbali (West-Central Africa), Lake Mbalang (North Cameroon) and Lake Chad: Regional Synthesis	193

List of Table

Tableau I.1. Monthly precipitation values (1935-2018), temperatures (1980-2019) according to the Mvan station in Yaoundé.	11
Tableau I.2. Monthly precipitation values (1996-2019) according to the Edea station	12
Tableau I.3. Monthly precipitation values (1997-2019) according to the Ngaoundere station	13
Tableau II.1. Classifications and particle size scales	41
Table IV.1. Thickness, color, grain size distribution, texture and relative humidity of Lake sediments	75
Table IV.2. Total organic carbon (TOC) and organic matter (OM) in % from the studied lakes	85
Table V.1. Position of the main detected dust infrared band peaks with transition assignment	94
Table V.2. Chemical composition (wt.%) of minerals analyzed by SEM-EDS in sediments from the Ossa lakes Complex	96
Table V.3. Major element composition (wt.%) and element ratios of sediments from the Simbock Lake	103
Table V.4. Trace element concentrations (in ppm) and element ratios in sediments from the Simbock Lake	105
Table V.6. Major elements (wt. %) and some element ratios in sediments from the Ossa lakes Complex.....	111
Table V.8. Rare earth elements (ppm) in sediments from the Ossa lakes Complex.....	113
Table V.9. Major elements (wt. %) and some element ratios in sediments from the Ngaoundaba Lake.....	118
Table V.10. Trace elements (ppm) in sediments from the Ngaoundaba Lake	119
Table V.11. Trace elements (ppm) in sediments from the Ngaoundaba crater Lake.....	120
Table V.11. Heavy metal, enrichment Factor	124
Table V.11. Heavy metal, enrichment Factor	125
Table V.13. Heavy metal, enrichment Factor	126
Table VI.1. Radiocarbon dating of organic sedimentary carbon of cores sediments.....	131
Table VI.2. Eigenvalues, inertia and cumulative inertia of the CFA axes	140
Table VI.3. Spatial distribution of species along the Ossa core.....	146
Table VI.4. Eigenvalues, inertia and cumulative inertia of the CFA axes	147
Table VI.5. Spatial distribution of species along the Ngaoundaba core.....	153
Table VI.6. Eigenvalues, inertia and cumulative inertia of the CFA axes	155

List of abbreviations

AMS	: Accelerator Mass Spectrometry
BP	: Before Present
CF	: Contamination Factor
CIA	: Chemical Index of Alteration
CIW	: Chemical Index of Weathering
EF	: Enrichment Factor
FT-IR	: Fourier Transform Infrared
HREE	: High Rare Earth Element
ICV	: Index of Compositional Variability
I-geo	: Geo-accumulation Index
LOI	: loss-On-Ignition
LREE	: Light Rare Earth Element
OM	: Organic Matter
PAAS	: Post Archean Australian Average Shales
pH	: Potential for Hydrogen
PIA	: Plagioclase Index of Alteration
PLI	: Pollution Load Index
REE	: Rare Earth Elements
SEM-EDS	: Scanning Electron Microscope-Energy Dispersive X-ray Spectroscopy
TOC	: Total Organic Carbon
UCC	: Upper Continental Crust
WIP	: Weathering Index of Parker
XRD	: X-Ray Diffraction
XRF	: X-ray Fluorescence

Abstract

Lakes can be viewed as the most attractive and expressive characteristics of a landscape. Lacustrine sediments provide a historical record of the conditions of the local catchment environments. They are considered as a sensitive tool to investigate the weathering conditions, provenance, and to understand the redox conditions in the depositional environment, because sediment composition is controlled by the nature of the source rocks, climatic and tectonic factors of the source area. The aim of this thesis is reconstructing the paleoenvironment of three regions (Yaoundé, Dizanguè and Ngaoundéré) from Cameroon during the last 2000 years using a multiproxy approach including sedimentology, petrology and radiocarbon dating.

Sediments samples, taken from a raft and polyvinyl chloride (PVC) pipes under study are classified as shales, iron-shales, iron-sands, and arkoses and are composed of high water and organic matter contents. They essentially derived from felsic, intermediate and mafic rocks which likely correspond to nearby extensive granitic, gneissic and basaltic basement rocks. According to the mineralogical analyses carried out, the studied lakes sediments are made of quartz, kaolinite, smectite, hematite, goethite, feldspars, rutile and calcite with traces of illite, vivianite and ilmenite. The quartz grains shapes which are generally sub-rounded would have undergone a long fluvial transport and sometimes less. These grains confirm a physical and chemical alteration of the surrounding rocks and quite far away. The sediments from the center of the Ngaoundaba Lake could be the result of aeolian transport.

Weathering indices including chemical index of alteration (CIA~ 79–96.7); chemical index of weathering (CIW~ 85–98.8) and plagioclase index of alteration (PIA~ 92.6–99.1), associate to A-CN-K plots suggest that the intensity of weathering was moderate to higher for almost all sediment lakes relative to central part of Ngaoundaba sediments samples. This differentiation can be related to active tectonism during the deposition of the sediments from the center of the Ngaououndaba lake, whereas, it's related to passive in the other lakes. The $\text{SiO}_2/\text{Al}_2\text{O}_3$, $\text{Al}_2\text{O}_3/\text{Na}_2\text{O}$, and $\text{K}_2\text{O}/\text{Na}_2\text{O}$ ratios (2.1–12.5, 11.8–521.3 and 0.9–16 respectively), and the index of chemical variability (ICV), indicate a low compositional maturity for all the lacustrine sediments (~ 0.2–0.7) compared with central part of the Ngaoundaba Lake samples (~ 0.9–1.8). The values of U/Th, V/Cr and Ni/Co (0.1–0.42, 0.2–1.53 and 1.2–5.5 respectively) suggest an oxic depositional condition for all studied samples. The average Sr/Ba ratios for the sediments from the three sediment lakes suggest a depositional paleoenvironment with low salinity. From studied samples, high LREE/HREE and the average Ce/Ce* for lacustrine

sediment varying from 0.62 to 1.3. These low negatives to positive Ce anomalies may suggest a depositional milieu in a freshwater and a well oxygenated condition. The low values of P_2O_5/Al_2O_3 and V/Al_2O_3 ratios in the selected lake sediments were deposited in a shallow marine and fluvial depositional environments with an increase depositional environments water depth environmental condition. However, it should be noted that according to radiocarbon dating, the studied sediments are dated to the Holocene. The range values of Rb/Sr (0.04–0.7) and Ga/Rb (0.3–2.5) ratios for the Simbock, Ossa and Ngaoundaba lakes from the southern and northern Cameroon are low, suggesting warm and humid condition during the deposition of sediments. Likewise, the palynological assemblages along the Simbock, Ossa and Ngaoundaba cores show significant variations with arboreal species in South-Cameroon and forest-savannah in North-Cameroon and therefore confirm the present tropical climatic conditions.

Keywords: Sedimentology, petrology, paleoenvironment, lacustrine sediments, northern and southern Cameroon.

Résumé

Les lacs peuvent être considérés comme les plus attrayante et les plus expressive des caractéristiques d'un paysage. Les sédiments lacustres fournissent un traceur historique des conditions des environnements dans les bassins versants locaux. Ils sont considérés comme un outil sensible pour étudier les conditions d'altération, la provenance et pour comprendre les conditions d'oxydoréduction dans l'environnement de dépôt. La composition des sédiments est contrôlée par la nature des roches mères, les facteurs climatiques et tectoniques de la zone d'origine. L'objectif de cette thèse est de reconstruire le paléoenvironnement de trois régions (Yaoundé, Dizanguè et Ngaoundéré) du Cameroun au cours des 2000 dernières années en utilisant une approche multidisciplinaire comprenant la sédimentologie, la pétrologie et la datation au radiocarbone.

Les échantillons de sédiments, prélevés sur un radeau et des tuyaux en polyvinyl chloride (PVC) pour cette l'étude sont classifiés d'argiles-ferrugineuse, de sables-ferrugineux et d'arkoses. Ils sont composés de fortes teneurs en eau et en matière organique. Ils proviennent essentiellement de roches felsiques, intermédiaires et mafiques qui correspondent probablement à des roches du socle granitique, gneissique et basaltique étendues situées à proximité des lacs étudiés. Selon les analyses minéralogiques effectuées, les sédiments lacustres étudiés sont constitués de quartz, de kaolinite, de smectite, d'hématite, de goethite, de feldspaths, de rutile et de calcite avec des traces d'illite, de vivianite et d'ilménite. Les formes des grains de quartz qui sont généralement sub-arrondis, ils auraient subi un long et parfois court transport fluvial. Ces grains confirment une altération physique et chimique des roches environnantes et assez lointaines. Les sédiments du centre du lac Ngaoundaba seraient par contre le résultat d'un transport éolien.

Les indices d'altération tels que l'indice chimique de l'altération météorique (CIA~ 79-96,7) ; l'indice chimique d'altération chimique (CIW~ 85-98,8) et l'indice d'altération des plagioclases (PIA~ 92,6-99,1), associés aux parcelles A-CN-K suggèrent que l'intensité de l'altération des roches sources était modérée à très élevée pour presque tous les sédiments lacustres par rapport à la partie centrale des échantillons de sédiments de Ngaoundaba. Cette différenciation peut être liée au tectonisme actif pendant le dépôt des sédiments du centre du lac Ngaououndaba, alors qu'elle est liée au tectonisme passif dans les autres lacs. Les rapports $\text{SiO}_2/\text{Al}_2\text{O}_3$, $\text{Al}_2\text{O}_3/\text{Na}_2\text{O}$, et $\text{K}_2\text{O}/\text{Na}_2\text{O}$ (2,1-12,5 ; 11,8-521,3 et 0,9-16 respectivement), et l'indice de variabilité chimique (ICV), indiquent une faible maturité compositionnelle pour tous

les sédiments lacustres ($\sim 0,2-0,7$) par rapport à ceux de la partie centrale des échantillons du lac Ngaoundaba ($\sim 0,9-1,8$). Les valeurs de U/Th, V/Cr et Ni/Co ($0,1-0,42$; $0,2-1,53$ et $1,2-5,5$ respectivement) suggèrent un état de dépôt oxydique pour tous les échantillons étudiés. Les moyennes des rapports Sr/Ba pour les sédiments des trois lacs sédimentaires suggèrent un paléoenvironnement de dépôt avec une faible salinité. D'après les échantillons étudiés, les rapports LREE/HREE élevé et les anomalies en Ce (Ce/Ce^*) pour les sédiments lacustres varient de 0,62 à 1,3. Ces faibles anomalies négatives à positives de Ce peuvent suggérer un milieu de dépôt en eau douce et un état bien oxygéné. Les faibles valeurs des rapports $\text{P}_2\text{O}_5/\text{Al}_2\text{O}_3$ et $\text{V}/\text{Al}_2\text{O}_3$ dans les échantillons de sédiments lacustres sélectionnés ont été déposées dans un milieu marin et fluvial peu profond, avec une augmentation des conditions environnementales des milieux de dépôt en eau profonde. Cependant, il convient de noter que, selon la datation au radiocarbone, les sédiments étudiés sont datés de l'Holocène. Les valeurs des rapports Rb/Sr ($0,04-0,7$) et Ga/Rb ($0,3-2,5$) pour les lacs Simbock, Ossa et Ngaoundaba au sud et au nord du Cameroun sont faibles, ce qui suggère un climat chaud et humide pendant le dépôt des sédiments. De même, les assemblages palynologiques le long des carottes de Simbock, d'Ossa et de Ngaoundaba montrent des variations significatives des espèces arboricoles au Sud-Cameroun et de forêt-savane au Nord-Cameroun et confirment donc les conditions climatiques tropicales actuelles.

Mots-clés : Sédimentologie, pétrologie, paléoenvironnement, sédiments lacustres, Nord et Sud du Cameroun.



General introduction

Imagination is more important than knowledge because knowledge is limited while imagination encompasses the whole world.

-Albert Einstein-

1. Overview

Curiously, it is not easy to give the exact definition of lakes. Without denying the connections with tributaries and effluent, a lake has no direct relationship with the sea. It does not influence it, since it is an inland body of water. On the contrary, it is the watershed that dominates the lake, since it is a continental body of water. The major and the main consequence of the lack of communication with the ocean is the development of an identity specific to each lake, its operation in closed circuit. If the latter is old enough, its most prominent manifestation is biological endemism. A lake is therefore a continental body of water, that is, separated from the sea, dominated by its feeding basin and developing its own personality (Touchart, 2000).

Lakes in the strict sense are pieces of water that have a central region in which the depth of the water is sufficient to prohibit the arrival of the littoral flora. Ponds are lakes so shallow that submerged coastal flora can be found everywhere (Bayly and Williams, 1973). In a lake, unlike ponds and wetlands, there is a staging, that is, a sustainable organization of most phenomena such as sediment deposits in the vertical dimension.

Lakes can be viewed as the most attractive and expressive characteristic of a landscape. Lake sediments provide a historical record of the conditions of the local catchment environments. They are considered as a sensitive tool to investigate the weathering conditions, provenance, and to understand the redox conditions in the depositional environment, because sediment composition is controlled by the nature of the source rocks, climatic and tectonic factors of the source area.

2. Problem statement

Lake sediments are archives of climatic variations and pollution in the environment. Trace and major element signals recorded in sediments allow the reconstruction of historical events, both natural and anthropogenic in origin. The reconstruction of anthropogenic-induced changes in lake trophic state from lacustrine archives can provide a better understanding of present-day lake processes and chemical fluxes with respect to pre-industrial conditions and long-term variations.

Sediment characteristics are commonly governed by several factors, such as provenance, tectonic setting, maturity and climate in a depositional environment (Verma and Armstrong-Altrin, 2013; Sharma et al., 2013; Tawfik et al., 2018; Madhavaraju et al., 2019). An understanding of sedimentation processes involved in the origin of transport and deposition

of lake sediments is of paramount importance in understanding sedimentological and environmental conditions (Nesbitt and Young, 1982; Ekoa Bessa et al., 2018; Ramos-Vázquez and Armstrong-Altrin, 2019). Anthropogenic activities, concentrated along the terraces of rivers, lakes and estuaries, urbanization, tourism, fishing and agricultural activities have considerably complicated the natural pace of lakes and estuarine sedimentation processes (Kaotekwar et al., 2019). Organic matter (OM) and total organic carbon (TOC) in lake sediments mainly involves humic substances and other organic compounds (Zhang et al., 2017). Organic matter content in lake sediments provides crucial information for studies of paleoenvironments, the evolution of climate change and the effects of human activity on local and regional ecosystems.

Petrology of lacustrine sediments is overseen by factors like provenance and weathering conditions (Kuscu et al., 2018; Armstrong-Altrin et al., 2019). Mineralogy and chemical composition of sediments mostly provide large information on weathering conditions and provenance (Bhatia 1983; Roser and Korsch 1986; Benayad et al., 2013). Verma and Armstrong-Altrin (2013, 2016) have warned in the use of discrimination diagrams for provenance studies using major element geochemistry. However, geochemistry of lacustrine sediments has widely been used to evaluate provenance, weathering conditions and paleoclimate (Kasanzu et al., 2008; Armstrong-Altrin et al., 2018; Abu and Sunkari, 2020).

Five categories of lakes are present in Cameroon: Crater lakes (e.g., Ngaoundaba Lake, Lake Nyos); subsidence lakes (e.g., Ossa Lake, Dibi Lake); Bassin lakes (e.g., Lake Chad); artificial lakes (e.g., Simbock Lake, municipal Lake of Yaoundé) and other lakes (e.g., le lac des Jumeaux).

From several lakes of Cameroon, numerous studies are mainly focused on water quality, heavy metal contaminations, fish species and pollution; paleoenvironmental reconstruction with palynology and rarely on radiocarbon dating (Kwon et al., 2012; Nguetsop et al., 2013; Barkai et al., 2014; N'nganga et al., 2018). Geochemical, mineralogical studies are very few in Cameroon Lakes, which are more influenced by natural processes and sometimes human activity.

3. Objectives

In this study, the selected lakes have different formation context: artificial (Simbock), subsidence (Ossa Complex) and crater (Ngaoundaba). Their study has a double importance.

Firstly, because their sediments can be used to reconstruct the paleoenvironmental evolution of the studied area. Secondly, sediments of these lakes will provide a record of the increased anthropogenic and natural processes using various physical and petrological features from strongly urbanized area (Simbock, Yaounde) to naturally preserved ones (Ossa and Ngaoundaba).

This study was focused on a paleoenvironmental reconstruction during the last 1000 yrs BP., using a multiproxy approach including sedimentology, geochemistry and mineralogy, which will be applied to the selected lakes to retrace and compare their respective depositional environments. To attain this objective, it will be important to characterize the physical features, the petrology including mineralogy and geochemistry without neglecting the environmental statut of selected lakes.

The results of this study provide important insight for future research on lakes in Cameroon and over the world with the new and simple methods. This study will help in short-term to understand the characteristics of lakes formed in different contexts and in a long-term will more understanding on the last event which occurred in Cameroon and Central Africa. It is the first of its kind in the sub-region to embrace this approach to solving both environmental and paleoenvironmental studies. This thesis will build local capacity teaching, learning, deposition system and research both in Cameroon and the sub-region at the undergraduate, graduate and postgraduate levels that will be trained using a wide array of new approaches to geoscience.

4. Methodology

To achieve the objectives of this study, a major literature review was conducted throughout the study on lakes over the country and the world. several field campaigns were conducted and several cores were taken from a raft and polyvinyl chloride (PVC) pipes, and seven were selected for this study. In the laboratory, a description based on color and manual texture was carried out. Sedimentological analyses such as grain sizes, microtextures, residual humidity, color determination and organic matter were carried out in the laboratories of the University of Yaoundé I. Other analyses such as mineralogy, geochemistry and radiocarbon dating were also realized. Details on the methods and analytical procedures are to be provided in the third chapter of this thesis.

5. Thesis outline

The present thesis has been organized into three parts of seven chapter preceded by this general introduction which highlights an overview, the problem statement, the main objectives, the methodology and the thesis outline and followed by conclusions and suggestions.

The first part in the background consist of chapters one, two and three, the second part gives the results and the interpretations and it is composed of chapters four, five and six. The last part, namely discussion gives the different discussions from results in chapter seven.

The first chapter is dedicated to the presentation of the natural setting and the geology of the Yaoundé, Dizangué and Ngaoundéré regions.

The second chapter takes into account the literature review, focusing on synthesis of work on sedimentology, mineralogy and geochemistry. It also focuses on a brief overview of lakes in Cameroon.

The third chapter is focused on methods and materials used to perform the different objectives which permits to reach to results.

The fourth chapter focuses on the determination of different characteristics including residual humidity, physical features, shapes of grains and organic matter content of sediments.

The fifth chapter deals with the mineralogy and the chemistry of their different phases; geochemical distribution and environmental status of lacustrine sediments.

The sixth chapter addresses the dating and paleoenvironmental reconstruction of sediments using the lake sediments as archives.

An overall account on the provenance, tectonic setting, maturity, paleoweathering, depositional environments, paleoclimate linked to paleoreconstruction is provided in the last chapter as synthesis and discussions.



Part one: Background

The first part concerns the natural environment, previous work and methods. It is subdivided into three chapters: the first deals with the description of the natural environment of the various sites, the second with the state of current knowledge of the lakes and previous work on lakes in Cameroon and the third on the different materials and methods used in this study.



Chapter I: Natural setting

The student is not a container you have to fill, but a torch you have to light. If we knew what we were doing, it wouldn't be called research anymore, would it ?

-Albert Einstein-

This chapter provides a general overview of the natural environment of the studied areas, their climate, water regime, vegetation, geomorphology, soils and geology. It also describes observations in the country. Essential information for this chapter is obtained from previous work on Cameroon's hydroclimatic regimes, notably that of Olivry (1986), Suchel (1987), Lienou et al. (2005), Anonymous (2010), Viviane Djoufack (2011), etc.

1.1. Location

Cameroon is very stretched in latitude, covering a length of about 1300 km on its north-south axis, compared to nearly 900 km on the east-west axis. It shares 4700 km of border with 6 neighbouring countries (Nigeria, Chad, Central African Republic, Republic of Congo, Gabon and Equatorial Guinea) including 1700 km with Nigeria, and 400 km of coastline on the Atlantic Ocean (figure 1a). Its relief ranges from 0 to 4095 m at the summit of Mount Cameroon. From the climatic point of view, about 4/5th of the country's surface area belongs to the humid climate zone, while tropical climates of dry nuance concern the remaining 1/5th. The natural environment defines all the physical characteristics that influence the existence of human beings on earth. From this point of view, the diversity of Cameroon's landscapes constitutes one of its main originalities. It is essentially due to its extension from the equator to the Sahelian zone; its opening to the ocean through the Gulf of Guinea, gateway to the monsoon flow on the African continent; its location at the crossroads of the West and Central African climatic domains and its orography, its soils and geology are varied. Lakes included in this study are located in the following regions: Central for Lake Simbock, Littoral for Lake Ossa and Adamawa for Lake Ngaoundaba.

Site1: Simbock Lake

Lake Simbock is located in Yaoundé, the political capital of Cameroon, Mfoundi Division, central region, subdivided into seven subdivisions over an area of about 310 km². It occupies the western edge of South Cameroon plateau between the parallels 3° and 5° North and the meridians 11° and 13° East. The lake studied is located in the Subdivision of Yaounde VI in the south-western part of the town, in the Simbock neighborhood, precisely at 03°48' N and 11°27' E (Figure I.1b).

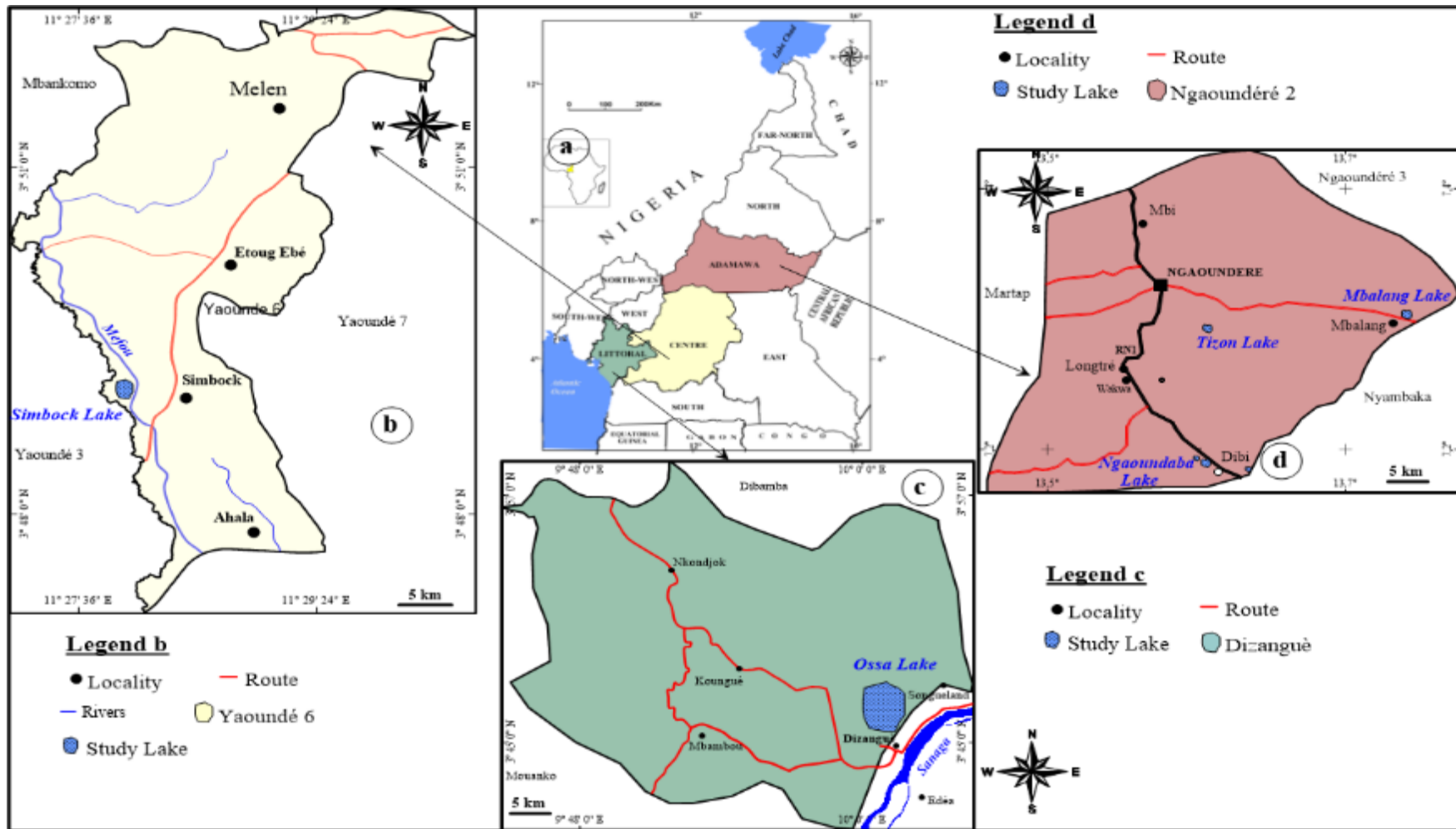


Figure I.1. Location of Cameroon and the different sites studied: a) Administrative map of Cameroon; b) Lake Simbock; c) Lake Ossa and d) Lake Ngaoundaba

Site2: Ossa Lake

Lake Ossa is located in the town of Dizangue, Division of the District of the same name, Sanaga Maritime Division, Littoral Region. It is located at the western part of Edéa and owes its influence on the presence of an agro-industrial complex specialized in the cultivation of oil palm. Access is facilitated by the D58, which starts from the N3 at the municipality of Edea II, runs alongside the Sanaga River and permits to join the town on about 11 km on an earth road. Located at an altitude of 8 m above sea level, fits in a rectangle of N-S orientation approximately 10 x 12 km sides, whose extreme coordinates are 03°45.7'-03°53' of north latitude and 09°90'-10°04.2' of east longitude (Figure I.1c).

Site3: Ngaoundaba Lake

Lake Ngaoundaba culminate at an altitude of 600 m, it is located 15 km from Ngaoundere, the capital of Adamawa Region, Vina Division. Ngaoundere or Navel Mountain is located on a high plateau of 1200 meters above sea level; it is a transistion town between the North and the South. Geographically it is located between 7°19'28 - 7°21'21 of North latitude; and 13°33'52- 13°35'56 of East longitude (Figure I.1d).

1.2. Climate

According to the rainfall regime, succession of seasons and incidentally of the thermal regime, the Cameroonian territory has been divided into different climatic zones that can be grouped into two major classes separated by a line that approximately corresponds to latitude 4°30 N: tropical climate with two seasons to the north of this line and equatorial climate with four seasons to the south. Taking in consideration the regional nuances imparted by the main factors of climate, including contrasting relief, latitude and location in relation to the sea, several patterns of climatic regions have been proposed (Figure I.2).

Site1: Simbock Lake (Yaoundé)

The climate of the study area was characterized based on rainfall and thermal data obtained at the Yaounde weather station for a period of 60-years from 1935 to 2019. The total annual rainfall and temperatures are 1560.9 mm and 24.4 °C respectively (Table I.1; Figure I.3). Climate characterization was based on the calculation of monthly aridity index of DeMartonne (1942) and ombrothermics curves by Bagnouls and Gaussen (1957).

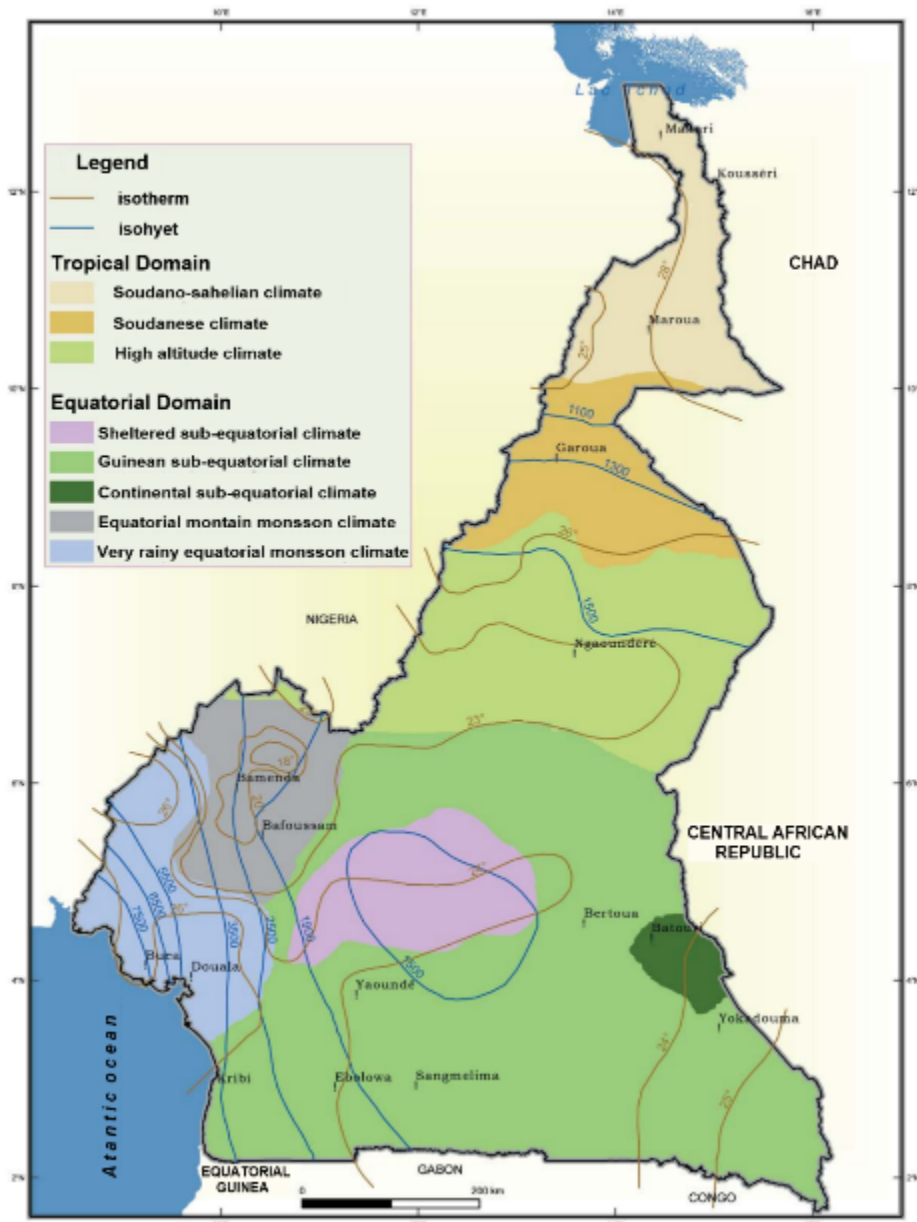


Figure I.2. Climate map of Cameroon (Anonymous, 2010)

The dry periods correspond to the months of December, January, and July; whereas the months of April, May, September, October correspond to the wet periods (Figure I.3).

Tableau I.1. Monthly precipitation values (1935-2018), temperatures (1980-2019) according to the Mvan station in Yaoundé.

	Jan.	Feb.	Mar.	Apr.	May	Jun.	Jul.	Aug.	Sept.	Oct.	Nov.	Dec.	An.
P (mm)	20.4	47.7	119.6	164.4	205.5	155.2	99.7	125.9	218.1	267.0	109.2	28.2	1560.9
T (° C)	24.1	25.4	25.3	25.4	24.1	23.8	24.5	24.4	24.2	24.3	24.1	24.1	24.4
Ia	10.3	22.4	52.6	66.9	70.3	52.6	26.8	37.3	77.2	97.8	54.2	13.1	48.4

The ombrothermal curves show that this region is subject to an equatorial climate of four-seasons distributed as follows:

- a long dry season from mid-November to mid-February;
- a small rainy season from mid-February to June;
- a long rainy season from August to November;
- a small dry season in July.

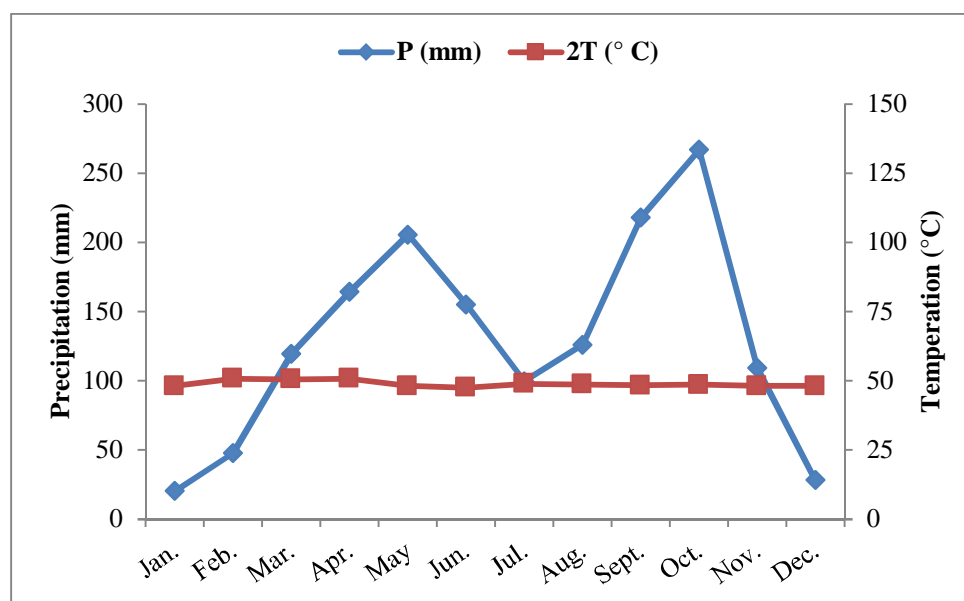


Figure I.3. Ombrothermal curves of Yaounde town (1935- 2019), according to Bagnouls and Gausse (1957).

Site2: Ossa Lake (Dizangué)

Lake Ossa is located in the deltaic zone of the Littoral (few kilometres away from the Atlantic Ocean). The climate of the study area was characterized using rainfall and thermal data obtained at the Edea weather station for a period of 13-years from 1996 to 2019. Total annual rainfall and temperatures are 2535.41 mm and 27.2 °C, respectively (Table I.2; Figure I.4). The climate characterization was made from the calculation of the monthly aridity index of De Martonne (1942) and the ombrothermal curves of Bagnouls and Gausse (1957).

Tableau I.2. Monthly precipitation values (1996-2019) according to the Edea station

	Jan.	Feb.	Mar.	Apr.	May	Jun.	Jul.	Aug	Sept.	Oct.	Nov.	Dec.	An.
P(mm)	24.48	45.06	135.36	225.71	268.33	224.81	266.13	427.55	422.89	330.9	136.75	27.44	2535.41
T (°C)	28.8	28.4	29.3	27.9	27.5	26.6	25.5	25	25.6	26.4	27.4	28	27.2
Ia	19.8	22.4	20.5	18.9	17.6	14.9	11.3	9.9	12.4	15.5	17.6	18.1	16.58

The ombrothermal curves show that this region is subject to a maritime equatorial Cameroonian climate with two seasons distributed as follows:

- a rainy season from April to October;
- a dry season from November to March.

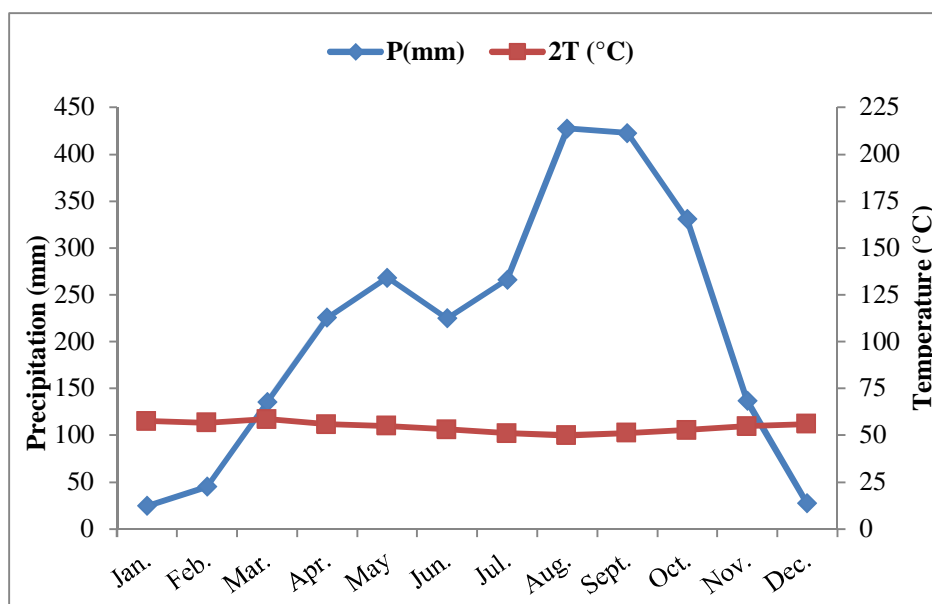


Figure I.4. Ombrothermal curves of the town of Dizangue (1996- 2019), according to Bagnouls and Gausson (1957).

Site3: Ngaoundaba Lake (Ngaoundere)

The Adamawa region is subject to a transitional tropical climate between the dry tropical climate in the North and the humid tropical climate in the South. It is a climate tempered by the position in altitude (high altitude tropical climate as defined by Olivry (1986)). The dry season is marked by a dry wind coming from the North, the harmattan, which is transformed into a dry and hot wind, generating temperatures that can reach 28.7°C. The rainy season is characterized by a period of violent thunderstorms (at the beginning of the season) and an average temperature of 22 °C. Annual rainfall reaches an average height of 1510 mm in Ngaoundere.

Tableau I.3. Monthly precipitation values (1997-2019) according to the Ngaoundere station

	Jan.	Feb.	Mar.	Apr.	May	Jun.	Jul.	Aug.	Sept.	Oct.	Nov.	Dec.	An.
P (mm)	0	0	40	130	200	200	250	270	230	130	10	0	1510
T (°C)	21	22	23	23	22	22	22	21	21	21	21	21	22

The ombrothermal curves shows that this region is subject to a tropical Sudano-Guinean climate characterized by two seasons distributed as follows:

- a dry season that lasts five months from November to March;
- a rainy season that lasts seven months from April to October.

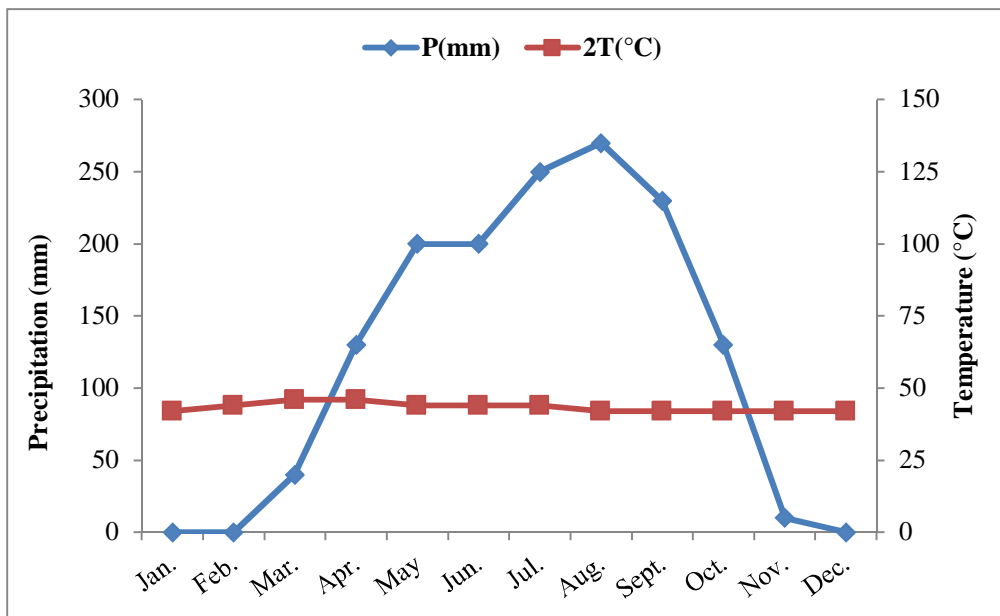


Figure I.5. Ombrothermal curves of the city of Ngaoundere (1997- 2019), according to Bagnouls and Gausson (1957)

1.3. Hydrography

Orography orient of the main axes of the hydrographic network in Cameroonian territory. Thus, one can distinguish two preferential directions of water courses: SSW-NNE is concord with the "Cameroon line" and the other, and NW-SE dominated by the southern part of the Benue River and tributaries of the Congo. In the north, rivers originating mainly from the northern slopes of the Adamawa and Mandara Mountains converge into two main drains:

- the Benue, formed by its three main tributaries (Upper Benue, Mayo Kebi and Faro), is oriented towards Nigeria in the ditch that takes its name;
- the Logone, formed by its main branches the Vina and Mbere in Cameroon and the Pende in Chad, drains the north-eastern limit of the Adamawa. It crosses the former catchment area in the Bongor locality and enters the Chadian plain where the gentle slopes give's a network characteristic of the Sahel up to its confluence with the Chari at Kousséri. On the north-eastern and eastern flanks of the Mandara Mountains, descend from torrential streams (the Mayos: temporary streams in Peulh) which then disappear into the sand dunes and mud of the Chadian basin plain. One of these Mayos, the best studied, the Mayo Tsanaga, chosen in this study as

representative of the northern zone of Cameroon. In the southern part, the plateau slopes are mainly drained by the Lom and Djerem, forming the upper Sanaga, and the Mbam, receiving the Noun from the western highlands. The flow axes approximately first follow the north-south direction on the high peaks. This direction bends to meet of the Sanaga fault. This accident imposes on the main course of the river the N30°E direction, parallel to that of the Cameroon line, which it follows until its mouth in the coastal plain.

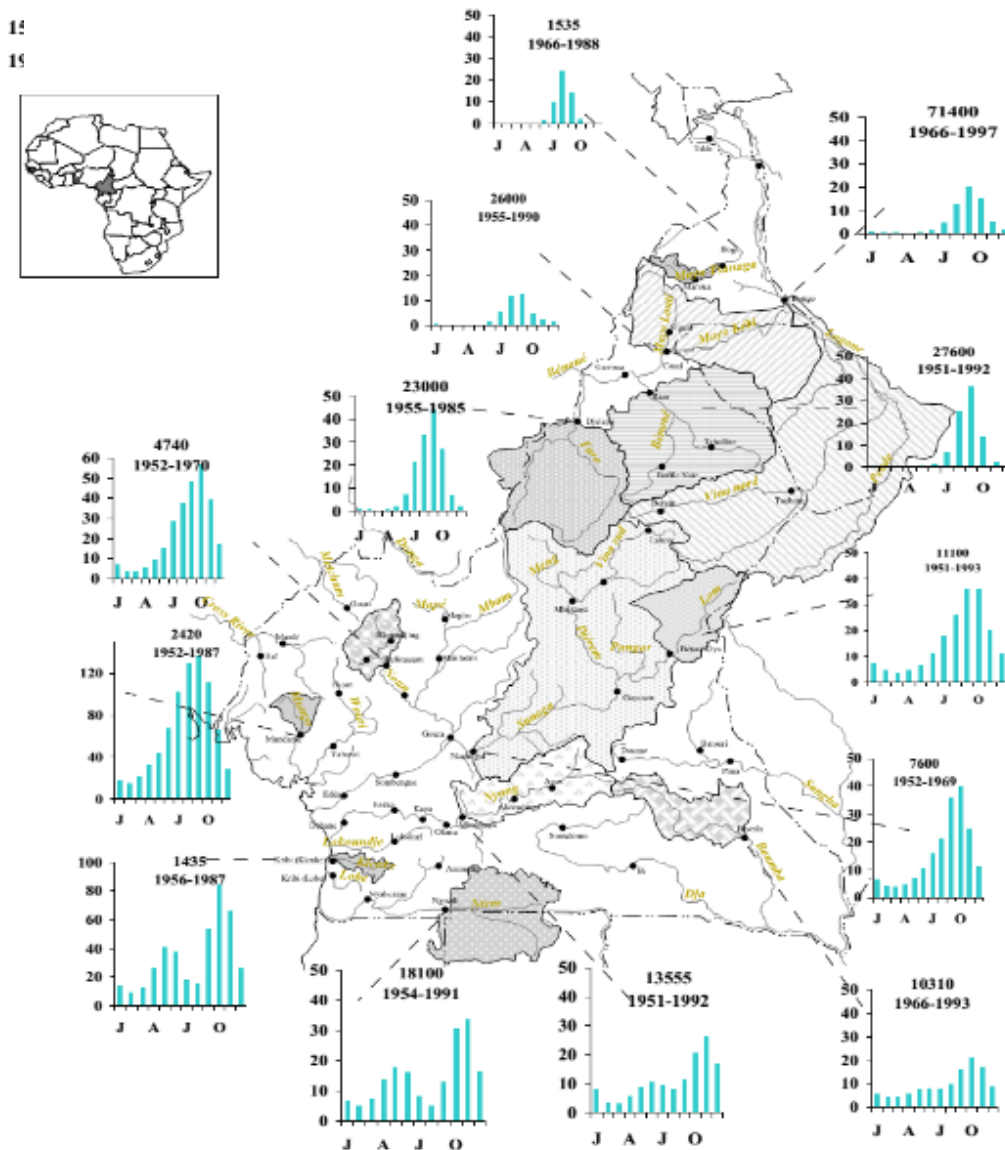


Figure I.6. Natural hydrological regimes of Cameroon: specific monthly production in $l.km^{-2}.s^{-1}$ (Lienou et al., 2005)

The relief of the central part of the southern Cameroonian plateau defines a watershed that directs the Kadei and all the Boumba-Dja eastwards towards the Congo basin. The Nyong and Ntem are the mains rivers in the southern coast and flow towards the ocean. The Kienke also belongs to this group. In the south-western part of the country, the chain of peaks forming the Cameroonian ridge directs the Cross River towards Nigeria and the Wouri and Mungo rivers towards the north coast (Figures I.6).

Site1: Simbock Lake (Yaoundé)

The hydrographic regime of Yaounde and its surroundings is equatorial (Onguené Mala, 1993). The Mfoundi, Anga'a and Mefou are the three main rivers that drain the entire town of Yaounde (Olivry, 1986). In the south-western sector of Yaounde, which is located in the Mefou sub-basin, the rivers have a NW - SE flow direction.

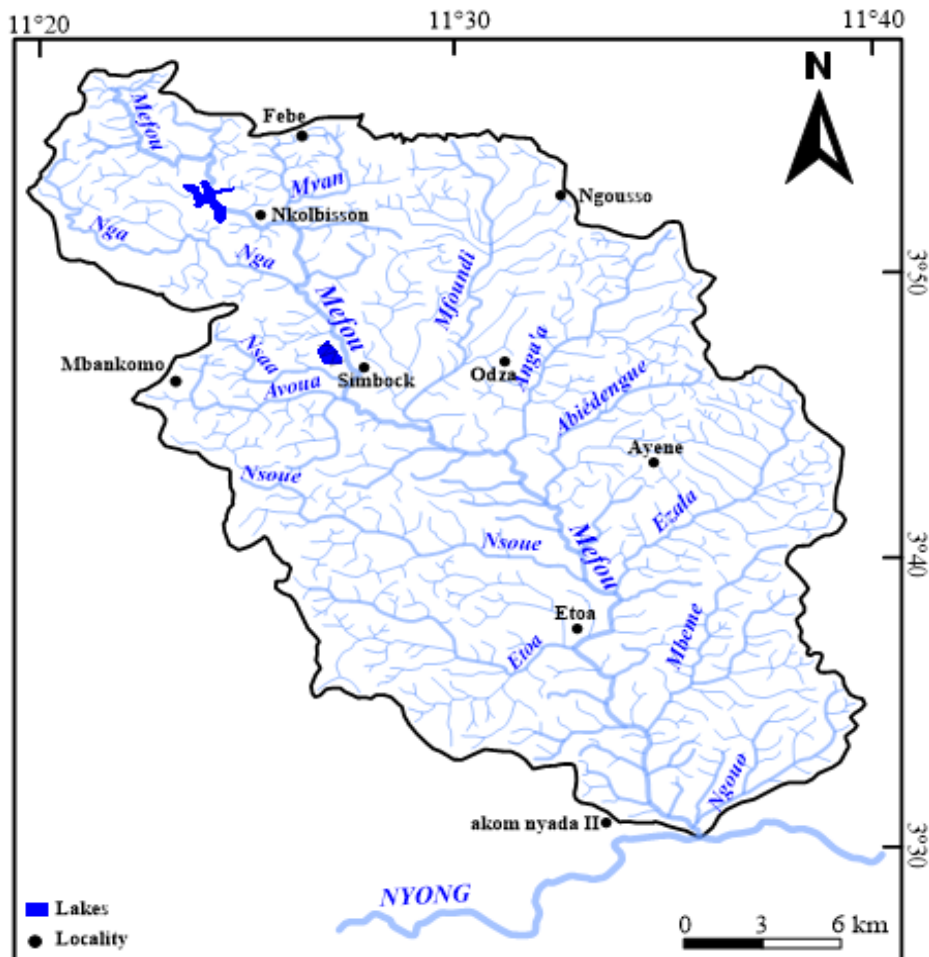


Figure I.7. Location of Lake Simbock in the sub-catchment of the Mefou (Ndam Ngoupayou et al., 2007a)

Most of these rivers have their source at the foot of the Eloumdem Mountains (1209 m). The main rivers are Nsaa, Mga, Avoua, Ossoe and Ngoue, which are all tributaries of the Mefou and Ezola, Biyeme which are tributaries of the Mfoundi. The hydrographic network is of dendritic type with a rectangular and branched tendency (Figure I.7). This sub-basin directly and/or indirectly feeds Lake Simbock.

Site2: Ossa Lake (Dizangué)

Dizangue is surrounded by lakes and the most important is Lake Ossa having a surface area of 5000 ha containing species of protected animal such as Lamentin and a group of 18 islets, true tourist wonders. River Sanaga meanders through the municipality at a distance of 8 km. It's part of the great Sanaga basin (Figure I.8). There are also some rivers such as the Mbanda River, Mbongo River, Kwakwa River, etc. (Figure I.8). There is also the Atlantic Ocean on the side of Ndigle Island.

Surface water in the Ossa basin has a conductivity of 17.8 uS.cm^{-1} (normalized for 25°C) and a pH of 7.0. The conductivity is very low and concentrations of SO^- and Mg^{2+} are particularly low compared to tropical and temperate lakes. Most of the ions are brought into waters by weathering of rocks of the catchment area and/or by meteoric inputs (geographic journal of Cameroon, 1992). According to the trophic classification of lakes based on water transparency, N, P and chlorophyll concentrations, Lake Ossa is oligotrophic. Compared to average rainfall values collected inside the ground of Cameroon, ionic ratio values are significantly lower. Decrease in Ca/Na, K/Na and Cl/Na ratios is due to sodium inputs through rock weathering. Waters are unsaturated with respect to siderite, but estimates should be considered with caution as colloidal iron is not retained by the 1.2 ppm filters (Wirrmann, 1992).

Site3: Ngaoundaba Lake (Ngaoundere)

The Ngaoundaba Lake, located in the Adamawa plateau which is the "water tower of Cameroon". It gives rise to numerous rivers that feed three of the four basins of the national hydrographic network: the Djerem, which rises at an altitude of around 1100 m, 40 km north of Meiganga, and receives two tributaries (Vina of the south and Beli). It flows into the Sanaga with the Lom (Olivry, 1986); the Vina and Mbere which flow eastwards; the Benue and its tributaries; the Faro and Deo which flow northwards before flowing into the Niger. It is worth mentioning the presence of several lakes inherited from the long volcanic history of the region. The best known are the Tizon, Nosole Mbalang and Ngaoundaba lakes near the town centre of Ngaoundere.

generally extend at the foot of the Mandara Mountains, between Duck's Beak and Lake Chad (Donfack, 1988). These are industrial rice-growing areas (Yagoua). The severity of climatic conditions heralds the Sahelian and desert climates of Sudanese Africa (Letouzey, 1985).

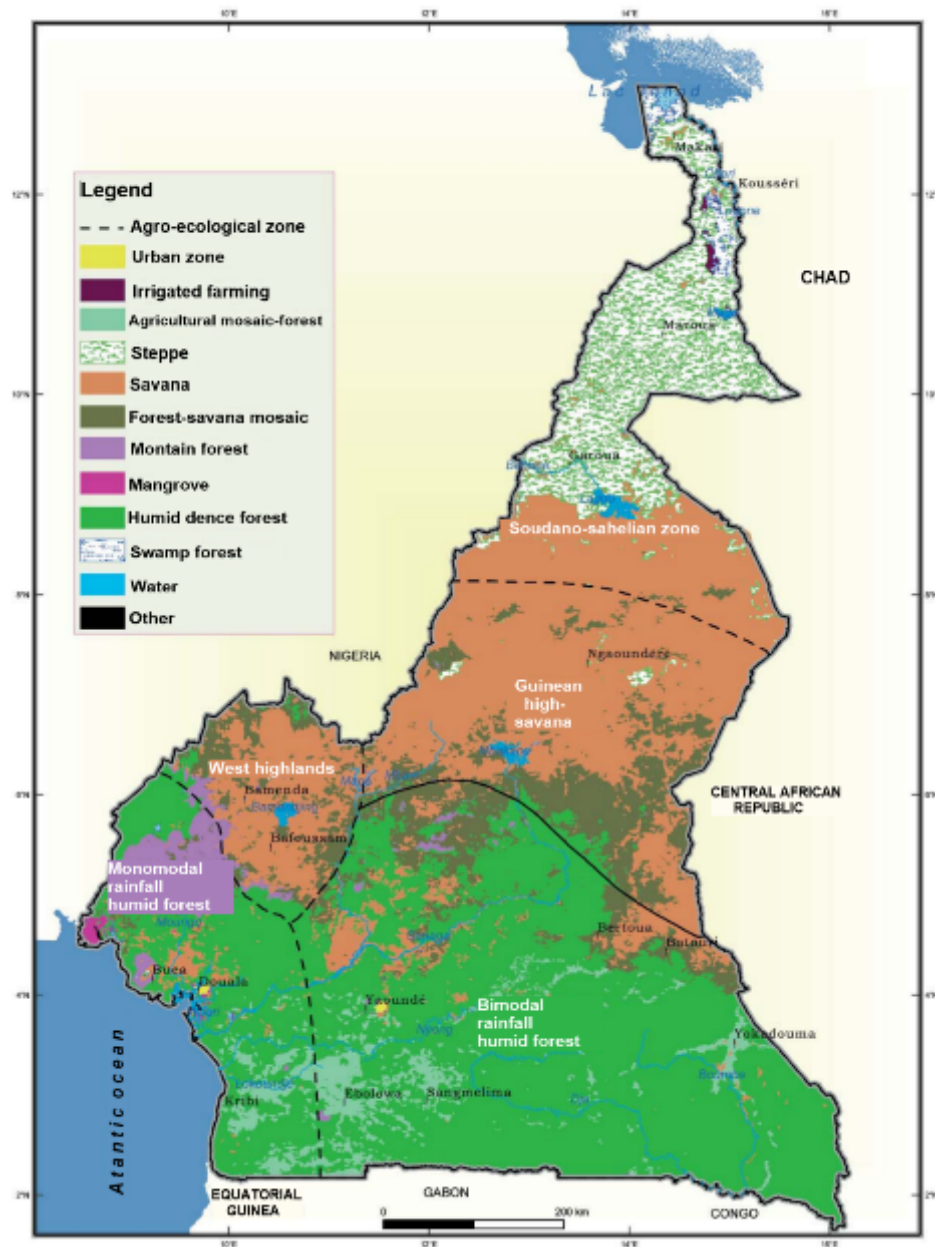


Figure I.9. Vegetation distribution of Cameroon (Letouzey, 1985)

At the latitudes of Adamawa in the Sudanian domain, vast Sudano-Guinean shrubby and wooded savannas can be found on an altitude of about 900-1500 m. The mountain forest and Afro-Subalpine grassland occurs on Cameroon and Oku Mountains 2800 m above sea level. These high-altitude formations are areas of volcanism and grazing.

All the plant formations of southern Cameroon belong to the Congo-Guinean region (Santoir et al., 1995). These plant formations are organised into two groups: the dense deciduous forest and the evergreen humid dense forest domain: the dense humid forest is located in the northernmost zone of the Congo-Guinean region, in contact with the Sudano-Zambian region. It is subdivided into Guineo-Sudanian perennial savannah and Guineo-Congolian semi-caducifolia forest. The first are located on either side of the Sanaga River, north of the forest formations. They are predominantly herbaceous with scattered trees and shrubs. The semi-caducifoliated forests, on the other hand, are composed of dense humid semi-caducifoliated rainforest or semi-deciduous forest with Sterculiaceae-Ulmaceae. They are not easy to demarcate because they gain over other types of vegetation during agricultural clearing.

On the shores of the Atlantic Ocean we find landscapes of mangroves (about 2500 km²) which constitute an enormous evapotranspiration potential. The average annual relative humidity exceeds 50 % almost everywhere, even in the dry season, and the annual thermal amplitudes are below 2 °C.

Site1: Simbock Lake (Yaoundé)

The work of Villiers (1995) characterizes the vegetation of Yaoundé which is covered by a dense semi-caducifoliated and ulmaceous forest. However, as a result of increasing anthropic action, Yaoundé is degraded into a secondary forest populated by grasses, lianas, palms, shrubs and few large trees. In the localities surrounding, the generally penetrated landscape consists of food crop plantations separated from each other by a few patches of secondary forest or shrubby savannah. Under anthropogenic action, this forest is gradually being replaced by a secondary forest populated by grasses, palms and shrubs. In this zone of dense rainforest, edaphic formations may be associated, mainly in swampy areas where raphias, mitragyne and uapaca are found. The hillsides are where cassava, groundnuts, maize and, in places, cocoa trees are planted. Cassava, groundnuts, maize and in some places cocoa trees are planted on hillsides, while vegetables and various market garden product (salads, carrots, tomatoes, etc.) are grown in marshy areas (Figure I.10).



Figure I.10. Vegetation around Lake Simbock

Site2: Ossa Lake (Dizangué)

Vegetation found in the islets and catchment of the Reserve is a coastal forest in the Guinean-Congolian ombrophilic zone with the dominant species being the *Lophira alata* and *Irvingia gabonensis*. The reserve is generally represented by a subtype of the lowland Biafran evergreen forest or Atlantic coastal forest (Letouzey, 1985) in the Ossa Lakewatershed consisting of trees such as: umbrella tree (*Musanga cecropioides*), frake (*Terminalia superba*) and the iroko (*Milicia excelsa*). On the south-eastern edge, a swampy forest takes over (*Pandanlis*, *Raphia*, *Mitragyne*, *Uapanca*); we also find: *Lophira alata* (family *Ochnaceae*, called Bongossian Ewondo), *Sacoglottis gabonensis*, of South American origin, the only African representative of the *Humiriaceae* family (bidou), *Cynornetra hankei* (*Caesalpinaceae*, *ekep*), *Codaeddis* (*Olacaceae*, *ewomé*) while a secondary forest be it adult or young, colonizes the north (Wirmann, 1992). In the west, industrial crops occupy the whole riparian zone (palm oil and rubber from the Dizangué plantation), in association with food crops. The catchment area is occupied by 95 % forest, 5 % agricultural crops and less than 1 % grass (Figure I.11).



Figure I.11. Vegetation around Lake Ossa

Site3: Ngaoundaba Lake (Ngaoundere)

The Adamawa plateau has a buffer vegetation between the forest in the south and the steppe in the north. plateaux are covered by Sudano-Guinean shrubby savannahs with thick, fire-resistant grasses and shrubs. It stretches from the slopes of volcanic edifices to the ravines, a savannah with more trees than on the plateau, but which is subject to extensive agricultural clearing. While many forest galleries develop along rivers and in river valleys. But this vegetation has taken a serious blow with the advanced desertification phenomenon. It is gradually degrading to grassy savannah in the northern plain. The vegetation around Lake Ngaoundaba is a wooded savannah and a mid-Sudanian open forest (Figure I.12).



Figure I.12. Vegetation around Lake Ngaoundaba

1.5. Orography

According to the importance of altitude, a distinction is made between mid-altitude plateaus and depressions which are essentially made up of the southern Cameroonian plateau, the Atlantic lowlands and the northern plains. Mountains and high plateau are also distinguished and account for nearly a quarter of the country's surface area (Figure I.13).

Lowlands consist mainly of the Atlantic lowlands (coastal plains) and Northern Cameroon plains. In the centre, the Douala Sedimentary Basin extends to Nigeria through the Ndian and Rio del Rey plains. The plains and depressions of North Cameroon are erected against the Atlantic and are therefore frequently exposed to the harmattan blast. Here, we find a topography of low altitudes that evokes more aridity than the abundant rains encountered further south. They are mainly formed by 2 depressions: the upper Benue basin and the Lake Chad plain. The Diamare plain extends between the Chad basin and the Benue basin with an altitude of 500 m.

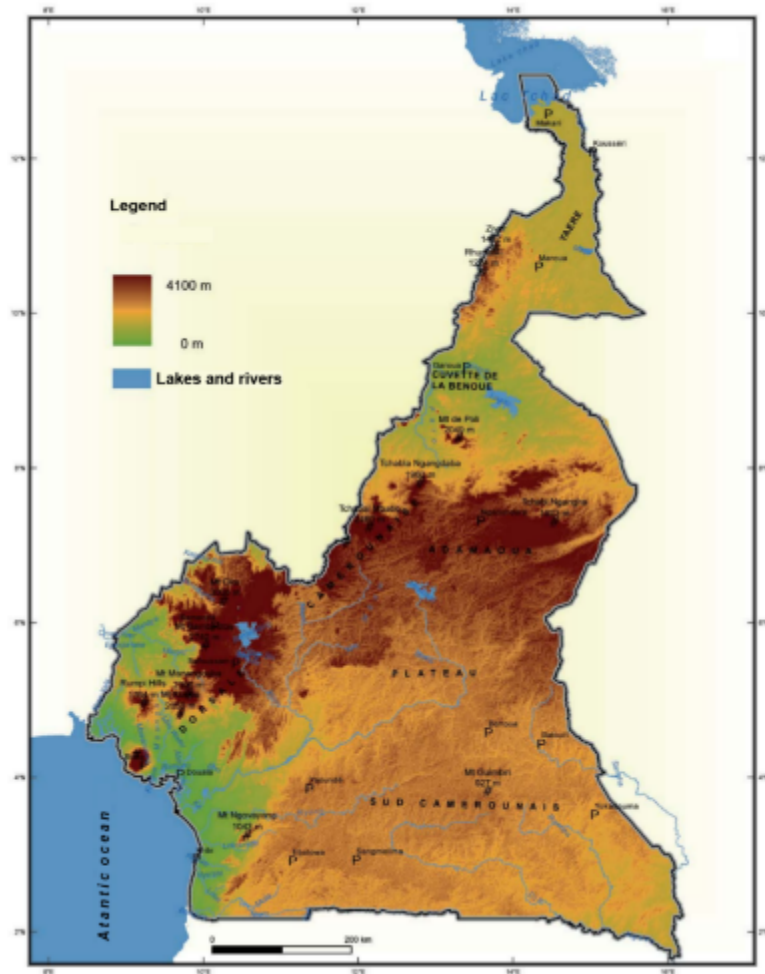


Figure I.13. Distribution of relief in Cameroon (Anonymous, 2010)

There are mountain ranges and high plateaus that stretch from Mount Cameroon to the Central African Republic over a length of about 400 km. This assembly is commonly called the Cameroonian Dorsal or the highland ridge. Altitudes peak between 2000 and 3000 m in its central part while the Bamileke Plateau in the south-west has peaks between 1200 and 1600 m. The Bamboutos Mountains culminate at 2700 m. At the southern part of the ridge, in the first escarpments of the Nkongsamba region, one first note of all some modest peaks, then the first important domes such as Mount Kupe and the Manegoumba Mountains which culminate at 2064 and 2411 m respectively. The Mbo Plain follows this system of reliefs and thus established the link with the highlands of the Bamileke country (Tchawa, 1991; Valet, 1980; Dongmo, 1981; Morin, 1981; Fotsing, 1990). The Adamawa Plateau extends the growth of highlands eastward, 150-300 km wide. It dominates the Benue basin by a series of steep ledges known as cliffs. Adamawa extends southwards by two platforms that extend on either side of the Djerem depression: the first platform has the Central African border as its axis and joins up with the Southern Cameroonian Plateau.

The second platform, which is located between the Mbam and the Djerem, has a compartmentalized relief whose altitudes are around 1530 m (Suchel, 1988). In the southern Cameroonian plateau, relief has many disparities following an east-west trajectory, with altitudes peaking at about 1585 m in the Ngoro massif to the north. To the south, the Ntem massif reaches 1400 m.

Site1: Simbock Lake (Yaoundé)

Yaounde region, which culminates at an altitude of about 750 m, is located on the western edge of the Southern Cameroonian Plateau and has the characteristics of a peneplain (Kueté, 1990) with a hummocky "half-orange" pattern of hills that are strongly undulating in detail. Southern Cameroonian plateau is a vast relief unit resulting from the morphology of the basement.

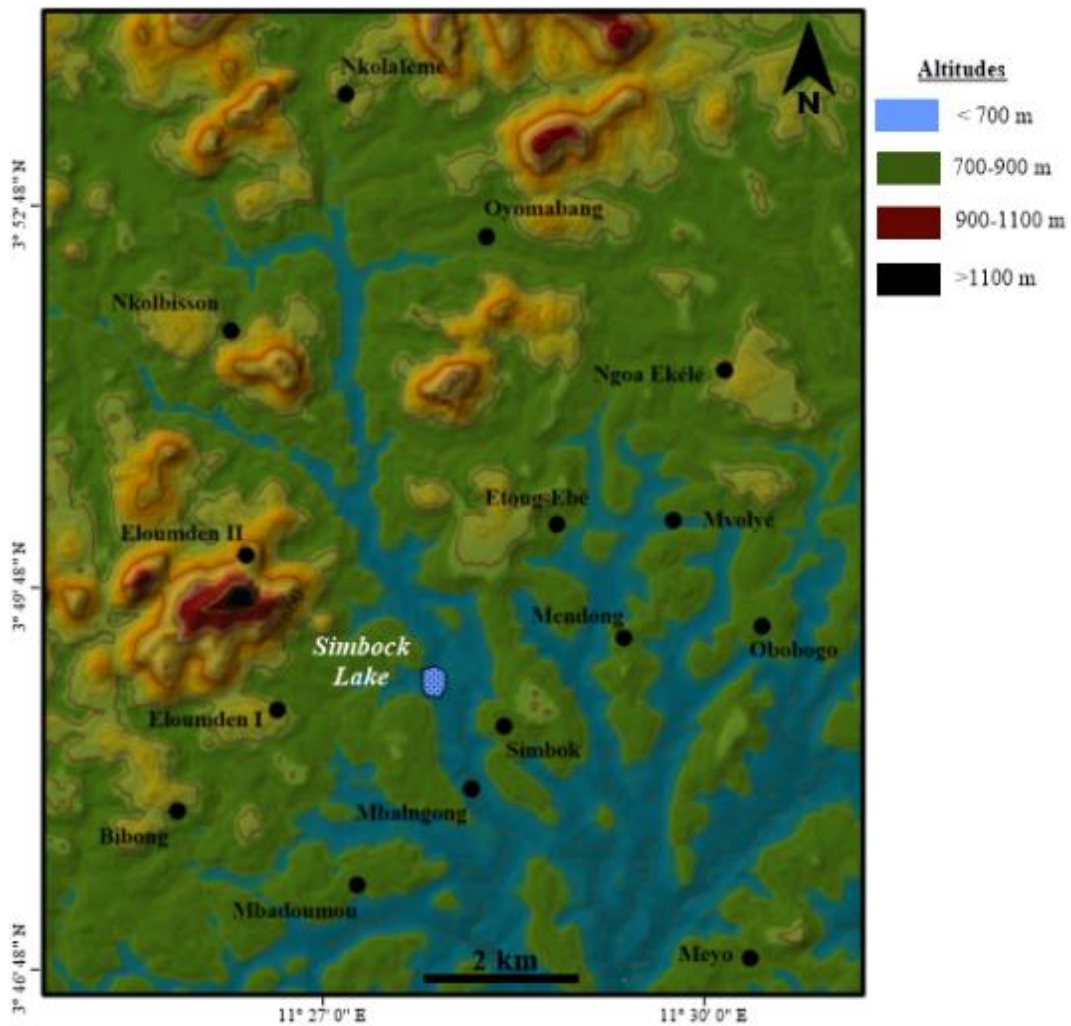


Figure I.14. Relief of the Yaoundé area

The valleys are sometimes widened into swampy basins. The monotony of this relief is broken in the south-west and on the watershed by residual mounds of hills, evidence of older flattened surfaces (Santoir and Bopda, 1995). In the studied area, four geomorphological units were distinguished (Figure I.14):

- the first unit with altitudes lower than 700 m corresponds to valleys. It occupies about 40 % of the area;
- the second unit whose altitudes are between 700 m and 900 m corresponds to the low plateaux. It occupies about 55 % of the area;
- the third unit is between 900 m and 1100 m. It represents the residual mounds that extend over about 4 % of the area;
- the fourth unit whose altitude is higher than 1100 m occupies about 1 % of the area and corresponds to mountains.

Site2: Ossa Lake (Ngaoundere)

The region is low with a lowland relief below 100 m.

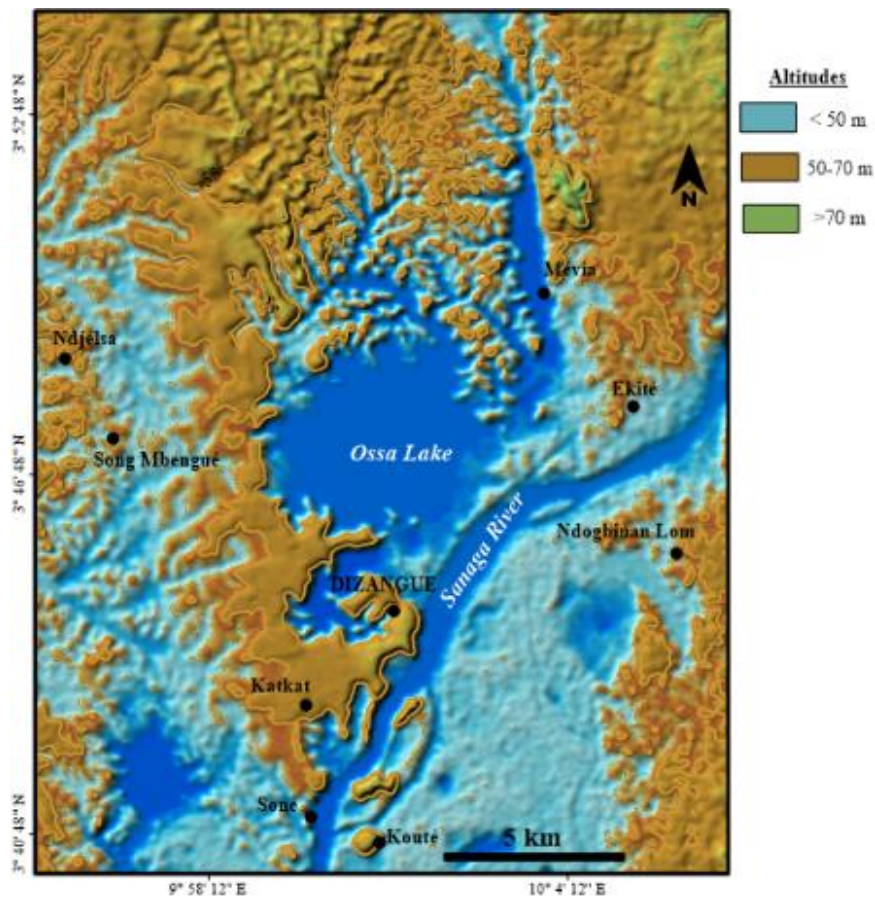


Figure I.15. Relief around Lake Ossa

The town of Dizangue called "Beach at the western part of Lake Ossa more precisely the part called Mwembe. The southern coast of the lake is indented. It is marked at the southern entrance of the town by a steep cliff with a difference of 41 m height. We surveyed 33 m along the road side of the Sanaga River, at the water catchment, pumping point and 74 m from the center of the town (Figure I.15). The banks of the lake have steep slopes, rapidly rising to maximum heights of 70/80 meters. Rock outcrops represent less than 1% of the catchment area. The lake has a digitized relief, reflecting the formation of the water body by flooding of the lower parts of the lake. A single river joins the lake with the Sanaga flowing to the south-east (Wirrmann, 1992).

Site3: Ngaoundaba Lake (Ngaoundere)

The Ngaoundere Plateau is cut by the Vina River and is dominated by granitic "inselberg" massifs consisting of phonolite and trachyte extrusions and by volcanic edifices of Neogene to subterranean age.

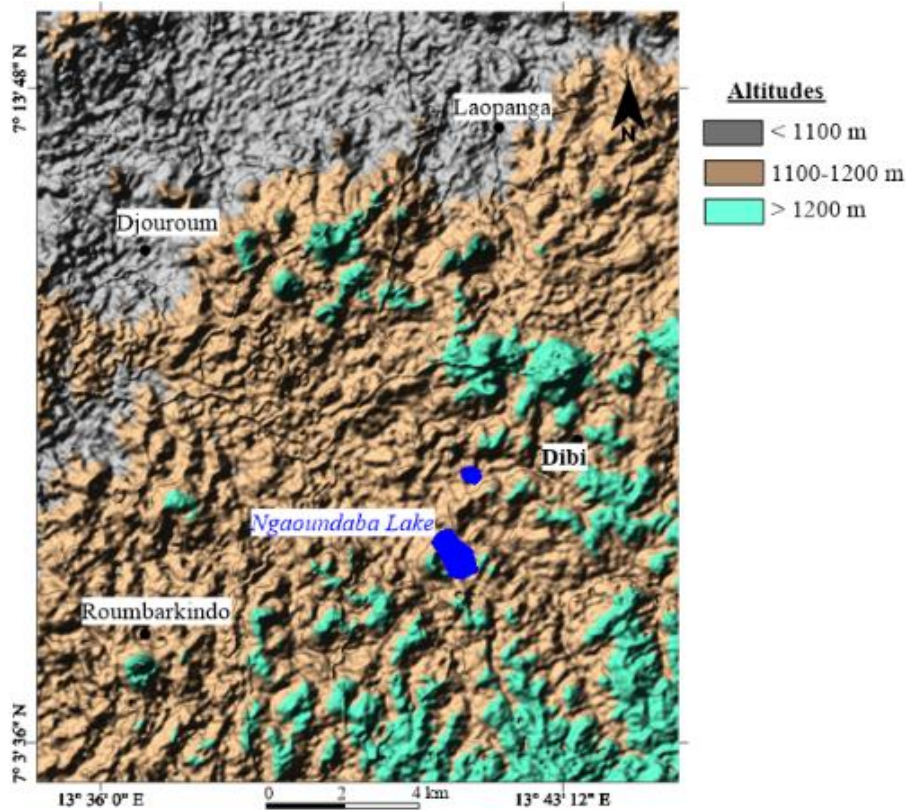


Figure I.16. Relief around Lake Ngaoundaba

The are consisting of basaltic slag cones often associated with phreatomagmatic craters explosion (Temdjim, 2005). These include Ngao Pag-Hay (altitude of 1231 m), Ngao Nday (1324 m) and Ngao Sey (1231 m) which are trachy-phonolitic massifs as well as Ngao Ndin (1237 m) which is a Strombolian cone.

The distributions of geomorphological units such as: valleys (altitude <1000 m), plateaux (1000-1200 m) and hills or summits (>1200 m) according to Eno Belinga (1984) which distinguished six main groups in the Adamawa according to altitude and clasified the volcanic district of Ngaoundere in group II, that is between 1000 and 1200 m (Figure I.16).

1.6. Soils

The diversity of soils in Cameroon is due to the great variety of source rock, topographical factors, age and the different bioclimatic environments in which they are formed. These soils have several facies related to their spatial representativeness, at the state of degradation and their use by humans. Their list is not exhaustive but, among the main soils encountered in Cameroon (Figure III.17), we can list the following:

- ferralitic soils which cover about two thirds of the country's surface area, are found at the southern of the 8th parallel (Muller, 1978; Onguene, 1993). These are red, deep, loose, clayey and porous soils that are suitable for forest-type vegetation. These soils are poor in nutrients, acidic and very vulnerable to erosion;
- hydromorphic soils are characterized by an excess of water and have a grey, discoloured horizon. They are encountered in the Lake Chad plain during the rainy season (Pias, 1956; Vernier, 1988). They contain swelling clay (verticas), but the presence of excess water is not permanent, and they turn into pseudogley soils during low-water periods. Hydromorphic soils are also found in the southern part of the country, in the mangrove areas along the seashore (hydromorphic gleyed soils);
- poorly evolved soils that develop on recently deposited materials such as wind-blown deposits from the Lake Chad cordillera or deposits of volcanic ash from the West Cameroon massifs (Martin, 1961); Vertisols that present a coherent, clayey and dark-coloured profile that crack deeply in a dry state. They are encounterd in regions with alternating wet and dry seasons such as in Northern Cameroon (Mahop et al., 1995). Their variation in water content is accompanied by seasonal swelling and shrinkage;

- andosols and eutrophic brown soils that are young and have a homogeneous profile. They are developed on basic volcanic formations, associated with crude and poorly evolved minerals. Andosols are rich in water and organic matter but are very sensitive to erosive processes. Eutrophic brown soils, on the other hand, have abundant humus and rich in mineral matter. Both soils are favourable for agriculture, but their fertility decreases with increasing leaching and induration.

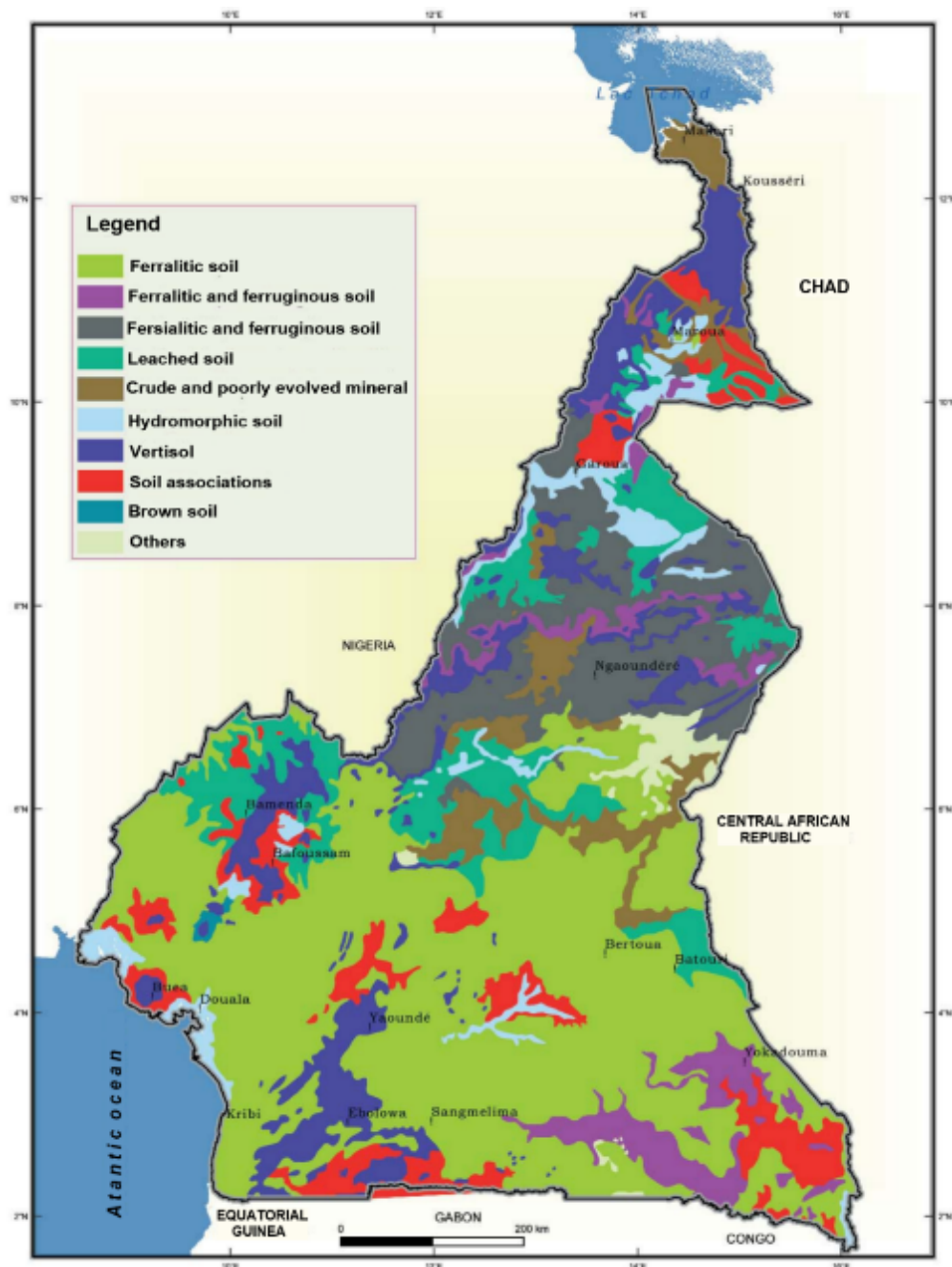


Figure I.17. Soil distributions in Cameroon (Anonymous, 2010)

Site1: Simbock Lake (Yaoundé)

The region of Yaounde and its surroundings belong to the Southern Cameroonian plateau (Yongue, 1986). This plateau has two classes of soils: ferrallitic and hydromorphic soils.

➤ Red ferrallitic soils and yellow ferrallitic soils: red ferrallitic soils have a thickness that varies between 2 and 25 metres (Ngon Ngon, 2007). In total, three (03) sets follow one another from bottom to top: an alteritic set that presents two facies: a facies with a preserved structure (isalterite) in which the structure of the parent rock can be recognised and a facies with a partially preserved structure (alloterite) in which the structure of the parent rock can be recognised in some places; a gluvial complex corresponding to ferruginous accumulations (armour, nodules); a loose clayey complex containing some rare nodules in contact with the gluvial complex (Yongue, 1986). These soils are made of materials consisting of an assemblage of clays (kaolinite), oxyhydroxides and iron oxides (goethite, hematite) and aluminium oxides (gibbsite). Yellow ferrallitic soils are located at the bottom of the slope. They are composed of quartz, kaolinite and goethite (Onguene Mala, 1993).

➤ Hydromorphic soils are found in poorly drained lowlands. These soils are characterized by the accumulation of poorly decomposed organic matter on top of a sandy and clayey set (Bekoa, 1994).

Site2: Ossa Lake (Dizangue)

Soils of the study area are yellow ferrallitic soils on sedimentary rocks (Segalen, 1994). They have a sandy to sandy-clayey texture. These soils constitute of kaolinite, quartz, gibbsite, hematite, and goethite (Segalen, 1994). In the north-eastern part of the catchment, at the east of Mevia, in addition to the constituents listed above, feldspar and micas are observed in the soils in small quantities. The soil profile presents the following succession of horizons on the Dizangue mound: a whitish alteration horizon with yellow or purplish, sandy patches in which the sedimentary structures (channels) are still preserved; a sandy yellow horizon with reddish brick armour blocks up to 6 m thick; a 3 m thick yellow horizon with layers of heterometric ferruginous nodules packed in a fine sandy to sandy-clayey soil. On some steep slopes, horizons with ferruginous nodules outcrop; a thin, sandy, yellow-brown humus horizon, surmounted by a thin litter (Kossoni, 2003).

Site3: Ngaoundaba Lake (Ngaoundere)

The soils of Ngaoundere belong to the great group of ferrallitic soils (Segalen, 1967; Muller, 1978). These soils are of two types (Segalen et al., 1967; Muller, 1978; Segalen, 1994):

- red soils formed on ancient basalts. They are very humiferous, characterized by a high clay content (40 to 60 %), a conductivity of about 10 meq, a pH of about of 5.5 and a fairly constant iron concentration of 15 to 20 %;
- brown soils, frequent on more recent basaltic rocks. They are generally very permeable, shallow, of the profile, variable texture, sometimes rich in organic matter (up to 12 %) and nitrogen. Cuirasses also plays an important role in regional pedology; their ferruginous nature is evident. The cuirass is the result of erosion and are of non-climatic origin (Bachelier and Laplante, 1953).

1.7. Geology

The geological formations encountered in Cameroon are essentially of Precambrian age (Basement Complex), resulting from the remobilisation of the Archean basement, on which the "Intermediate Series" and the "Dja Formation" are based (Bessoles, 1969). Figure I.18 shows the main geological formations in the Cameroonian territory described by Nzenti (1994), Toteu (2006), Nkoumbou et al. (2014). The Cameroonian part of the Congo Craton known as the "Ntem Complex" of Archean and Palaeoproterozoic age covers the southern part of the country. It is mainly composed of tonalites, trundjemites, granites, granulites and green rocks. The main geological formations belonging to the Pan-African Range consists of three main domains (North, Central and South) covering the rest of the country. They consist of micaschists, gneisses, migmatites and granites. The Poli and Lom groups form entities affected by a weaker metamorphism. The volcano-sedimentary deposits of Mangbei mark the end of the pan-African tectono-metamorphic evolution in Cameroon. They are part of a regional ensemblage with outcrops in the Lake Lere region near Mangbei and at Hoye near Poli.

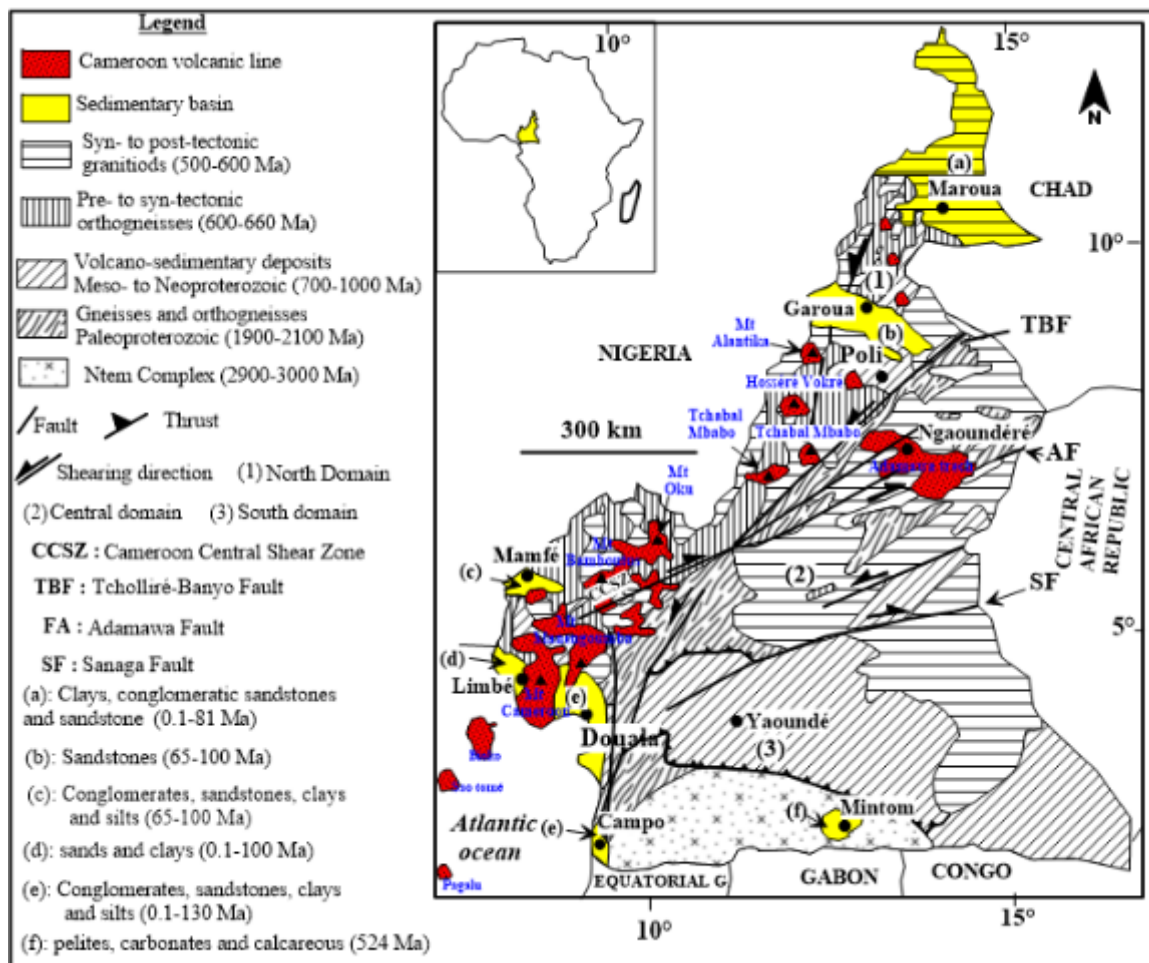


Figure I.18. Geological map of Cameroon (Nkoubou et al., 20114, modified)

Sedimentary basins form relatively small subsidence zones in the coastal region (Douala and Mamfe basins), the South (Mimtom basin), the North (Benoue basin), and Southern Chad:

- the coastal sedimentary basin located on the edge of the Gulf of Guinea corresponds to a subsiding trench formed from the Cretaceous and gradually deepening towards the ocean. The main formations are essentially black marls and clays as well as sandstones;
- the Benue basin is made up of detrital sediments of Cretaceous and Quaternary age that lie directly on the crystalline basement. The Cretaceous is represented by sandstones at the western part of Garoua, consolidated clays and sandstone limestones. The Quaternary forms terraces along the edges of the rivers and the argillaceous in the flood zones;
- the basin of the northern extreme is part of the Chadian basin. It is a spreading zone of tertiary, quaternary and current alluvial deposits. The formations are essentially sandy, clayey to sandy-clayey, sandstone and limestone. The first significant volcanic manifestations are attributed to

a period between the late Cretaceous and the Upper Eocene, giving rise to the thick formations that cover the western and Adamawaa highlands. In the south-west, these lava flows are interbedded in the Douala Basin. In relation with the western fracture, new volcanic manifestations of an acidic nature gave rise in the late Neocene, to (Manengoumba, Bamboutos, Nkogam, Mbapit, Mbam) massifs, as well as a few small massifs in the north. The only volcano still active is Mount Cameroon, whose historical eruptions are numerous and varied. Of the seven best documented eruptions of the 20th century, three occurred in the last twenty years (1982, 1999 and 2000). Despite of the various types of damages, these eruptions, through the quantities of volcanic ash and pozzolans deposited, contribute to the extraordinary fertility of the soils of the region and provide materials for civil engineering.

Site1: Simbock Lake (Yaoundé)

The Yaounde series is made up of the formations of Pan-African chain of ages 540- 600 Ma. These formations belong to the ancient metamorphic basement of the Cameroon Basement Complex (Toteu et al., 1994), consisting of paraderived and orthoderived deformations. These deformations are intrusive in paraderived formations. Paraderived metamorphites are formed of various paragneisses, micaschists and quartzites. Whereas the orthoderived formations consist of pyriclasites (pyroxene gneisses and plagioclases) with associated pyroxene and amphibole gneisses, pyroxenites and biotitites (Owona et al., 2003; Figure I.19 C). The Yaoundé series is affected by two deformation phases D1 and D2. The first phase D1, affect only paragneisses, which is marked by a compositional bedding $S_{0/1}$, a high degree of metamorphism and the beginning of partial in-situ migmatization. The second phase D2 affects orthoderived migmatitis and micaschists. It takes up the markers of the first phase in the paragneiss and this results in $S_{0/1/2}$ structures. This phase is accompanied by a partial in-situ fusion marked by the placement of mobilisats in the shear planes (Owona et al., 2003).

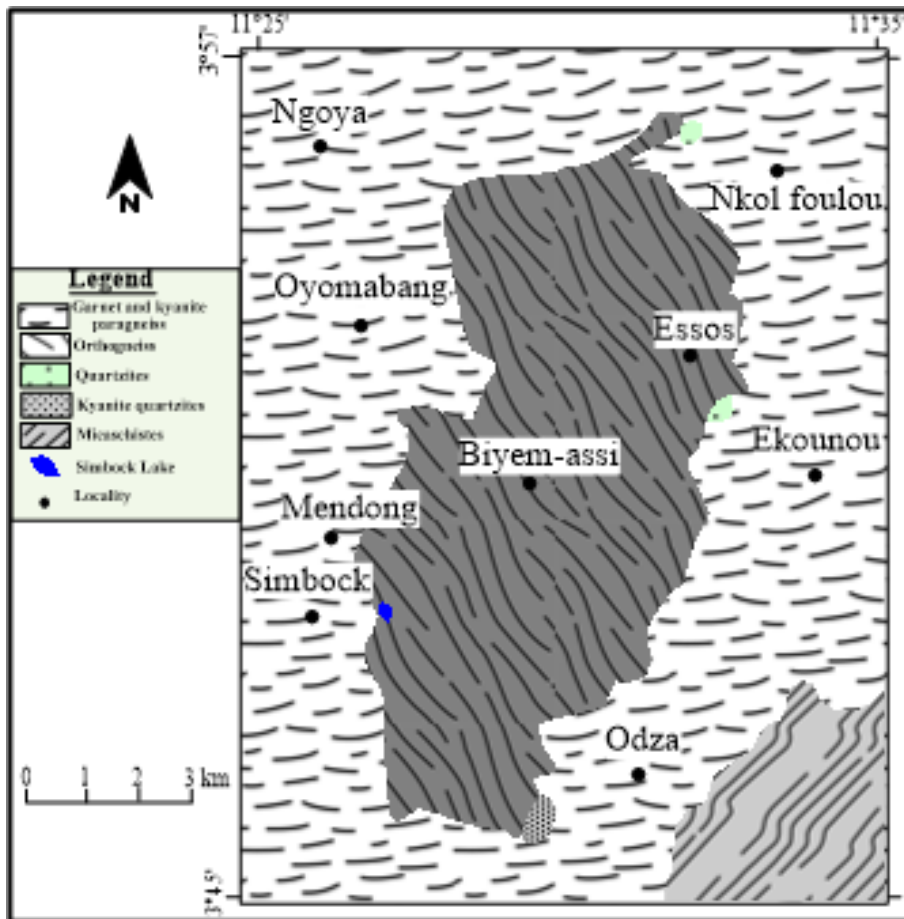


Figure I.19. Geological map of the south-western part of the Yaoundé (Owona et al., 2003)

Site2: Ossa Lake (Dizangué)

The Ossa lake system is located near the continental edge of the coastal sedimentary basin of Cameroon. This basin, bounded at its eastern edge by two major fault clusters N150-N170 E and N40-N65 E (Njiké-Ngaha, 1984), was filled by continental sediments and towards the western edge by marine sediments (Njiké-Ngaha, 1984). The sub-base of the studied area is characterized by steppe structure, over the entire continental edge of the Douala Basin and a consequence of the north-southern continental flexure. It is a very characteristic basement structure at the edge of the sedimentary basins of Africa at the south of Sahara (Reyre, 1966). This structure is thought to result from added effects of regressive erosion from the basement level and normal longitudinal faults generated by basement tectonics (Reyre, 1966; Njiké-Ngaha, 1984). The Sanaga axis would thus correspond to a major fracture at the northern edge of the Congo Craton (Figure I.20). The emplacement of Lake Ossa, unlike surrounding lakes, is likely related to the release of ancient fractures (Njiké-Ngaha, 1984) that created horsts and grabens on the basement surface. The latter would have subsided progressively according to

the overloading of Cretaceous and Tertiary sediments in the Douala Basin. The release of the faults, by accentuation of subsidence, gave rise to multitude of small fractures along which small streams of the northern part of Lake Ossa and Lake Mévia flowed. These streams, initially directed towards the axis of the Sanaga River, would have been blocked by the accumulation of the low alluvial terrace of the Sanaga River, thus allowing water to be retained and giving rise to the lake at least in its present configuration.

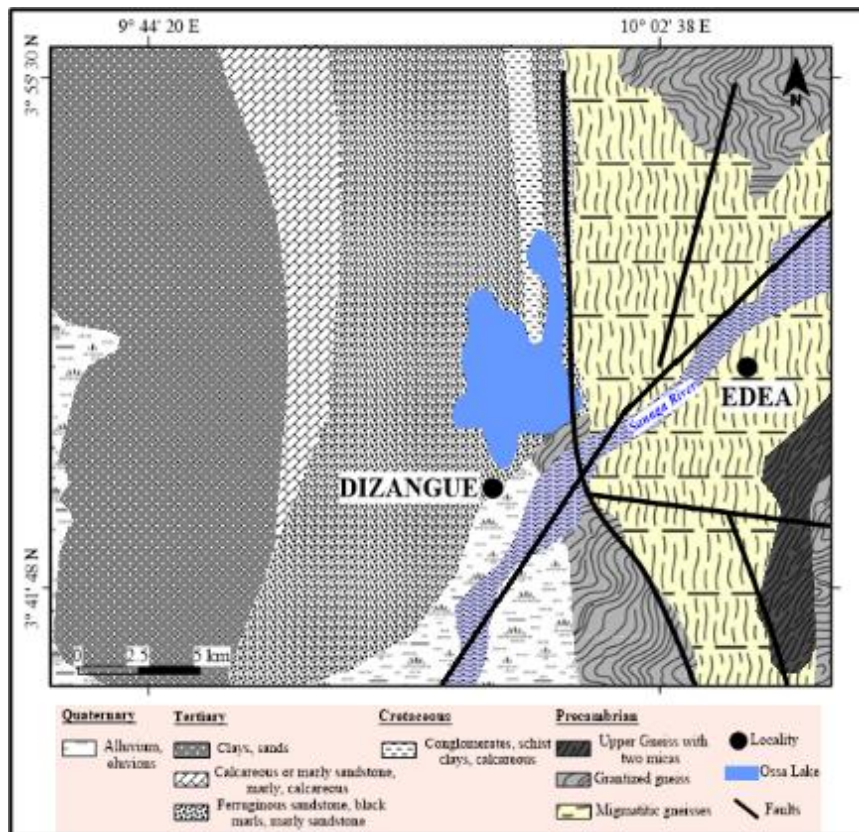


Figure I.20. Geological map of Dizangue and Lake Ossa (Dumort, 1968)

The geological formations are the sedimentary rocks characteristic of the Dizangue (terminal continental) series for the major part of the catchment. They are cross-stratified ferruginous sandstones of Paleocene age. A thin band of schistose clays with sandstone intercalations and rare calcareous episodes of Upper Cretaceous age is present in northern of Mevia (Figure I.20). Bedrock outcrops are rare in Dizangué area, due to a thick colluvial and soil cover (about 20 m) that is almost homogeneous over the entire catchment of the lake. Some few outcrops of kaolinic sandstone are found at the base of certain road trenches (Dizangue-Mariemberg road) or at the bends of major rivers, and of ferruginous and marly sandstone at the sources of streams (northern Mevia). Note that the boundary with the basement is about 2 km northeast of Lake Mevia (Kossoni, 2003).

Site3: Ngaoundaba Lake

The Adamawa plateau, with an average altitude of 1100 m are covered by huge basaltic flows accompanied by trachytes and trachyphonolites (Temdjim 1986, 2005; Ngounouno, 2000). In the centre of the plateau, swampy valleys dotted with volcanic mounts and cones are found (Figure I.21). Volcanism covers the northern, eastern and southern zones (Ngounouno, 2000). In the town of Ngaoundere, surface formations consist of the Pan-African granitogneissic basement represented by granites of Ordovician age, gneisses and Pan-African migmatites. In addition, basalts, trachytes and phonotrachytes can also be encountered (Eno Belinga, 1984; Ngounouno et al., 2000). The presence of metadiorites in the form of enclaves of the Paleoproterozoic basement is also noted (Toteu et al., 1994).

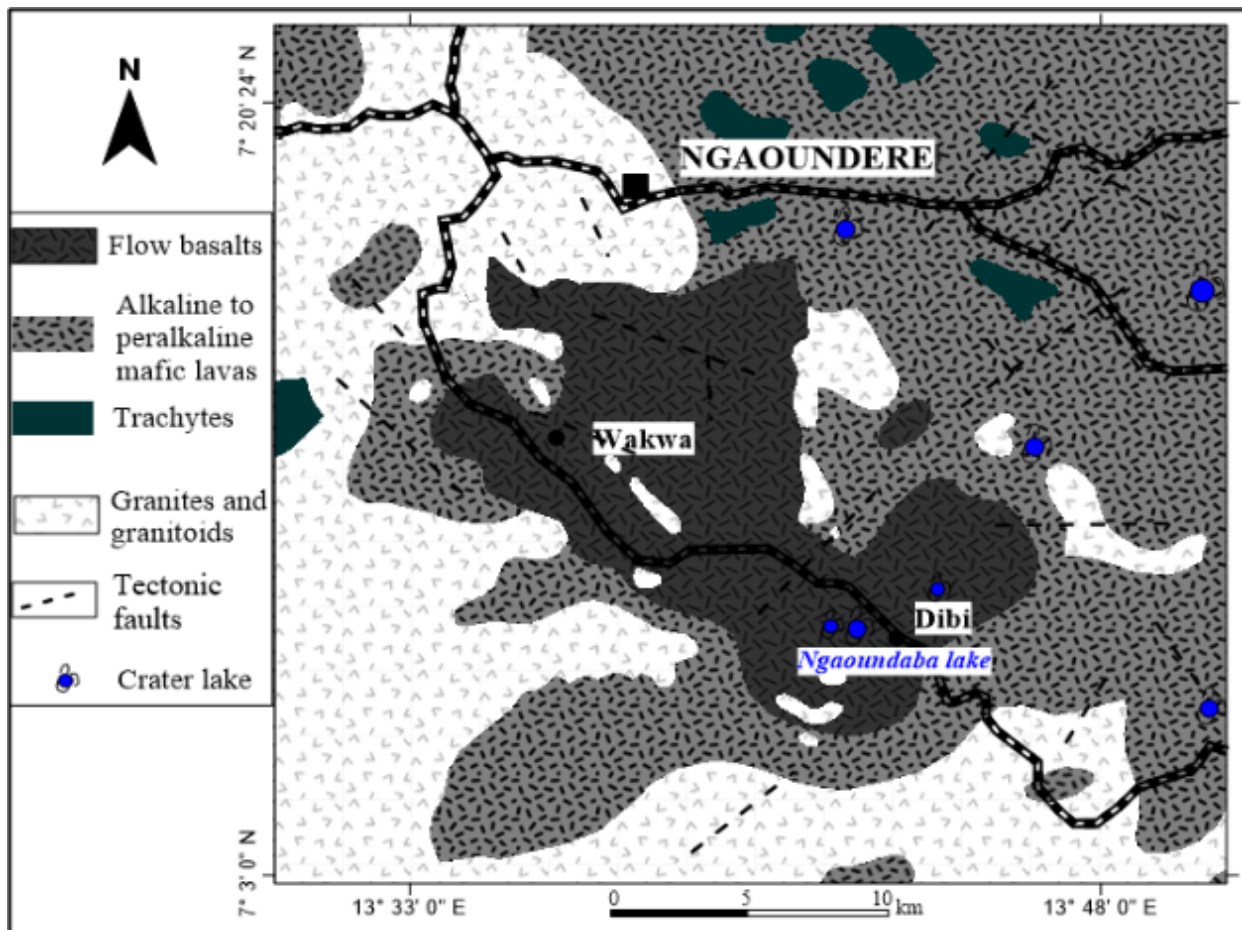


Figure I.21. Geological map of the Ngaoundaba area (Temdjim et al., 2010)

Conclusion

Cameroon is a country characterized by great climatic, phytogeographic, pedological and even geological diversity. The regions of Yaounde, Dizangue and Ngaoundere are located in the middle of the forest, coastal and plateau areas of Cameroon and are subject to various climates depending on the region. They are marked by the presence of rocks of diverse nature. The weathering of the lithological substratum leads to the formation of red or yellow ferrallitic soils, brown soils and hydromorphic soils located in a geomorphological variation ranging from mountains to plateaus through plains.



Chapter II: Literature review

*« The more knowledge there is, the less ego. The less knowledge, the more ego.
The effort to unite wisdom and power rarely and only very briefly succeeds »
-Albert Einstein-*

This chapter is firstly focused on the literature review on five aspects: the first concerns the definitions of concepts concerning sediments, lakes and pollution; the second is a synthesis of work on the sedimentology in lake and river; the third will focus on previous work on the mineralogy of lake and river sediments; the fourth concerns the current state of knowledge on the geochemical behavior of elements in lakes and river sediments; and the last is oriented towards a literature review on the pollution of lakes. Secondly, it will give a brief overview of lakes in Cameroon.

II.1. Concepts and definitions

II.1.1. Sediments

The term sediment, from the Latin *sedimentum*, is a collection of more or less coarse particles or precipitated matter that has separately undergone a certain transport; it is a loose deposit left by water, wind and other erosive agents and, according to its origin, may be continental, fluvial, glacial, lacustrine or marine. Sediments are generally referred to as sediments when the deposit is recent, especially if it is still in its environment of formation, and it is still waterlogged (Foucault and Raoult, 1995).

Sediments are defined as continental or marine deposits consisting of particles that result from the weathering or disintegration of pre-existing rocks and the precipitation of suspended solids that passes through the water column (Lesven, 2008; Ramarosan, 2008).

According to Ramade (2002), sediments are defined as a deposit of loose material of various nature of mineralogical or biogenic origin. Clastic (or mineralogical) particles originate from emergent rocks that are eroded by physical, chemical and/or biological alteration processes (Chamley, 2000). Organic (or biogenic) debris is a ubiquitous component of sediments that can lead to a black or dark grey colour of deposits (Chamley, 2000).

II.1.2. Lake sediments

Sediments deposited at the bottoms of lakes are results of all interactions within and on lake system. The spatial, lateral and vertical distribution of sediments and their physical, mineralogical and chemical nature are determined by the overall characteristics of the catchment and lake basin (Berthois, 1975; Reineck et al., 1980). The distribution of particles depends on several factors: material size, origin, hydrodynamic processes (during transport and deposition) and diagenetic processes that may influence the size of certain categories of

particles (Folk, 1980; Cojan and Renard, 1995). Indeed, sedimentation in marine environment is evaluated at 1 cm/year whereas in lake systems known as generally calm environments, it is of order of 1 mm/year (Forel, 1892).

II.1.3. Sediment granulometry

Sediments are also defined by the size of the particles they are made up of. The size of the particles depends on the presence or absence of very fine particles (diameter less than one micrometre) transported by wind and large blocks (greater than one metre in size) carried by glaciers. Sediments are classified according to various particle size scales (Table II.1).

II.1.4. Origin of sediments

Particles that make up sediment vary in size and consist of organic and inorganic compounds from four distinct sources (Lin et al., 2001):

- a terrigenous source, meaning that particles come from the erosion of the surface land. This source is enriched by various inputs such as aeolian, volcanic and glacial inputs, without forgetting fluvial inputs and/or runoff, which alone constitute the most important cumulative input. In the case of marine sediments, the contribution from coastal erosion itself must be taken into consideration;
- an endogenous source, referring to particles that come from the sedimentation basin, such as macrophyte debris (aquatic plants, microphytes) or shell fragments of organisms;
- a neoformation-related source, corresponding to alteration, transfer and precipitation phenomena that may occur in the sedimentation basin or within the sediment during diagenesis;
- an anthropogenic source that can be ex-situ and in-situ. In the first case, it includes all agricultural, industrial and domestic discharges that end up in river inputs. This fraction is rich in organic matter, nutrients and micropollutants. It can also contribute to suspended materials. In the second case, it encompasses all human and industrial port activities (loading of goods, fishing, fueling, maintenance of navigation equipment). Generally, this source is heavily contaminated, leading to an increase in sedimentation rate.

II.1.5. Sedimentation and water decontamination

Sedimentation in aquatic environments is defined as the process of depositing sediment at the bottom of water. Heavy metals have a strong affinity for suspended solids (SS) transported by water bodies. Sedimentation therefore appears to be a phenomenon that favours

the decontamination of aquatic ecosystems. Indeed, it appears that the half-life of lead in sediments is 1700 years as compared to only 25 days in the water column (Ramade, 2005).

Tableau II.1. Classifications and particle size scales (Wentworth, 1922)

Phi	PHI - mm CONVERSION $\phi = \log_2 (d \text{ in mm})$ $1 \mu\text{m} = 0.001 \text{ mm}$		Fractional mm size and Decimal inches	SIZE TERMS (after Wentworth, 1922)		SIEVE SIZES		Intermediate diameters of natural grains equivalent to sieve size	Number of grains per mg		Settling Velocity (Quartz, 20°C)		Threshold Velocity for traction cm/sec		
	mm	mm		ASTM No. (U.S. Standard)	Tyler Mesh No.	Quartz spheres	Natural sand		Spheres (Gibbs, 1971) cm/sec	Crushed	(Reyn., 1949)	(modified from Hjulstrom, 1939)			
-8	256	10.1"		BOULDERS ($> -3\phi$)											
-7	128	5.04"			COBBLES										
-6	64.0	2.52"		PEBBLES		2 1/2"	2"								
-5	32.0	1.26"			very coarse	1 1/2"	1 1/2"								
-4	16.0	0.63"			coarse	3/4"	.742"								
-3	8.00	0.32"			medium	5/8"	.525"								
-2	4.00	0.16"			fine	3/8"	.371"								
-1	2.00	0.08"			Granules	5/16"	.315"								
0	1.00	1			very coarse	4	4								
1	.500	1/2			coarse	5	5	1.2	.72	.5					
2	.250	1/4			medium	8	8	.86	2.0	1.5					
3	.125	1/8			fine	10	10	.59	5.6	4.5					
4	.062	1/16		very fine	12	12	.42	15	13						
5	.031	1/32		SAND	14	14	.30	43	35						
6	.016	1/64			coarse	16	16	.215	120	91					
7	.008	1/128			medium	20	20	.155	350	240					
8	.004	1/256			fine	25	25	.115	1000	580					
9	.002	1/512		very fine	30	30	.080	2900	1700						
10	.001	1/1024		SILT	35	35									
					coarse	40	40								
				medium	45	45									
				fine	50	50									
				very fine	60	60									
				CLAY	70	70									
					Clay/Silt boundary for mineral analysis	80	80								

Notes:
 Note: Some sieve openings differ slightly from phi mm scale
 Note: Sieve openings differ by as much as 2% from phi mm scale
 Note: Applies to subangular to subrounded quartz sand (in mm)
 Note: Applies to subangular to subrounded quartz sand
 Stokes Law (R = 6r²v)

Note: The relation between the beginning of traction transport and the velocity depends on the height above the bottom that the velocity is measured, and on other factors.

However, heavy metals remain trapped in sediments, if it is deeply buried enough to be protected from physico-chemical exchange phenomena at the water-sediment interface and from resuspension processes leading to its release into aquatic environment (Ramade, 2002).

In any case, this sediment-heavy metal affinity is at the origin of a concentration phenomenon and storage of pollutants in recent deposits during the process of sedimentation. The percentage of metals in some phases (sediment) represents 90 % of the metals contained in aquatic systems (Calmano et al., 1993).

II.1.6. Impact of lake sediments in pollution

Because of its environmental impact, the study of heavy metal pollution in the lake environment mobilized researchers for several decades. Sediments, which are the repositories of heavy metals (Mercury, Lead, Cadmium and other toxic chemicals), form an integral part in the cycle of these elements. Heavy metal content in sediments vary in the same direction as those in the source and reservoir bedrock (Lisk, 1972). These contents also depend on the influence of several processes involved in diagenesis of sediments. Consequently, the distribution, solubility and movement of these elements remain related to the physico-chemical properties of the sediments (Korte et al., 1976). In aquatic systems, sediments are studied by their role as an indicator of environmental contamination because of their ability to bind pollutants. According to Calmano et al. (1994), more than 90% of the heavy metals released in these ecosystems are trapped in sediment matrix. If these sediments can be considered as traps for trace metal elements (TMEs), they also represent a potential source of pollution.

II.1.7. Lakes

Lakes can be considered as the most attractive and expressive features of a landscape; they are important carbon sinks. Sediments in the lake provide a history of the conditions of local capture environments surrounding the lakes (Lone et al., 2017). The main concentrations and trace elements of terrigenous sediments are considered a sensitive tool for studying the alteration state of source rocks, provenance, and for understanding the redox state in the depositional environment, thus sediments composition is controlled by the parental rocks, climate and tectonic factors of the source region (Armstrong-Altrin et al., 2004; Mortazavi et al., 2014; Madhavaraju, 2015; Yu et al., 2016). A lake is a large body of freshwater on land, consisting of rivers and other water courses that feed or drain the lake. Although by some dimensions, some salty water lakes are considered as inland seas, lakes are inland and are not part of the ocean; therefore, are distinct from lagoons, and are larger and deeper than ponds, while remaining a waterbody by definition.

Lakes can be distinguished from a river or stream by the movement, flow of water: if streams are lotic systems, lakes, like ponds, are lentic systems. However, most lakes are fed and drained by rivers and streams.

II.1.8. Origin and typology of lakes

Origin of a lake can be: natural, its origin results from processes that shape reliefs (volcanism, glaciation); artificial, totally anthropogenic, these lakes result from extractive activities (gravel pits); anthropogenic, these lakes are created on a river and correspond essentially to dam lakes or reservoirs. Homogeneous zones from the point of view of geology, relief and climate, in fact hydro-eco-regions (HEr) constitute one of the main criteria used in the typology and delimitation of rivers and lakes. Three types of shape (Figure II.1) specify the overall configuration of the water body, namely:

- “L” shape if they are shallow lakes, with a largely predominantly littoral zone.
- “P” shape for deep lakes, with a reduced littoral zone.
- “LP” shape for lakes with both deep and extensive littoral zones, where the basin may be symmetrical or asymmetrical.

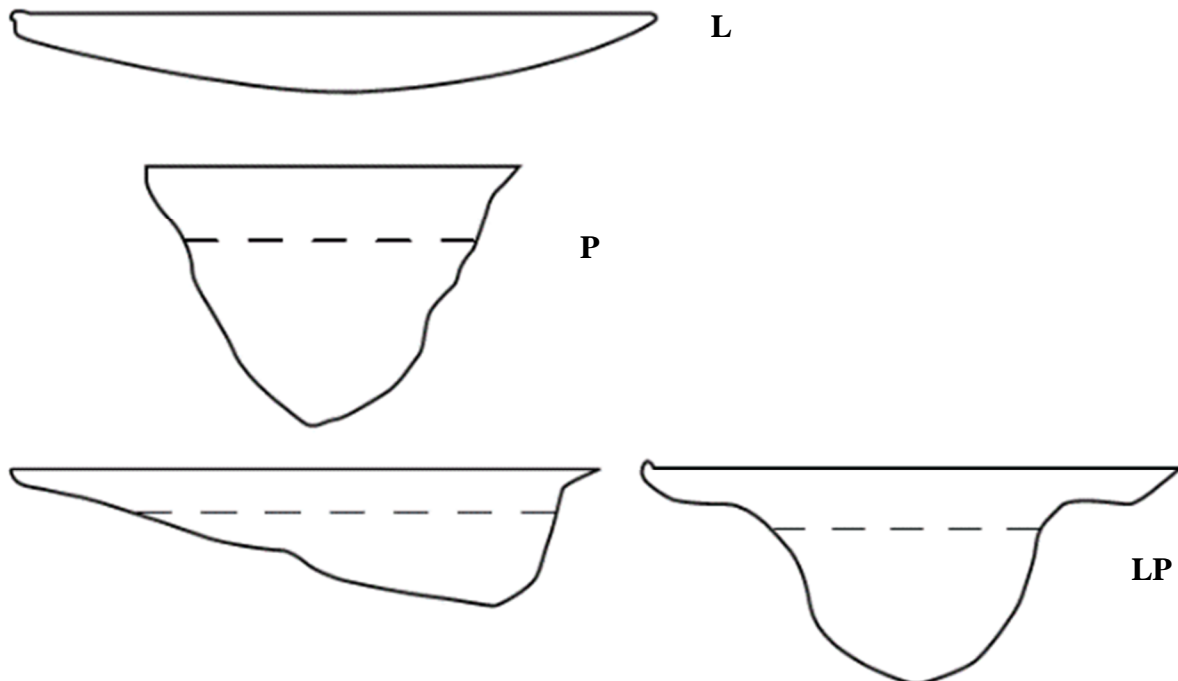


Figure II.1. Different shapes of lakes

The intersection of all these criteria (HEr, shape, origin) determines the typology of the lake.

II.1.9. Evolution of a lake

A lake generally has three stages (Lisk, 1972):

- an oligotrophic stage: this is the "young" stage of the lake. It's pure (weakly mineralized) and clear waters, which are not very nourishing, contain a small number of plant and animal species that are essentially represented by plankton with a low concentration of organic matter.
- a mesotrophic stage: over time, waters of the lake receive additions of organic and mineral matter. Zooplankton and phytoplankton species develop and make it possible to feed larger organisms. Their corpses accumulate at the bottom, decomposed by bacteria, provide mineral matter which, recycled in the aquatic environment, contributes in water enrichment. This bacterial activity consumes oxygen and thus depletes the deep layers of the lake;
- an eutrophic stage: enrichment in organic matter continues, and because of the increasing of oxygen deficit, mineralization becomes slower; the lake gradually closes. Its shallow shores are invaded by vegetation, and after a more or less long period of time, it eventually fills up. This natural phenomenon, known as eutrophication, is often accelerated by artificial inputs of nitrates and phosphates that stimulate plant development (for example, even if these drifts are diminishing: leaching of fertilizers used in agriculture, industrial and urban wastewater discharges, etc.).

This evolutionary cycle is found in a pond; it is clearly accelerated (a few decades) compared to the duration of that of a lake. This cycle, involving nitrogen, phosphorus, carbon and oxygen, in three stages, is finally found in aquariums and the low volume makes the nitrogen cycle very fast (Figure II.2).

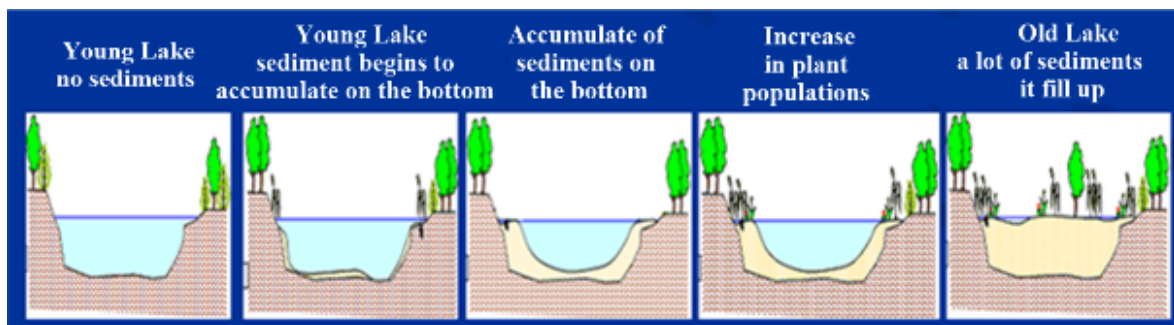


Figure II.2. Evolution of a lake

II.1.10. Some methodologies of lake sediment sampling

Lake sediment sampling is done at several scales and depends on what is being sought. Thus, it can be done on the water, on human beings of the environment and on sediments themselves. Sampling can be done at depth or on the surface according to the discipline and the study carried out.

Sampling can be done using (Figure II.3):

- a stainless steel corer for superficial sediments (1);
- a Vertical Polycarbonate WaterMark Water Bottle for water sampling (2);
- a manual "Beaker" corer for sampling undisturbed sediments (3);
- sediment skips from vanveen, ekman, ponar, boxcorer, ... (4);
- a BOTTOM/UWITEC percussion corer designed for use in subglacial shelf settings (5);
- a gravity corer designed to collect surface sediment cores in subglacial shelf settings (6);
- a hand auger for taking edge sediment samples (7);
- a sand shovel: this is a shovel made of stainless steel or ordinary unpainted steel, also known as a mason's shovel;
- a drawer shovel: telescopic system with a 50 cm long parallelepiped shovel with a sliding lid and a check valve at the base. It also bears the trade name 'Vrijwit'. It allows samples to be taken from thicker layers of sediment or from the banks or from a bridge;
- a Peat Sampler (8);
- a Peterson mud sampler (XDB0201) (9);
- a Mackereth compressed air corer (10);
- a vibrocore system (11) ...

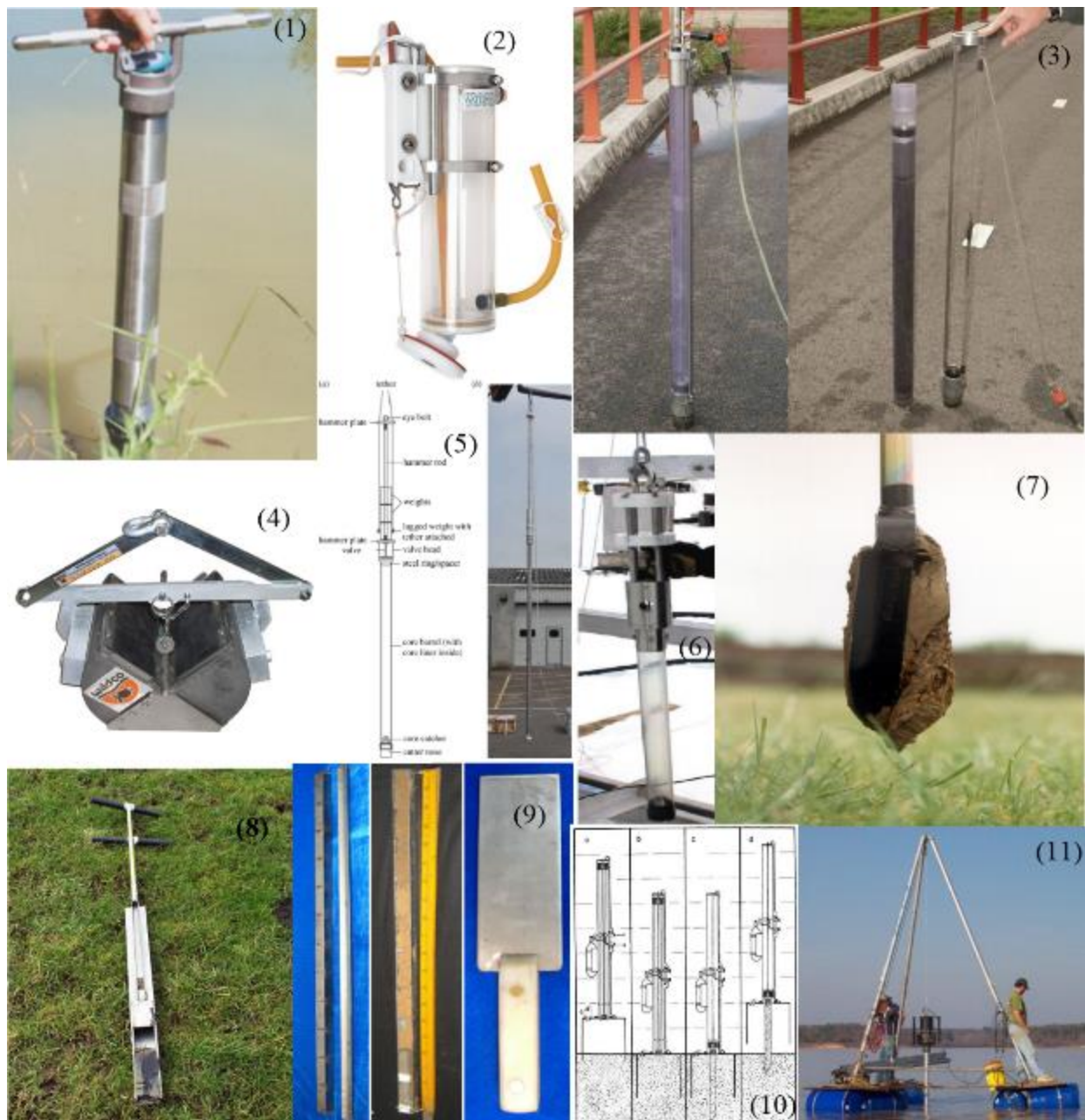


Figure II.3. Some core drills

II.1.11. Pollution

An aquatic environment is said to be polluted when its equilibrium is permanently altered by the input of excessive quantities of toxic substances from natural or anthropogenic origin. In an aquatic environment, we cannot talk of water pollution without sediment pollution. Sediments often constitute a reservoir of pollutants, particularly trace metal elements (TMEs), and subsequently become a potential source of contamination for water. There are multiple sources of pollution which can be classified into two major categories:

- Anthropogenic pollution

The sources of this pollution are multiple: combustion, industry, waste storage and incineration, agriculture, livestock.

- Natural pollution

Natural pollution is caused by various agents:

- **physical agents:** includes insoluble inert matter of any size that can remain suspended in water. They have no chemical or biological activity. Whether sand, silt or clay, these materials are largely the result of erosion. Rain, snow and ice cause compact rocks, loose deposits or soils to disintegrate.
- **organic chemicals:** runoff from areas with vegetative cover carries all kinds of organic matter into streams and lakes. These organic materials often come from the breakdown of plant matter. This colouring organic pollution often results in the appearance of acidic macromolecules such as humic or fulvic acid, leading to a significant decrease in pH.
- **inorganic chemical agents:** inorganic chemical pollutants appear in water when soil and geological formations are leached by precipitation. This leaching causes a solubilisation of salts that constitute the lithosphere and the presence of toxic ions in water drainage. The geological nature of the soil conditions and the types of ions. The quantity and quality of precipitation determine the intensity of this phenomenon. Trace metallic elements are the most common inorganic pollutants found in aquatic environments.
- **biological agents:** water courses contain a multitude of organisms of all sizes forming specific food chains. The natural contribution of organic or inorganic elements can modify these balance temporarily or permanently by promoting or inhibiting the growth of certain organisms.

II.1.12. Characteristic parameters of pollution

A wide variety of water pollution indicator parameters exist (physical, chemical or biological). However, some analyses are conducted on both water and sediments (Ineris, 2006). Many parameters characterize pollution: Suspended solids (SS); 5-day biochemical oxygen demand (BOD5); chemical oxygen demand (COD); pH; temperature; redox potential; organic matter; residual moisture; pollution load index; enrichment factor (EF) ; geo-accumulation index; definition and calculation of metal flux; geochemical modeling; mineralogical

characterization by X-ray diffraction; particle size by laser diffraction; determination of percentage of total carbon and sulphur; measurement of electrical conductivity; etc.

II.2. Previous work on sedimentological characterization of lake sediments

The deposits of Bilanko wood depression in Congo are made up of a succession of clays of various colours, surmounted by sands. Numerous plant fragments of centimetric size are present in variable quantity according to the levels. Granulometric analysis showed the presence of few grains of shiny, limpid sand, showing no recent impact marks. Radiocarbon dating was carried out on a piece of wood located between 48 and 54 cm depth, the age obtained is 10,850 \pm 200 years B.P. (Elenga and Vincens, 1990).

Sediments of Lake Tanganyika in Eastern Africa have a granulometry that varies from muds to sands with a silty to clayey texture of dark olive-grey colour. These sediments are estimated to be approximately 3,700-1,200 *cal.*, yr. BP based on ^{14}C dating (Cohen et al., 2006). According to Anne Beaudoin (2014), Nettilling Lake sediments in Canada are composed mainly of fine silts and sands (with sizes ranging from 4 to 125 μm). Colours are dark yellowish brown (10YR 4/6) and dark grey (10YR 4/1). Based on ^{14}C dating, these sediments are dated to be approximately 11,000 years B.P.

Lake Caço in north-eastern Brazil, is made up of a sandy substratum which dates to the Pleistocene. These sediments consist of fine-grained sands and silts and organic matter. Colours ranging from greenish-brown to black, dated from radiocarbon 5610 to 20000 years B.P. (Jacob, 2003).

In two northern alpine lakes, the facies show good to medium sorting and a high average grain size (50-140 μm), which reflects high energy transport conditions and thus a high current, the particles vary from coarse silts to "true clays". Thin section shows that the sediments are mainly composed of detrital particles: clastic particles and organic particles mainly observed in coarse sediment laminae. Organic particles corresponding to the remains of terrestrial vegetation existing between the silt-clay laminae and the coarse silt and sand laminae dated between 8890 *cal.*, BP (\pm 120) and attests to their presence at the site since this period (Giguët-Covex, 2010).

In the Sahel of Tunisia, description of lithofacies based on the lithological nature, granulometry and variation of colour shows that the cores are composed of three types of

detrital facies: a fine to very fine sandy facies, mixed facies: sandy-clayey and clayey-sandy and fine facies: clayey-silty to clayey. The most complete sequences begin at the base with clays followed by a sandy-clay or sandy-clayey horizon; and ends with sands. These sediments are rich in organic matter of terrestrial origin (Raja Chairi, 2005).

Potrok Aike lagoon in Portugal consists of three facies: fine sands, coarse silts and fine silts. Thus, a multitude of pumice fragments, called micropumices and originating from the tephra of the catchment, enriched the detrital material since the last ice age. These materials are enriched in TOC with values between 1 and 10% which could reflect the redox conditions of the environment (Jouve et al., 2015).

Lakeshore soils are generally sandy, in Cameroon according to Ngos et al. (2003) The soils of the lakeshore of Assom, Bousemi and Ngwana are sandy in nature, probably resulting from repeated flooding by the surrounding rivers. Within the lake, the sediments are generally sandy-clayey. Similarly, the sediments of Ngaoundere's Mbalang and Tizon lakes are mud to conglomerate, ranging from fine to coarse sands with silty to clayey texture with high concentrations of organic matter, and at some sandy levels from grey to dark grey and yellowish in some places. Radiocarbon dating revealed that Lake Mbalang has a sedimentation rate of 0.93 mm/yr and Tizon Lake has a sedimentation rate of 1.58 mm/yr. These sediments are dated at 6400 cal years BP and TOC values increase from the bottom to the top (Ngos et al., 2005).

In Lake Ossa in Cameroon, Kossoni (2003) highlighted two particle size fractions: the sandy fraction ($> 50 \mu\text{m}$) and the pelitic fraction ($50 \mu\text{m}$). In some necessary cases, a second sand fraction ($> 315 \mu\text{m}$) was evaluated. A highly compacted grey clay level has the characteristics of a hydromorphic gley type soil, dark grey (5Y 4/1) colour with brown siderite granules. Then, a muddy black organic-clay level of very dark grey (10 YR 3/1) colour up to 170 cm, with vivianite aggregates observed. From 170 cm, sediments show a very clear change: between 170 and 101 cm, very light medium to coarse sands are observed, the colour are from very dark grey (5Y 3/1) to olive grey (5Y 5/2) with clayey footsteps between 140 and 130 cm, then between 100 and 95 cm. upper, from 100 to 20 cm, sands are less and less coarse towards the top, they are very dark greyish brown in colour (2.5 Y 3/2). The top of the core (0-20 cm) has a fine, dark, clayey-organic muddy level of dark olive grey (5Y 3/2) colour. These sediments are radiocarbon dated to 9210 years cal., BP.

The Lake Fonjak depositional sequence in the North Cameroon displays eight lithofacies made up of : light greenish grey clayey mud ; black clayey mud mostly composed

of volcanic ash ; light grey silty clayey mud ; dark grey sandy layer with coarse rounded fragments of volcanic rocks ; light grey silty mud ; dark grey silty mud ; light grey silty mud ; dark grey silty mud with few rootlets, and an herbaceous peat. In this depositional sequence, organic matter contents range from 9 to 59 %. A correlation between the age-depth model and lithofacies of this depositional sequence suggests Late Pleistocene sediments at the base and Late Holocene sediments at the top. Radiocarbon dating of these lacustrine sediments were deposited since 13,339 cal yr BP (N'nanga, 2019).

II.3. Previous work on the mineralogical characterization of sediments

Chemical elements in alluvial sediments depend on their grain size and mineralogical composition (Sawyer, 1986; Kasanzu et al., 2008; Bhuiyan et al., 2011). Similarly, the classification of alluvial sediments determines the distribution of minerals in different fractions that depend on the composition and degree of alteration of the source rock (Hoffmann 2005; Das et al., 2006; Marques et al., 2011). Similarly, Ndjigui et al. (2014) showed that most of the minerals in the Ngaye River reveal the presence of smectites, kaolinite, quartz, illite, small proportion of rutile, amphibole, olivine, pyroxene, feldspar, ilmenite, goethite and hematite. Sandy fractions having large proportions of quartz and most abundant minerals in the fine fractions (silts and clays) being kaolinite and smectites. Similarly, Fadil-Djenabou et al. (2015) showed that the mineral composition of the sediments of the Ngaye River consists of quartz, kaolinite, muscovite-illite and smectites associated with goethite, feldspar, amphibole and anatase.

According to Young et al. (2012), the composition of active sediments in a stream is influenced by the source, lithology, climate, weathering, hydraulics and transport of these sediments. According to Jacob (2003), X-ray diffractometry of Lake Caço sediments reveals a mineralogy consisting of quartz, amorphous silica, siderite and goethite.

The mineralogy of two northern alpine lakes consists of vivianite, calcite, quartz, iron oxides such as magnetite and hematite, and clay minerals (Giguet-Covex, 2010). According to the work of Lambert (1997) in Lake Neuchâtel (Switzerland), most of the material harvested consists of carbonates, with calcite contents ranging from 50 to 70 %. Other main minerals present are phyllosilicates, quartz, potassium feldspar, plagioclases, ankerite and dolomite.

Phyllites are represented by three minerals (kaolinite, illite and smectites) characteristic of deposits of the region Sahel in Tunisia (Raja Chairi, 2005). In addition, they are also made up of non-clayey minerals such as: quartz, calcite and evaporites (gypsum and halite).

The mineralogy of sediments of the Potrok Aike lagoon in Portugal was determined by X-ray diffractometry and SEM-EDS (Scanning Electron Microscope-Energy Dispersive X-ray Spectroscopy) analysis by Nuttin et al., 2013 and Jouve et al., 2012. According to the first, these sediments consist of: quartz, calcite, feldspar, smectite-chlorite, kaolinite-chlorite, mica, pyroxene and amphibole. According to the second, they consist of carbonates (calcite and monohydrocalcite); silicates (quartz, anorthite, sodium-calcite feldspar and muscovite); and clayey minerals (clinochlore of the chlorite group).

Mineralogical analysis of sediments of Dojran Lake in Macedonia revealed that the mineralogy of the lake's surface and base sediments is closely related to the predominant metamorphic, volcanic and igneous rocks of the Dojran region. The mineralogical assemblage of the lake sediments is mainly composed of quartz, feldspar, clay minerals, calcite and micas, as well as small amounts of augite and hornblende (Šmuc et al., 2015).

The mineralogical assemblage of the orthogneiss of the SW of Yaounde is composed of kaolinite, quartz, goethite, anatase and incidentally hematite (Ndjigui et al., 2013). Similarly, lateritic clays and hydromorphic clay materials in the region of Yaounde are essentially kaolinitic with the presence of quartz, goethite, hematite and incidentally rutile, anatase and halloysite (Ngon Ngon et al., 2009).

According to the XRD, the mineralogy of sediments of Lake Mbalang consists of clayey minerals and volcanic elements. This mineralogy consists mainly of quartz, feldspar, kaolinite and some traces of gibbsite. In Tizon Lake, volcanic minerals such as pyroxenes and olivine are also present (Ngos et al., 2005). Similarly, sediments of Lake Ossa (Kossoni, 2003) are composed of quartz, kaolinite, gibbsite, amorphous silica and feldspar, muscovite, vivianite, siderite, hornblende, augite and illite. The Holocene sediments of the Lake Fonjak (N'anga, 2019) exhibit in XRD data various minerals assemblages with relative contents varying from 15 to 42 % for quartz ; 19–37 % for kaolinite ; 12–37 % for micas ; 5–18 % for serpentine ; 1–9 % for feldspars ; 5–7 % for gibbsite and 11 % for olivine. As far as detrital minerals are concerned, they are : quartz, orthoclase, siderite, vivianite, hornblende, plagioclase and opaque minerals.

II.4. Previous work on the geochemical characterization of sediments

The geochemistry of clastic sediment deposits provides information on the source rock that feeds them (McLennan et al., 1993). Similarly, composition of the source rock, grain size and sediment geochemistry are dependent on alteration and diagenesis processes (Sawyer, 1986).

In two northern alpine lakes, the fine sediment laminae are enriched in aluminum while silicon and calcium are more concentrated in the laminae containing coarser particles. Sediments appeared to be rich in silica (~68 wt. %) and aluminum (~12 wt. %) and poor in calcium (~4 wt. %), alkaline and alkaline earth metals, as well as phosphorus and titanium oxides (Giguet-Covex, 2010). In the sediments of the Potrok Aike lagoon in Portugal (Jouve et al., 2012), calcium, Ti, Mn, Fe and Si were mainly detected. The values of Ti and Fe are low, i.e. 1.21- 3.71 wt. % Fe and 0.13-0.42 wt. % Ti, which is generally used as an indicator of detrital input as it reflects a river feeding and by extension allows the determination of paleohydrological variations. It also permits the determination of physical erosion of surrounding rocks (Cohen, 2003). The Dojran Lake in Macedonia, more than 65 % of major elements are in almost all samples would represent Si-Al-Fe components, reflecting a relatively high proportion of quartz, feldspar, clayey minerals and micas present in the surface sediments of the lakes. CIA values of approximately 67 % in the samples suggest that the lake's catchment is undergoing a moderate degree of alteration (Šmuc et al., 2015).

Sediments from the Ngaye River have moderate to high SiO₂ content (~38.06-91.72 wt. %), with an average of ~64.89 wt. % SiO₂. The proportions of Al₂O₃ increase while those of SiO₂ decrease, sandy fraction being more siliceous than the source rock while fine-grained sediments are more aluminous. Silts and clays are enriched in Ti and P, but the proportions of Ti being high in fine-grained sands indicates the presence of rutile and/or ilmenite (Ndjigui et al., 2014). Similarly, materials from the SW of Yaoundé has a high composition of Al₂O₃ (22.48 wt. %) and TiO₂ (1.36 wt. %) relative to orthogneiss. The values of Fe₂O₃, MnO, MgO, CaO, Na₂O and K₂O decrease considerably from the source rock to the dark materials (Ndjigui et al., 2013). The work carried out by Ngon Ngon (2007) shows that Yaounde migmatic gneisses are characterised by high SiO₂ contents (60.27 - 62.99 wt. %). The contents of Al₂O₃ (15.07 - 16.20 wt. %) and Fe₂O₃ (6.84 - 9.34 wt. %) are low while the contents of MnO, MgO, CaO, Na₂O, K₂O, TiO₂ and P₂O₅ are very low (less than 3 wt. %). According to Ndjigui et al. (2013), trace elements of the locality of Simbock have been grouped into five groups whose alkaline (Li, Rb,

Cs) and alkaline earth metals (Be, Sr, Ba) contents are very low in the sediments compared to the source rock ; those of scandium, V, Cr, Co, Ni and Cu are low; yttrium, Nb, Mo, Hf and W show low concentrations with the exception of Zr; the other metals (Ga, Zn, Cd, In, Sn, Sb, Ti and Pb) show similar behaviour with those of the previous group. Thorium has very low values in contrast to uranium, whose concentrations considerably increase from source rock to sediment.

Chemical analyses of the clayey materials of Missole II, showed that rare earth elements spectra normalized to chondrite show an enrichment in LREE, compared to HREE and a negative anomaly in Eu. These characteristics are attributed to a felsic source rock (Ngon Ngon et al., 2012). Similarly, rare earths elements have a very high composition, over 100 ppm in unaltered samples and vary from 49 to 96 ppm in altered samples. Several ferruginous samples have very low rare earth elements values ranging from 39 to 47 ppm. All altered samples are highly enriched in rare earth elements (LREE/HREE ~ 3-86). The light rare earth elements have very positive correlations with heavy rare earth elements. Overall, high concentrations of rare earth elements contain: La, Ce, Pr, Nd, Sm, Gd and Dy (Ndjigui et al., 2013).

II.5. Previous work on sediment pollution

High concentration of Fe relative to other metals is due to the high values of Fe in the earth crust. The average sediments at the sampling stations of Otamiri River (Nigeria) shows that the river sediments are unpolluted and formed under excellent conditions. According to the EF, no heavy metal enrichment was observed at that river, except for Zn and Ni for which moderately severe enrichment was observed. Same observation was made for Pb at some locations. The Pollution Load Index (PLI) of stations shows that river sediments are formed under perfect conditions (Iwuoha et al., 2012).

Heavy metal measurements in the sediments of Lake Ahémé in Benin are compared with water quality standards and results obtained by other authors on Beninese rivers and water bodies such as the Porto Novo lagoon and the Okpara River, Benin (Dimon et al., 2014). It emerges that Lake Ahémé is polluted by chemical substances that come from anthropic activities (managerial waste discharges, biomedical waste, leaching, domestic wastewater discharges) carried out along its banks. These pollutions contribute to the destruction of the ecosystem, destruction that mainly results in the disappearance or rarefication of certain aquatic species (Dimon et al., 2014).

Average concentrations of trace elements in Dojran Lake sediments (SE, Republic of Macedonia) are in the following order: Au < Sb < Cr < Co < Pb < Cu < As < Ni < Zn. According to the FE calculation values, surface sediments of Dojran Lake have low enrichment in Cr, Zn, Pb, Cu and Co, moderately enriched in Ni, Au and Sb, medium enrichment in Au, high enrichment in Sb and very severely enrichment in As. These values are believed to be derived from a number of geological parameters such as weathering of surrounding rocks and anthropogenic sources (Šmuc et al., 2015).

Concentrations of heavy metals in sediments of lakes Bini and Dang showed high levels of Pb, Fe and Cd. Iron values show very low enrichment compared to all metals except Pb and Cd, which ranged from moderate enrichment for Lake Bini to very high enrichment for Lake Dang. The levels of contamination obtained by I-geo suggest for Cr, Fe, Cu, Ni and Zn, a slight contamination of the both lakes, while Cd and Pb present a contamination varying from moderate to strong for Lake Bini and very strong for Lake Dang (Oumar et al., 2014).

Ekengele Nga et al. (2012) focused on the determination of the degree of pollution in the Municipal Lake of Yaounde. This study shows that sediments in the central part of the lake are contaminated in Pb, Cd, Cu, Zn, and Cr according to the contamination factor (CF) and polluted according to the geoaccumulation calculation (I-geo). These sediments have an anthropogenic source.

Demanou and Brummett (2003), in two lakes of Yaounde, determine the concentrations of fecal bacteria and heavy metals (Cr, Cd, Hg, Pb and Zn) in fish, sludge and water in these lakes. That study shows that despite the high heavy metal content, fishes of these lakes are increasing in size and weight but are not a danger to human nutrition.

Waters of Lake Mwembe, periodically flooded areas between Ossa and Mwembe, the outlet of Lake Ossa and occasionally waters of southern and eastern Ossa are characterized by high nitrate content. Except for the eastern of Lake Ossa, these environments are close to industrial plantations located at the southwest part of the lake. These plantations could thus be the source of nitrate pollution. This hypothesis seems to be confirmed by the absence of nitrates in the Sanaga River and Lake Mevia, which are potential sources of other ionic inputs into Lake Ossa (Kossoni, 2003).

II.6. Some studies of lakes in Cameroon

Cameroon has about 39600 km² of continental (inland) water bodies made up of rivers (1000 km²), flood plains and marshes (34000 km²), natural lakes (1800 km²) and artificial reservoirs (2800 km²). These water bodies biologically contain rich and very varied ecosystems, especially in the Sanaga, Boumba and coastal rivers. Lake environments are also very rich from a biological point of view and crater lakes presenting the greatest diversity. Fish fauna of lakes and rivers in southern Cameroon is currently highly sought after by aquarists and is the subject of very little controlled international trade. Five categories of lakes are found in Cameroon: Crater lakes or volcanic lakes (e.g., Nyos, Barombi Mbo, Oku, Tizon); tectonic or subsidence lakes (e.g., Ossa, Dissoni, Ejanghan); basin lakes (e.g., Lake Chad); reservoir lakes (e.g., Lagdo, Mbakaou, Mapé, Bamendjim dams) or artificial lakes (e.g., Yaounde municipal lake, mefou lakes of which Lake Simbock is a part, ponds); and other lakes (e.g., twin lakes). Several other lakes have been the subject of several studies. These include:

II.6.1- Yaoundé

Located in the Central region, Yaoundé is the capital of Cameroon. This city abounds in more than ten lakes, all of which are artificial, dating back to the 1930s. It has many industries and institutions; it is one of the most populated cities in the country. On the scientific level, studies have been carried out and the majority have focused on the quality of the water. The work on pollution has been carried out mainly in the municipal and IRAD lakes of Yaounde. They focused on physico-chemical parameters and heavy metals (Joly and Assako, 2001; Fezeu et al., 2009; Kwon et al., 2012; Naah, 2013; Ekengele et al., 2015). Others have focused on water quality and fish species in these lakes (Ekengele et al., 2015; Ajaejah et al., 2017; Ndjama et al., 2017).

II.6.2- Dizangué (Ossa Lakes Complex)

The Ossa lake Complex is a set of 7 subduction lakes including Ossa, Mevia and Mwembe, which consist of Holocene sediments that likely retained valuable information about sedimentary processes. Previous investigations in Ossa complex were based mainly on paleoenvironmental studies, pollution and fish species including bacteriology. The paleoenvironment of Lake Ossa is focus on radiocarbon dating, combined with pollen and diatom data (Reynaud-Farrera et al., 1996; Nguetsop et al., 1998; Wirmann et al., 2001; Giresse et al., 2005; Nguetsop et al., 2010; Debret et al., 2014), environmental changes, climatic

variability and paleovegetation record (Reynaud Farrera et al., 1996). It is also suspected that Sanaga River related impact may have been significant through a large part of the sedimentary history of the lake (Wirrmann et al., 2001; Nguetsop et al., 1998, 2004; Kossoni and Giresse, 2010). However, the pollution aspect of the lakes of the Ossa Complex was characterized by high heavy metals (Nzieleu et al., 2014). On the other hand, several studies have identified within the order of Siluriformes several species with strong potential in aquaculture. *Chrysichthys auratus* is a species abundantly fished and commercialized in the Lake Ossa Faunal Reserve (Nack et al., 2015, 2018; Bahanack et al., 2016).

II.6.3- Ngaoundere

Numerous studies were carried out in Ngaoundere on paleoenvironment and pollution. Most of these studies are focused on late Holocene paleoclimate variations and paleoenvironmental reconstruction (Ngos et al., 2008; Vincens et al., 2010; Giresse and Ngos, 2011; Lebamba et al., 2012). They emphasized on the progressive replacement of forest by woody savannah around 3000 cal yr BP (Nguetsop et al., 2013; Lebamba et al., 2016; N'anga et al., 2018). Pollution of Ngaoundere lakes, was assessed by the physico-chemical properties and heavy metals identification on waters and sediments from lakes Mofole, Birni and Dang near the urbanized area of Ngaoundere (Oumar et al., 2014; Tsamo et al., 2017).

II.6.4- Work on other lakes

Like in the three selected cities for this study, the work in the lakes was carried out throughout the Cameroonian territory. They cover practically all areas of geosciences and biosciences, but the most recurrent ones are carried out on lakes located around the volcanic line of Cameroon and in crater lakes. This work for some gives the ecological status, the risks that these lakes may cause and warns about probable disasters that may occur with the living creatures around these lakes (Green, 1972; Kusakabe et al., 1989; Freeth, 1990; Kusakabe et al., 2008; Gufler, 2009; Yong et al., 2014; Yoshida et al., 2015); it also provides an overview of the paleoenvironment of Cameroon through microfossil and radiogenic dating studies and morphological studies of the country's lakes (Giresse et al., 1994; Assi-Kaudjhis et al., 2008; Lebamba et al., 2010; Mimpfoundi and Ndassa, 2016; Stager et al., 2017). In addition, work in Cameroonian lake environments reports on water quality, fish species and bacteria and links these to pollution (Tatsadjieu et al., 2009; Musilovà et al., 2014; Michaels et al., 2015; Martin

et al., 2015; Kamtchueng et al., 2016; Tamungang et al., 2016; Tenyang et al., 2016; Tabi et al., 2017; Sone et al., 2017; Tombi et al., 2017).

Conclusion

Cameroon, Africa in miniature abounds in large type of lakes like those encountered in the world. They come in many forms and have many origins. Their sedimentological and mineralogical characteristics are similar to those of others in the world according to their climatic zone and their context of formation. The work carried out in these lakes is in a variety of fields; all the same, several of these lakes have not yet been studied, still less by using recent methods by making comparisons between lakes with different formation contexts. In addition, informations on the geochemistry and pollution of the country's lakes is limited in the sediments they contain.



Chapter III: Material and methods

« Put your hand on a stove for a minute and it feels like an hour. Sit next to a pretty girl for an hour and it feels like a minute. That's relativity »

-Albert Einstein-

This chapter is focus on methods and materials used to get results. It's starts on the field with details of sampling collection with the different materials used. It's continuous with presentation of various analytical procedures performed in this study such as grain sizes, relative humidity, color determination, total organic carbon, mineralogical and geochemical analysis.

III.1. Field work

Many have been done, but field work in different periods for the three locations. In September 2017, in November 2018 and September 2019 respectively for Simbock Lake, Ossa lake Complex and Ngaoundaba Crater lake. The equipments includ: a raft (Figure III.1) that was mounted on the studied sites; a GPS receiver; a 1/200000 topographic map of the localities; a digital camera; a cutlass; a hacksaw; many polyvinyl chloride (PVC) pipes of 63 Φ ; a sledgehammer; a sellotape; a compass; a field notebook and markers; etc...



Figure III.1. Sampling procedure used in the lakes

Protocole

Ten cores of size varying between 0.68 and 1.60 m were sampled manually using the PVC pipes. They are then packaged in such a way as to preserve the sedimentary signal. The following procedures were used:

1. the coring is done manually from a raft of wood placed at the sampling site (Figure III.1);
2. the pipe is driven into the sediment using a 5 kg sledgehammer and manual force;
3. it is then manually raised to the surface while plugging the bottom of the pipe to prevent sediment contamination;
4. using the sellotape or a PVC cap, to plug both ends of the pipe containing the core in order to avoid loss and the contamination of sediment;
5. the samples are arranged and marked from bottom to top in an order of succession.
6. the core is then identified, measured and photographed (Figure III.2).



Figure III.2. Exemple of some collected cores

For each core, the operation is repeated until the pipe can no longer sink into the mud due to compaction, the water depth, the length of the pipe or proximity to the substrate. The cores are taken from a restricted area (identified by its GPS coordinates) to ensure good correlation between the samples. Surficial sediments are sometimes made more fluid by surface water. Ten cores have been collected and seven cores were thus selected from the selected lakes (Figure III.3).

From the ten sampled cores, seven have been selected for this research. From the Ossa lakes Complex in Dizanguè three cores were selected. The first core namely LO were located in the Ossa Lake which, is the main lake of the Complex. The second is the MO core located in the Mwembe Lake which is one of the four major lakes of Ossa lakes Complex. The last core was sampled in the river which supply the lakes and link the Complex with the Sanaga River; this was codified as OL core (Figure III.3b). In the Simbock Lake in Yaoundé, two sampled

core sediments were selected. One core at the border and another one in the centre of the lake labelled NR and EB respectively (Figure III.3c). From the Ngaoundéré area, the sediments were cored in the Ngoundaba Lake where the core sediments were taken near the border (AZ) and the center of the lake (NL) (Figure III.3d).

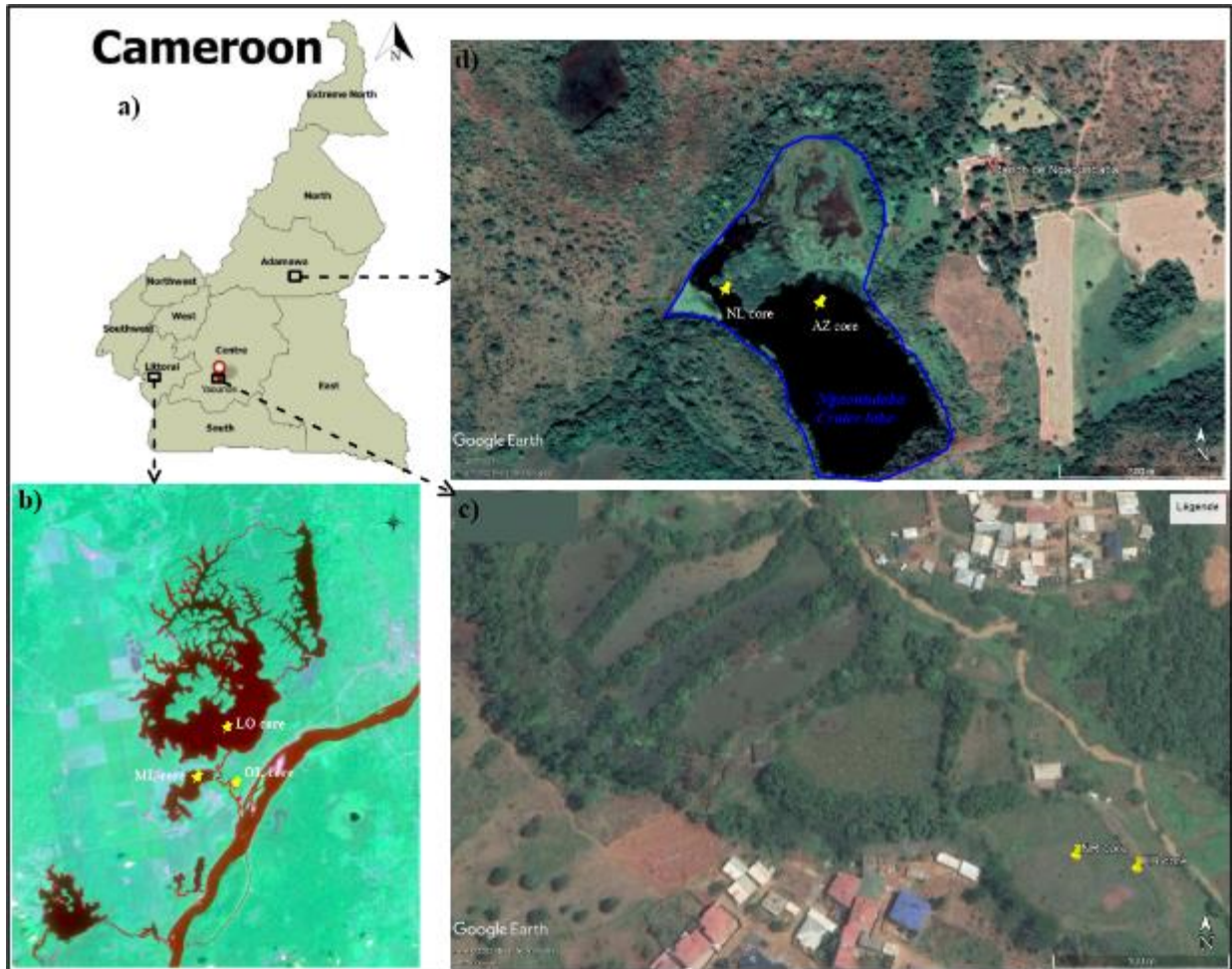


Figure III.3. Location map and samples location of: **a)** studied lakes in Cameroon **b)** Ossa lakes Complex in Dizanguè; **c)** Simbock Lake in Yaoundé and **d)** Ngaoundaba Lake in Ngaoundéré

III.2. Laboratory analyses

Laboratory work was carried out in several stages; from the opening of cores to the sampling of different sedimentary levels. After air dried, the samples were crushed using a pulverisette and an agate mortar for some of them in order to carry out sedimentological, mineralogical, geochemical (major, traces and rare earth elements), heavy metals analyses radiocarbon dating, diatoms and pollen grain analysis.

III.2.1. Sedimentological analysis

The macroscopic description of the seven selected cores is based on the colour, tone and texture of the sediments, the presence or absence of plant, rock or wood debris, the thickness of lithofacies, and an appreciation of the boundaries between the lithofacies. The first operation to be carried out was to delimit the different lithofacies. Colour is assessed when the sediments are still wet so that oxidation after opening the cores and their desiccation do not influence the description of their original colour, determined using the Munsell soil color chart. Texture is assessed by touch and taste, which is confirmed by grain sizes analyses.

III.2.1.1. Grain size analyses

Grain size distribution was carried out on all the samples (57) at the Department of Earth Sciences (University of Yaoundé I, Cameroon) according to Robinson-Köln's pipetting method for the silt- and clay-sized fractions (Singh, 2009). Sands were then separated using wet sieving. Twenty grams of the bulk sediment samples were treated with cold 1 M HCl and H₂O₂ to remove organic matter. Sodium hexametaphosphate has been added to deflocculate the samples. An aliquot of the bulk sediment below 2 mm grain-sized was separated in four fractions according to Ndjigui et al. (2014): coarse sands (2000-200 µm); fine sands (200-50 µm); silts (50-2 µm) and clays (< 2 µm). These can also be grouped into 3 main classes such as sands, silts and clays.

III.2.1.2. Residual humidity

Water contained in moist sediment is extracted by drying in an oven. This is the amount of bounded water remaining in the soil after drying in the open air. It was realized at the Department of Earth Sciences (University of Yaoundé I, Cameroon) on the 57 samples from 7 cores. The procedure is as follows: inside a clean, dry and tared container of weight M₁, place a sample of moist soil weighing at least 30g; after closing it with a lid, the whole is weighed, i.e. M₂ is the value of this weighing; then remove the lid and place it and the container in the oven at 105 °C for at least 15 to 16 hours. Drying will be considered satisfactory if two weighings carried out at 04 hours intervals have a difference of 0.1 %. Remove the container from the oven, cool it down and weigh it again; the value of this weighing is then M₃:

$$\omega (\%) = \frac{M_1 - M_3}{M_3 - M_1} \times 100$$

Where *M1*: weight of the empty box (or tared), *M2*: weight of the wet sample, and *M3*: weight of the dry sample.

III.2.1.3. Total Organic Carbon (TOC) and Organic Matter (OM)

The total organic carbon was determined in all selected sample sediments using a Primacs SLC analyser in the laboratories of the International Institute for Tropical Agriculture (IITA; Yaoundé, Cameroon). The Total Carbon (TC) was first determined by combustion at 105 °C. Then, the Inorganic Carbon (IC) was determined at 150 °C. Before the analysis begins, the sample is put in a test tube in which oxygen will be purged to remove CO₂. In order to decompose the inorganically bound carbon to the gaseous carbon dioxide, orthophosphoric acid is added to the sample. The flow of oxygen purges the carbon dioxide from the liquid into the IR detector to be measured again. The concentration of TOC is determined using the formulae: $TOC = TC - IC$. The amount of organic matter (OM) was obtained by the calculation of Walkley and Black (1934) formulae where $OM (\%) = TOC (\%) * 1.72$.

III.2.1.4. Scanning electron microscopic (SEM) observations of quartz grains

Quartz grains from Ossa lakes Complex and Ngaoundaba crater lake sediment sampled at different depths in the cores were hand-picked under the stereo zoom microscope and were prepared for SEM observations according to Trewin (1988). The grains were sputter-coated with platinum (~2 nm thickness) and examined at different scales using a *PHILLIPS XL-30* scanning electron microscope (SEM) at *Universidad Nacional Autónoma de México* (UNAM), Mexico. We followed the studies of Strand et al. (2003) and Vos et al. (2014) to study the quartz grain surface micro texture classification.

III.2.2. Mineralogical analysis

Mineralogical analyses were carried out using several methods for the different studied lakes. X-ray diffraction (XRD) for bulk sediments were realized in the three selected sites. However, SEM equipped with energy dispersive spectrometer (EDS) were done for aggregates and grains from Ossa lakes Complex and Ngaoundaba crater Lake. Fourier transform infrared (FT-IR) spectroscopy and X-ray diffraction of finest grain-sized fractions after specific treatments were applied for sediment from Simbock Lake.

III.2.2.1. X-ray diffraction for bulk sediments

Mineralogical analyses were carried out at the Geoscience Laboratories, Sudbury, Canada and at Botswana International University of Sciences and Technology (BIUST). The bulk mineralogy of the 45 selected samples was determined using XRD. Samples were prepared into powders by pulverizing with an agate mortar and pestle. Smear mounts of the powder were prepared on low background silicon disks for analysis. The analytical instrument (*PAN Analytical X'PERT PRO* diffractometer) was equipped with a monochromator using a Co K α radiation of 1.7854 Å over a range of 2.5°–35° 2 θ and a step size of 0.05° 2 θ /min at 40 kV and 45 mA. Minerals identification and quantified from XRD patterns using Rietveld refinement method (Ufer et al., 2008) and the “HighScores Plus software”.

III.2.2.2. Scanning electron microscopic equipped with energy dispersive spectrometer (SEM-EDS)

Sediments and aggregates from the Ossa Complex and Ngaoundaba Lake were selected as representative samples to determine the chemistry of different mineral phases in this study. The chemical composition of selected grains (aggregates) was acquired at the Petrology Laboratory, Institute of Geophysics, UNAM, using a *PHILLIPS XL-30* scanning electron microscope (SEM) equipped with EDAX spectrometer (EDS) system. Interpretation was done according to Armstrong-Altrin et al. (2017).

III.2.2.3. Fourier transform infrared (FT-IR) spectroscopy

FT-IR spectroscopy is a vibrational spectroscopy technique that can be used to optically probe molecular changes associated with minerals. The spectral bands in the vibration spectra are specific to the molecule and provide direct information on properties of chemical compositions. FT-IR peaks are relatively narrow and, in many cases, can be associated with vibration of a particular chemical bond (or single functional group) in the molecule. In addition, physical effect of the infrared is created by absorption and mainly influences the dipole and ion bands such as O-H, Al-OH and Si-O (Manoharan et al. 2012). Six powdered samples with high kaolinite proportion were analyzed using the *BRUKER OPTIK ALPHA* spectrometer in the Laboratory of Inorganic Chemistry, University of Yaoundé I. The infrared spectra were recorded at a wavelength range of 4000–400 cm⁻¹.

III.2.2.4. X-ray diffraction of the finest grain-sized

X-Ray Diffraction analyses were carried out on two selected samples with high kaolinite proportion at the Geological Institute of the University of Lausanne, Switzerland. The samples were prepared following the procedure of Adatte et al. (1996, 2002). The analytical instrument is equipped with a monochromator using a Cu-K α radiation ($\lambda = 1.540562 \text{ \AA}$) over a range 2-5 $^{\circ}$ 2Theta with a step of 0.02 $^{\circ}$ at 40 kV and 45 mA. The oriented samples were characterized using a *D8 BRUKER* Diffractometer in the University of Liege (Belgium). This analytical instrument is equipped with a Cu-K α radiation ($\lambda = 1.5406 \text{ \AA}$) at 35 kV and 45 mA. The diffraction patterns were obtained from 1.5 to 15 $^{\circ}$ 2Theta at a scanning rate of 1 $^{\circ} \text{ min}^{-1}$. Identification of minerals was done through observation of X-ray powder patterns before and after treatment by heating and with organic liquids according to several works (Brindley and Brown, 1980 ; Moore and Reynolds, 1989).

III.2.3. Geochemical analysis

These analytical methods are used to characterize lake sediments on one hand and to define conditions that prevailed during the establishment of sedimentary paleoenvironments on the other hand. These methods encompass the geochemistry of major elements, rare earths and trace elements. Fifty-seven samples from the three lakes were pulverized using an agate mortar and pestle. Geochemical analyses were carried out at the Geoscience Laboratories, Sudbury, Canada.

III.2.3.1. Major elements geochemistry

Major-element analysis is by X-ray fluorescence (XRF), test materials were prepared as glass discs, formed by mixing 1 part of weight (0.700 g) of the powdered sediment (dried at 110 $^{\circ}$ C) with 5 parts of weight of dried lithium metaborate/ tetraborate flux (*JOHNSON MATTHEY SPECTROFLUX IOOB*) and fusing in a muffle furnace for 15 min at 1100 $^{\circ}$ C in 95 % Pt-5 % Au crucibles. The melt was swirled repeatedly to ensure complete dissolution and homogenisation of the test material, then poured into a mould, which had been pre-heated on a hotplate, and pressed to form a thin (1.5 mm thick) flat-surfaced disc (35 mm diameter). A loss-on-ignition (LOI) measurement was undertaken on samples of dried sediment powder by heating in a pre-ignited silica crucible to 1000 $^{\circ}$ C for 1 hr and recording the percentage weight loss. The LOI determination is an essential part of the analytical programme for the major elements, accounting for constituents (e.g., H $_2$ O, CO $_2$) which cannot be measured directly by

XRF and are lost during glass formation, so requiring a correction to be made in the determination of the major elements.

III.2.3.2. Trace elements and rare earth elements (REE) geochemistry

The powders were prepared for ICP-MS analysis to determine lithophilic element concentrations by triacid etching in a closed vessel. The powders were treated in a diacid mixture (HCl + HClO₄) at 120 °C in a closed vessel for one week. The samples obtained after this phase were dissolved again in acid solutions (HNO₄ + HCl + HF) heated to 100 °C. The dissolved samples were analyzed using *PERKIN ELMER ELAN 9000 ICP-MS*. Initially, the analysis was performed using an IM100 analytical strip in which an average instrument weight responded for three certified reference materials prepared in the same manner as the blank for each element. Standard solutions were prepared for 30 samples together with a control after 10 samples were run each time. Data are reported for a wide range of transition metals. Due to uncertainty of element concentrations in the certified reference materials, the detection limits for the IM100 band are higher than the maximum capabilities (upper limits) of the instrument. When certain concentrations were found below the detection limit for the IM100 analytical band, the solutions were re-analyzed using a second group of 04 synthetic solutions of equal concentrations containing 14 rare earths, Y, U, Th, Zr, Nb, Ta, Rb and Sr. The detection limits obtained were very low. The accuracy of this method is estimated at 5%. (Burnham and Schweyer, 2004).

III.2.4. Heavy metals analysis

Samples sediments from selected intervals of the cores were digested using a mixture of HCl: HNO₃ (3:1) at 80 °C using an *AGILENT 4200 microwave plasma-atomic emission spectrometer* (MPAES) for heavy metal distribution (Fe, Mn, Cr, Cu, Pb and Zn) at University of Botswana and at BIUST. The digested sample solutions were analyzed using Inductively Coupled Plasma Optical Emission spectrometry (*ICP-OES*) 3000 XL (*Perkin Elmer*). The detection limits ranges from 0.05×10^{-6} to 4.0×10^{-6} mg/g depending on the elements. The quality assurance and quality control of analysis were assessed according to EPA standard using duplicates, standard reference materials and method blanks.

III.2.5. Radiocarbon dating (¹⁴C)

Three samples were taken from the OL core (base, middle and top) of Ossa Lake in the Southern Cameroon and 3 others from the NL core (base, middle and top) of Ngaoundaba Lake in the Northern part of the country. They were dated with radiocarbon dating (¹⁴C) at the Poznan Radiocarbon laboratory in Poland. The principle of this method consists in measuring specific activity of a sample, which is the number of rays β- emitted per gram of carbon per minute, and deducing, by calculation, the elapsed time. The physical and chemical pre-treatment for 2.5 g of samples consisted of : solubilizing the inorganic agents in 8-10% hydrochloric acid for 30 min with stirring; rinsing the samples with demineralized water; immersing the samples in a 0.5 M soda solution for 1 h while heating to 60 °C with stirring, controlling only the pH to remove humic and fulvic acids; rinsing again with demineralised water, neutralising the soda in order to avoid any trapping of atmospheric CO₂ by immersing the samples in a bath of HCl (8-10 %); checking the pH to ensure that the medium becomes acidic again; finishing with a last rinsing with demineralised water until the medium is neutralised; drying in an oven for 6 hours at 90 °C. The technique used for counting ¹⁴C is liquid scintillation using a *PERKIN ELMER TRI-CARB liquid scintillation counter*.

From the data obtained, an age-depth model can be established. It allows an age to be associated with each depth based on the data obtained by the ¹⁴C methods. There are several methods to establish the age-depth model of a core: linear interpolation, polynomial regression, spline interpolation. In this study, the method chosen is linear interpolation. Linear interpolation is a method for estimating the value taken by a continuous function between two determined points (Delachet, 1960). It consists in using the affine function (of the form $f(x) = m \cdot x + b$) passing through two determined points.

II.2.6. Analysis of diatoms

A total of 38 samples taken every 10 cm from one core per lake (mainly those near the centers of the lakes) were analyzed. The extraction of the diatoms and the preparation of the slides for microscopic observations were done following the standard method described by Bartabee (1986), which consists of chemical treatments with hydrogen peroxides to destroy the organic matter and deflocculate the clays, followed by successive washes with distilled water to remove the supernatant. Several steps were necessary for this purpose: hydrogen peroxide in the proportions of 3 volumes of mineralized water for one volume of 35 % hydrogen

peroxide to eliminate the organic fraction and to start the deflocculation of the clays. This reaction takes place under heat for 2 hours; diluted hydrochloric acid at ¼ is added drop by drop until the solution is discoloured under heat to eliminate the ologoelements; sodium hexametaphosphate diluted at 5 % was used to complete the deflocculation of the clays when it was not total after the hydrogen peroxide attack. Each step of this chemical treatment is followed by a minimum of 3 successive washes to remove the remaining solvent and suspended waste. During each wash, the beaker containing the mixture resulting from the chemical treatment is filled with distilled water and left to rest for 2 to 3 hours to allow the diatoms to settle. The supernatant consisting of the solvent and the fine suspended particles are removed by siphoning. The residual pellet containing the diatoms will be used for microscopic observations. This residual pellet obtained at the end of the chemical treatment is used for the preparation of slides for the qualitative analysis of taxa under the microscope. It is diluted in 200 to 300 mL of distilled water, then 0.2 mL of this solution is taken and deposited on a slide previously cleaned with alcohol. The solution, once air-dried, is placed on the slide on which naphrax used as mounting medium has been deposited. Three slides were mounted per sample. The identification at the specific level of the diatoms was done using the optical microscope OLYMPUS BH-2 equipped with a Nomarski interferential at 1000 X immersion magnification in the Laboratory of Animal Biology at the University of Dschang in Cameroon. Diatoms were counted following randomly selected vertical transects and a minimum of 400 individuals per sample was counted due to the low diatom content observed along some cores. The identification keys that have been used are those of Krammer and Lange-Bertalot (1991, 1993, 1999, 2000), Lange-Bertalot (1993), Gasse (1980, 1986), Simonsen (1987), Patrick and Reimer (1966), Hustedt (1930, 1962, 1966), Germain (1981), Krammer (1993, 1994), Foged (1977, 1982), Servant-Vildary (1978) and Werner (1976). The counting unit is the valve (half of an individual). However, diatom fragments with a size greater than or equal to 75 % of the valve or those with a complete central area (case of Pinnularia) are counted as whole valves.

II.2.7. Palynological analyses

Samples for pollen analysis were prepared using standard laboratory procedures: adding 10% HCl to dissolve carbonates, heating in 10% KOH to remove the humic fraction and at least 24-hour treatment with HF to remove the mineral fraction followed by Erdtman's acetolysis (Berglund and Ralska-Jasiewiczowa, 1986). Pollen and spores were counted with a biological microscope under 400× and 1000× magnification from the entire area of cover slide until the

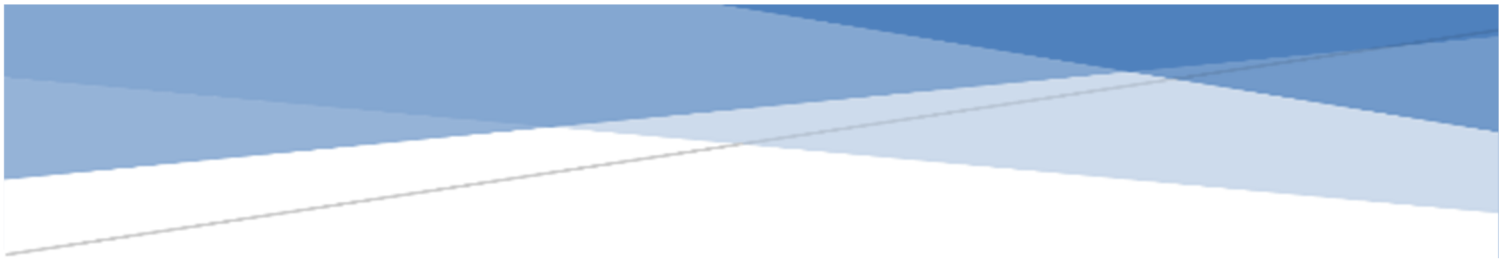
number of at least 200–250 pollen grains and spores was obtained (cf. Maley and Brenac, 1998). Pollen grains were identified using atlases (Maley, 1970; Sowunmi, 1973, 1995; Gosling et al., 2013; Schülerand and Hemp, 2016; Willis, 2020).

Percentages of pollen grains originating from forest and savannah communities were calculated as the ratio of an individual taxon and the TPS (total pollen sum); the TPS consisting of the sum of AP (arboreal pollen) and NAP (non-arboreal pollen but excluding any taxa originating from aquatic and wetland plants as well as spores and algae). Percentages of aquatic and wetland pollen taxa, as well as spores and algae, were calculated as the ratio of an individual taxon or alga and the TPS enlarged by this taxon or alga type.



Part two: Results and interpretations

The second part concerns the results obtained in selected lakes and their interpretations. It is subdivided into three chapters: the first chapter deals with the sediment characteristics, the second with the petrology and environmental aspect of lakes in Cameroon and the third focuses on the paleoenvironmental reconstitution.

An aerial photograph of a river delta or wetland landscape, showing a complex network of water channels and landforms. The water is a mix of dark blue and brown, while the land is green and brown. The overall scene is a dense, intricate pattern of natural features.

Chapter IV: Sedimentological characteristics of lake deposits

Don't try to become a successful man. Try to become a man of value. The value of a man lies in his ability to give, not in his ability to receive.

-Albert Einstein-

This chapter focuses on the determination of different characteristics of sediments through the selected samples. These characteristics include residual humidity, physical features, shapes of grains and organic matter content. It will help to gain insight into the constituent elements, provenance, degree of alteration and post-sedimentary processes occurred in different sites.

IV.1. Physical characteristics of sediments

The physical characteristics of sediments in this study are mainly composed of different sediments properties, water content (residual humidity), color, texture, thickness and grain sizes from different sites.

IV.1.1. Simbock Lake (Yaoundé)

Simbock Lake lies between 3°48'49.3''-3°48'51.8''N and 11°27'57.2''-11°28'00.8''E, at 691 m of altitude. It is the last of a succession of 7 lakes supplied by the Mefou River. It has a considerable evolution with time (Figure IV.1). The Simbock Lake has a diamond shape and a surface area of covers 4557 m² with 6835.5 m³ and about 1.5 m depth.



Figure IV.1. Evolution of Simbock Lake with time: 2002. The river bed is located at the right of the lakes; 2007. The bed of the stream is located at both sides of the lakes; 2013. The river bed is located at the left of the lakes and flooded; 2019. The river bed is located at the left of the lakes

Sediments from Simbock Lake were extracted by two cores: NR (119 cm) and EB (68 cm) with different colors and textures (Figures IV.2 and 3). The channel sediments of the Lake consist mostly of sand silt and clay sized particles. The studied sediments have an average grain size falling in a very fine sand (Table IV.1a). Relative humidity varies from 11.37 to 57.65 %, and high values are observed in the rich-clay samples.

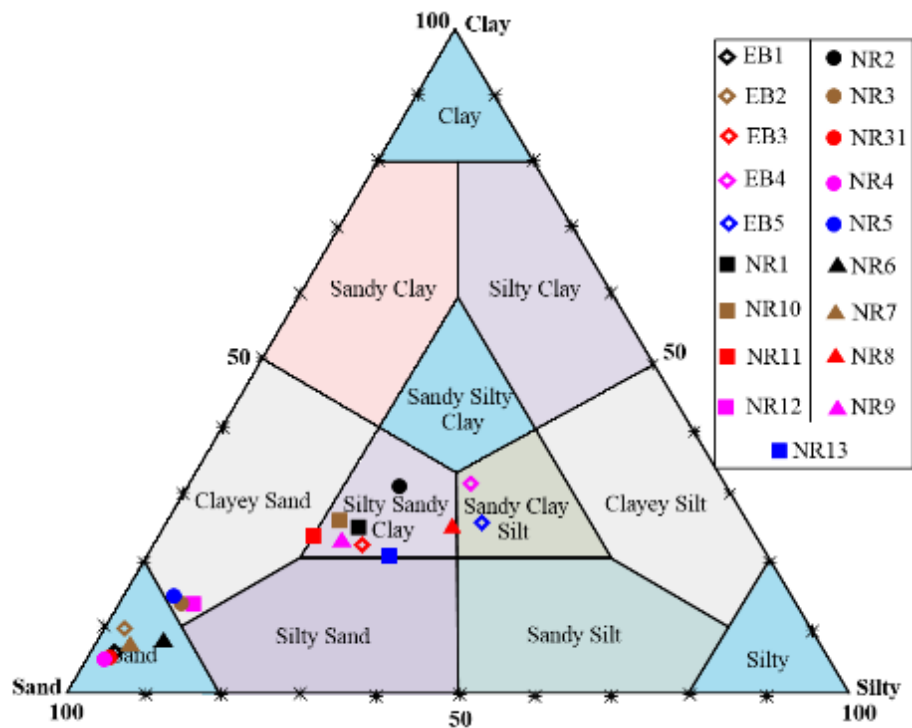


Figure IV.2. Simbock Lake sediments in the ternary textural diagram (Shepard, 1954)

NR core has 14 layers from the base to the top (Figure IV.3a). The base layer NR12 is 8 cm thick with organic laminae (past millimeter black organic waxes), light brown olive (2.5Y5/3) with clayey sand texture. NR5 is light brown olive (2.5Y5/6) due to some organic laminae, light clay to sandy clay and 11 cm thick. NR13 layer is 12 cm, light yellowish brown (2.5 Y 6/3) and light clayey sand texture, with organic laminae. NR4 layer is very light brown (10YR 7/3) with organic laminae (wood centimeter fragment), sandy and 8 cm thick. NR31 is an organic layer (wood fragments, root, and leaves); it is 9 cm thick, yellowish brown (10YR 5/6) and sandy clay. NR10 is 9 cm thick; sandy and yellowish brown (10YR 5/6). NR3 is an organic layer (wood fragments, roots, and leaves) blackish with some past slightly ochre along 8 cm. It is clayey sand and brown (10YR 5/3). NR9 layer has little organic matter. It is sandy clay and brown (10YR 5/3) with a thickness of 6 cm. NR8 layer has some yellowish organic

laminae with some wood fragments along a thickness of 9 cm. It is clayey and yellowish brown (10YR 5/6). Level NR2 is 5 cm; it has little yellowish organic laminates with some wood detritus. It is sandy clay and yellowish brown (10YR 5/4). NR7 is 7 cm in thickness; the level is sandy with dark brownish yellow colour (10YR 4/4). NR6 layer is a sandy level with yellowish brown colour (10YR 5/6). NR11 is 5cm in thickness, it's a vase, and the layer is sandy clay with dark yellowish-brown colour (10YR 3/4). NR1 is a vase; the layer is sandy clay with dark yellowish-brown colour (10YR 4/4), with 8 cm.

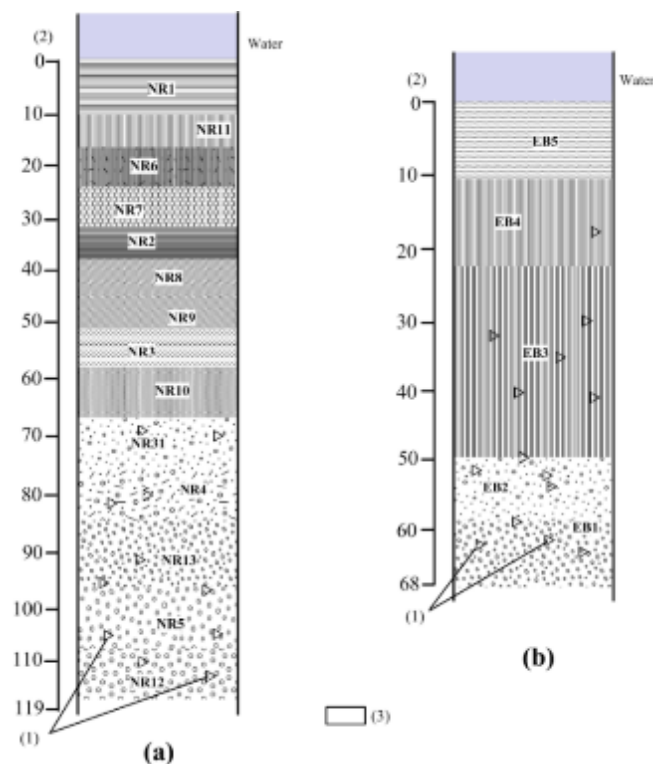


Figure IV.3. Macroscopic organization of core sediments from the Simbock Lake: **a)** NR core; **b)** EB core; (1) muscovite flake; (2) depth (cm) and (3) sample location

The EB core has 5 levels with positive grading from the base to the top (Figure IV.3b). EB1 is sandy and yellowish brown (10YR 5/4), slightly dense with many muscovite flakes. The layer is 14 cm thick. EB2 is sand, 7 cm thick and dark greenish brown (10YR 4/4) with centimetric ochre pebble and ferruginous. EB3 is compact, clayey and light yellowish brown (10YR 6/4) and it's 20 cm thick. EB4 is sandy clay and light greenish brown (2.5 Y 5/3), compact with some muscovite flakes and is 14 cm thick. EB5 is a muddy level, very compact with some liquids. It is clayey and light yellowish brown (2.5 Y 6/3) with 14 cm thickness.

Table IV.1. Thickness, color, grain size distribution, texture and relative humidity of Lake sediments

a) Simbock Lake

	NR Core														EB Core				
	NR12	NR5	NR13	NR4	NR31	NR10	NR3	NR9	NR8	NR2	NR7	NR6	NR11	NR1	EB1	EB2	EB3	EB4	EB5
Thickness (cm)	8	11	12	8	9	10	8	6	9	5	7	14	5	8	14	7	20	14	14
Color	Light brown olive	Light brown olive	Light yellowish brown	Very light brown	Yellowish brown	Yellowish brown	Brown	Brown	Yellowish brown	Yellowish brown	Yellowish brown	Yellowish brown	Dark yellowish brown	Dark yellowish brown	Yellowish brown	Dark greenish brown	Light yellowish brown	Light greenish brown	Light yellowish brown
% Sand size	78.88	80.25	49.15	91.64	91.88	52.27	80.74	50.23	34.27	41.93	87.42	85.03	58.27	51.32	89.45	86.82	32.62	31.91	58.05
% Silt size	10.27	8.54	31.83	2.3	2.14	23.45	8.06	21.99	38.1	29.52	3.98	5.35	17.75	23.8	3.05	2.48	37.78	33.83	22.2
% Clay size	10.85	11.21	19.02	6.06	5.98	24.28	11.2	23.11	27.62	28.55	8.6	9.63	23.98	24.88	7.5	10.7	29.7	34.26	19.75
Texture	Clayey sand	Clayey sand	Silty Sandy clay	Sand	Clayey sand	Silty Sandy clay	Clayey sand	Silty Sandy clay	Silty Sandy clay	Silty Sandy clay	Sand	Sand	Clayey sand	Silty Sandy clay	Sand	Sand	Silty Sandy clay	Sandy clay	Sandy clay
Humidity (%)	39.9	38.3	31.3	28.7	39.5	41.3	44.4	40.7	37.8	33.8	34.7	35.3	36.2	37.7	45.8	57.7	15	11.4	36

b) Ossa lakes Complex

	LO Core							OM Core							LO Core			
	LO1	LO2	LO3	LO4	LO5	LO6	LO7	OM1	OM2	OM3	OM4	OM5	OM6	OM7	OL1	OL2	OL3	OL4
Thickness (cm)	30	18	22	20	20	20	20	34	23	20	20	20	20	20	27	20	20	20
Color	Dark grey	Dark grey	Greyish brown	Greyish brown	Greyish brown	Greyish brown	Darkish greyish brown	Greyish brown	Darkish greyish brown	Darkish greyish brown	Darkish greyish brown	Very darkish greyish brown	Very darkish greyish brown	Very darkish greyish brown	Brown	Brown	Strong brown	Dark grey
% Sand size	7.20	6.11	9.34	6.24	7.67	0.42	1.89	0.43	0.23	0.09	0.27	0.78	0.77	3.88	1.46	36.01	17.85	52.83
% Silt size	68.32	70.44	74.32	72.92	73.17	76.28	72.85	84.36	73.93	76.12	76.71	79.43	77.12	74.95	62.37	38.11	46.67	33.41
% Clay size	26.28	23.45	16.34	20.84	19.27	23.3	25.27	15.21	25.84	23.79	23.01	19.78	22.12	21.2	35.15	25.41	35.48	13.76
Texture	Clayey silt	Clayey silt	Clayey silt	Clayey silt	Clayey silt	Clayey silt	Clayey silt	Silt	Clayey silt	Clayey silt	Clayey silt	Clayey silt	Clayey silt	Clayey silt	Sandy clay silt	Sandy clay silt	Sandy silt	Sandy silt
Humidity (%)	56.6	58.1	46.2	44.3	40.7	43.2	46	51.3	50.11	43.5	41.8	40.2	41.9	44.1	37	28.2	26.6	28.7

c) Ngaoundaba crater lake

	AZ Core									NL Core										
	AZ1	AZ2	AZ3	AZ4	AZ5	AZ6	AZ7	AZ8	AZ9	NL1	NL2	NL3	NL4	NL5	NL6	NL7	NL8	NL9	NL10	NL11
Thickness (cm)	16	10	10	10	10	10	10	10	10	16	10	10	10	10	10	10	10	10	10	10
Color	Dark grey	Dark grey	Dark grey	Very dark grey	Black	Black	Black	Darkish greyish brown	Darkish greyish brown	Dark grey	Dark grey	Dark grey	Very dark grey	Very dark grey	Black	Black	Black	Dark greyish brown	Dark greyish brown	Dark greyish brown
% Sand size	5.64	9.47	10.6	2.64	1.31	2.6	1.32	0.75	0.65	8.06	10.68	5.07	1.1	1.09	1.48	0.41	1.17	0.31	0.81	0.75
% Silt size	75.79	70.92	74.95	84.59	89.39	91.79	93.13	94.06	91.34	68.26	72.52	83.95	86.56	88.84	88.35	93.31	88.82	89.28	89.04	90.17
% Clay size	18.57	19.61	14.45	12.76	9.3	5.6	5.54	5.12	8	23.68	16.79	10.96	12.34	10	10.14	6.18	9.99	10.2	10.03	8.95
Texture	Clayey silt	Clayey silt	Clayey silt	Clayey silt	Clayey silt	Clayey silt	Clayey silt	Silt	Clayey silt	Clayey silt	Clayey silt	Clayey silt	Clayey silt	Clayey silt	Sandy clay silt	Sandy clay silt	Sandy clay silt	Sandy silt	Sandy silt	Sandy silt
Humidity (%)	63.2	71.6	70.5	69.8	69.7	68.7	67.3	66.8	65.8	61.5	60.9	59.6	70	64.6	63.8	63.4	69.7	71.1	71.7	72.3

200 < ϕ < 2000 μm (coarse sands); 200 < ϕ < 50 μm (fine sands); 50 < ϕ < 2 μm (silts); ϕ < 2 μm (clays).

IV.1.2. Ossa lake Complex (Dizanguè)

Ossa lake Complex is located between latitude 03°45.7' -03°53' and longitude 09°58' - 10°04' at 8 m a.s.l., in the eastern part of the Douala/Kribi-Campo Basin. Ossa Lake is the largest of a series of seven lakes in the complex; it is about 35 km from the Atlantic shore which was dammed during the Late Pleistocene by alluvial terraces. With a maximum width of about 7 km, Ossa is the largest lake (37 km²) of the complex, followed by Mevia (7 km²) and Mwembe lakes (3 km²) (Kossoni, 2003; Giresse et al., 2005). This lake system has a water surface area of about 3800 ha for a total surface area of 4500 ha. The maximum depth is 10 metres, with an average of 3 metres (Kling, 1988).

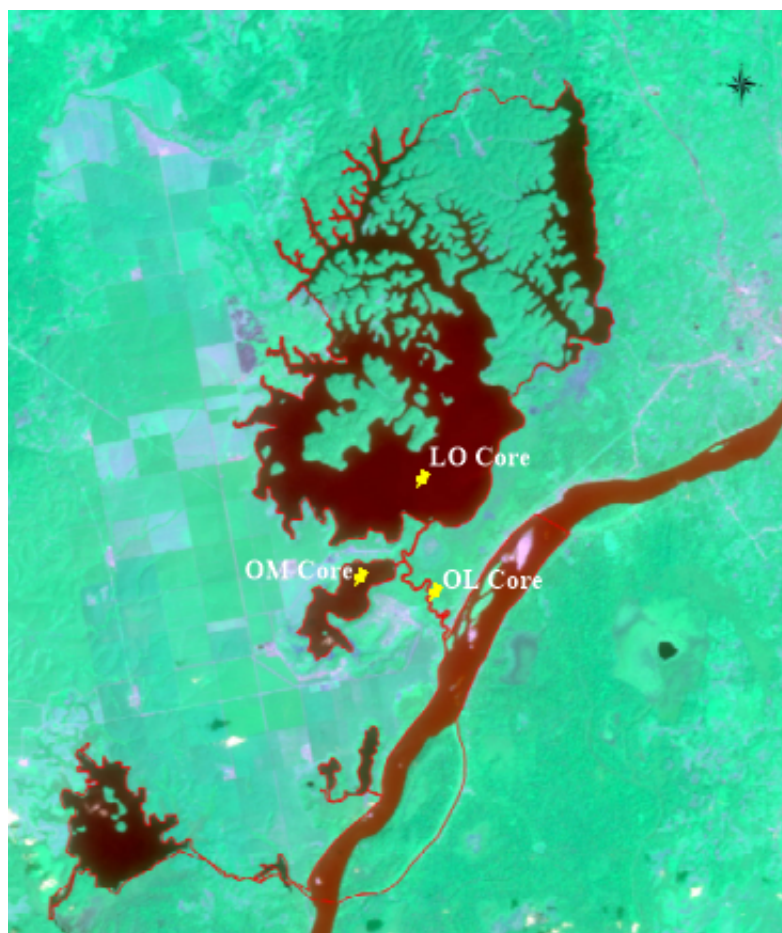


Figure IV.3. The Ossa Lakes Complex

The first core (LO) was retrieved in Ossa Lake, at 4.5 m water depth, it is 150 cm long. The second (OM) was collected in Mvembe Lake, the water depth was about 5.0 m and were about 157 cm of length. The last core (LO) was collected from the ridges of a water line, it is 87 cm long. The naked eye observations show that the cores are mainly composed of fine-

grayish- to brown-grained, with visible twigs and leaves. Relative humidity varies from 40.2 to 58.1 % with a mean of 46.2 % in the lakes, and from 26.6 to 37 % with an average of 30.1 % in the river sediments (Figures IV.4, 5; Table IV.1b).

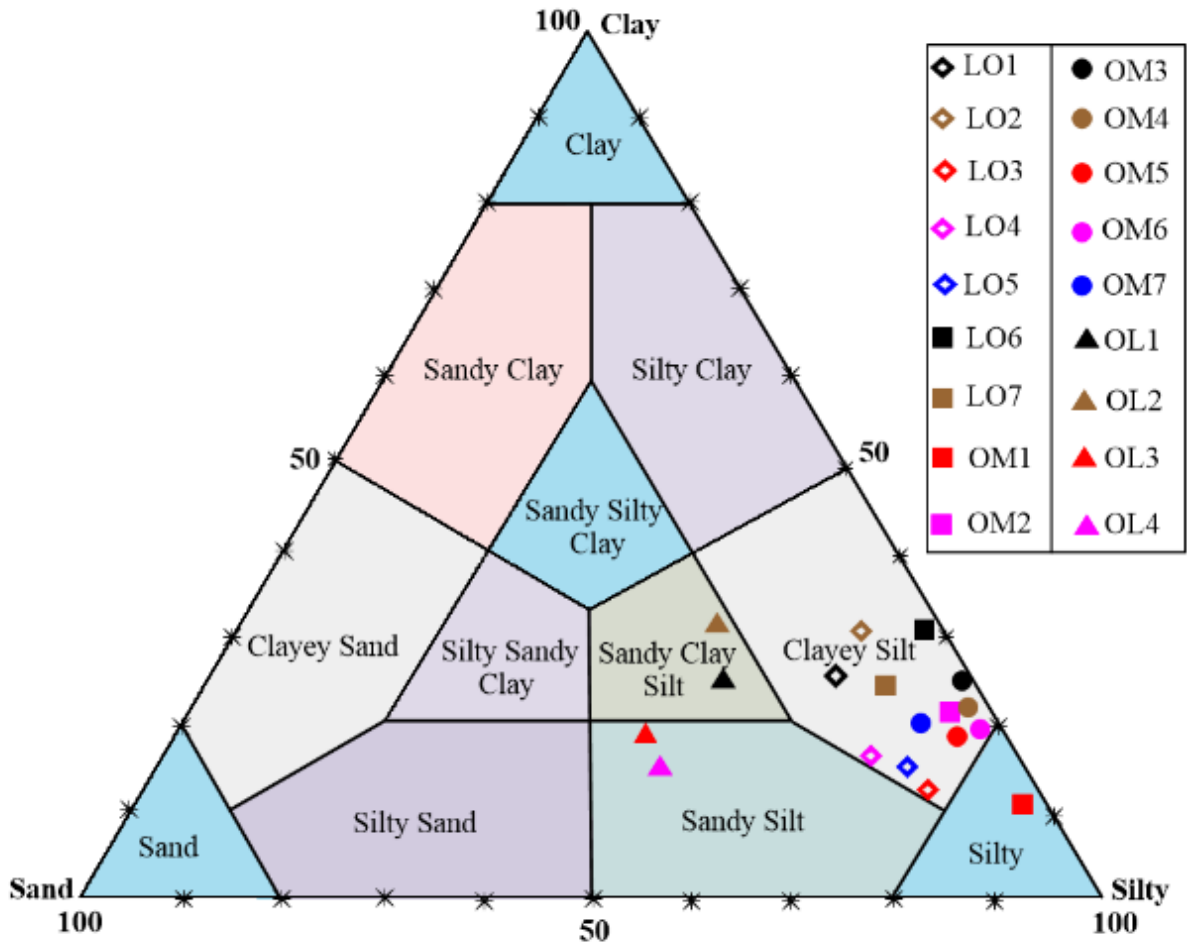


Figure IV.4. Ossa lakes Complex sediments in the ternary textural diagram (Shepard, 1954)

The grain size of the sediments is almost similar. The sampling was made at intervals of 20 cm for each core. LO core from Ossa Lake and OM core from Mwembe Lake has 7 sampling point for three layers each other. However, the river supplied core (OL) has 4 sampling points with three layers.

From the bottom to the top, the layers of LO core contain organic laminates (past millimeter black organic wakes, twigs, woods and leaves). The first layer is dark grey (2.5Y 4/1) with silty clay texture in samples LO1 and LO2. This layer is about 30 cm thick. The long silt texture layer of 80 cm thick is greyish brown (2.5Y 5/2). This layer is composed of samples LO3 to LO6. The last layer is the smallest with 20 cm thick. LO7 is the only sample of the

heavy silt layer, the color is dark greyish brown (2.5Y 4/2) (Figures IV.4, 5a; Table IV.1b). This layer has high organic debris than the others.

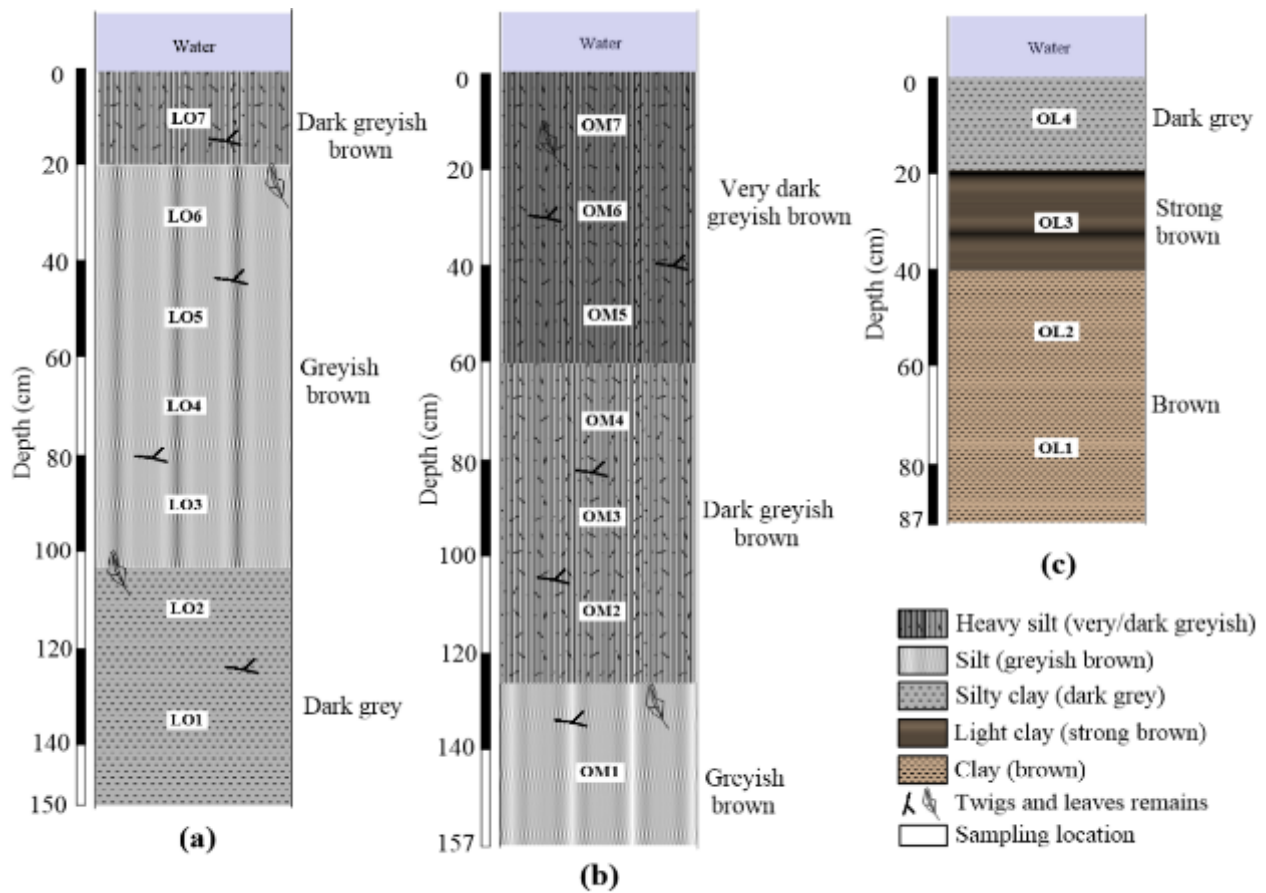


Figure IV.5. Macroscopic organization of core sediments from the Ossa lake Complex: **a)** LO core; **b)** OM core and **c)** OL core

OM core is the longest one of the set with 157 cm long and has high proportion of organic debris. The base layer is about 34 cm thick and composed only of sample OM1. The color is greyish brown (2.5Y 5/2) and has silt texture. The middle layer is dark greyish brown (2.5Y 4/2) in color, the texture is heavy silt. It is 63 cm long and composed of samples OM2 to OM4. The top layer has the same texture with the previous layer, it has also three samples (OM5 to OM7). With 60 cm thick, the color of the level is very dark greyish brown (2.5Y 3/2) (Figures IV.4, 5b; Table IV.1b).

The third core (OL), is the smaller core with 87 cm of length. The characteristics of this core are different from the others. The bottom layer is consisting of a clay texture with brown color (10YR 4/3). It is 47 cm thick with 2 samples (OL1 and OL2). Composed of light clay

texture, the middle layer of OL3 is strong brown (7.5YR 4/6). This layer is 20 cm thick. The top layer of OL core is also 20 cm thick with a silty clay texture and the color is dark grey (2.5Y 4/1) (Figures IV.4, 5c; Table IV.1b).

IV.1.3. Ngaoundaba crater Lake (Ngaoundéré)

Lake Ngaoundaba, 17 ha in area at 1160 m of altitude, has a maximum depth of 62 m with an average depth of 17 m (Kling, 1988). The lake area is continuously decreasing due to eutrophication and urbanization. This fish-bearing lake, where swimming and fishing take place, is one of the attractions of the Ngaoundaba ranch, which is a place renowned for its touristic capacity. Known as a maar, this crater lake is one of a multitude crater lake in the North of Cameroon and particularly in the Adamaoua region.



Figure IV.6. The Ngaoundaba Crater Lake

Two sediment cores from the Ngaoundaba Crater Lake (Figure IV.6). The Core AZ were sampled near the centre of the lake in a depth water of 8 m, with 96 cm of thickness. Near the left border and an eutrophication area, a core of 116 cm long labeled NL was sampled at 5 m depth. Physical features including relative humidity, grain size distribution and texture are listed in Table IV.1c, Figures IV.7 and 8. Relative humidity varies from 60 to 72 %, and the high values are observed in the top of the cores.

composed of 3 samples (NL6 to NL8) with 30 cm thick. This layer has both clayey silt and sandy clayey silt texture. The last level is a dark greyish brown (2.5Y 4/2) layer composed of 3 sampled points (from NL9 to NL11) of 30 cm thick. The texture of the layer is sandy silt (Figures IV.7 and 8b).

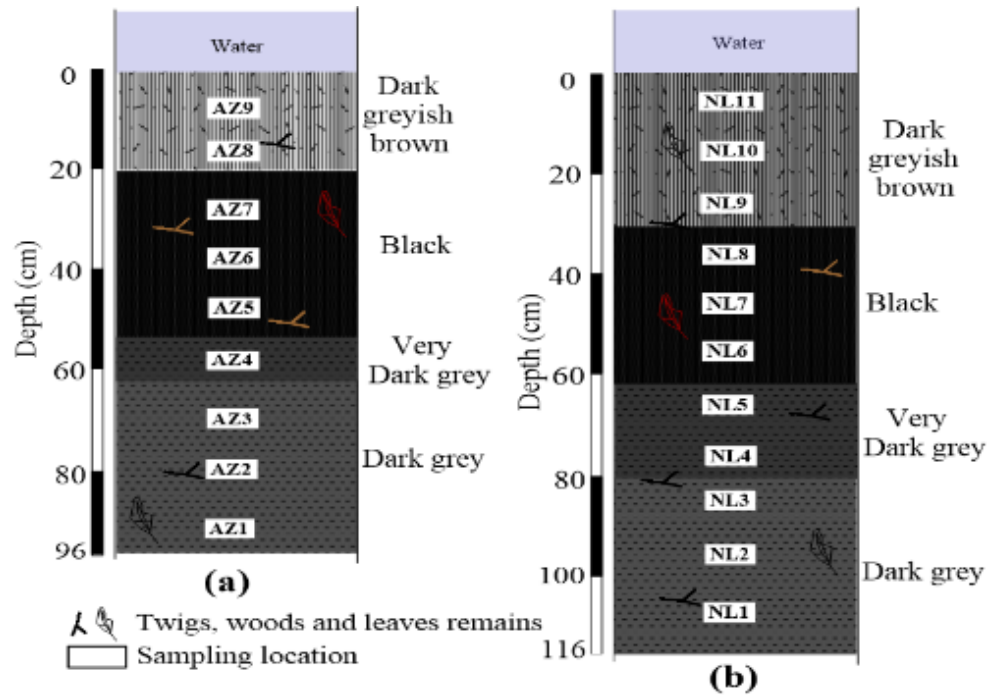


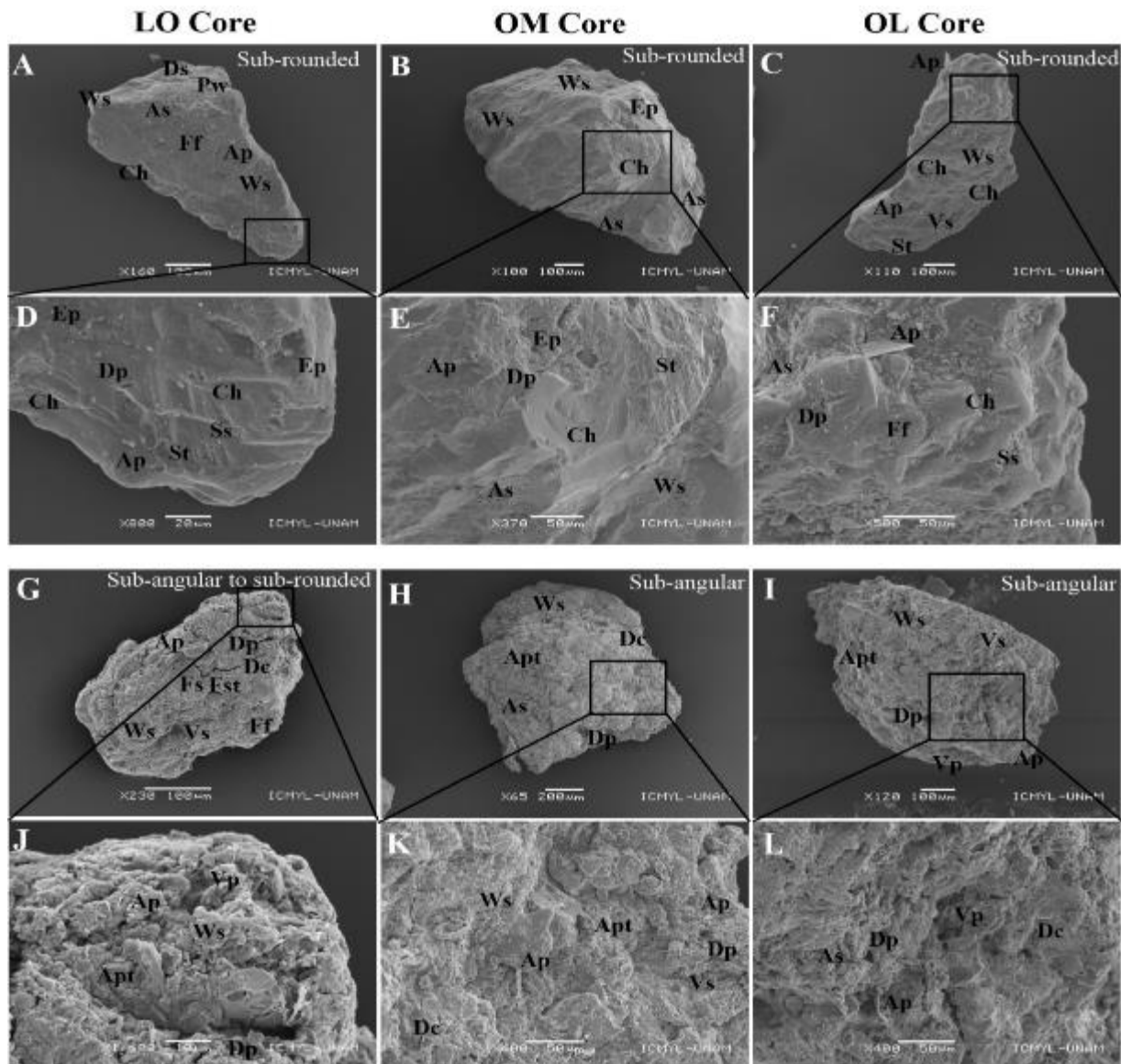
Figure IV.8. Macroscopic organization of core sediments from the Ngaoundaba Crater Lake: **a)** AZ core and **b)** NL core

IV.2. Quartz grain microtextures

Quartz grain microtexture were applied in Ossa lakes Complex and in Ngaoundaba Lake. Based on grain roundness, identified quartz grains were selected from each sample to be examined under SEM. In order to get detailed information about the genesis and conditions during transport, deposition of sediments, and post-sedimentary processes which formed the quartz grain surface, SEM analysis of the microstructures was carried out on quartz grain surfaces (Whalley and Krinsley, 1974; Traczyk and Woronko, 2010). Two stages including sharpness of grain edges (sub-rounded to angular) and identification of microstructures on the grain surfaces (Woronko, 2012) were applied for this study. In additional, on the grain surfaces, chemical and mechanical weathering have been noted. These sediments are dominated by sub-rounded sand grains.

IV.2.1. Ossa lake Complex

SEM images from these studied sites are composed of sand grains with physical alteration (Figures IV.9A-F) and chemical weathering (Figures IV.9G-L). The microtextures of the surface quartz grains from Ossa Lakes Complex present numerous features (Figures IV.9A-L).



Figures IV.9. SEM images of quartz grain surfaces and shapes from the Ossa lake Complex: A-F) sub-rounded shapes and surface grains and G-L) sub-angular to angular shapes (As: abrasive surface; Fs: fracture surface; Ff: fracture face; St: striation; Fst: fatigue striation; Sc: scaling; Dc: dissolution crust; Ws: weathering surface; Pw: preweathering surface; Dp: dissolution pit; Ep: etch pit; Ch: conchoidal fracture; Ap: adhered particle; Ss: straight step; Vs: vesicular shards; Vp: V-shaped pit; **Apt**: Amorphous precipitation)

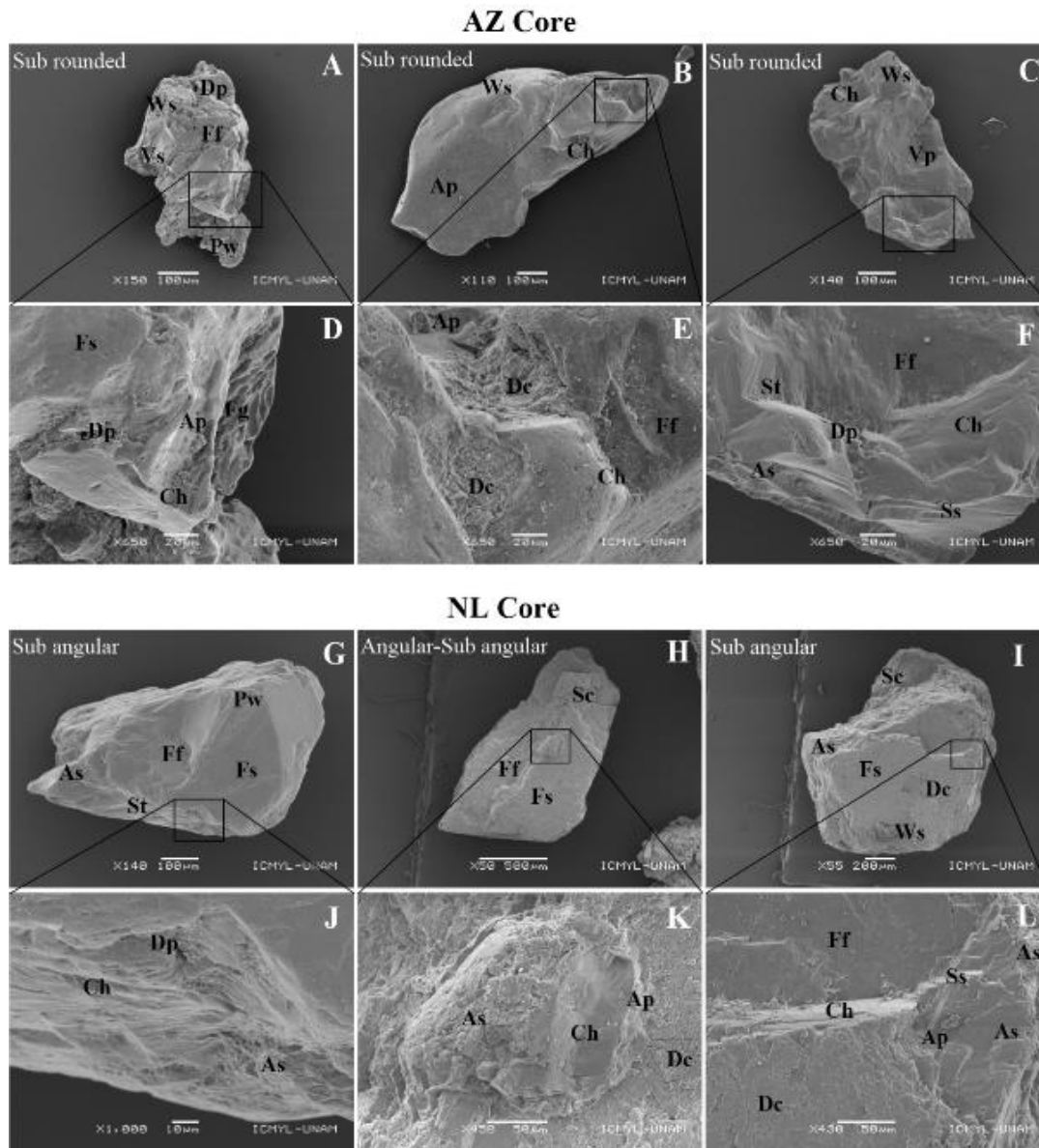
Microtextures due to mechanical alteration include fatigue striations, abrasive surfaces, striations, conchoidal fractures, straight step and V-shaped pits. Sand grains from Ossa Complex sediments presents various types of chemical features, such as scaling, amorphous precipitations, etch pits, dissolution crust, dissolution pits, weathering surface, and vesicular shards. Adhering particles located within pits and other impact regions on the surface of sand grains are produced by both mechanical and chemical features. The sub-rounded shape of the grain provides information about the distal provenance of the grain occur by a fluvial process and a long transport probably by the Sanaga River. The sub-angular shape could be the result of chemical weathering such as dissolution affected by sand grain during the short transport distance from the source rock which weakens the grain's shell and makes it vulnerable.

IV.2.2. Ngaoundaba Lake

The microtextures of the surface of quartz grains from different sample showed also both mechanical and chemical microtexture features (Figures IV.10A-F). The AZ core sand grains are mostly sub rounded (Figures IV.10A-C). However, those from NL core are sub angular to angular (Figures IV.10G-I). Microtextures due to mechanical weathering include fresh surfaces, abrasive surfaces, striations, conchoidal fractures, straight step and V-shaped pits. Most of the sand grains from Ngaoundaba Lake sediments showed various types of chemical features, such as scaling, preweathering surface, dissolution pits, weathering surface, and vesicular shards. Adhering particles located within pits and other impact regions on the surface of sand grains are produced by both mechanical and chemical features.

Surface microtextures embedded in grains can be related to some mechanical and chemical processes, whereas others may follow the principle of equifinality due to geological processes. The mechanical action of lacustrine sediments including fresh surfaces, abrasive surfaces, striations, conchoidal fractures, straight step and V-shaped pits that affect the surface texture of minerals. The effects of abrasion in abrasive surfaces and straight step are clearly engraved in the surface of the grains in this study, that reflect sustained high shear stress and conchoidal fractures on the subrounded edges. Straight step is generally characteristic of a tectonic origin, and can be related to fault systems (Mahaney, 2002), whereas conchoidal fractures are known on aeolian sands. In this study, these conchoidal fractures are both fresh and weathered. The latter coated by amorphous silica, it is clear a significant population of samples are reworked, possibly sourced from a warmer and more humid palaeoclimate and possibly involving aeolian transport. Fluvial action produced collisions between two grain

resulting in V-shaped pit which are interpreted to a deposition in high energetic subaqueous environments like the hillside of the Ngaoundaba Crater.



Figures IV.10. SEM images of quartz grain surfaces and shapes from the Ngaoundaba crater Lake: A-F) sub-rounded shapes and surface grains of core AZ and G-L) sub-angular to angular shapes and surface grains of core NL (As: abrasive surface; Fs: fracture surface; St: striation; Pw: preweathering; Sc: scaling; Dc: dissolution crust; Ws: weathering surface; Dp: dissolution pit; Ch: conchoidal fracture; Ap: adhered particle; Ss: straight step; Vs: vesicular shards; Vp: V-shaped pit; Fg: flinty globules)

IV.3. Total Organic Carbon (TOC) and influence on organic matter accumulation

The organic fraction of lake sediments is a mixture of organic compounds, including roots, wood chips, dead leaves, twigs and other biopolymers. These components in turn contain a wide range of organic functional groups in different molecular "environments" (Hedges and Oades, 1997). In the present research, organic matter is relatively high and varies from one lake to another. Their values are grouped in Table IV.2.

Table IV.2. Total organic carbon (TOC) and organic matter (OM) in % from the studied lakes

Simbock Lake			Ossa Lake Complex			Ngaoundaba Lake		
Sample	TOC (%)	OM (%)	Sample	TOC (%)	OM (%)	Sample	TOC (%)	OM (%)
NR12	2.20	3.78	LO1	7.77	13.36	AZ1	17.69	30.50
NR5	2.49	4.28	LO2	6.18	10.63	AZ2	20.43	35.22
NR13	2.52	4.33	LO3	4.26	7.33	AZ3	23.65	40.77
NR4	0.81	1.39	LO4	4.30	7.40	AZ4	21.32	36.76
NR31	2.89	4.97	LO5	4.72	8.12	AZ5	19.39	33.43
NR10	2.69	4.62	LO6	4.66	8.02	AZ6	20.89	36.01
NR3	2.70	4.64	LO7	4.52	7.77	AZ7	21.62	37.27
NR9	1.88	3.23	OM1	7.38	12.69	AZ8	18.24	31.45
NR8	2.06	3.54	OM2	6.10	10.49	AZ9	12.30	21.21
NR2	2.41	4.14	OM3	3.56	6.12	NL1	13.43	23.15
NR7	1.35	2.32	OM4	4.22	7.26	NL2	11.70	20.17
NR6	1.36	2.33	OM5	4.93	8.48	NL3	10.84	18.69
NR11	2.11	3.62	OM6	4.07	7.00	NL4	8.49	14.64
NR1	1.98	3.40	OM7	6.43	11.06	NL5	9.57	16.50
EB1	0.6	1.03	OL1	5.90	10.15	NL6	10.06	17.34
EB2	0.52	0.89	OL2	1.77	3.04	NL7	11.09	19.12
EB3	1.83	3.14	OL3	2.85	4.90	NL8	11.86	20.45
EB4	2.00	3.44	OL4	0.67	1.15	NL9	13.93	24.02
EB5	2.57	4.42				NL10	17.80	30.69
						NL11	19.36	33.38

IV.3.1. Simbock Lake

The sediments have a total organic carbon (TOC) ranging from 0.52 to 2.89 %. The organic matter (OM) varies from 0.89 to 4.97 % (Table IV.2). In the core NR, TOC values range between 0.81 and 2.89 % and OM varies from 1.39 to 4.97 %. In the core EB, TOC is between 0.6 and 2.57 % and OM varies from 0.89 to 4.42 %. The surface layer within the first 15 cm has the highest OM (4.42 %). It tends to decrease with depth (Figure IV.11). The abundance of organic matter is located in the center core (NR).

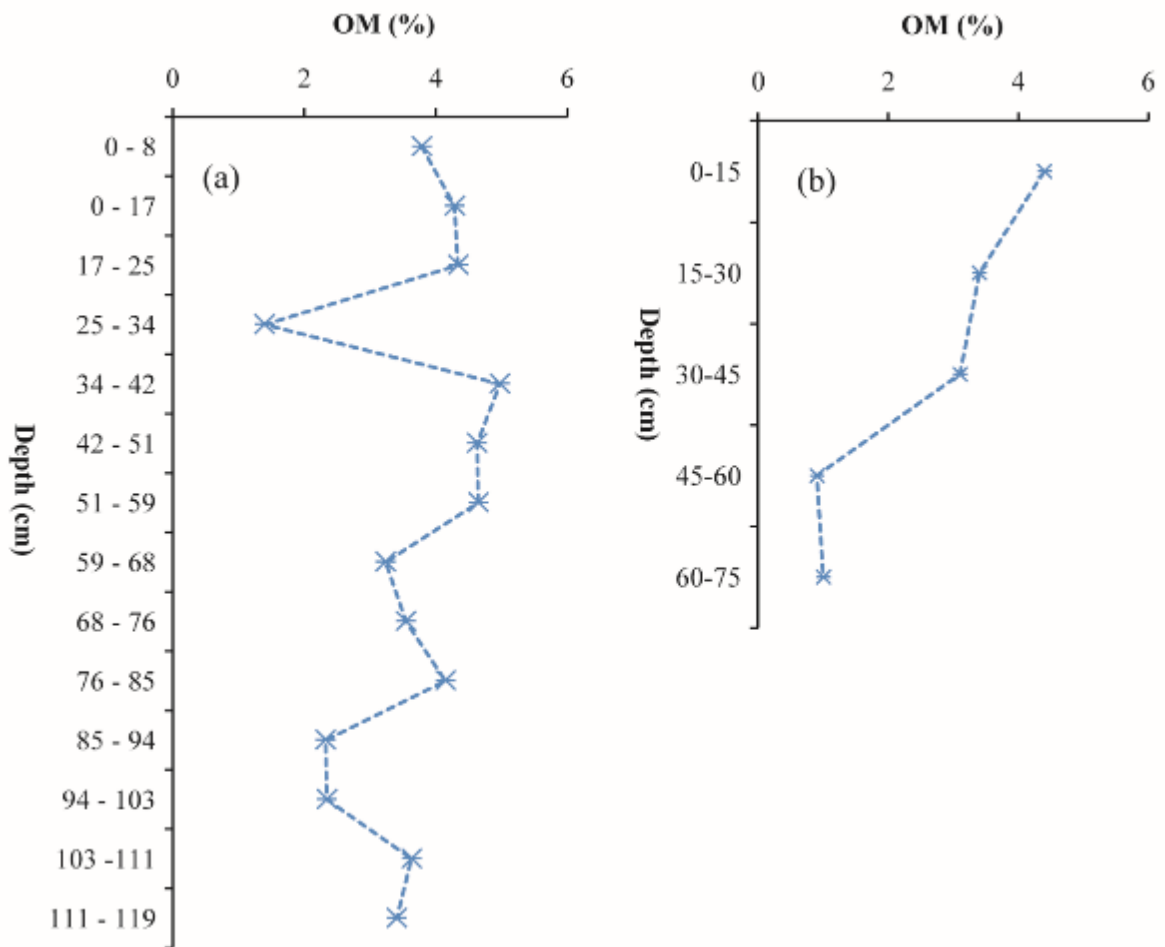


Figure IV.11. Vertical distribution of OM concentrations in sediments from Simbock Lake: a) NR core and b) EB core

IV.3.2. Ossa lake Complex

The content of the TOC of the sediment from the Ossa Lake Complex is shown in Table IV.2 and Figure IV.12, values in selected samples are generally higher than the values of the average shale (Wedepohl, 1971). They vary from 3.56 to 7.77 % with an average value of 5.94 %. This high TOC content can be linked to the presence of organic debris. From the TOC, OM content varies from 6.12 to 13.56 % in the sediments of the Ossa Lakes Complex. The supplying river sediment contents vary from 0.67 to 5.90 %, with a mean percentage of 2.8 and were the lowest TOC value is located in OL4 level from OL core. Organic matter of this core appears as the lowest and vary from 1.15 to 10.15 %.

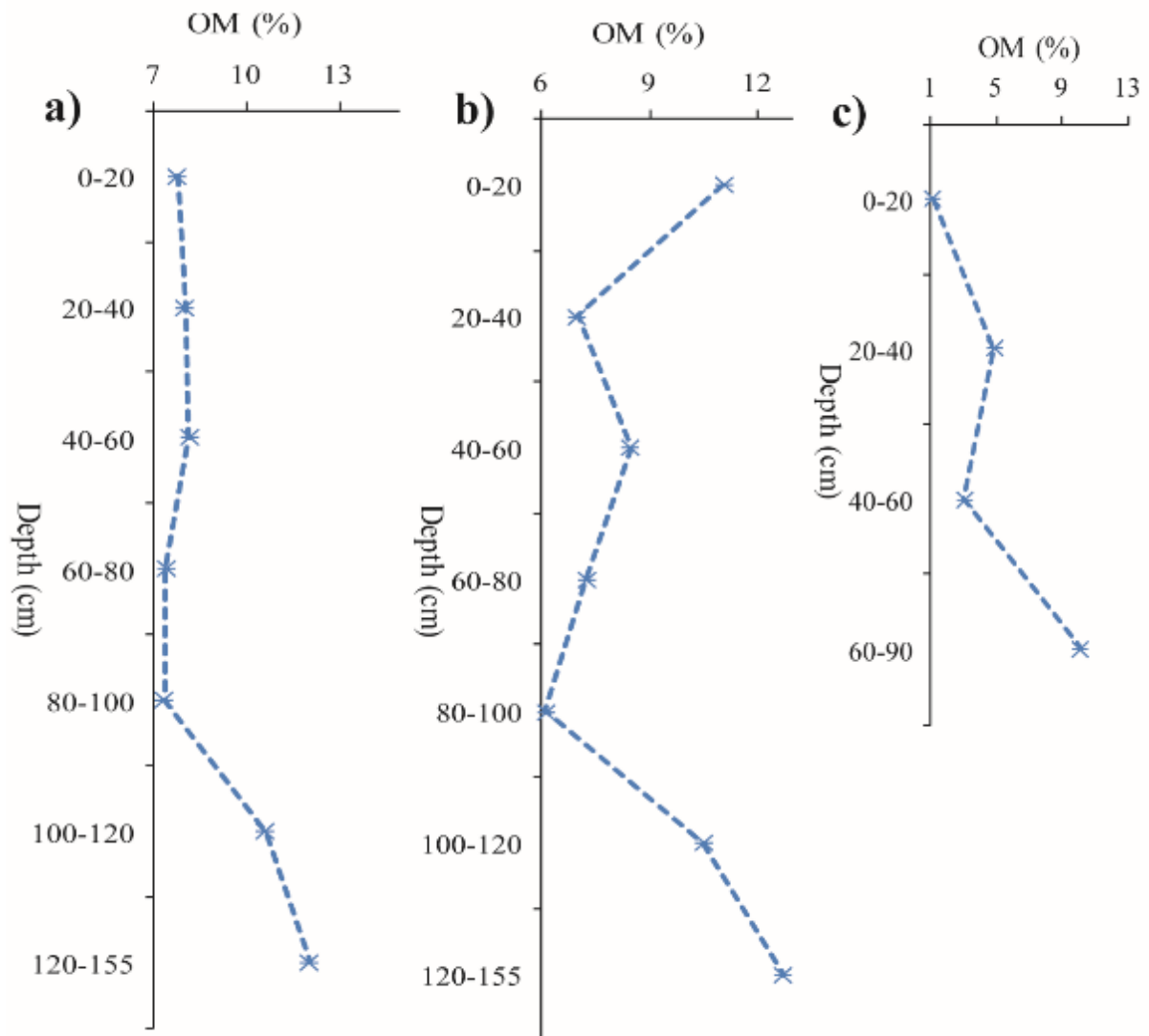


Figure IV.12. Vertical distribution of OM concentrations in sediments from Ossa lakes Complex: a) LO core; b) OM core and c) OL core

IV.3.3. Ngaoundaba Lake

In both cores AZ and NL, the concentrations of TOC vary from 12.3 to 23.7 % and 8.5 to 19.9 % respectively. It corresponds to high content of organic matter in the Lake sediments. This content is higher in AZ core with 21.2 to 40.8 %. In NL core it's about 14.6-24 % (Figure IV.13). These contents are slightly lower than the values recorded from previous studies in the Fonjack Lake (N'anga et al., 2018) from the Adamawa region.

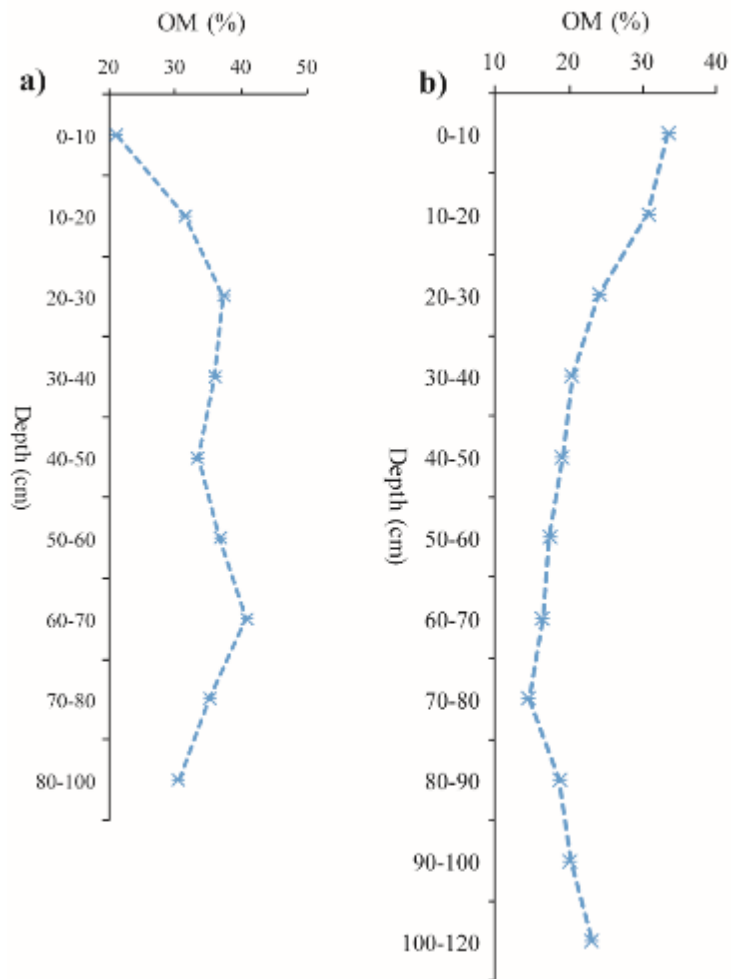


Figure IV.13. Vertical distribution of OM concentrations in sediments from Ngaoundaba Lake: a) AZ core and b) NL core

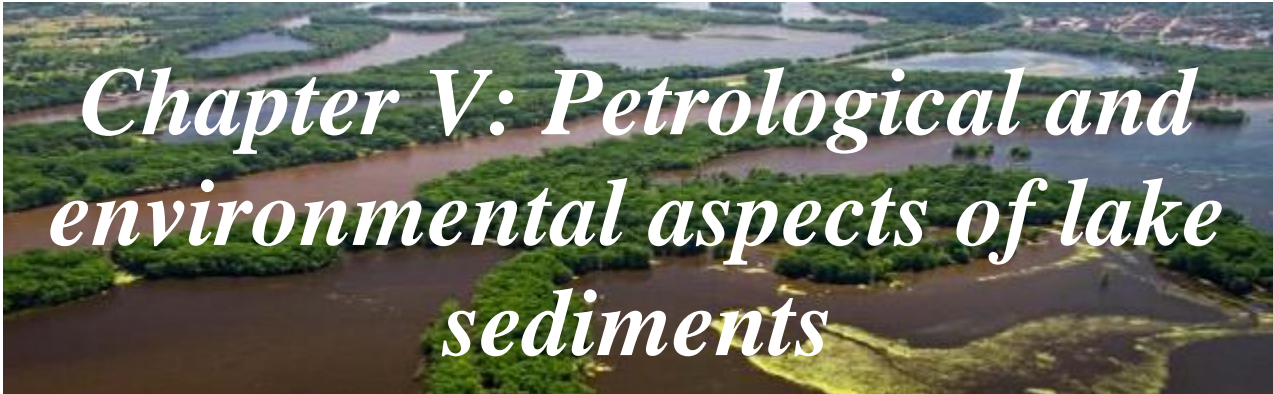
Conclusion

The sediments from studied lakes of South and North of Cameroon has characteristics which vary from one lake to another in some similarities.

Located in an urban area (Yaoundé), the artificial Simbock Lake is shallow with 1.5 m mean depth. The sediment pile is lower in the center and at the edge. The sediment from this lake are moderately humid with light brown to dark brown color. Grain sizes from these lakes show high content of sands and clay which confer to the sediment a clayey sand texture. The sediment samples from this lake would have undergone a long fluvial transport with high content of organic matter.

Known as one of the most popular lakes in Cameroon, the Ossa lake Complex is a subduction lake composed of several lakes in the Dizanguè region. This lake is deep and goes over 10 m with a very large pile of sediments. These sediments are mixed with some organic matter and are quite humid. The color of these sediments varies generally from dark brown to dark with a quite high proportion of organic matter. Sediment cores from this complex have high proportion of silts and clays with a clayey silt texture. The quartz grains shapes which are generally sub-rounded would have undergone a long fluvial transport and sometimes less. These grains confirm a physical and chemical alteration of the surrounding rocks and quite far away.

The last lake is a crater lake located near Ngaoundéré town in Northern Cameroon. Ngaoundaba crater Lake as it is called is very deep, up to 17 m on average with a very high-water depth and a large pile of very wet sediment. These sediments have a very high proportion of plant debris and the layer after the water is a herbaceous peat which favours a large percentage of organic matter. The overall dark pile of sediment consists of a high proportion of silt and moderate clay gives the sediment a clayey silt texture. The sand grains of this lake have sub-rounded shapes for the sediments from the center of the lake and mainly subangular for those at the edge. These sediments are the result of aeolian transportation for the sediments from the centre and low turbulent transport for those from edge.



*Chapter V: Petrological and
environmental aspects of lake
sediments*

What counts cannot always be counted, and what can be counted does not necessarily count.

-Albert Einstein-

This chapter deals with the mineralogy of the sediments of the studied lakes as well as the chemistry of their mineral phases. It also provides information on the geochemical distribution of the materials deposited on the lake bottoms in the South and North of the country. In this chapter, the degree of contamination of these lakes will also be assessed in order to determine their potential environmental impact. This will then give us a better compression of these sediments.

V.1. Mineralogy of lacustrine sediments

This part includes several methods using for the different area. It gives results and interpretations of bulk mineralogy, fine mineralogy after specific treatments, FT-IR spectrometry and mineral chemistry on phase minerals.

V.1.1. Simbock Lake

The mineralogical procession of Simbock Lake sediments was determined by bulk and fine mineralogy (XRD) associated to FT-IR spectrometry.

The mineral assemblages of the NR core are composed of quartz, illite, kaolinite, goethite, rutile, and feldspars (Figure V.1a). The principal peaks of kaolinite (7.16 and 3.58 Å) do not occur in NR2, NR8, NR31, and NR4 samples (Figure V.1a). In the previous samples, kaolinite is present in few amounts, which are relative to the sandy texture (Table V.1). The mineralogical composition of sediments from the EB core is similar to that of the previous one, with gibbsite as an additional mineral (Figure V.1b). Gibbsite is present in small amounts in the EB3, EB4, and EB5 samples while kaolinite occurs in small quantities in EB2 and EB1 samples as trace (Figure V.1b). The mineral assemblage of both core sediments is dominated by quartz (Figure V.1). The proportion of kaolinite is higher in the EB core than is that of NR (Figure V.1).

Two oriented samples (NR3 and EB4) were analyzed to confirm the presence of kaolinite, illite, and smectite (Figure V.2). In sample NR3, the diffraction peaks at 10.01 Å and 7.16 Å are not displaced during glycolation and confirm the presence of illite and kaolinite. The 7.16 Å diffraction peak disappears after firing at 550 °C as expected while the 10.01 Å peak remains observable (Figure V.2a). The increase in intensity of the 10.01 Å diffraction peak following thermal treatment at 550 °C is due to the collapse of the smectite diffraction peak at

10 Å. In sample EB4, the glycerol solvation clearly leads to the displacement of the diffraction peak at 14.04 Å to 14.16 Å, indicating the appearance of smectite (Figure V.2b).

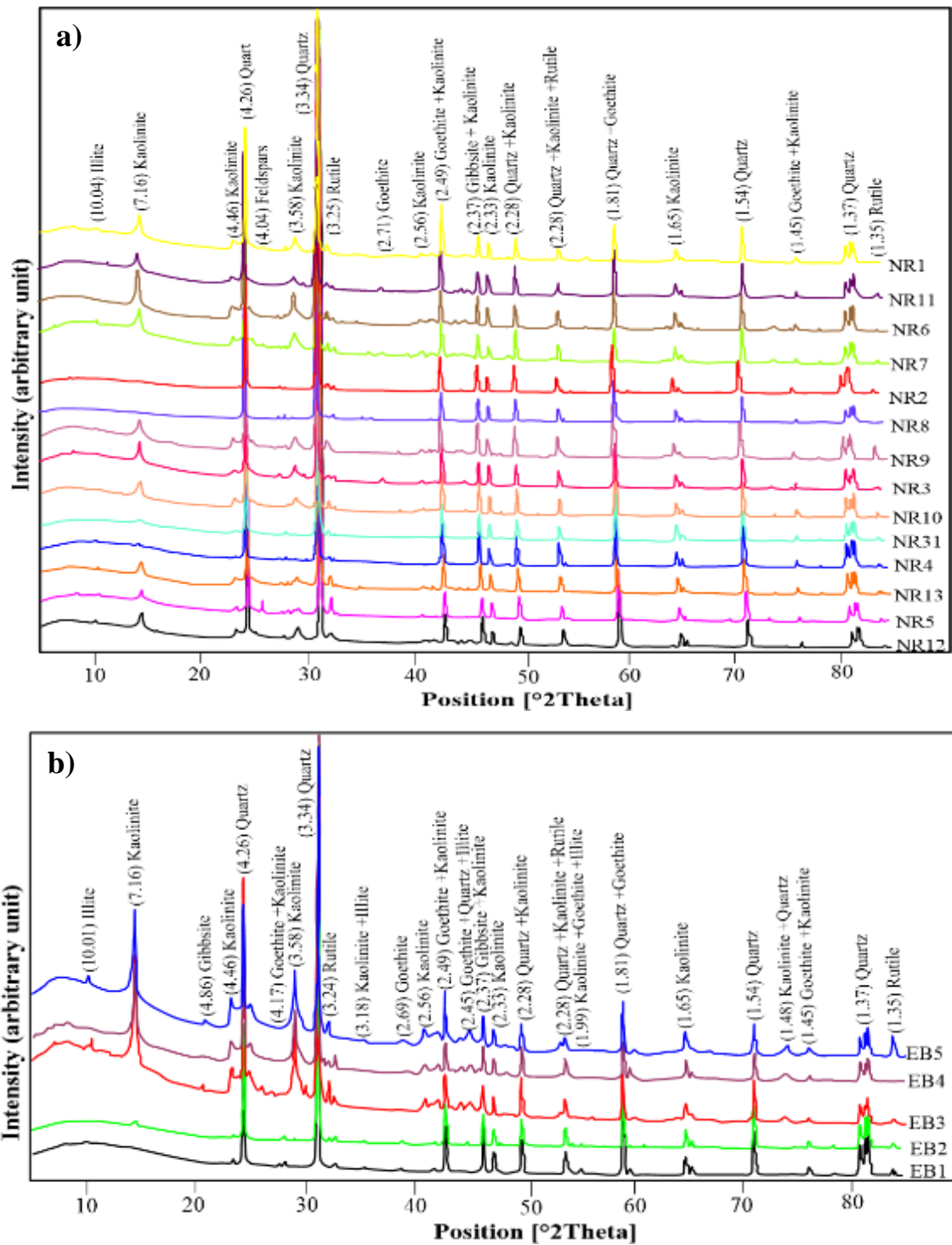


Figure V.1. X-ray diffraction spectra for Simbock Lake bulk sediments: **a)** NR core and **b)** EB core

The diffraction peaks at 10.03 Å and 7.16 Å are not sufficiently displaced during glycolation and further confirm the presence of illite and kaolinite. The 7.16 Å diffraction peak disappears

after firing at 550 °C as expected while the 10.01 peak remains observable. The increase in intensity of the 10.03 Å diffraction peak following thermal treatment at 550 °C is because of the collapse of the smectite diffraction peak at 10 Å which is an additional evidence of smectite.

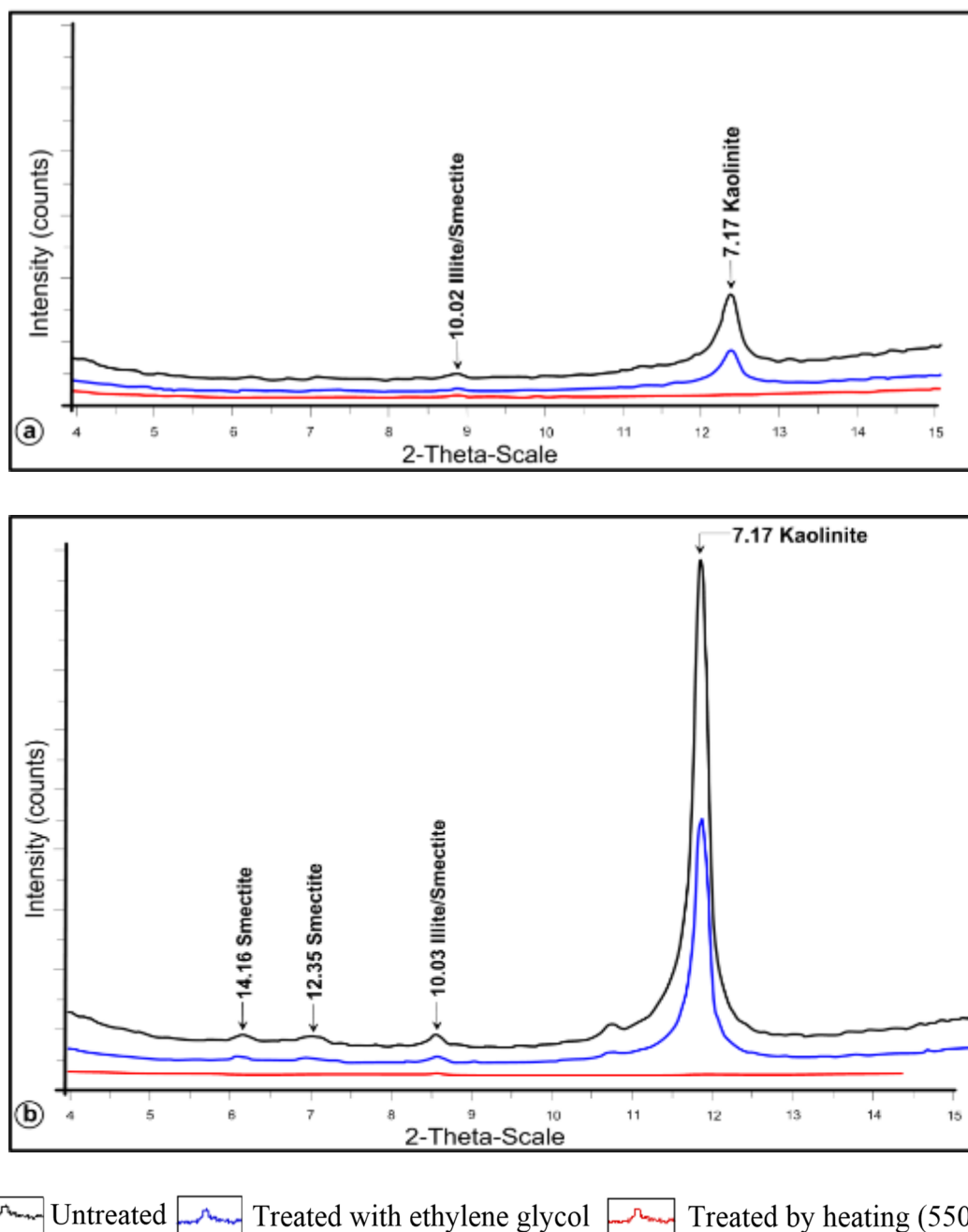


Figure V.2. X-ray diffraction spectra of the finest grain-sized fractions for after specific treatments: **a)** Sample NR3 of NR core and **b)** Sample for sample EB4 of EB core

The FT-IR spectra are typical of kaolinite minerals (Figure V.3). The bands at 3691, 3664, 3652, and 3620 cm^{-1} in the EB series are characteristic stretching bands of O–H bonds in the kaolinite structure (Figure V.3a, Table V.1). In the NR series, the bands at 3694 and 3620

cm-1 are the only kaolinite O–H bands observable (Figure V.3b, Table V.1) and is an indication that the kaolinite in these samples is less ordered in comparison to that of the EB samples.

Table V.1. Position of the main detected dust infrared band peaks with transition assignment

Wave number (cm ⁻¹)	NR core			EB core			Assignment
	NR6	NR3	NR1	EB5	EB4	EB3	
3694-3691	3694	3694	3694	3691	3691	3691	OH stretching of inner-surface hydroxyl groups
3664	-	-	-	3664	3664	3664	OH stretching of inner-surface hydroxyl groups
3652	-	-	-	3652	3652	3652	OH stretching of inner-surface hydroxyl groups
3620	3620	3620	-	3620	3620	3620	OH stretching of inner hydroxyl groups
1627-1623	1627	1627	-	1623	1623	1623	in-plane Si–O stretching
1107	-	-	-	1107	1107	1107	in-plane Si–O stretching
1032-1025	1032	1032	1032	1025	1025	1025	Si–O stretching
1004	-	-	-	1004	1004	1004	in-plane Si–O stretching
912-911	912	912	912	911	911	911	OH deformation of inner hydroxyl groups
790-785	785	785	785	790	790	790	OH deformation linked to Al ³⁺ , Mg ²⁺
745	-	-	-	745	745	745	Si–O, perpendicular
684-681	684	684	684	681	681	681	Si–O, perpendicular
530-526	530	530	-	526	526	526	Al–O–Si deformation
461	-	-	-	461	461	461	Si–O–Si deformation
447	447	447	447	-	-	-	Si–O–Si deformation

(–) not detected

The bands at 3691 cm-1 or 3694 cm-1 are assigned to surface O–H, in-phase stretching vibration; the bands at 3664 and 3652 cm-1 are attributed to the surface O–H, out-of-phase stretching vibration and the band at 3620 cm-1 is known as the inner O–H stretching vibration (Frost et al. 2001; Mbey et al. 2013). The characteristic band at 3664 cm-1 is indicative of improved crystallized kaolinite in the EB samples. A Si–O stretching at 1107 cm-1 and Si–O–Si symmetric stretch at 1004 cm-1 and a bending vibration of Al–OH at 911 cm-1 and a –OH (Al–OH) translational vibration at 790 are observed. The stretching bands of Si–O in quartz are also observable at 745 cm-1 and 681 cm-1 (Figure V.3). In addition, Si–O–Si deformation bands appeared at 447 (or 461) cm-1 and the bands at 530 (or 536) cm-1 are associated with both Si–O–Al and Si–O–Si deformations. The sand enrichment in the NR samples causes the bands at 687 cm-1 to be better developed in comparison to their counterparts in the EB samples at 681 cm-1 (Figure V.3).

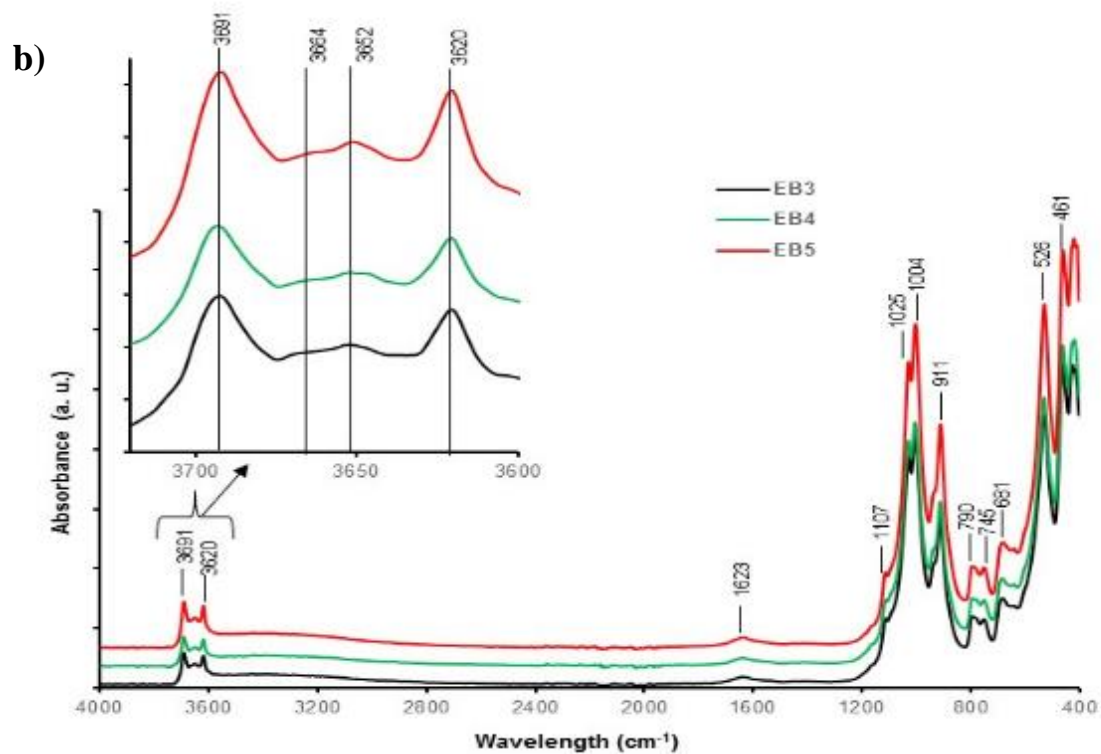
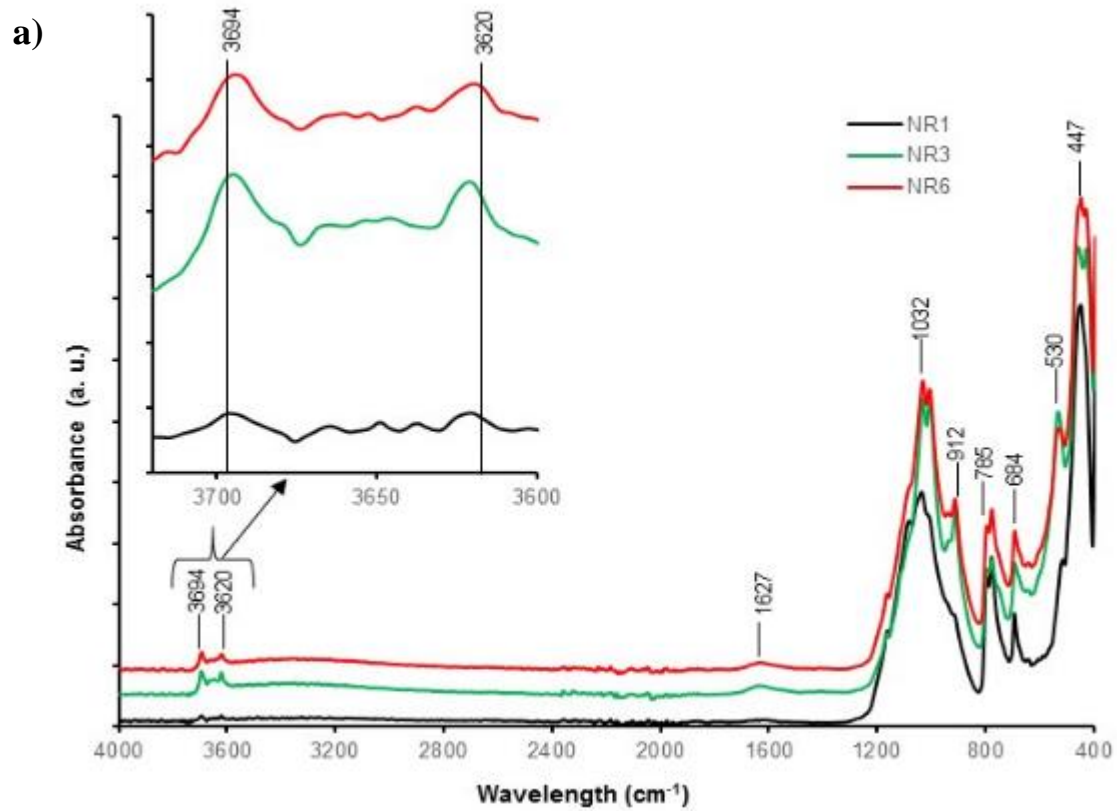


Figure V.3. FT-IR spectra of the sediments from the Simbock Lake: a) core NR and b) core EB

V.1.2. Ossa Lake Complex

In the Dizanguè lake Complex, the mineralogy was determined using bulk mineralogy by XRD and SEM-EDS.

The bulk mineralogy of the core samples (n = 18) using XRD revealed no remarkable variation in the mineralogical assemblages of different level of the cores OL, OM and LO, while the dominant minerals are quartz and clay minerals. X-ray diffraction studies revealed mostly the presence of kaolinite, quartz, illite, rutile, goethite, gibbsite, feldspars, vivianite and illite-smectite in the Ossa lake Complex (Figure V.4a-c). The three cores have the same mineral phase consisting predominantly of kaolinite (18.75–22.32 %), quartz (18.75–22.22 %) and illite (16.66–21.80 %), in addition to moderate proportions of rutile (9.38–12.5 %), goethite (6.24–9.38 %) and gibbsite (5.55–6.25 %) with feldspar, vivianite, illite-smectite and undetermined minerals being minor constituents (<5 wt.%).

Scanning electron microscope (SEM) images at 500 µm indicated the presence of mineral assemblages similar to the XRD. Thus, the aggregates of the cores from Ossa Complex are mainly composed of kaolinite, quartz, rutile, illite, goethite, vivianite, zircon and feldspars (Figure V.4a and b).

Table V.2. Chemical composition (wt.%) of minerals analyzed by SEM-EDS in sediments from the Ossa lakes Complex

Element	Kaolinite	Rutile	Goethite	Feldspar	Zircon	Illite	Vivianite
Na ₂ O	0.88	0.25	0.39	0.07	0.00	0.64	0.00
MgO	0.97	0.00	0.00	5.15	0.13	0.15	0.23
Al ₂ O ₃	16.58	0.44	8.83	16.74	0.25	10.71	2.14
SiO ₂	58.03	0.41	3.53	44.81	21.96	57.12	3.63
K ₂ O	2.32	0.25	0.00	4.67	0.39	4.24	0.34
CaO	1.01	0.23	0.35	2.52	0.00	1.69	0.00
TiO ₂	1.87	97.59	1.12	1.93	0.78	2.59	0.40
Cr ₂ O ₃	0.03	0.00	9.31	0.00	0.00	0.00	0.07
MnO	1.13	0.00	0.00	0.77	0.00	0.52	0.37
FeO	15.37	0.67	76.47	20.87	0.00	0.88	57.81
NiO	1.83	0.15	0.00	2.47	1.25	1.48	0.00
Cl	0.00	0.00	0.00	0.00	0.00	0.00	0.12
P ₂ O ₅	0.00	0.00	0.00	0.00	0.00	0.00	34.90
ZrO ₂	0.00	0.00	0.00	0.00	75.24	0.00	0.00
Total	100.00	100.00	100.00	100.00	100.00	100.00	100.00
N.F	10.11	6.08	6.01	5.69	4.29	6.24	19.71

N.F. Normalization factor

Chemical composition is consistent with the mineralogy data (Table V.2 and Figure V.5).

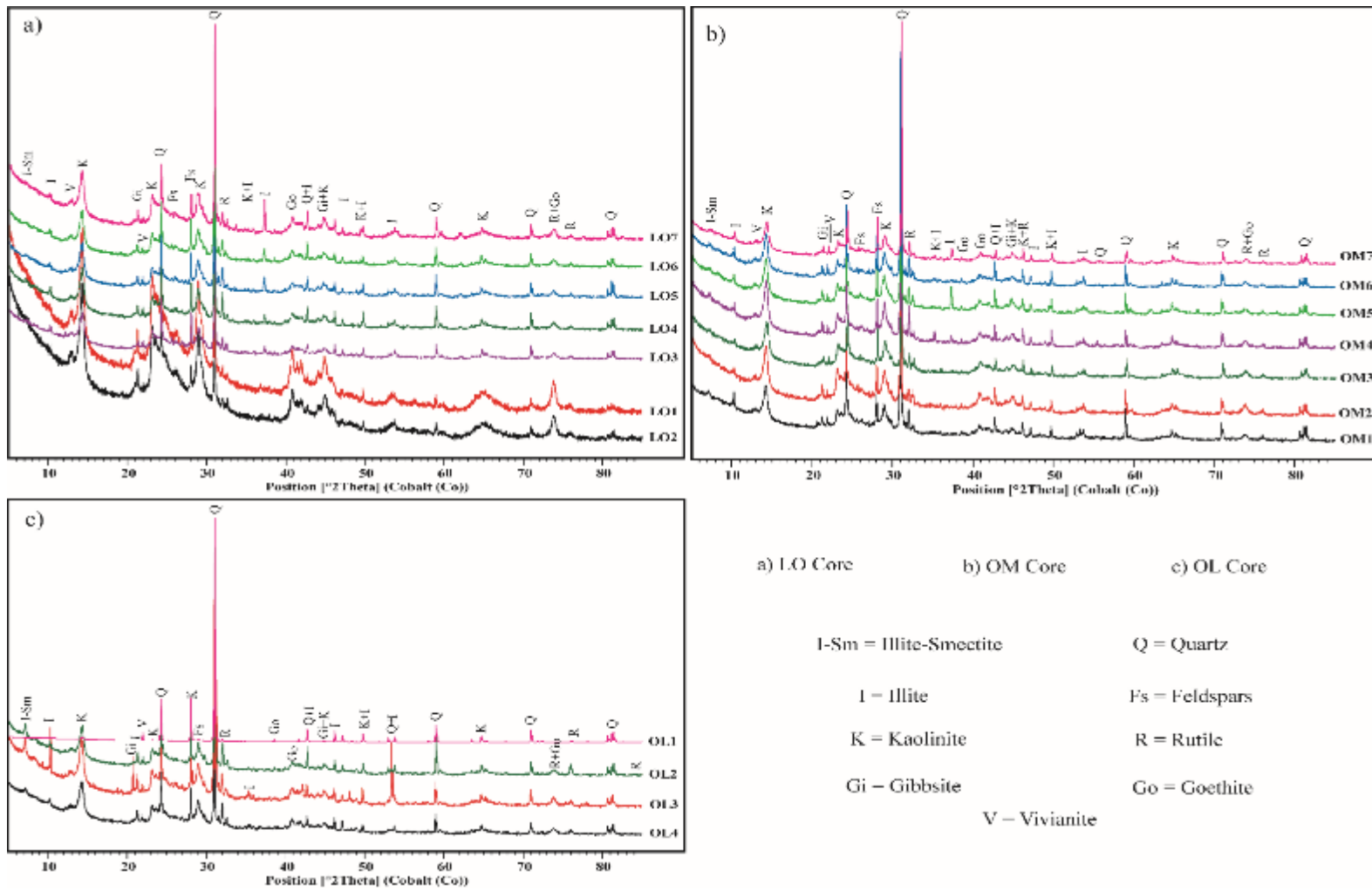


Figure V.4. X-ray diffraction spectra for sediments from Ossa lakes Complex

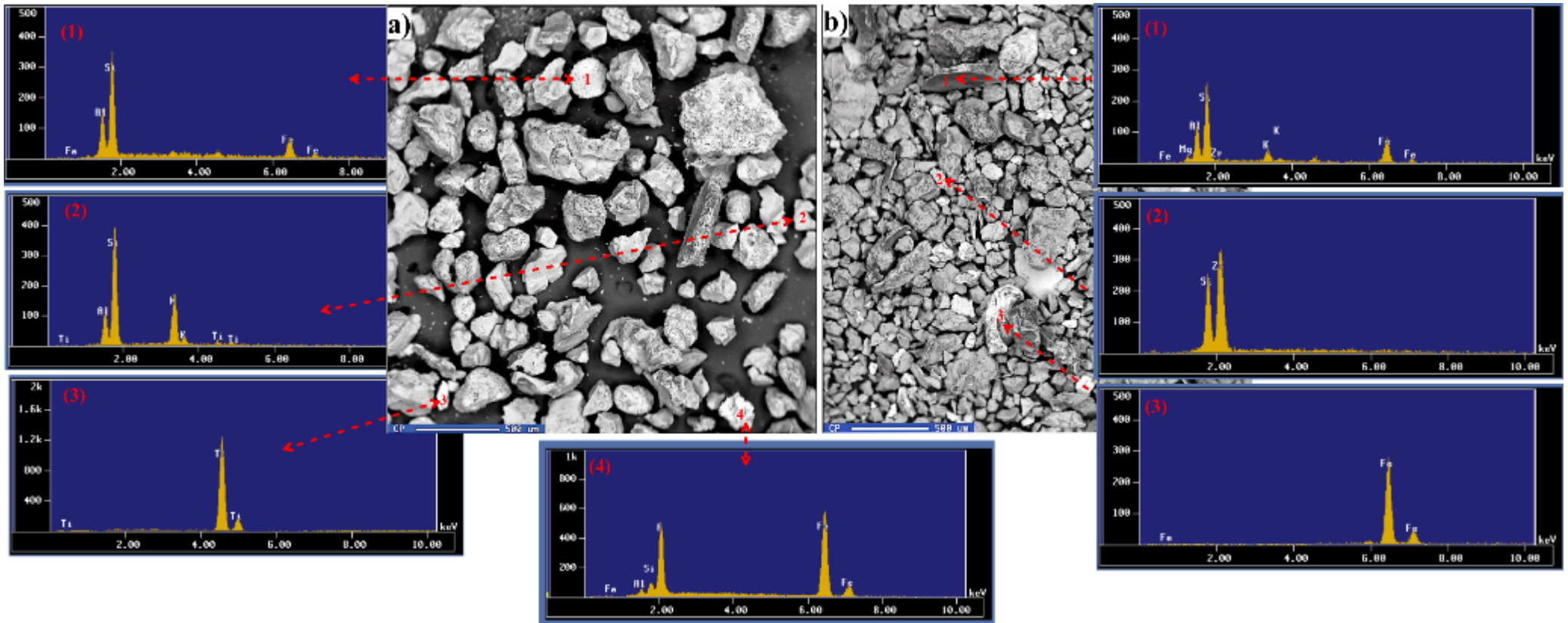


Figure V.5. Scanning electron microscope and SEM-EDS spectrum for sediments from the Ossa lakes Complex: **a)** core MO with **1)** kaolinite; **2)** illite; **3)** vivianite and **4)** rutile; **b)** core OL with **1)** feldspars; **2)** zircon and **c)** goethite

The chemical composition of samples (n = 8) from Ossa lake Complex shows high content of SiO₂, Al₂O₃ and FeO in some grains confirm the presence of kaolinite (Figure V.5a1); rutile (Fig. 5a4) and goethite (Fig. 5b3). Illite is mainly composed of SiO₂, Al₂O₃ and K₂O (Figure V.5a2). In Figure V.4b1, feldspars are distinguished by the presence of Al₂O₃ and SiO₂ with moderate proportion of FeO and trace of MgO and K₂O. Zircon is a natural zirconium silicate, it is not identified in XRD pattern but present in almost all selected sample cores (Figure V.5b2). Similarly, vivianite, which is a hydrated iron phosphate mineral common in all geological environments is identified in Ossa lake Complex, revealed by the presence of high content of FeO and P₂O₅ (Figure V.5a3).

V.1.3. Ngaoundaba Lake

In this site, the mineralogy was determined using bulk mineralogy by XRD and SEM-EDS as the previous site.

Mineralogical analyses of bulk sediments from Ngaoundaba Lake is reported in figure V.6. Almost all sediment samples in the Lake are mineralogically similar. They are mainly composed of quartz, kaolinite and hematite, with minor amounts of feldspars, rutile and calcite. Illite and ilmenite occur in trace amounts.

SEM/EDS images at 500 μm confirm a mineral assemblage similar to those of XRD. Thus, the grains and aggregates of the core sediments from Ngaoundaba Lake except Quartz are mainly composed of kaolinite, ilmenite, hematite, illite, feldspars and rutile (Figure V.7a and b).

EDS analysis showed that the mineral deposits that formed on Lake samples sediments were mainly composed in oxides of silica, alumina, chromium, iron, phosphorous, titanium, calcium, magnesium, manganese and potassium, with high contents of silica, alumina and iron. This high content of SiO₂, Al₂O₃ and FeO in some grains confirm the presence of kaolinite (Figure V.7a2). The presence in high proportion of SiO₂, TiO₂ and FeO in aggregates confirm the presence of Ilmenite (Figure V.7a1). A very significant fraction of the as-received ilmenite concentrate appeared to be TiO₂ (rutile; Fig. 6b3), which still remained as TiO₂. Very high content of FeO refer to hematite in the grain samples (Figure V.7a3). Illite is mainly composed of SiO₂, Al₂O₃ and K₂O (Figure V.7b1). The presence of Al₂O₃ and SiO₂ in high contents, with moderate proportion of FeO and trace of MgO and K₂O feldspar is distinguished (Figure V.7b2).

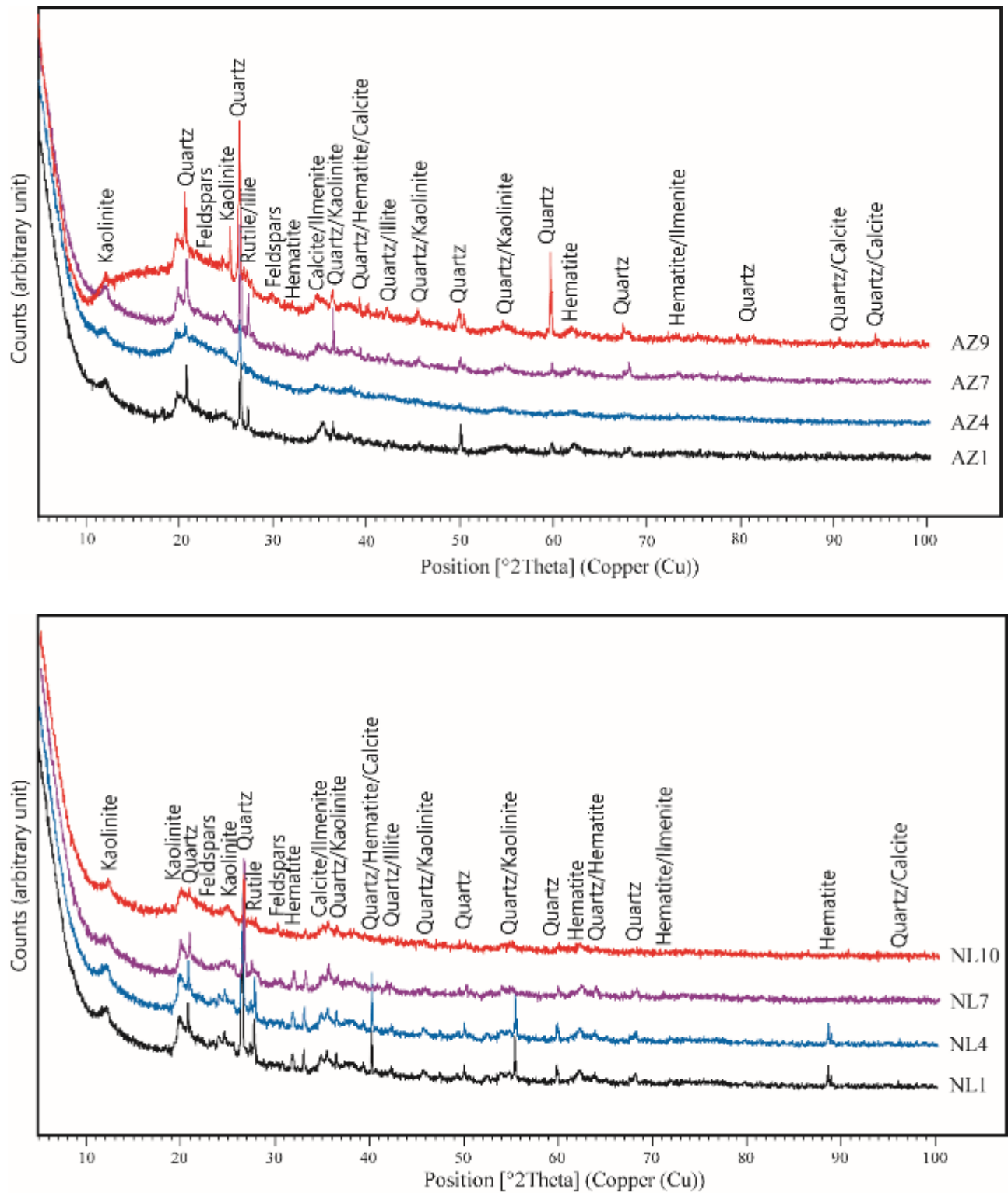


Figure V.6. X-ray diffraction spectra for sediments from Ngaoundaba Crater lake: a) core LO and b) core MO

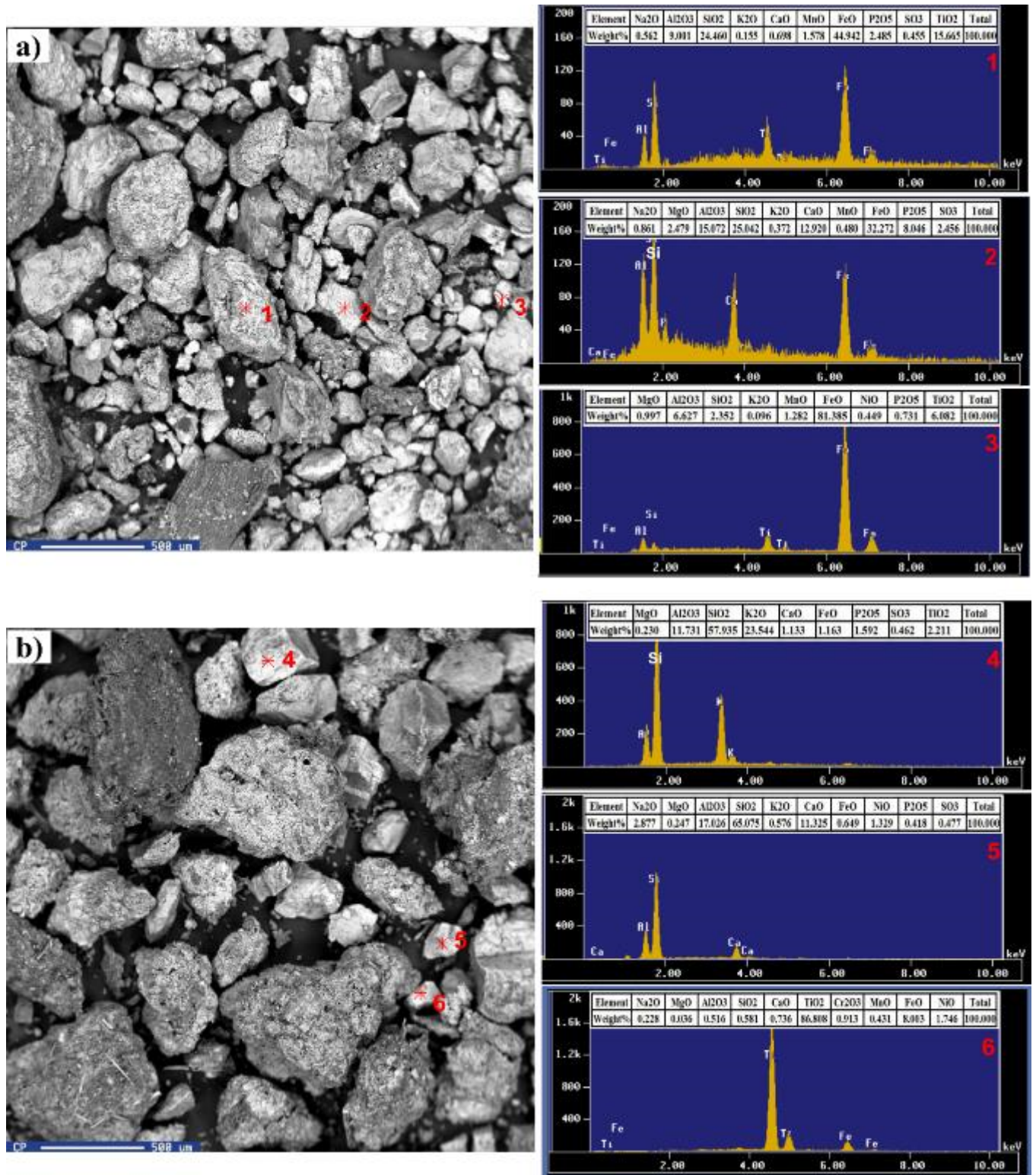


Figure V.7. Scanning electron microscope and SEM-EDS spectrum for grains from the Ngaoundaba Lake: **a)** core AZ with **1)** ilmenite; **2)** kaolinite; **3)** Hematite and **4)** rutile; **b)** core NL with **1)** illite; **2)** feldspars and **3)** rutile

V.2. Geochemistry of lacustrine sediments

The geochemistry (major, trace and rare earth elements) of rocks involves those from the three studied sites (Simbock Lake, Ossa lakes Complex and Ngaoundaba Lake). Sediments from these areas vary in their chemical composition. Their study will provide an in-depth knowledge of their chemical composition and throw more light on the eventual chemical changes after their weathering.

V.2.1. Simbock Lake

V.2.1.1. Major elements

It is noted that all sediments are in order of importance SiO_2 (mean value of 70.46 wt.% for the sediments, 71.55 wt.% in NR core and 67.41 wt.% in EB core), Al_2O_3 (mean value of 12.94 wt.% for the sediments, 11.76 wt.% in NR core and 16.25 wt.% in EB core) and Fe_2O_3 (mean value of 7.87 wt.% for the sediments, 4.32 wt.% in NR core and 4.61 wt.% in EB core). The alkali and alkali earth contents ($\text{Na}_2\text{O} + \text{K}_2\text{O} + \text{CaO} + \text{MgO}$) are relatively low (mean value of 1.07 wt.% in NR core and 0.08 wt.% in EB core). Average TiO_2 contents are 1.75 wt.% and confirm the presence of rutile. The P_2O_5 contents are relatively low (mean value of 0.17 wt.%; Table V.3). Figure V.8 shows negative correlations of almost all the oxides with silica which confirm the abundance of quartz in the core sediments of the Lake.

The Index of Compositional Variability (ICV) is calculated to evaluate mineralogical maturity of sediments. To understand and measure the extent of chemical weathering of the surface area, the Chemical Index of Alteration (CIA) was calculated according to Nesbitt and Young (1984); PIA is also estimated in these sediments. For these indices, CaO^* is the CaO in silicate minerals and the other oxides were recalculated again to 100% taking CaO^* instead of $\text{CaO}_{(\text{total})}$. The mass ratio $\text{SiO}_2/\text{Al}_2\text{O}_3$ is moderately high with a mean value of 6.32, 6.85 for NR core and 4.84 for EB core, and indicates that these sediments contain more components rich in SiO_2 than in Al_2O_3 . The $\text{K}_2\text{O}/\text{Na}_2\text{O}$ ratio is around 0.13 for all the samples, 0.16 for NR core and 0.07 for EB core (Table V.3), this is indicative of the high Na_2O contents in this environment.

Table V.3. Major element composition (wt.%) and element ratios of sediments from the Simbock Lake

	d.l.	NR core															EB core					Average	
		NR12	NR5	NR13	NR4	NR31	NR10	NR3	NR9	NR8	NR2	NR7	NR6	NR11	NR1	Av. 1	EB1	EB2	EB3	EB4	EB5	Av. 2	n = 19
SiO ₂	0.04	65.18	75.91	66.79	86.02	82.74	65.58	70.79	65.02	80.34	63.49	83.3	61.02	68.58	66.95	71.55	86.42	80.31	58.88	58.45	53.01	67.41	70.46
Al ₂ O ₃	0.02	14.36	9.45	13.55	6.86	7.34	13.96	11.12	14.07	8.61	14.49	7.32	16.4	13.03	14.06	11.76	9.39	12.68	19.1	19.24	20.85	16.25	12.94
Fe ₂ O ₃	0.01	5.76	2.93	5.17	1.49	2.03	4.84	4.55	5.74	2.68	5.99	2.02	6.71	5.06	5.5	4.32	0.68	1.62	6.32	6.58	7.87	4.61	4.4
MnO	0.002	0.16	0.11	0.17	0.11	0.13	0.29	0.24	0.5	0.1	0.48	0.17	0.37	0.32	0.16	0.24	0.16	0.03	0.11	0.12	0.13	0.11	0.2
MgO	0.01	0.21	0.18	0.2	0.13	0.13	0.24	0.2	0.23	0.12	0.26	0.11	0.23	0.24	0.23	0.19	0.12	0.16	0.27	0.28	0.28	0.22	0.2
CaO	0.006	0.13	0.12	0.13	0.11	0.11	0.14	0.13	0.16	0.08	0.17	0.1	0.12	0.16	0.17	0.13	0.08	0.09	0.12	0.13	0.14	0.11	0.13
Na ₂ O	0.02	0.13	0.08	0.13	0.06	0.07	0.13	0.09	0.13	0.14	0.07	0.14	0.12	0.07	0.07	0.10	0.02	0.02	0.05	0.05	0.04	0.04	0.08
K ₂ O	0.01	0.69	0.67	0.68	0.52	0.58	0.71	0.75	0.7	0.57	0.6	0.57	0.68	0.67	0.69	0.65	0.26	0.32	0.7	0.69	0.6	0.51	0.61
TiO ₂	0.01	1.74	2.07	1.81	2.01	2.02	1.73	1.76	1.88	2.18	1.79	2.05	1.72	1.95	1.82	1.90	0.76	1.16	1.66	1.65	1.58	1.36	1.75
P ₂ O ₅	0.002	0.18	0.15	0.18	0.07	0.1	0.25	0.17	0.25	0.13	0.25	0.09	0.23	0.21	0.18	0.17	0.03	0.07	0.23	0.23	0.26	0.16	0.17
LOI	0.05	10.34	7.54	10.36	2.39	4.09	11.2	9.55	9.9	4.46	11.23	3.84	11.54	8.6	9.37	8.17	1.02	2.44	11.5	11.72	14.25	8.19	8.18
Sum	-	98.95	99.25	99.23	99.8	99.38	99.13	99.42	98.62	99.44	98.97	99.76	99.21	98.94	99.24	99.24	98.81	98.91	99.02	99.21	99.07	99.00	99.18
ICV	-	0.57	0.58	0.56	0.57	0.61	0.53	0.63	0.61	0.62	0.6	0.63	0.57	0.6	0.57	0.59	0.19	0.24	0.45	0.46	0.48	0.36	0.52
CIA (%)	-	93.79	91.54	93.51	90.87	90.57	93.44	91.96	93.43	91.6	94.51	90.04	94.69	93.54	93.82	92.67	96.34	96.72	95.62	95.69	96.42	96.16	93.58
PIA (%)	-	98.13	97.74	98.02	97.4	97.35	98	97.9	97.88	97.34	98.29	96.57	98.5	98.17	98.27	97.83	98.95	99.12	99.06	99.06	99.14	99.07	98.32
SiO ₂ /Al ₂ O ₃	-	4.54	8.03	4.93	12.54	11.27	4.7	6.37	4.62	9.33	4.38	11.38	3.72	5.26	4.76	6.85	9.2	6.33	3.08	3.04	2.54	4.84	6.32
Na ₂ O/K ₂ O	-	0.19	0.12	0.19	0.12	0.12	0.18	0.12	0.19	0.25	0.12	0.25	0.18	0.1	0.1	0.16	0.08	0.06	0.07	0.07	0.07	0.07	0.13

d.l.: detection limits.

ICV = (Fe₂O₃* + K₂O + Na₂O + CaO + MgO + TiO₂)/Al₂O₃ from Cox et al. (1995).

CIA (%) = (Al₂O₃ / (Al₂O₃+CaO*+Na₂O+K₂O)) × 100 from Nesbitt and Young (1984).

PIA = [(Al₂O₃ - K₂O) / (Al₂O₃ + CaO* + Na₂O - K₂O)] × 100 from Fedo et al. (1997). Where CaO* correction was using followed the procedure of McLennan et al. (1993).

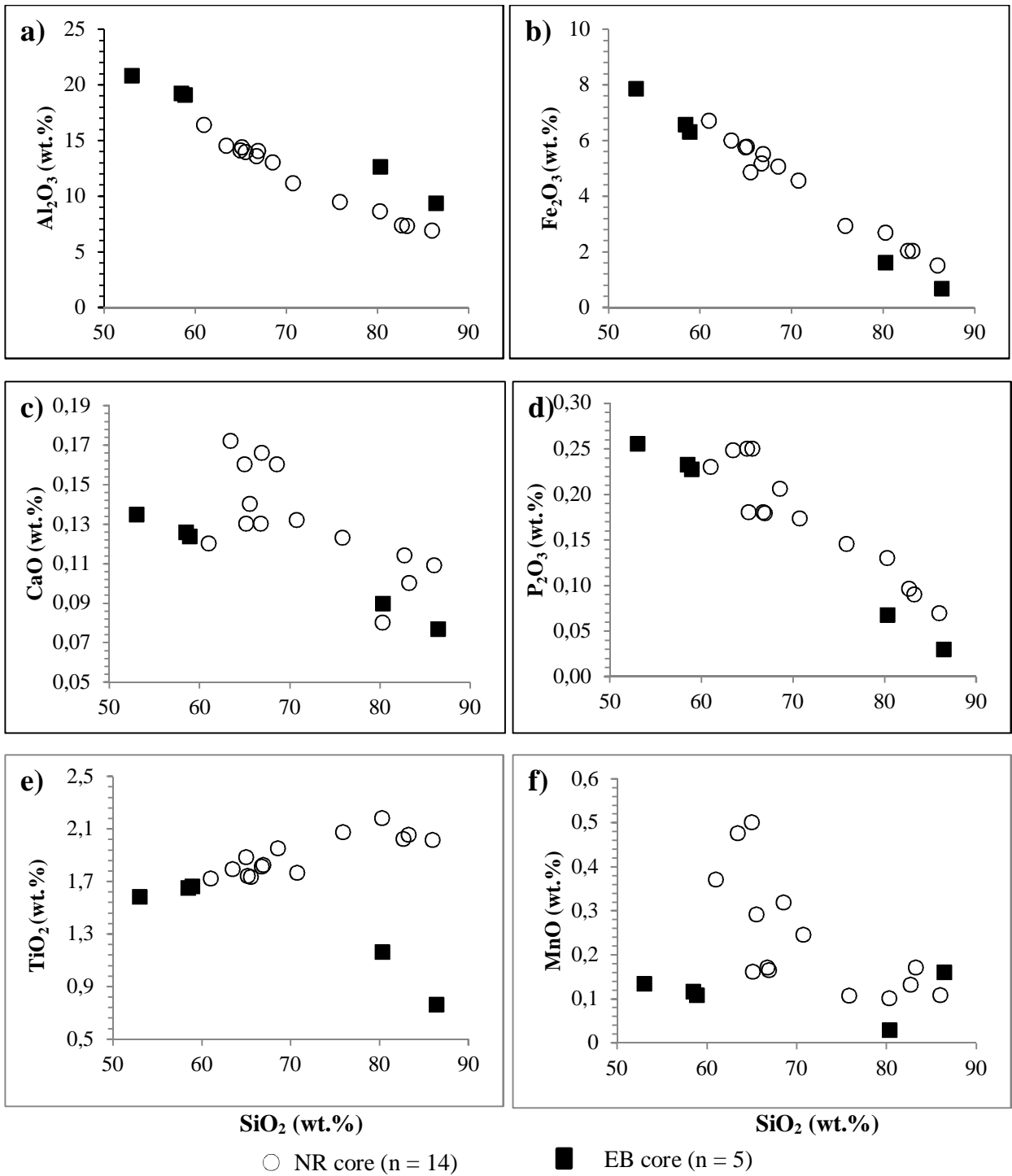


Figure V.8. Binary diagrams of selected major elements in Simbock Lake sediments

V.2.1.2. Trace elements

Trace element concentrations and their mean values in Lake Simbock sediments are gathered in Table V.4. These elements have been subdivided into three groups: elements whose contents are greater than 100 ppm (Cr, Ba, Zr and V).

Table V.4. Trace element concentrations (in ppm) and element ratios in sediments from the Simbock Lake

	d.l.	NR core														EB core						Average n = 19	
		NR12	NR5	NR13	NR4	NR31	NR10	NR3	NR9	NR8	NR2	NR7	NR6	NR11	NR1	Av.1	EB1	EB2	EB3	EB4	EB5		Av. 2
Cr	3	100	91	98	71	70	106	104	106	78	125	885	137	109	108	156	76	107	156	153	144	127	145
Ni	0.7	41	23	39	10	14	45	35	45	17	53	28	47	40	42	34	10	18	58	58	61	41	36
Co	0.13	26.03	18.82	27.71	7.9	11.23	33.41	25.33	38.03	12.87	41.29	11.73	39.03	30.66	26.72	25.05	7.15	13.09	35.86	35.57	34.05	25.14	25.08
Zn	1.8	92	65	88	28	36	116	88	115	47	140	37	112	92	92	82	20	34	124	125	119	84	83
Sc	1.1	14	8	13	4	6	14	13	15	6	18	5	16	14	15	12	5	7	22	21	21	15	13
Cu	1.4	39	51	35	15	25	40	46	43	40	49	71	42	31	37	40	8	13	44	45	47	31	38
Ba	0.8	356	346	373	253	303	389	437	411	292	423	295	466	360	355	361	117	152	400	381	346	279	340
Pb	0.18	28.1	13.7	20.4	7.7	9.7	22.2	17.5	22.4	10.4	21.4	8.9	23.8	19.2	21.5	17.64	4.6	7.6	26.4	26.4	28.5	18.70	17.68
Y	0.05	21.48	15.36	20.76	6.73	10.06	26.31	20.85	25.56	9.85	29.94	8.78	24.8	23.5	21.73	18.98	5.63	11.99	30.45	29.39	26.83	20.86	19.47
Ga	0.04	18.85	11.69	17.68	7.26	8.16	18.87	15.48	19.31	9.7	20.94	8.43	23.03	17.71	18.31	15.39	8.08	11.59	26.95	26.78	28.24	20.33	16.69
Th	0.01	24.07	34.41	26.28	20.37	25.98	22.62	30.27	22.45	24.73	25.5	20.6	22.68	30.63	27.05	25.55	5.13	12.63	24.8	23.31	22.64	17.70	23.48
U	0.01	3.37	3.59	3.52	2.05	2.96	3.58	3.69	3.69	2.77	3.51	2.52	3.72	3.8	3.47	3.30	0.91	1.7	3.56	3.69	3.52	2.68	3.14
Zr	6	429	400	399	219	292	553	508	459	293	497	276	520	484	410	410	114	196	459	449	397	323	387
Li	0.4	11.7	7.1	11	3.9	4.9	12.3	9	12.4	5.7	13.9	4.7	12.3	10.9	10.8	9.33	3.9	5.8	14.7	14.8	17.9	11.42	10
Sb	0.04	0.16	0.09	0.14	0.05	0.06	0.14	0.12	0.14	5.7	0.16	0.1	0.13	0.13	0.15	0.52	<d.l.	0.04	0.16	0.16	0.2	0.14	0.44
Nb	0.02	35.48	48.6	35.57	48.91	45.14	36.28	36.03	36.18	44.75	37.08	43.03	31.53	40.07	39.81	39.89	16.79	24.07	29.3	28.84	27.64	25.33	36.06
Hf	0.14	11.14	10.68	10.51	6.07	7.63	14.51	13.09	12.14	7.86	12.57	7.58	13.49	12.73	10.78	10.77	3.09	5.33	11.7	11.71	10.19	8.40	10.15
Be	0.04	0.96	0.81	0.95	0.42	0.41	1.07	1.07	1	0.44	1.25	0.4	1.33	0.95	0.95	0.86	0.39	0.57	1.71	1.67	1.56	1.18	0.94
Cd	0.01	0.13	0.12	0.11	0.07	0.09	0.17	0.16	0.21	0.09	0.27	0.09	0.18	0.16	0.11	0.14	0.09	0.1	0.2	0.21	0.17	0.15	0.14
Mo	0.08	1.64	1.33	1.69	0.92	1.07	2.13	1.52	1.91	1.07	2.12	2.77	2.28	1.78	1.72	1.71	0.54	0.78	1.99	2.04	2.18	1.51	1.66
Sn	0.16	2.81	2.93	2.67	2.49	5.65	2.91	2.66	2.81	2.83	2.84	2.81	3.8	2.87	2.99	3.08	0.89	1.46	2.93	3.08	3.01	2.27	2.87
W	0.05	1.58	2.05	1.56	2.03	1.99	1.63	1.61	1.57	1.99	1.58	2	1.36	1.77	1.73	1.75	0.68	1.05	1.24	1.25	1.25	1.09	1.57
Cs	0.01	1.63	0.75	1.57	0.31	0.48	1.85	1.09	1.89	0.58	1.92	0.43	1.65	1.56	1.55	1.23	0.21	0.5	1.85	1.86	2.08	1.30	1.25
Rb	0.11	27.92	20.94	27.14	13.35	16.18	28.83	26.97	30.18	16.28	32.24	14.87	23.61	28.62	28.4	23.97	7.27	11.83	30.53	28.51	19.93	19.61	22.82
Sr	0.6	41.8	41.1	42.4	33.4	36.5	43.5	47.4	43	32.9	46.5	34.7	46.7	43.8	43.6	41.24	16.6	20.1	48	45.9	41	34.32	39.42
Ta	0.007	2.16	2.92	2.11	2.88	2.6	2.19	2.1	2.24	2.6	2.18	2.63	1.9	2.43	2.34	2.38	1.09	1.52	1.79	1.75	1.75	1.58	2.17
In	0.0018	0.07	0.03	0.06	0.01	0.02	0.07	0.05	0.07	0.028	0.07	0.02	0.09	0.06	0.06	0.05	0.02	0.03	0.09	0.1	0.1	0.07	0.06
Tl	0.002	0.42	0.24	0.44	0.11	0.17	0.55	0.31	0.61	0.18	0.58	0.16	0.48	0.47	0.43	0.37	0.08	0.15	0.47	0.48	0.54	0.34	0.37
V	0.8	134	121	150	92	93	144	126	145	101	162	n.a	150	145	141	131.05	60	98	177	176	173	137	133
Rb/Sr	-	0.67	0.5	0.64	0.4	0.44	0.67	0.57	0.7	0.5	0.7	0.42	0.5	0.65	0.65	0.57	0.44	0.59	0.63	0.62	0.49	0.55	0.58
K ₂ O/Rb	-	24.71	32	25.06	38.95	38.85	24.63	27.81	23.19	35.01	18.61	38.33	28.8	23.41	24.3	28.83	35.76	27.05	22.93	24.2	30.11	28.01	26.87

n.a.: non analyzed; d.l.: detection limits; d.l.: detection limits.

Elements with concentrations between 10 and 100 ppm such as Ni, Co, Zn, Sc, Cu, Pb, Y, Ga, Th, Nb, Rb and Sr); and the last group with contents below 10 ppm such as U, Li, Sb, Hf, Be, Cd, Mo, Sn, W, Cs, Ta, In and Tl.

V.2.1.3. Rare earth elements (REE)

The REE distribution in the core sediments from the Simbock Lake was measured to identify their provenance. The total concentrations, as well as mean, minimum, maximum and standard deviation values are presented in Table V.5. The high REE contents in all samples could be due to their absorption by the component minerals of the fine materials. Sediments are highly enriched in REE (77.53 – 404.58 ppm) and LREE compared to HREE (LREE/HREE ratio varies from 17.64 to 54.58) as well as the negative Eu anomaly ($Eu/Eu^* \sim 0.38 - 0.9$) and high ratio of $(La/Yb)_N$ are observed throughout the cores. Singh (2009) suggested the importance presents the splitting of REEs during the various progressive stages of the weathering. The two cores sediments have similar chondrite-normalised REE pattern with overlapping abundances and negative anomaly in Eu (Figure V.9a-b) with $(La/Yb)_N$ ratios ranging between 12.3 and 48.17 (Table V.5). LREE and HREE show variable fractionation with $(La/Sm)_N$ values ranging between 3.54 and 4.24. The $(Gd/Yb)_N$ values range between 1.93 and 5.02 (Table V.5).

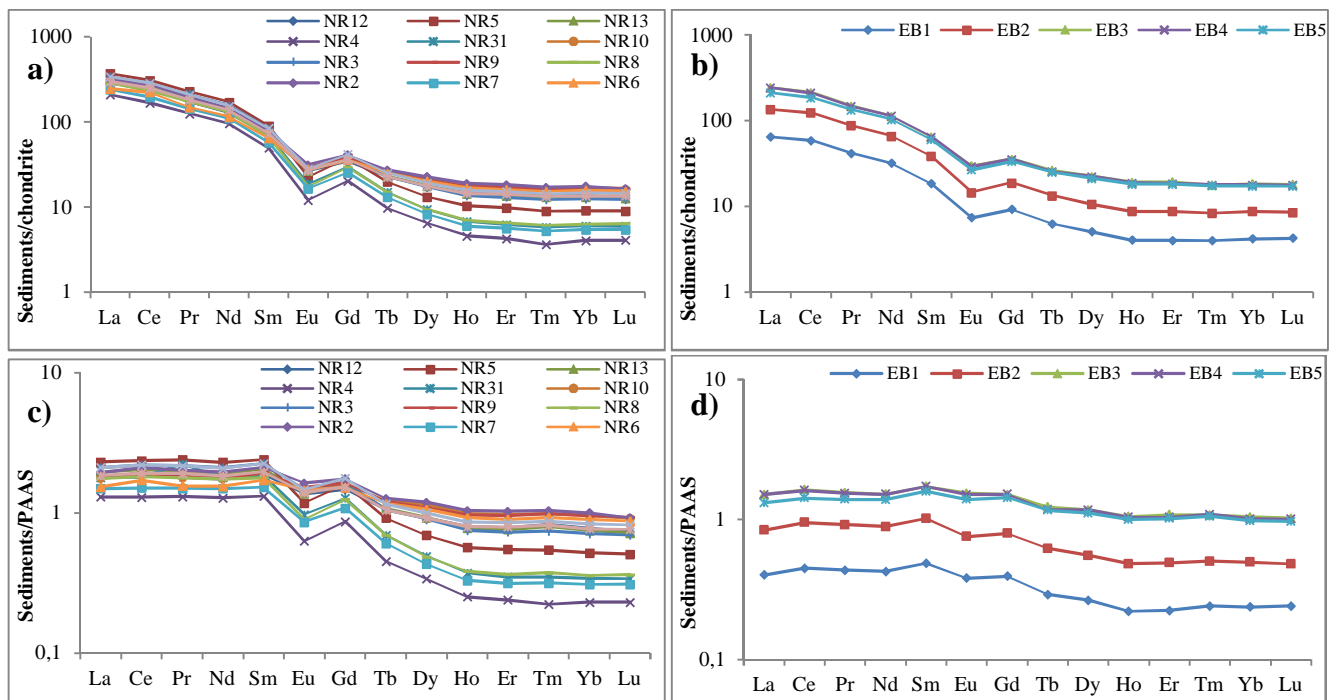


Figure V.9. REE patterns of Simbock Lake sediments: **a)** Chondrite-normalized (McDonough and Sun, 1995) for NR core; **b)** Chondrite-normalized (McDonough and Sun, 1995) for EB core; **c)** PAAS-normalized (McLennan, 1989) for NR core; **d)** PAAS-normalized (McLennan, 1989) for EB core

Table V.5. REE concentrations (ppm) of the sediments Simbock Lake

	d.l.	NR Core														EB Core					Average n = 19
		NR12	NR5	NR13	NR4	NR31	NR10	NR3	NR9	NR8	NR2	NR7	NR6	NR11	NR1	EB1	EB2	EB3	EB4	EB5	
La	0.10	68.82	88.11	74.73	49.52	68.42	67.25	80.32	67.61	67.28	74.18	56.78	58.31	80.58	70.56	15.35	32.1	57.64	57.46	50.08	62.37
Ce	0.12	149.05	187.57	162.04	102.95	142.2	151.99	174.28	154.41	144.15	167.7	120.1	136.12	174.94	152.65	35.75	75.75	129.55	128.48	113.5	137.01
Pr	0.01	15.78	21.08	17.34	11.56	9.7	15.83	19.14	15.95	15.76	17.8	13.22	13.73	19.15	16.86	3.83	8.13	13.76	13.62	12.31	14.45
Nd	0.06	58.68	77.81	64.89	43.47	60.54	59.85	71.62	60.04	58.97	66.31	50.39	52.36	70.3	62.46	14.46	30.17	51.33	51.48	47.01	55.38
Sm	0.03	10.36	13.29	11.41	7.32	10.32	10.7	12.45	10.74	9.9	11.71	8.45	9.54	12.54	10.91	2.7	5.66	9.52	9.55	8.84	9.78
Eu	0.00	1.48	1.27	1.48	0.68	1.05	1.63	1.59	1.64	0.97	1.76	0.93	1.56	1.58	1.5	0.41	0.81	1.67	1.63	1.51	1.32
Gd	0.01	6.85	7.48	7.4	4.03	5.94	7.56	7.66	7.6	5.82	8.15	5.04	7.05	8.24	7.11	1.83	3.72	7.02	7.05	6.65	6.43
Tb	0.00	0.82	0.71	0.83	0.35	0.54	0.95	0.82	0.93	0.54	0.98	0.47	0.9	0.9	0.81	0.23	0.48	0.95	0.91	0.9	0.74
Dy	0.01	4.27	3.24	4.32	1.58	2.31	5.32	4.19	5.08	2.28	5.55	2.02	4.95	4.68	4.31	1.24	2.59	5.48	5.47	5.2	3.9
Ho	0.00	0.79	0.56	0.77	0.25	0.37	0.98	0.74	0.95	0.38	1.03	0.33	0.91	0.85	0.79	0.22	0.48	1.04	1.03	0.99	0.71
Er	0.01	2.24	1.56	2.16	0.68	1	2.79	2.08	2.72	1.04	2.92	0.9	2.57	2.42	2.26	0.64	1.4	3.08	2.95	2.9	2.02
Tm	0.00	0.33	0.22	0.32	0.09	0.14	0.4	0.3	0.4	0.15	0.42	0.13	0.38	0.35	0.33	0.1	0.2	0.44	0.44	0.43	0.29
Yb	0.01	2.2	1.46	2.11	0.65	0.97	2.69	2	2.7	1.01	2.82	0.87	2.52	2.35	2.17	0.67	1.4	2.95	2.86	2.77	1.96
Lu	0.00	0.32	0.22	0.31	0.1	0.15	0.39	0.3	0.4	0.16	0.4	0.13	0.38	0.35	0.33	0.1	0.21	0.44	0.44	0.42	0.29
REE	-	321.98	404.58	350.12	223.23	303.63	328.33	377.49	331.17	308.41	361.73	259.74	291.28	379.23	333.05	77.53	163.11	284.85	283.36	253.5	296.65
LREE	-	311.02	396.61	339.29	219.53	298.17	314.81	367.06	318	302.85	347.61	254.91	278.67	367.32	322.05	74.33	156.34	270.48	269.26	239.9	286.75
HREE	-	10.96	7.97	10.83	3.7	5.46	13.52	10.43	13.18	5.55	14.12	4.84	12.61	11.91	11	3.2	6.76	14.37	14.1	13.6	9.9
LREE/HREE	-	28.37	49.76	31.34	59.33	54.58	23.28	35.19	24.14	54.53	24.62	52.69	22.09	30.85	29.28	23.25	23.11	18.82	19.1	17.64	32.74
Ce/Ce*(1)	-	1.09	1.05	1.09	1.04	1.34	1.13	1.08	1.14	1.07	1.12	1.12	1.16	1.08	1.07	1.13	1.13	1.11	1.11	1.11	1.11
Ce/Ce*(2)	-	1.04	1	1.04	1.02	0.62	0.98	1.01	0.97	1.01	0.99	0.99	0.96	1.02	1.02	0.99	1	0.99	0.99	0.99	0.98
Eu/Eu*(1)	-	0.54	0.39	0.49	0.38	0.41	0.55	0.5	0.55	0.39	0.55	0.43	0.43	0.47	0.52	0.57	0.54	0.62	0.61	0.6	0.5
Eu/Eu*(2)	-	0.83	0.6	0.63	0.59	0.63	0.85	0.77	0.85	0.6	0.85	0.67	0.9	0.73	0.8	0.88	0.84	0.96	0.94	0.93	0.78
(La/Yb) _N	-	21.3	41	24.11	51.75	48.17	16.98	27.28	17.04	45.39	17.87	44.34	15.69	23.29	22.09	15.56	15.55	13.29	13.67	12.3	25.61
(La/Sm) _N	-	4.15	4.14	4.09	4.22	4.14	3.93	4.03	3.93	4.24	3.96	4.2	3.82	4.01	4.04	3.55	3.54	3.78	3.76	3.54	3.95
(Gd/Yb) _N	-	2.52	4.14	2.84	5.02	4.98	2.27	3.1	2.28	4.68	2.34	4.68	2.26	2.84	2.65	2.21	2.15	1.93	2	1.95	2.99

d.l.: detection limits.

$$\text{Ce/Ce}^*(1) = (\text{Ce}_{\text{sample}}/\text{Chondrite})/(\text{La}_{\text{sample}}/\text{La Chondrite})^{1/2} (\text{Pr}_{\text{sample}}/\text{Pr Chondrite})^{1/2}.$$

$$\text{Ce/Ce}^*(2) = (\text{Ce}_{\text{sample}}/\text{PAAS})/(\text{La}_{\text{sample}}/\text{La PAAS})^{1/2} (\text{Pr}_{\text{sample}}/\text{Pr PAAS})^{1/2}.$$

$$\text{Eu/Eu}^*(1) = (\text{Eu}_{\text{sample}}/\text{Eu Chondrite})/(\text{Sm}_{\text{sample}}/\text{Sm Chondrite})^{1/2} (\text{Gd}_{\text{sample}}/\text{Gd Chondrite})^{1/2}.$$

$$\text{Eu/Eu}^*(2) = (\text{Eu}_{\text{sample}}/\text{Eu PAAS})/(\text{Sm}_{\text{sample}}/\text{Sm PAAS})^{1/2} (\text{Gd}_{\text{sample}}/\text{Gd PAAS})^{1/2}.$$

$$(\text{La/Yb})_N = (\text{La}_{\text{sample}}/\text{La Chondrite})/(\text{Yb}_{\text{sample}}/\text{Yb Chondrite}).$$

$$(\text{La/Sm})_N = (\text{La}_{\text{sample}}/\text{La Chondrite Sm}_{\text{sample}}/\text{Sm Chondrite}).$$

$$(\text{Gd/Yb})_N = (\text{Gd}_{\text{sample}}/\text{Gd Chondrite})/(\text{Yb}_{\text{sample}}/\text{Yb Chondrite}).$$

V.2.2. Ossa lake Complex

V.2.2.1. Major elements

Concentrations of major and trace elements geochemistry of Ossa Lake complex include Ossa Lake (OL; n = 7), Mwembe Lake (OM; n = 7) and the supplied river (LO; n = 4) samples are shown in Tables V.6-7. The sediments from Ossa lakes complex has similar variations except top sample (OL4) from the river supplied core.

The Ossa complex sediments have higher abundance of SiO₂, Al₂O₃ and Fe₂O₃ varying from 32.37 to 54.26 wt% (avg. 47.32 wt%), 18.42 to 23.12 wt% (avg. 20.94 wt%) and 5.56 to 10.44 wt% (avg. 8.46 wt%), respectively; these high values are linked to predominance of clay minerals in these fine sediments. Moderate content of TiO₂ are also seen in Ossa Lakes complex varying from 0.95 to 1.6 wt.% (avg. 0.77 wt%). The alkali, alkaline-earth, MnO and P₂O₅ contents in the sediments are < 1, except for K₂O which content vary from 0.56 to 2.09 wt% (avg. 1.66 wt%). Those samples content also high concentration of Loss on ignition (LOI) which vary from 10.74 to 39.73 (avg. 17.74 wt%) and can be explained by the presence of high content of organic matter and clay minerals. Different trends are shown in OL4 sample sediments with 91.81 wt%; 3.87 wt% and 0.78 wt% respectively for SiO₂, Al₂O₃ and Fe₂O₃ (Table 2), this sample has low content of LOI (1.94 wt%). The correlation between the major elements and Al₂O₃ without sample OL4 which different trend is shown in Figure 6. The negative correlation between SiO₂ and Al₂O₃ is due to the fact that most of the silica is sequestered in quartz (Bessa et al., 2018). Positive correlation of TiO₂ with Al₂O₃ suggests that TiO₂ is probably associated with rutile, silicates and sometime phyllosilicates, especially with illite and Illite-smectite. The positive correlation of Fe₂O₃, P₂O₅ and MgO with Al₂O₃ (Figure V.10) suggests that their distribution is mainly controlled by silicates and phyllosilicates (Bal Akkoca et al., 2019). Numerous weathering indices and elemental ratios have been used in several studies to determine paleoweathering processes and the source rock alteration degree (Bessa et al., 2018; Ongboye et al., 2019). Among them, the Chemical Index of Alteration (CIA); the Plagioclase Index of Alteration (PIA) and Chemical Index of Weathering (CIW) are used in this study to evaluate the intensity of chemical weathering in the source area. In addition, the weathering degree and probable source rocks composition are also defined by A-CN-K (Al₂O₃-CaO* + Na₂O-K₂O) triangular plot by Nesbitt and Young, 1984. For this study, CaO* values are accepted only if CaO < Na₂O; when CaO > Na₂O, it is assumed that the concentration of CaO equals that of Na₂O (McLennan et al., 1993). In this lake sediments, CIA values of

sediment samples from Ossa Lake complex range from 84.4 to 96.1 (avg. ~ 88.1), indicating intense-degree of chemical weathering of the gneissic source rocks. This high chemical weathering is confirmed by high PIA (avg. ~ 94.7) and CIW (avg. ~ 95.2) values (Table 2).

V.2.2.2. Trace elements

Table 3 shows the concentrations of trace elements present in the 18 selected samples from Ossa complex sediments with different trend concentrations for OL4 sample. The transitional trace elements (eg. Co, Sc, Cr, Ni, V, Cu, and Zn) concentrations show low variation in the studied sediments. High-field-strength elements (e.g., Th, U, Zr and Hf) point to their presence in heavy minerals such as zircon that have been delivered from metamorphosed and felsic source rocks. The moderate concentration of Sr and Nb in sediments is observed, which may be due to the presence of feldspar in these lake sediments. Large-ion lithosphere elements (e.g., Rb, Ba, and Sr) with high to moderate content suggests their incorporation in sheet silicates, such as illite and illite-smectite, and sorption onto clay mineral surfaces.

V.2.2.3. Rare earth elements (REE)

Table V.8 shows concentrations with some useful ratios of rare earth elements (REE) and the sums of REE (Σ REE), light REEs (LREE compose of La, Ce, Pr, Nd, Sm and Eu) and heavy REE (Σ HREE compose of Gd, Tb, Dy, Ho, Er, Tm, Yb and Lu), it's note that OL4 sample has content out of the other samples. The Σ REE contents range from 170.9 to 341.2 ppm with 43.1 ppm for sample OL4, the LREE/HREE ratios range from 8.1 to 11.6, reflecting a strong enrichment of LREE in all sediments. LREE enrichments in these sediments are also evident by high $(La/Yb)_N$ ratios which ranging from 8.3 to 13.7. Indeed, REE shows moderate to high fractionation as seen by $(Gd/Yb)_N$ ratios varying from 1.1 to 2.2 in the studied sediments. This fractionation during weathering process is confirm by high ratio of $(La/Yb)_N$ (ranging from 3.1 to 4.9). The REE spectra normalized relative to the chondrite (Taylor and McLennan, 1985) confirm the LREE-abundance and reveal strong negative Eu anomalies ($Eu/Eu^* \sim 0.58-0.8$) and the homogeneity of spectra except for sample OL4 (Figure V.11a) confirming the influence of surrounding geology in the Ossa Lake watershed. The normalization of REE to the PAAS (Taylor and McLennan, 1985) is similar to chondrite normalization except the dispersion in REE patterns and positive Eu anomalies (Figure V.11b).

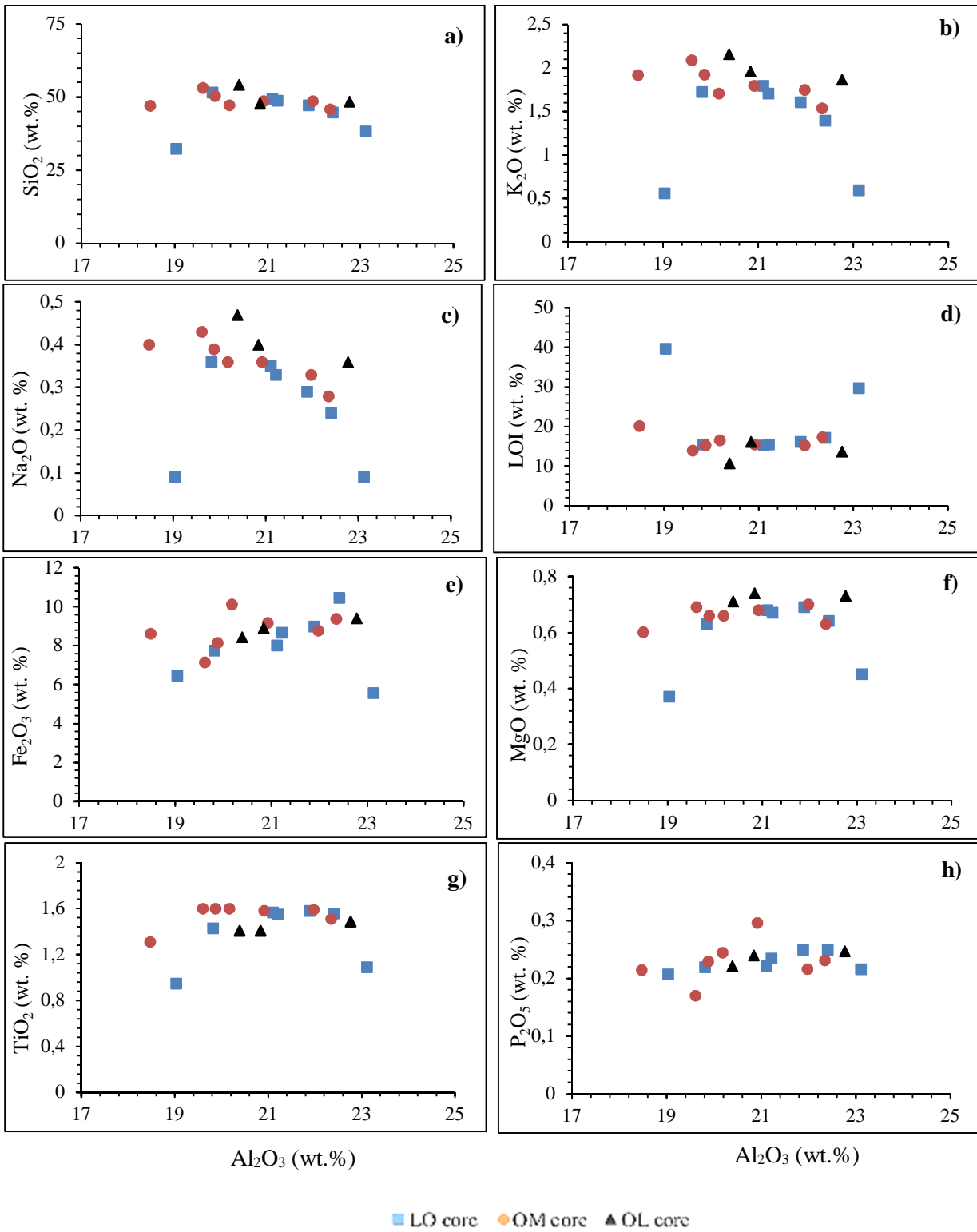


Figure V.10. Hacker diagram of Al_2O_3 versus major oxides showing the distribution of Ossa lake Complex samples

Table V.6. Major elements (wt. %) and some element ratios in sediments from the Ossa lakes Complex

Elements	d.l.	LO core							OM core							OL core			
		LO1	LO2	LO3	LO4	LO5	LO6	LO7	OM1	OM2	OM3	OM4	OM5	OM6	OM7	OL1	OL2	OL3	OL4
SiO ₂	0.04	32.37	38.36	51.58	49.59	48.79	47.21	44.77	47.07	45.86	48.59	48.71	47.25	53.22	50.4	47.85	48.48	54.26	91.81
Al ₂ O ₃	0.02	19.04	23.12	19.82	21.11	21.22	21.89	22.41	18.48	22.35	21.98	20.92	20.18	19.61	19.88	20.84	22.77	20.39	3.87
Fe ₂ O ₃	0.01	6.45	5.56	7.73	8.01	8.66	8.97	10.44	8.61	9.36	8.77	9.15	10.1	7.13	8.14	8.9	9.39	8.41	0.78
TiO ₂	0.01	0.95	1.09	1.43	1.57	1.55	1.58	1.56	1.31	1.51	1.59	1.58	1.6	1.6	1.6	1.41	1.49	1.41	0.77
CaO	0.006	0.243	0.185	0.324	0.312	0.32	0.295	0.265	0.363	0.27	0.308	0.324	0.367	0.363	0.36	0.454	0.293	0.34	0.05
K ₂ O	0.01	0.56	0.6	1.73	1.8	1.71	1.61	1.4	1.92	1.54	1.75	1.8	1.71	2.09	1.93	1.96	1.87	2.16	0.08
MgO	0.01	0.37	0.45	0.63	0.68	0.67	0.69	0.64	0.6	0.63	0.7	0.68	0.66	0.69	0.66	0.74	0.73	0.71	0.06
MnO	0.002	0.024	0.021	0.054	0.055	0.074	0.063	0.067	0.044	0.046	0.051	0.064	0.119	0.045	0.063	0.145	0.083	0.053	0.005
Na ₂ O	0.02	0.09	0.09	0.36	0.35	0.33	0.29	0.24	0.4	0.28	0.33	0.36	0.36	0.43	0.39	0.4	0.36	0.47	0.06
P ₂ O ₅	0.002	0.207	0.216	0.22	0.222	0.235	0.25	0.25	0.214	0.231	0.216	0.296	0.244	0.17	0.229	0.24	0.247	0.221	0.024
LOI	-	39.73	29.83	15.57	15.35	15.56	16.26	17.22	20.27	17.37	15.35	15.58	16.61	13.95	15.29	16.2	13.73	10.74	1.94
TOTAL	-	100.09	99.58	99.56	99.15	99.23	99.22	99.37	99.38	99.54	99.74	99.57	99.29	99.42	99.06	99.26	99.55	99.27	99.46
K ₂ O/Na ₂ O	-	6.22	6.67	4.81	5.14	5.18	5.55	5.83	4.8	5.5	5.30	5	4.75	4.86	4.95	4.9	5.19	4.60	1.33
Al ₂ O ₃ /TiO ₂	-	20.04	21.21	13.86	13.45	13.69	13.85	14.37	14.11	14.80	13.82	13.24	12.61	12.26	12.43	14.78	15.28	14.46	5.03
SiO ₂ /Al ₂ O ₃	-	1.70	1.66	2.60	2.35	2.30	2.16	2.00	2.55	2.05	2.21	2.33	2.34	2.71	2.54	2.30	2.13	2.66	23.72
CIA	-	95.48	96.07	86.65	87.23	87.84	89.03	90.67	84.48	89.62	88.06	86.99	86.92	84.38	85.50	85.84	87.85	84.54	93.34
PIA	-	98.42	98.70	93.82	94.37	94.69	95.48	96.36	92.57	95.74	94.87	94.14	93.93	92.69	93.27	93.43	94.86	92.84	95.23
CIW	-	98.47	98.74	94.37	94.86	95.13	95.82	96.60	93.35	96.04	95.29	94.65	94.46	93.48	93.94	94.06	95.29	93.61	95.33
ICV	-	0.39	0.31	0.58	0.57	0.58	0.56	0.57	0.66	0.55	0.57	0.61	0.67	0.61	0.62	0.63	0.57	0.63	0.50

d.l.: detection limits.

CIA (%) = $[\text{Al}_2\text{O}_3 / (\text{Al}_2\text{O}_3 + \text{CaO}^* + \text{Na}_2\text{O} + \text{K}_2\text{O})] \times 100$ from Nesbitt and Young (1984).PIA (%) = $[\text{Al}_2\text{O}_3 - \text{K}_2\text{O} / (\text{Al}_2\text{O}_3 + \text{CaO}^* + \text{Na}_2\text{O} - \text{K}_2\text{O})] \times 100$ from Fedo et al. (1995).CIW (%) = $[\text{Al}_2\text{O}_3 / (\text{Al}_2\text{O}_3 + \text{CaO}^* + \text{Na}_2\text{O})] \times 100$ from Harnois (1988).ICV (%) = $(\text{Fe}_2\text{O}_3 + \text{K}_2\text{O} + \text{CaO} + \text{Na}_2\text{O} + \text{MgO} + \text{MnO} + \text{TiO}_2) / \text{Al}_2\text{O}_3$ from Cox et al. (1995). Where CaO* correction was using followed the procedure of McLennan et al. (1993).

Table V.7. Trace elements (ppm) in sediments from the Ossa lakes Complex

	d.l.	LO core							OM core							OL core			
		LO1	LO2	LO3	LO4	LO5	LO6	LO7	OM1	OM2	OM3	OM4	OM5	OM6	OM7	OL1	OL2	OL3	OL4
Cr	3	135	131	120	133	125	113	108	136	132	144	133	133	132	109	115	125	115	62
V	0.8	153.2	141.6	131.2	142.8	139.9	138.5	148.3	137.4	129.6	151.9	144.6	147.4	160.5	129.2	128.6	139.3	127.4	44.6
Ni	0.7	54.9	52.5	48.7	53	51.8	53.2	52.4	54	50.3	58.3	53.5	53.8	54.7	42.3	47.9	52.9	42.6	10.7
Zn	1.8	97	85.1	84.6	92	88.2	73	79.3	99.8	90.3	102.4	96.6	96.5	94.6	84.6	84.9	93.2	76.8	12.2
Cu	1.4	35.5	34.9	31.4	34.6	33.9	38.5	42.1	34.5	33.1	36	34.8	35.9	40	35.3	31.7	34.8	30.9	4.3
Co	0.13	27.14	26.33	23.17	26.12	26.53	17.22	23.35	26.19	24.23	29.28	29.64	27.83	28.66	26.18	26.07	25.79	20.06	2.54
Sc	1.1	16.4	16.4	15.5	17	15.8	15.4	16.1	17	16.6	18.9	16.6	16.2	14.9	14.7	16.9	17	15.7	4.4
Ba	0.8	524.9	604.4	650.6	657.9	650.6	282.7	316.2	865.2	840.4	761.9	663.9	612.8	478.9	782.3	837.9	648.1	736	59.2
Sr	0.6	80.1	95.2	102.2	109.6	111.6	41.6	54.3	142.3	140.2	137.8	112.8	100.5	77.3	128.3	144.8	100.2	132.9	15.7
Li	0.4	26.3	26	22.2	25.5	25.1	24.3	19.8	24.9	23.5	26.2	26.6	25.2	26.1	19.7	22.8	24.5	21.5	3.9
Sb	0.04	0.2	0.2	0.2	0.21	0.2	0.14	0.16	0.22	0.22	0.23	0.2	0.19	0.17	0.22	0.21	0.24	0.24	0.22
Rb	0.11	24.89	31.74	35.6	39.58	38.91	12.81	27.48	65.18	60.6	57.12	38.66	26.26	21.66	61.22	66.04	43.96	52.56	3.67
Cs	0.013	2.89	3.13	3.15	3.28	3.14	2.44	2.66	3.48	3.38	3.37	3.32	3.12	2.68	3.21	3.55	3.62	3.38	0.60
Th	0.018	19.67	18.66	20.81	19.23	17.71	17.09	18.45	22.08	20.35	20.37	19.33	19.62	20.7	19.25	19.99	20.01	17.99	4.19
Zr	6	294	314	342	380	387	114	126	449	468	416	384	351	322	392	381	391	412	411
Nb	0.028	34.44	34.65	32.58	36.03	34	22.33	19.5	36.65	35.85	38.07	36.06	35.08	33.65	30.26	34.55	35.08	33.14	15.48
U	0.011	4.38	4.24	4.76	4.29	3.97	3.51	3.57	4.95	4.9	4.59	4.47	4.58	4.47	4.38	4.33	4.78	4.16	1.19
Hf	0.14	7.26	7.96	8.96	9.07	9.2	2.93	3.1	10.94	11.69	9.64	9.01	8.41	7.2	9.97	9.33	9.72	10.24	10.73
Mo	0.08	1.53	1.51	1.42	1.63	1.62	1.72	1.7	1.55	1.47	1.68	1.49	1.62	1.6	1.57	1.71	1.7	1.56	0.52
W	0.05	1.51	1.41	1.51	1.46	1.3	1.16	1.01	1.5	1.46	1.41	1.45	1.48	1.33	1.4	1.39	1.55	1.41	1.09
In	0.0018	0.1	0.09	0.1	0.09	0.09	0.09	0.09	0.1	0.09	0.09	0.1	0.1	0.1	0.09	0.09	0.1	0.09	0.02
Ta	0.007	2.2	2.16	2.23	2.17	2.03	1.46	1.24	2.33	2.29	2.22	2.15	2.15	1.94	1.95	2.17	2.25	2.08	1.04
Y	0.05	31.47	31.79	32.56	32.36	30.82	23.88	33.65	40.4	36.8	39.87	34.78	32.17	30.54	38.03	37.59	35.17	31.69	4.6
Ga	0.04	30.8	30.1	29.03	29.45	28.65	31.69	25.86	28.03	27.2	29.14	29.68	31.21	33.05	26.39	29.21	31.84	27.77	5.35
Pb	0.18	32.54	31.71	33.83	32.93	30.07	41.35	35.88	34.92	33.83	32	35.1	34.12	36.55	41.07	32.64	34.59	36.1	10.19
Be	0.04	3.02	2.98	2.68	2.92	2.87	2.65	2.58	3.03	2.88	3.2	3.16	2.97	3.16	2.5	2.68	2.87	2.41	0.2
Cd	0.013	0.09	0.09	0.1	0.12	0.11	0.08	0.18	0.15	0.13	0.13	0.12	0.1	0.08	0.14	0.11	0.09	0.06	0.01
Sn	0.16	3.69	3.67	3.77	3.59	3.48	3.46	2.95	3.31	3.55	3.43	3.79	3.68	3.94	3.6	3.71	3.89	3.57	1.09
Tl	0.002	0.6	0.59	0.63	0.6	0.6	0.5	0.5	0.61	0.58	0.58	0.62	0.62	0.54	0.64	0.65	0.66	0.62	0.06
U/Th	-	0.22	0.23	0.23	0.22	0.22	0.21	0.19	0.22	0.24	0.23	0.23	0.23	0.22	0.23	0.22	0.24	0.23	0.28
Ni/Co	-	2.02	1.99	2.1	2.03	1.95	3.09	2.24	2.06	2.08	1.99	1.8	1.93	1.91	1.62	1.84	2.05	2.12	4.21
Sr/Cu	-	2.26	2.73	3.25	3.17	3.29	1.08	1.29	4.12	4.24	3.83	3.24	2.8	1.93	3.63	3.65	4.3	2.88	4.57
Rb/Sr	-	0.31	0.33	0.35	0.36	0.35	0.31	0.51	0.46	0.43	0.41	0.34	0.26	0.28	0.48	0.23	0.4	0.44	0.46

d.l.: detection limits.

Table V.8. Rare earth elements (ppm) in sediments from the Ossa lakes Complex

	d.l.	LO core							OM core							OL core			
		LO1	LO2	LO3	LO4	LO5	LO6	LO7	OM1	OM2	OM3	OM4	OM5	OM6	OM7	OL1	OL2	OL3	OL4
La	0.1	44	48.1	48.4	47.4	45.1	34.2	59.4	68.4	60	62.8	49.9	43.7	34.2	61.9	63.5	53	50	9
Ce	0.12	97.96	107.38	109.6	104.89	102.52	72.53	137	153.71	136.08	139.32	113.26	98.23	78.67	146.93	145.66	122.63	116.68	20.96
Pr	0.014	10.93	11.82	11.97	11.25	11.26	8.39	14.4	16.63	14.78	15.02	12.38	11.15	8.79	15.62	15.09	12.79	12.27	1.86
Nd	0.06	40.39	43.19	44.37	41.2	41.09	30.55	53.17	60.19	53.16	55.01	45.32	40.22	30.99	56.79	55.03	46.95	44.74	6.57
Sm	0.026	8.08	8.69	8.54	8.29	8.09	6.36	9.87	11.22	10.29	10.36	8.74	8.32	6.79	10.75	10.37	8.7	8.60	1.15
Eu	0.0031	1.83	1.84	1.96	1.77	1.84	1.48	2.26	2.47	2.22	2.37	1.96	1.80	1.65	2.36	2.26	1.96	1.82	0.20
Gd	0.009	6.81	6.98	7.36	6.75	6.63	5.40	8.04	9.10	8.41	8.31	7.23	7	5.89	8.70	8.19	7.23	6.91	0.92
Tb	0.0023	1.01	1.04	1.08	0.98	0.95	0.80	1.12	1.33	1.20	1.21	1.06	1.02	0.91	1.26	1.18	1.1	0.97	0.13
Dy	0.009	5.83	5.99	6.31	5.72	5.56	4.66	6.23	7.50	6.71	6.85	6.23	5.82	5.22	7.12	6.73	6.39	5.83	0.82
Ho	0.0025	1.15	1.17	1.27	1.13	1.08	0.92	1.19	1.47	1.35	1.35	1.23	1.18	1.06	1.42	1.3	1.26	1.13	0.17
Er	0.007	3.41	3.3	3.55	3.30	3.11	2.53	3.32	4.13	3.96	3.88	3.52	3.33	3.03	3.99	3.7	3.61	3.32	0.51
Tm	0.0019	0.47	0.48	0.52	0.48	0.45	0.38	0.47	0.59	0.58	0.57	0.53	0.50	0.46	0.60	0.54	0.53	0.47	0.08
Yb	0.009	3.14	3.14	3.49	3.15	2.94	2.35	2.94	3.91	3.67	3.56	3.32	3.17	2.81	3.86	3.56	3.51	3.14	0.63
Lu	0.002	0.45	0.46	0.50	0.44	0.43	0.32	0.42	0.57	0.55	0.54	0.49	0.46	0.43	0.56	0.5	0.52	0.46	0.09
ΣREE	-	225.46	243.57	248.91	236.74	231.05	170.85	299.83	341.23	302.94	311.14	255.15	225.90	180.91	321.85	317.61	270.18	256.33	43.08
LREE	-	203.19	221.02	224.84	214.80	209.90	153.50	276.11	312.63	276.53	284.88	231.56	203.42	161.10	294.35	291.91	246.03	234.11	39.74
HREE	-	22.27	22.55	24.07	21.94	21.15	17.35	23.73	28.60	26.41	26.26	23.60	22.48	19.81	27.49	25.70	24.15	22.22	3.34
LREE/HREE	-	9.13	9.80	9.34	9.79	9.92	8.85	11.64	10.93	10.47	10.85	9.81	9.05	8.13	10.71	11.36	10.19	10.53	11.90
Ce/Ce*	-	1.08	1.09	1.10	1.10	1.10	1.04	1.13	1.10	1.11	1.10	1.10	1.08	1.10	1.14	1.14	1.14	1.14	1.24
Eu/Eu*	-	0.75	0.72	0.75	0.72	0.77	0.77	0.78	0.74	0.73	0.78	0.75	0.72	0.80	0.74	0.75	0.75	0.72	0.58
(La/Yb) _N	-	9.52	10.42	9.42	10.23	10.43	9.90	13.73	11.89	11.10	11.97	10.23	9.37	8.27	10.91	12.12	10.26	10.82	9.77
(La/Sm) _N	-	3.40	3.46	3.54	3.57	3.48	3.36	3.76	3.81	3.64	3.79	3.56	3.28	3.14	3.60	3.82	3.80	3.63	4.87
(Gd/Yb) _N	-	1.75	1.80	1.71	1.73	1.83	1.86	2.21	1.88	1.85	1.89	1.76	1.79	1.70	1.83	1.86	1.67	1.78	1.18

d.l.: detection limits.

$$\text{Ce/Ce}^* = (\text{Ce}_{\text{sample}}/\text{Ce}_{\text{chondrite}})/(\text{La}_{\text{sample}}/\text{La}_{\text{chondrite}})^{1/2}(\text{Pr}_{\text{sample}}/\text{Pr}_{\text{chondrite}})^{1/2}.$$

$$\text{Eu/Eu}^* = (\text{Eu}_{\text{sample}}/\text{Eu}_{\text{chondrite}})/(\text{Sm}_{\text{sample}}/\text{Sm}_{\text{chondrite}})^{1/2}(\text{Gd}_{\text{sample}}/\text{Gd}_{\text{chondrite}})^{1/2}.$$

$$(\text{La/Yb})_N = (\text{La}_{\text{sample}}/\text{La}_{\text{chondrite}})/(\text{Yb}_{\text{sample}}/\text{Yb}_{\text{chondrite}}).$$

$$(\text{La/Sm})_N = (\text{La}_{\text{sample}}/\text{La}_{\text{chondrite}})/(\text{Sm}_{\text{sample}}/\text{Sm}_{\text{chondrite}}).$$

$$(\text{Gd/Yb})_N = (\text{Gd}_{\text{sample}}/\text{Gd}_{\text{chondrite}})/(\text{Yb}_{\text{sample}}/\text{Yb}_{\text{chondrite}}).$$

REE are subdivided into LREE (La, Ce, Pr, Nd, Sm and Eu) and HREE (Gd, Tb, Dy, Ho, Er, Tm and Lu).

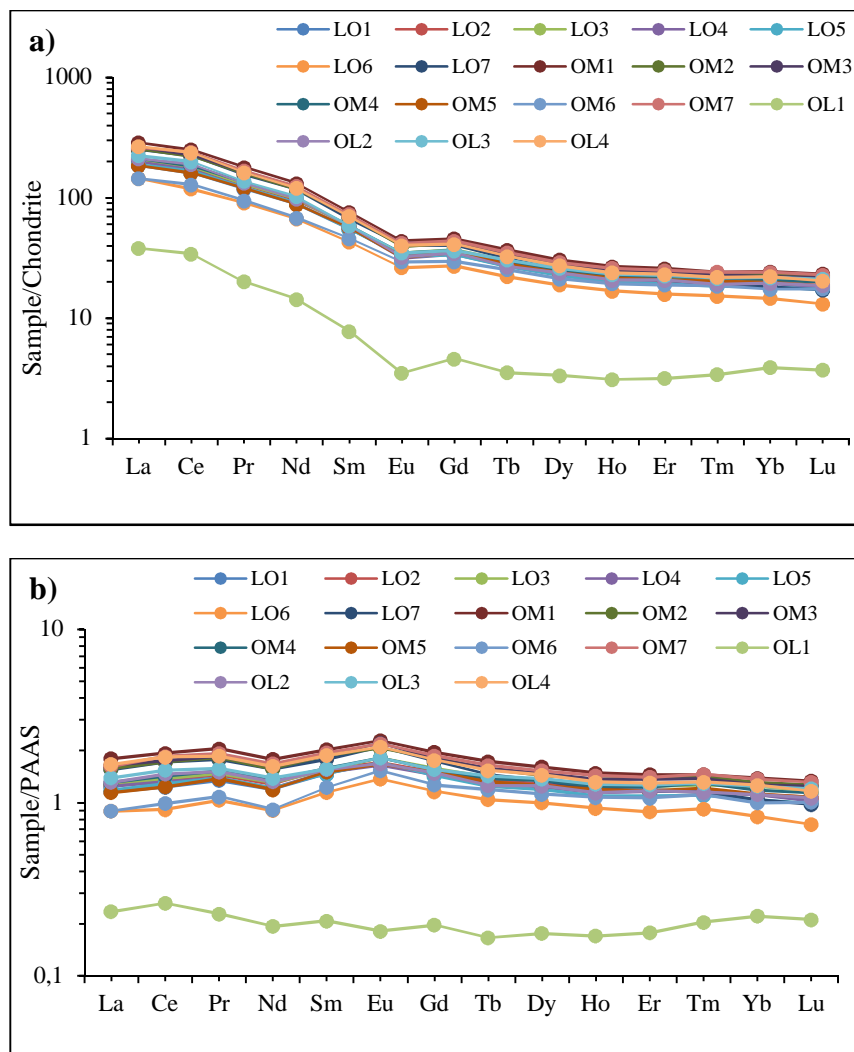


Figure V.11. REE patterns of the lacustrine sediments: **a)** Chondrite-normalized (McDonough and Sun, 1995) and **b)** PAAS-normalized (Taylor and McLennan, 1985)

V.2.3. Ngaoundaba Lake

V.2.3.1. Major elements

Concentrations of major elements geochemistry of sample sediments from Ngaoundaba Crater Lake (core AZ; n = 9 and core NL; n = 11) are listed in Tables V.9. The major oxides selected for the present course included SiO₂, Al₂O₃, Fe₂O₃, MgO, CaO, Na₂O, K₂O, TiO₂, P₂O₅ and MnO. These element oxides have highest concentrations in the core located in the border (NL) than the one in the center of the studied lake. The concentration of SiO₂ varies from 14.23 to 17.59 wt.% in AZ sediments and from 31.32 to 33.97 wt.% in NL sediments. Al₂O₃ concentration in AZ sample sediments varies from 3.65 to 5.97 wt.%. In NL core samples, alumina varies from 12.54 to 14.86 wt.%. With concentration varies from 2.33 to 3.98 wt.%,

iron oxide is moderately represented in AZ core sediments. Fe_2O_3 is more represented in NL core sediments and varies from 6.45 to 9.78 wt.%. Concentration of TiO_2 is considerably represented in the Lake sediments. The higher concentration of TiO_2 is represented in NL core sediments were value range from 2.14 to 3.21 wt.%. In AZ core sediments these values are < 1 wt.%. The others element oxides have concentrations < 1 wt.% in almost sediment samples from Ngaoundaba Lake. In addition, high to very high content of loss on ignition (LOI) are observe the studied lake sediments. The LOI central core sediments are very high, the content is from 70.90 to 75.30 wt.%. However, LOI vary from 36.90 to 40.40 wt.% in the border core sediment. Low positive (Figure V.12a-b) and negative (Figure V.12c-d) correlation suggests that elements from each core has differents sediments provenance and various source rocks ot they not variated too much. The mass ratio $\text{SiO}_2/\text{Al}_2\text{O}_3$ is moderate and varies from 2.38 to 4.78 for AZ core and 2.16 to 2.76 for NL core, and indicates that these sediments contain more components rich in SiO_2 than in Al_2O_3 . The $\text{K}_2\text{O}/\text{Na}_2\text{O}$ ratio is around 0.87 and 4 for for AZ core and 1.52 to 2.2 for NL core (Table V.9), this is indicative of the high Na_2O contents in this environment. High ratio of $\text{Al}_2\text{O}_3/\text{TiO}_2$ (3.95-9.33) confirm the present of zircon wich can be link to the presence of clay minerals such as kaolinite and illite.

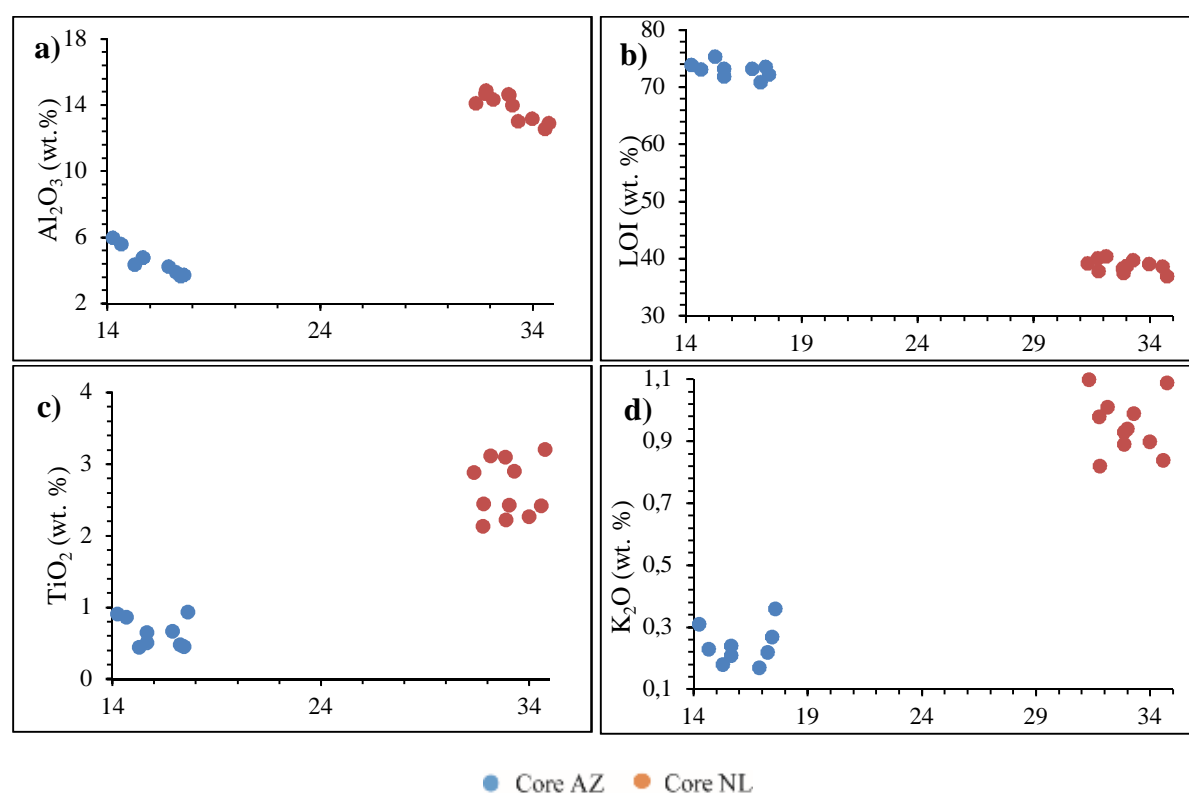


Figure V.12. Hacker diagram of SiO_2 versus some major oxides showing different sources of sediment from Ngaoundaba crate Lake

In the present study, numerous weathering indices have been calculated to determinate the source area weathering degree (Table V.9) including chemical index of alteration (CIA); chemical index of weathering (CIW); weathering Index of Parker (WIP) and index of compositional variability (ICV). The range values of CIA from the lacustrine sediments of Ngaoundaba are from 54.13 to 73.51% and from 78.99 to 83.31% in AZ and NL cores respectively. The same trends are observed in CIW results with 56.58 to 76.68% and from 84.27 to 87.94% respectively in AZ and NL cores. However, the WIP values, with an opposite trend have similar values in the studied core sediments, ranging from 24.42 to 36.94%. Lacustrine sediments from Ngaoundaba Crater Lake have almost similar values of ICV varying between 1.07 and 1.90 in AZ core sediments and between 0.86 and 1.12 in NL core sediments. Moreover, chemical indices such as CIA and WIP values are well correlate in the bottom core and quite well in the border core sediments, exhibiting moderate and greater CIA and smaller WIP values respectively for AZ and NL cores (Table V.9). The above correlations suggest that these indices of weathering, despite their different methods of assessing the degree of weathering of lake sediments, can be significantly influenced by the size of the sediment grains. (Sun et al., 2018). The variation of chemical indices values of studied sediments can be attributed to the variation in the source rocks composition. For sediments studies, $ICV > 1$ is compositionally immature and $ICV < 1$ suggests a compositionally mature sediment (Cox et al., 1995). However, sediments from the bottom of the lake are immature and the moderate weathering character of these sediments is confirmed. Whereas, sediment from the border are generally mature with intense weathering.

V.2.3.2. Trace elements

Elements with relatively high contents in the Ngaoundaba are Barium > Sr > Ni > Zr > V > Cu > Co. They show higher concentrations in either the border core (NL) of the lake (Table V.10). Like in the previous lake, high-field-strength elements (e.g., Th, U, Zr and Hf) point to their presence in heavy minerals such as zircon that have been delivered from recycled and felsic source rocks. The moderate concentration of Sr and Nb in sediments is observed, which may be due to the presence of feldspar in these lake sediments. Large-ion lithosphere elements (e.g., Rb, Ba, and Sr) with high to moderate content suggests their incorporation in sheet silicates, such as illite and kaolinite, and sorption onto clay mineral surfaces.

V.2.3.3. Rare earth elements (REE)

The REE contents are variable in the sediments from Ngaoundaba Lake, between 83 and 100.35 ppm for AZ core and between 254.84 and 292.33 ppm for NL core (Table V.11). In these core sediments, REE shows moderate to high fractionation as seen by $(Gd/Yb)_N$ ratios varying from 1.19 to 3.95. Contrary to other lake deposits in the sub-region (e.g., Ekoa Bessa et al., 2018; N'nganga et al., 2018), the sediments from this study are characterized by moderate light REE (LREE) abundance with respect to heavy REE (HREE; $LREE/HREE \sim 9.01-12.23$). LREE enrichments in studied sediments are also evident by high $(La/Yb)_N$ and $(La/Yb)_N$ ratios, ranging from 3.33 to 4.95 and 6.54 to 20.38 respectively. Amongst the REE in these materials, cerium is the most abundant element in the sediments. In AZ core, Ce values ranging between 35.9 and 45.7 ppm and from 108.5 to 143.8 ppm in NL samples (Table V.11).

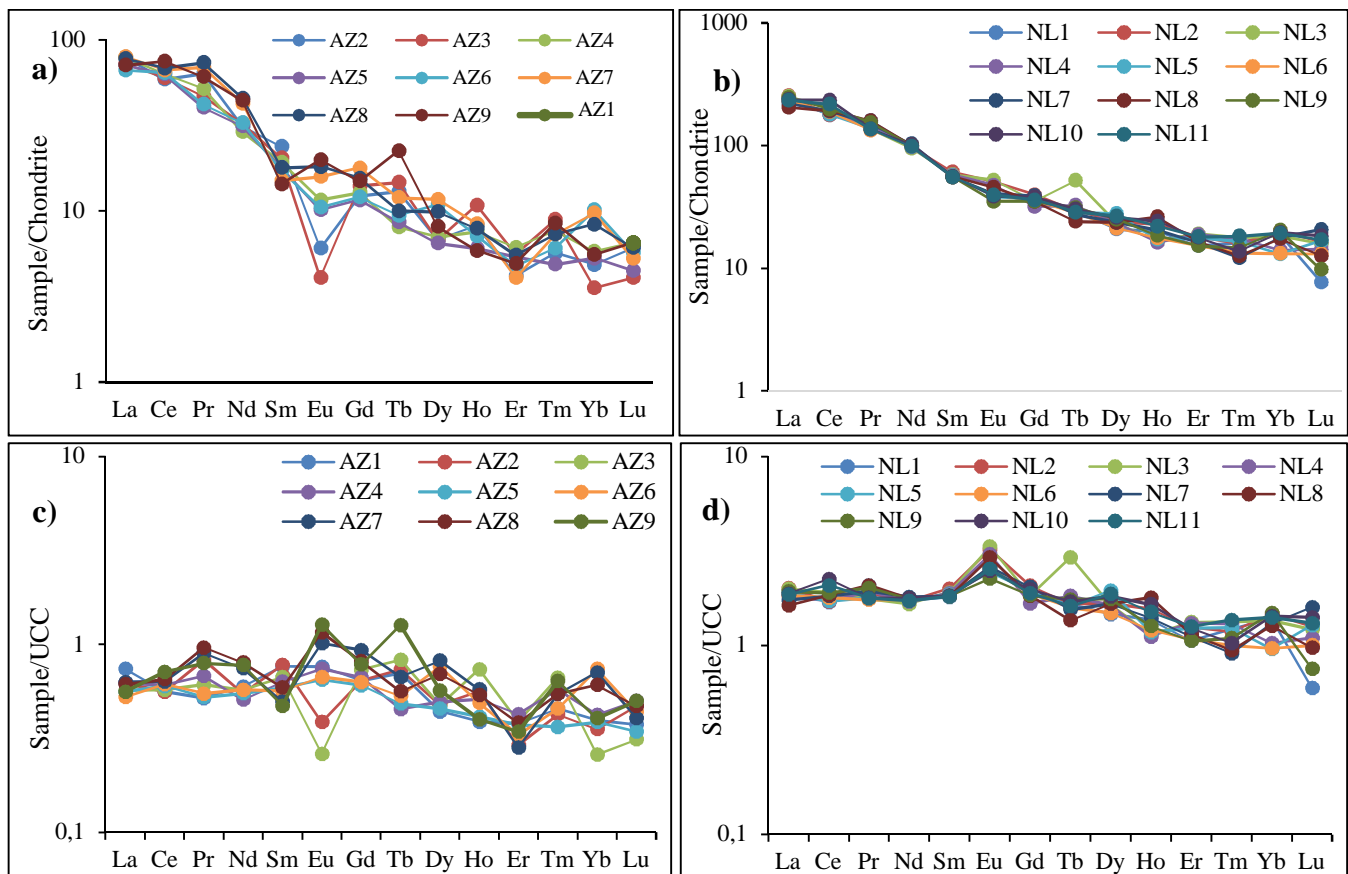


Figure V.13. REE patterns of Ngaoundaba Lake sediments: **a)** Chondrite-normalized (McDonough and Sun, 1995) for NR core; **b)** Chondrite-normalized (McDonough and Sun, 1995) for EB core; **c)** PAAS-normalized (McLennan, 1989) for NR core; **d)** PAAS-normalized (McLennan, 1989) for EB core

Table V.9. Major elements (wt. %) and some element ratios in sediments from the Ngaoundaba Lake

	d.l	Core AZ									Core NL										
		AZ1	AZ2	AZ3	AZ4	AZ5	AZ6	AZ7	AZ8	AZ9	NL1	NL2	NL3	NL4	NL5	NL6	NL7	NL8	NL9	NL10	NL11
SiO ₂	0.04	14.23	14.65	17.43	15.65	15.27	16.87	15.65	17.23	17.59	32.12	32.85	31.76	32.87	33.01	33.97	34.56	31.79	31.32	34.74	33.28
Al ₂ O ₃	0.02	5.97	5.59	3.65	4.76	4.33	4.21	4.75	3.87	3.71	14.34	14.65	14.67	14.6	13.98	13.18	12.54	14.86	14.09	12.89	13.03
Fe ₂ O ₃	0.01	3.12	2.67	2.34	3.03	2.41	2.87	3.98	3.78	2.98	6.45	7.64	7.87	9.25	8.67	8.23	8.37	9.78	9.32	8.83	7.56
TiO ₂	0.01	0.91	0.87	0.46	0.51	0.45	0.67	0.65	0.48	0.94	3.12	3.1	2.14	2.23	2.43	2.27	2.42	2.45	2.89	3.21	2.91
CaO	0.006	0.89	1.2	1.26	1.17	1.21	1.12	1.34	1.21	0.96	0.71	0.68	0.78	1.01	0.7	0.69	0.74	0.67	0.62	0.64	0.68
K ₂ O	0.01	0.31	0.23	0.27	0.21	0.18	0.17	0.24	0.22	0.36	1.01	0.93	0.98	0.89	0.94	0.9	0.84	0.82	1.1	1.09	0.99
MgO	0.01	0.43	0.47	0.51	0.48	0.5	0.61	0.59	0.62	0.66	0.53	0.55	0.56	0.6	0.55	0.59	0.61	0.63	0.47	0.51	0.61
MnO	0.002	0.03	0.042	0.032	0.035	0.03	0.039	0.051	0.016	0.025	0.191	0.213	0.231	0.2	0.18	0.14	0.15	0.19	0.11	0.09	0.12
Na ₂ O	0.02	0.12	0.17	0.31	0.21	0.07	0.09	0.07	0.04	0.09	0.46	0.47	0.63	0.54	0.51	0.41	0.51	0.53	0.62	0.66	0.65
P ₂ O ₅	0.002	0.11	0.29	0.18	0.17	0.12	0.12	0.23	0.27	0.18	0.19	0.32	0.23	0.27	0.24	0.27	0.33	0.31	0.29	0.26	0.3
LOI	-	73.9	73.1	73.5	73.2	75.3	73.2	71.8	70.9	72.2	40.4	38.3	40.1	37.5	38.7	39.1	38.6	37.8	39.2	36.9	39.7
Total	-	100.02	99.28	99.94	99.43	99.87	99.97	99.35	98.64	99.70	99.52	99.70	99.95	99.96	99.91	99.75	99.67	99.83	100.03	99.82	99.83
K ₂ O/Na ₂ O ₃	-	2.58	1.35	0.87	1.00	2.57	1.89	3.43	5.50	4.00	2.20	1.98	1.56	1.65	1.84	2.20	1.65	1.55	1.77	1.65	1.52
Al ₂ O ₃ /TiO ₂	-	6.56	6.43	7.93	9.33	9.62	6.28	7.31	8.06	3.95	4.60	4.73	6.86	6.55	5.75	5.81	5.18	6.07	4.88	4.02	4.48
SiO ₂ /Al ₂ O ₃	-	2.38	2.62	4.78	3.29	3.53	4.01	3.29	4.45	4.74	2.24	2.24	2.16	2.25	2.36	2.58	2.76	2.14	2.22	2.70	2.55
CIA	-	73.51	67.35	54.13	63.81	63.30	64.00	62.82	60.72	61.90	82.03	82.93	80.67	79.83	81.71	81.95	80.21	83.31	80.85	78.99	79.42
CIW	-	76.68	69.43	56.58	65.81	65.16	65.84	65.05	63.07	66.21	87.50	87.94	85.67	84.27	86.88	87.23	85.16	87.67	86.78	85.14	84.97
ICV	-	1.07	1.20	1.77	1.37	1.36	1.57	1.62	1.83	1.90	0.88	0.90	0.86	0.96	0.94	0.95	1.04	0.94	1.01	1.12	1.03
WIP	-	27.53	30.07	36.94	30.60	27.00	25.43	28.03	25.34	29.65	27.21	25.21	29.51	26.84	26.12	24.42	25.22	24.66	29.48	29.21	29.63

d.l.: detection limits.

CIA (%) = $[\text{Al}_2\text{O}_3 / (\text{Al}_2\text{O}_3 + \text{CaO}^* + \text{Na}_2\text{O} + \text{K}_2\text{O})] \times 100$ from Nesbitt and Young (1984).

PIA (%) = $[\text{Al}_2\text{O}_3 - \text{K}_2\text{O} / (\text{Al}_2\text{O}_3 + \text{CaO}^* + \text{Na}_2\text{O} - \text{K}_2\text{O})] \times 100$ from Fedo et al. (1995).

WIP (%) = $(\text{CaO}^* / 0.7 + 2\text{Na}_2\text{O} / 0.35 + 2\text{K}_2\text{O} / 0.25 + \text{MgO} / 0.9) \times 100$, from Parker (1970).

ICV (%) = $(\text{Fe}_2\text{O}_3 + \text{K}_2\text{O} + \text{CaO} + \text{Na}_2\text{O} + \text{MgO} + \text{MnO} + \text{TiO}_2) / \text{Al}_2\text{O}_3$ from Cox et al. (1995). Where CaO* correction was using followed the procedure of McLennan et al. (1993).

Table V.10. Trace elements (ppm) in sediments from the Ngaoundaba Lake

	d.l.	Core AZ									Core NL										
		AZ1	AZ2	AZ3	AZ4	AZ5	AZ6	AZ7	AZ8	AZ9	NL1	NL2	NL3	NL4	NL5	NL6	NL7	NL8	NL9	NL10	NL11
Ba	1	243	168	143	356	148	278	165	198	267	467	423	675	521	596	533	487	387	467	597	520
Ni	20	79	47	67	78	40	38	46	85	76	127	110	187	145	165	152	212	134	187	154	145
Cu	1.4	48.4	42.5	54	44.8	44.8	40.1	52.9	46.4	39	60.2	66.1	64.5	67.2	68.8	69.5	74.1	69.1	73.2	64.2	74.5
Sc	1	8	12	6	6	5	8	9	8	5	10	21	17	18	21	18	19	21	12	17	19
Be	1	6	4	5	7	8	8	8	7	8	1	3	3	2	3	1	4	1	2	2	3
Co	0.2	19.1	23.2	41.9	19.7	20	20.8	28.9	31.3	30	44.5	42.4	39.7	42.7	40.9	41.2	41.8	38.2	33.9	38.6	38.2
Cs	0.1	1.4	1	0.9	0.6	0.8	0.8	0.7	0.8	1	1.1	1.5	1.7	1.4	1.2	1.2	0.9	1.1	1.2	1.2	1.3
Ga	0.5	4.9	6.1	6.4	6.1	5.6	5.9	6	5.8	5.9	15.4	17.3	19.3	20.4	17.9	18.1	18.8	18.3	23.2	22.2	20.9
Hf	0.1	1.7	5.7	1.7	1.1	1.5	1.9	2.7	3.8	3.6	7.8	11.7	6.8	4.7	6.2	6.3	8.8	9.3	6.9	5.9	5.7
Nb	0.1	11.5	16.4	12.3	21.2	11.2	11.9	11.7	10.2	10.9	43.8	52.8	57.1	56.9	49.3	51.7	52.7	50.8	55.8	48.9	49
Rb	0.1	11.9	13.7	16.6	10.9	11.1	16.5	10.8	13.4	17.4	50.8	56.1	42.7	31.8	41.4	43.7	44.7	38.1	49.8	52.2	65.3
Sr	0.5	103.4	107.8	110.4	132	118.7	114.8	117.3	121.9	119	132.3	142.2	119.3	121.4	121	120.7	120.9	118.4	115.5	132.1	121.4
Ta	0.1	0.6	1.3	0.9	0.8	0.8	1.2	1.8	1.4	1.7	3.4	2.9	4.6	3.8	3.7	3.2	2.8	2.9	3.2	2.1	1.9
Th	0.2	3.2	3.8	4.6	4.1	3.8	3.6	3.9	4.5	5.5	13.8	14.1	15.3	16.8	10.4	11.3	15.2	11.5	16.3	14.5	11.4
U	0.1	1.3	0.8	0.8	1	0.9	1.5	1.4	1.1	0.9	3.2	3.6	3.1	2.9	2.1	2.5	2.3	2.8	1.9	2.4	2.1
V	8	84	96	78	59	62	68	76	87	67	151	134	129	135	154	154	134	145	176	134	156
Zr	0.1	74.3	67.4	61.9	71.8	62	85.9	82.2	75.9	80.9	187.8	198.1	252.7	201.9	353.8	256.6	189.9	223.4	298.1	276.9	264
Y	0.1	8.7	9.4	7.1	7.9	8.7	8.4	9.9	9.5	10.4	24.9	25.7	28.2	35.2	21.3	25.2	28.5	24.8	27.8	30.8	31.4
U/Th	-	0.41	0.21	0.17	0.24	0.24	0.42	0.36	0.24	0.16	0.23	0.26	0.20	0.17	0.20	0.22	0.15	0.24	0.12	0.17	0.18
Ni/Co	-	4.14	2.03	1.60	3.96	2.00	1.83	1.59	2.72	2.53	2.85	2.59	4.71	3.40	4.03	3.69	5.07	3.51	5.52	3.99	3.80
Rb/Sr	-	0.12	0.13	0.15	0.08	0.09	0.14	0.09	0.11	0.15	0.38	0.39	0.36	0.26	0.34	0.36	0.37	0.32	0.43	0.40	0.54

d.l.: detection limits.

Table V.11. Trace elements (ppm) in sediments from the Ngaoundaba crater Lake

	Core AZ										Core NL										
	d.l.	AZ1	AZ2	AZ3	AZ4	AZ5	AZ6	AZ7	AZ8	AZ9	NL1	NL2	NL3	NL4	NL5	NL6	NL7	NL8	NL9	NL10	NL11
La	0.1	22.2	18.7	17.1	18.7	16.8	15.7	18.9	18.4	16.8	57.8	60.1	59.7	54.8	56.9	55	52.1	48.7	57.8	56.2	55.7
Ce	0.1	36	35.9	36.7	38.8	38.5	39.3	40.7	41.8	45.7	108.5	109.1	121.8	110.7	109.9	114.7	116.9	117.8	121.6	143.8	132.7
Pr	0.02	3.67	5.87	4.34	4.81	3.72	3.89	6.38	6.82	5.64	14.76	13.45	12.56	13.67	12.7	12.37	13.79	14.74	14.29	12.65	12.59
Nd	0.3	15.5	14.2	14.8	13.2	14.3	14.9	19.4	20.8	20.2	45.3	44.5	43.1	44.3	45.1	45.5	46.9	46	45.7	46.2	44.7
Sm	0.05	3.44	3.51	3.01	2.85	2.64	2.54	2.23	2.65	2.12	8.13	8.98	8.56	8.51	8.36	8.24	8.22	8.2	8.18	8.23	8.19
Eu	0.02	0.67	0.34	0.23	0.65	0.57	0.59	0.89	1.02	1.12	2.25	2.83	2.93	2.67	2.15	2.27	2.29	2.56	1.98	2.18	2.23
Gd	0.05	2.43	2.43	2.78	2.54	2.3	2.39	3.54	3.09	2.97	7.13	7.87	6.98	6.35	7.34	7.07	7.74	6.96	6.98	7.53	7.16
Tb	0.01	0.45	0.47	0.53	0.29	0.31	0.34	0.43	0.36	0.81	1.05	1.06	1.87	1.17	1.04	1.01	0.99	0.87	1.12	1.09	1.03
Dy	0.05	1.54	1.67	1.66	1.73	1.59	2.67	2.87	2.43	1.99	5.12	5.87	5.78	5.73	6.82	5.2	5.82	5.82	6.17	6.36	6.54
Ho	0.02	0.31	0.45	0.59	0.41	0.33	0.39	0.46	0.43	0.32	1.09	1.25	0.91	0.89	0.94	0.96	1.12	1.43	1.01	1.32	1.2
Er	0.03	0.87	0.67	0.89	0.98	0.86	0.76	0.65	0.88	0.79	2.43	2.87	3.05	3.01	2.84	2.46	2.57	2.65	2.43	2.84	2.89
Tm	0.01	0.15	0.14	0.22	0.19	0.12	0.15	0.18	0.18	0.21	0.4	0.39	0.44	0.43	0.41	0.33	0.3	0.31	0.36	0.34	0.45
Yb	0.05	0.87	0.78	0.57	0.93	0.85	1.63	1.56	1.34	0.89	3.04	3.23	2.97	2.26	2.11	2.12	2.87	2.79	3.27	3.14	3.09
Lu	0.01	0.12	0.15	0.1	0.16	0.11	0.14	0.13	0.15	0.16	0.19	0.4	0.39	0.35	0.41	0.32	0.51	0.31	0.24	0.45	0.42
ΣREE	-	88.22	85.28	83.52	86.24	83	85.39	98.32	100.35	99.72	257.19	261.9	271.04	254.84	257.02	257.55	262.12	259.14	271.13	292.33	278.89
LREE	-	81.48	78.52	76.18	79.01	76.53	76.92	88.5	91.49	91.58	236.74	238.96	248.65	234.65	235.11	238.08	240.2	238	249.55	269.26	256.11
HREE	-	6.74	6.76	7.34	7.23	6.47	8.47	9.82	8.86	8.14	20.45	22.94	22.39	20.19	21.91	19.47	21.92	21.14	21.58	23.07	22.78
LREE/HREE	-	12.09	11.62	10.38	10.93	11.83	9.08	9.01	10.33	11.25	11.58	10.42	11.11	11.62	10.73	12.23	10.96	11.26	11.56	11.67	11.24
Ce/Ce*	-	0.96	0.83	1.03	0.99	1.18	1.22	0.90	0.90	1.14	0.90	0.93	1.08	0.98	0.99	1.06	1.06	1.06	1.02	1.30	1.21
Eu/Eu*	-	0.71	0.35	0.24	0.74	0.71	0.73	0.97	1.09	1.36	0.90	1.03	1.16	1.11	0.84	0.91	0.88	1.03	0.80	0.84	0.89
(La/Yb) _N	-	17.33	16.29	20.38	13.66	13.43	6.54	8.23	9.33	12.82	12.92	12.64	13.66	16.47	18.32	17.62	12.33	11.86	12.01	12.16	12.25
(La/Sm) _N	-	4.03	3.33	3.55	4.10	3.97	3.86	5.29	4.34	4.95	4.44	4.18	4.36	4.02	4.25	4.17	3.96	3.71	4.41	4.26	4.25
(Gd/Yb) _N	-	2.26	2.52	3.95	2.21	2.19	1.19	1.84	1.87	2.70	1.90	1.97	1.90	2.27	2.81	2.70	2.18	2.02	1.73	1.94	1.87

d.l.: detection limits.

$$Ce/Ce^* = (Ce_{sample}/Ce_{chondrite}) / (La_{sample}/La_{chondrite})^{1/2} (Pr_{sample}/Pr_{chondrite})^{1/2}.$$

$$Eu/Eu^* = (Eu_{sample}/Eu_{chondrite}) / (Sm_{sample}/Sm_{chondrite})^{1/2} (Gd_{sample}/Gd_{chondrite})^{1/2}.$$

$$(La/Yb)_N = (La_{sample}/La_{chondrite}) / (Yb_{sample}/Yb_{chondrite}).$$

$$(La/Sm)_N = (La_{sample}/La_{chondrite}) / (Sm_{sample}/Sm_{chondrite}).$$

$$(Gd/Yb)_N = (Gd_{sample}/Gd_{chondrite}) / (Yb_{sample}/Yb_{chondrite}).$$

REE are subdivided into LREE (La, Ce, Pr, Nd, Sm and Eu) and HREE (Gd, Tb, Dy, Ho, Er, Tm and Lu).

Cerium is followed by lanthanum and neodymium, and the lowest concentration in this REE is obtained for lutetium (Table V.11). The Ngaoundaba sample sediments show almost no slightly positive or negative Ce anomalies, varying from 0.83 to 1.30. The Eu values ranging from 0.24 to 1.16 from the sediment samples show strong to negligibly negative anomaly. Variation of chondrite- and UCC-normalized REE patterns of the Ngaoundaba Lake suggest various sediments provenance (Figure V.13).

V.3. Environmental statut of lakes

Environmental indices (EF and *I-geo*) coupled with statistical methods were used to assess the environmental status of the lake ecosystem. Heavy metals in lacustrine milieu is known by the human effect and sometimes by the weathering input from source rock. (Xiao et al., 2014). In this study, heavy metals such as Fe, Al, Mn, Cr, Cu, Pb, Zn, Ni, V and Co depending of their presence or not in the studied lakes.

The EF values are grouped in five different categories: $EF \leq 2$ characteristic of absence to minimal enrichment; $2 < EF \leq 5$ due to moderate enrichment; $5 < EF \leq 20$ with significant enrichment; $20 < EF \leq 40$ which represent very high enrichment and $EF > 40$ characteristic of extremely high enrichment (Loska et al., 1997).

The *I-geo* can be grouped into six classes which is representative of sediment quality. These different classes are: $I-geo < 0$ (0; unpolluted); $0 < I-geo \leq 1$ (1; unpolluted to moderately polluted); $1 < I-geo \leq 2$ (2; moderately polluted); $2 < I-geo \leq 3$ (3; moderately to strongly polluted), $3 < I-geo \leq 4$ (4; strongly polluted) and $4 < I-geo \leq 5$ (5; strongly to extremely polluted) (Singh et al., 1997).

V.3.1. Simbock Lake

For the accuracy of the Heavy metals analysis, results showed good linearity over a wide concentration range for the studied metals (Al, Cr, Ni, V, Zn, Cu, Pb and Co) in border and center sample cores from Simbock Lake. The results are shown in Table V.11. These results have shown that the highest metal concentrations were located in the border sediments of the lake. On average basis, the metals follow a decreasing concentration order in the central core (NR) in mg/kg : Al (62298.1) > V (131.1) > Cr (99.1) > Zn (82) > Cu (40) > Ni (34.1) > Co (25.1) > Pb (17.6) and Al (82057.9) > V (135.8) > Cr (122.5) > Zn (84) > Ni (39.9) > Cu (32.8)

> Co (25.1) > Pb (18.5) in the central core (EB). Comparison between the average concentrations of heavy metals in the different sites and samples shows that the average Al concentration is higher than that of other metals. This average Al concentration and those of V, Cr and Co in sample sediments are up to the average shale (80,000 mg/kg) (Turekian and Wedepohl, 1961) reference values. The average concentration of the other metals in this study is less than the reference values of average shale (Turekian and Wedepohl, 1961).

The Enrichment factor (EF), is a simple and easy tool for assessing enrichment degree and comparing the contamination of different environmental biota. Table V.11 shows the enrichment factors (EF) of the studied metals core samples. Cu shows the highest average values (3.24 mg/kg) in the middle of the central core NR. As shown in table V.11, the EF values show a similar behavior. Almost all the studied metals of the sediments from Simbock Lake with $EF < 2$, suggesting absence to minimal enrichment in the lake. This minimal enrichment could be attributed agricultural activities in the mefou watershed.

The geo-accumulation index is a quantitative measure of the degree of pollution in sediments (Singh et al., 2017). Table V.11 present the geo-accumulation index for the quantification of heavy metal accumulation in the sediments of the Simbock Lake. The I-geo grades for the sediments vary from one metal to another and between sample location (Table V.11). All metals in this studied area remain in grade 0 (unpolluted) in all samples, suggesting that the sediments of the study area are under the background value. This may be due leaching of rocks and to the non-use of pesticides and fertilizers in agriculture.

V.3.2. Ossa lake Complex

The basic descriptive statistical values and spatial distributional patterns of the studied trace metals are presented in Table V.12. On the average basis, the metals follow a decreasing concentration order in all the studied core samples but with different value $Fe > V > Cr > Zn > Ni > Cu > Co > Cd$. The higher values are located in OM core from Mwembe Lake and lowest in OL core from river which supply the lakes of the Complex. Comparison of the average concentrations of heavy metals in the different sites and samples shows that the average Fe concentration is higher (61207.5 mg/kg) than that of other metals. This average concentration of iron in sediments is up to the Average Shale (47200 mg/kg) (Turekian and Wedepohl, 1961) reference values. Others metals such as Cr, V, Zn and Co have also values which are up to the average shale values of these sediments. On the other hand, the average concentrations of the other metals in this study are less than the reference values of average shale (Turekian and

Wedepohl, 1961). These values can be attributed to the result of the natural weathering and leaching of rocks.

The enrichment factors of heavy metals in Ossa lakes Complex were as shown in Table V.12. The EF in the study core sediments is generally less than 2 and shows that the sediments of these lakes area might have natural input inflow of most of the heavy metals.

The geo-accumulation index of heavy metals both studied samples of Ossa Complex showed that the sediments were not polluted (Table V.12). They fall in class 0. This could be attributed to the non-use of fertilizers in agricultural activities.

V.3.3. Ngaoundaba Lake

The vertical distribution of studied trace metals (mg/kg) from the AZ and NL cores are presented in Table V.13. Its reveals that the mean concentrations (mg/kg) of selected heavy metals were found in a decreasing order Fe (6.94 – 200.30) > Mn (0.04 – 13.63) > Cr (0.05 – 1.33) > Zn (0.02 – 0.95) > Cu (0.11 – 0.89) > Pb (0.03 – 0.82). However, all metals are under the background values (Turekian and Wedepohl, 1961).

Statistic variations of EF are presents in Table 3. This study showed that selected heavy metals are characteristic of minimal to moderate enrichment ($1 < EF < 5$) except for samples NL1, NL3 and NL4 of the border core of the study lake. Enrichment factor for the selected metals including Mn, Cr, Cu, Pb and Zn in sample NL3 varying from 7.59 to 19.69. This is related to significant enrichment of selected metals in NL3 sample. The same trend can be recognized in NL4 sample except for Cu and Pb with $EF > 40$ related to extremely high enrichment. This extremely high enrichment is also affected in sample NL1 with copper (Table V.13).

The geo-accumulation index of the selected heavy metals in both cores of Ngaoundaba Lake showed that the sediments were not polluted (Table V.13), they fall in class 0 with $I\text{-}geo < 0$.

In this study, the environmental risk assessment of heavy metals suggests low to moderate contamination from border to the bottom of the lake sediments (Table V.13). This can be attributed to their incorporation by anthropogenic influences mainly from tourism, artisanal fishing and sometimes agriculture which is in strong agreement with the sampling area.

Table V.11. Heavy metal, enrichment Factor (EF; Wedepohl, 1995) and Geo-accumulation Index (I-Geo; Müller, 1979) for the sediments from Simbock Lake, calculated based on background values (Turekian and Wedepohl, 1961)

Core		NR core														EB core				
Element		NR12	NR5	NR13	NR4	NR31	NR10	NR3	NR9	NR8	NR2	NR7	NR6	NR11	NR1	EB1	EB2	EB3	EB4	EB5
Heavy metals	Al	76008	50018	71720	36309	38850	73890	58858	74473	45573	766956	38745	8680	68968	74420	49701	67115	101096	101837	110359
	Cr	100	91	98	71	70	106	104	106	78	125	85	137	109	108	76	107	156	153	144
	Ni	40.7	23.2	38.7	10.1	14.2	44.8	34.6	45.2	16.8	53.4	27.7	46.7	39.5	42.2	9.7	18.3	57.9	58.4	61.2
	V	134.1	121.1	150.2	91.8	93.2	144.4	126.2	145.2	100.6	161.7	131.1	150.2	145.2	140.5	59.9	98	177.2	175.5	172.8
	Zn	92	65	88	28	36	116	88	115	47	140	37	112	92	92	20	34	124	125.00	119
	Cu	39.1	50.9	34.8	15.2	24.8	40.3	45.8	43.1	40.1	49.3	70.6	41.8	31.4	36.8	7.5	12.7	44.4	44.9	46.9
	Pb	28.1	13.7	20.4	7.7	9.7	22.2	17.5	22.4	10.4	21.4	8.9	23.8	19.2	21.5	4.6	7.6	26.4	26.4	28.5
	Co	26.03	18.82	27.71	7.9	11.23	33.41	25.33	38.03	12.87	41.29	11.73	39.03	30.66	26.72	7.15	13.09	35.86	35.57	34.05
EF	Al / Al	1	1	1	1	1	1	1	1	1	1	1	1	1	1	1	1	1	1	1
	Cr / Al	1.17	1.62	1.21	1.74	1.60	1.28	1.57	1.27	1.52	1.45	1.95	1.40	1.40	1.29	1.36	1.42	1.37	1.34	1.16
	Ni / Al	0.63	0.55	0.63	0.33	0.43	0.71	0.69	0.71	0.43	0.82	0.84	0.63	0.67	0.67	0.23	0.32	0.67	0.67	0.65
	V / Al	1.09	1.49	1.29	1.56	1.48	1.20	1.32	1.20	1.36	1.30	2.08	1.06	1.30	1.16	0.74	0.90	1.08	1.06	0.96
	Zn / Al	1.02	1.09	1.03	0.65	0.78	1.32	1.26	1.30	0.87	1.54	0.80	1.09	1.12	1.04	0.34	0.43	1.03	1.03	0.91
	Cu / Al	0.91	1.81	0.86	0.74	1.13	0.97	1.38	1.03	1.56	1.14	3.24	0.86	0.81	0.88	0.27	0.34	0.78	0.78	0.76
	Pb / Al	1.48	1.10	1.14	0.85	1.00	1.20	1.19	1.20	0.91	1.12	0.92	1.10	1.11	1.16	0.37	0.45	1.04	1.04	1.03
	Co / Al	1.44	1.58	1.63	0.92	1.22	1.90	1.81	2.15	1.19	2.27	1.27	1.89	1.87	1.51	0.61	0.82	1.49	1.47	1.30
I-Geo	Al	-0.66	-1.26	-0.74	-1.72	-1.63	-0.70	-1.03	-0.69	-1.40	-0.65	-1.63	-0.47	-0.80	-0.69	-1.27	-0.84	-0.25	-0.24	-0.12
	Cr	-10.23	-10.36	-10.26	-10.72	-10.74	-10.14	-10.17	-10.14	-10.59	-9.91	-10.46	-9.77	-10.10	-10.12	-10.62	-10.13	-9.59	-9.62	-9.70
	Ni	-11.53	-12.34	-11.60	-13.54	-13.04	-11.39	-11.76	-11.37	-12.80	-11.13	-12.08	-11.33	-11.57	-11.47	-13.59	-12.68	-11.02	-11.00	-10.94
	V	-9.81	-9.95	-9.64	-10.35	-10.33	-9.70	-9.89	-9.69	-10.22	-9.54	-9.84	-9.64	-9.69	-9.74	-10.97	-10.26	-9.40	-9.42	-9.44
	Zn	-10.35	-10.85	-10.41	-12.07	-11.70	-10.01	-10.41	-10.03	-11.32	-9.74	-11.66	-10.07	-10.35	-10.35	-12.55	-11.79	-9.92	-9.91	-9.98
	Cu	-11.58	-11.20	-11.75	-12.95	-12.24	-11.54	-11.36	-11.44	-11.55	-11.25	-10.73	-11.49	-11.90	-11.67	-13.97	-13.21	-11.40	-11.38	-11.32
	Pb	-12.06	-13.10	-12.52	-13.93	-13.59	-12.40	-12.74	-12.39	-13.49	-12.45	-13.72	-12.30	-12.61	-12.45	-14.67	-13.95	-12.15	-12.15	-12.04
	Co	-12.17	-12.64	-12.08	-13.89	-13.38	-11.81	-12.21	-11.62	-13.19	-11.50	-13.32	-11.59	-11.93	-12.13	-14.03	-13.16	-11.71	-11.72	-11.78

Table V.11. Heavy metal, enrichment Factor (EF; Wedepohl, 1995) and Geo-accumulation Index (Igeo; Müller, 1979) for the sediments from Ossa Complex, calculated based on background values (Turekian and Wedepohl, 1961)

Core		LO Core							OM Core							OL Core			
Elements		LO1	LO2	LO3	LO4	LO5	LO6	LO7	OM1	OM2	OM3	OM4	OM5	OM6	OM7	OL1	OL2	OL3	OL4
Heavy metals	Fe	45111.30	38886.64	54063.62	56021.94	60568.04	62736.18	73017.36	60218.34	65463.84	61337.38	63995.10	70639.40	49867.22	56931.16	62246.60	65673.66	58819.54	5455.32
	Cr	135	131	120	133	125	113	108	136	132	144	133	133	132	109	62	115	125	115
	V	153.2	141.6	131.2	142.8	139.9	138.5	148.3	137.4	129.6	151.9	144.6	147.4	160.5	129.2	44.6	127.4	139.3	128.6
	Ni	54.9	52.5	48.7	53	51.8	53.2	52.4	54	50.3	58.3	53.5	53.8	54.7	42.3	10.7	42.6	52.9	47.9
	Zn	97	85.1	84.6	92	88.2	73	79.3	99.8	90.3	102.4	96.6	96.5	94.6	84.6	12.2	76.8	93.2	84.9
	Cu	35.5	34.9	31.4	34.6	33.9	38.5	42.1	34.5	33.1	36	34.8	35.9	40	35.3	4.3	30.9	34.8	31.7
	Co	27.14	26.33	23.17	26.12	26.53	17.22	23.35	26.19	24.23	29.28	29.64	27.83	28.66	26.18	2.54	20.06	25.79	26.07
	Cd	0.09	0.09	0.10	0.12	0.11	0.08	0.18	0.15	0.13	0.13	0.12	0.10	0.08	0.14	0.01	0.06	0.09	0.11
EF	Fe / Fe	1	1	1	1	1	1	1	1	1	1	1	1	1	1	1	1	1	1
	Cr / Fe	1.57	1.77	1.16	1.25	1.08	0.94	0.78	1.18	1.06	1.23	1.09	0.99	1.39	1.00	0.52	0.92	1.11	11.06
	V / Fe	1.23	1.32	0.88	0.93	0.84	0.80	0.74	0.83	0.72	0.90	0.82	0.76	1.17	0.82	0.26	0.70	0.86	8.56
	Ni / Fe	0.84	0.94	0.63	0.66	0.59	0.59	0.50	0.62	0.53	0.66	0.58	0.53	0.76	0.52	0.12	0.45	0.62	6.09
	Zn / Fe	1.07	1.09	0.78	0.82	0.72	0.58	0.54	0.82	0.69	0.83	0.75	0.68	0.94	0.74	0.10	0.58	0.79	7.73
	Cu / Fe	0.83	0.94	0.61	0.65	0.59	0.64	0.60	0.60	0.53	0.62	0.57	0.53	0.84	0.65	0.07	0.49	0.62	6.09
	Co / Fe	1.49	1.68	1.06	1.16	1.09	0.68	0.79	1.08	0.92	1.19	1.15	0.98	1.43	1.14	0.10	0.76	1.09	11.87
	Cd / Fe	0.33	0.38	0.29	0.33	0.29	0.20	0.39	0.40	0.31	0.34	0.30	0.23	0.26	0.37	0.03	0.15	0.24	3.14
I-geo	Fe	-0.65	-0.86	-0.39	-0.34	-0.23	-0.17	0.04	-0.23	-0.11	-0.21	-0.15	0.00	-0.51	-0.31	-0.19	-0.11	-0.27	-3.70
	Cr	-9.03	-9.08	-9.20	-9.06	-9.15	-9.29	-9.36	-9.02	-9.07	-8.94	-9.06	-9.06	-9.07	-9.34	-10.16	-9.27	-9.15	-9.27
	V	-8.85	-8.97	-9.08	-8.95	-8.98	-9.00	-8.90	-9.01	-9.09	-8.86	-8.94	-8.91	-8.79	-9.10	-10.63	-9.12	-8.99	-9.10
	Ni	-10.33	-10.40	-10.51	-10.38	-10.42	-10.38	-10.40	-10.36	-10.46	-10.25	-10.37	-10.36	-10.34	-10.71	-12.69	-10.70	-10.39	-10.53
	Zn	-9.51	-9.70	-9.71	-9.59	-9.65	-9.92	-9.80	-9.47	-9.61	-9.43	-9.52	-9.52	-9.55	-9.71	-12.50	-9.85	-9.57	-9.70
	Cu	-10.96	-10.99	-11.14	-11.00	-11.03	-10.84	-10.72	-11.00	-11.06	-10.94	-10.99	-10.95	-10.79	-10.97	-14.01	-11.16	-10.99	-11.13
	Co	-11.35	-11.39	-11.58	-11.40	-11.38	-12.01	-11.57	-11.40	-11.51	-11.24	-11.22	-11.31	-11.27	-11.40	-14.77	-11.79	-11.42	-11.41
	Cd	-19.52	-19.52	-19.46	-19.21	-19.27	-19.77	-18.58	-18.81	-19.08	-19.03	-19.15	-19.40	-19.74	-19.00	-22.38	-20.08	-19.59	-19.31

Table V.13. Heavy metal, enrichment Factor (EF; Wedepohl, 1995) and Geo-accumulation Index (Igeo; Müller, 1979) for the sediments from Ngaoundaba crater Lake, calculated based on background values (Turekian and Wedepohl, 1961)

Core		Core AZ									Core NL										
Sample		AZ1	AZ2	AZ3	AZ4	AZ5	AZ6	AZ7	AZ8	AZ9	NL1	NL2	NL3	NL4	NL5	NL6	NL7	NL8	NL9	NL10	NL11
Heavy metals	Fe	6.94	176.60	34.88	13.50	200.30	164.89	216.89	213.70	121.96	95.53	199.30	201.60	189.49	187.81	173.20	218.70	143.70	118.90	132.80	120.10
	Mn	0.04	8.83	4.77	1.46	10.49	10.99	11.76	11.08	4.77	2.65	13.63	11.79	9.99	7.40	6.87	4.97	4.89	5.40	3.34	2.91
	Cr	0.05	0.73	0.87	0.81	1.01	1.33	1.14	0.94	0.35	0.23	0.48	0.63	0.65	0.71	0.76	0.69	0.56	0.27	0.66	0.55
	Cu	0.76	0.44	0.65	0.89	0.60	0.67	0.69	0.49	0.37	0.11	0.23	0.27	0.37	0.36	0.39	0.37	0.28	0.26	0.26	0.21
	Pb	0.03	0.07	0.23	0.82	0.34	0.23	0.10	0.11	0.03	0.04	0.22	0.27	0.25	0.22	0.13	0.15	0.17	0.09	0.11	0.12
	Zn	0.02	0.42	0.66	0.95	0.54	0.58	0.52	0.46	0.17	0.17	0.65	0.89	0.84	0.77	0.55	0.54	0.32	0.18	0.34	0.32
EF	Fe / Fe	1	1	1	1	1	1	1	1	1	1	1	1	1	1	1	1	1	1	1	1
	Mn / Fe	3.25	2.93	2.19	2.20	1.26	1.89	2.52	1.40	1.34	0.33	2.78	7.59	6.01	2.91	3.70	3.01	2.88	2.17	1.54	3.80
	Cr / Fe	1.64	1.80	2.00	2.31	1.67	2.06	1.19	2.62	2.41	3.96	2.16	13.01	31.53	2.63	4.22	2.77	2.30	1.52	1.28	1.27
	Cu / Fe	1.39	2.06	2.02	2.38	1.79	2.03	2.26	2.08	1.82	115.16	2.61	19.69	69.34	3.16	4.29	3.35	2.42	3.14	1.23	1.22
	Pb / Fe	3.16	3.17	2.73	1.81	1.67	2.72	1.82	1.94	2.41	0.95	0.94	15.63	143.91	4.03	3.36	1.13	1.18	0.67	0.87	2.55
	Zn / Fe	2.20	2.20	2.03	1.57	1.22	1.10	0.77	1.28	1.33	1.73	1.18	9.37	34.84	1.33	1.76	1.18	1.06	0.67	0.90	1.63
I-geo	Fe	-2.55	-2.57	-2.58	-2.61	-2.51	-2.69	-2.77	-2.73	-2.77	-4.01	-2.60	-3.31	-3.72	-2.55	-2.63	-2.51	-2.52	-2.76	-2.87	-2.55
	Mn	-2.03	-2.11	-2.24	-2.27	-2.41	-2.42	-2.37	-2.58	-2.64	-4.49	-2.16	-2.43	-2.94	-2.08	-2.06	-2.04	-2.06	-2.43	-2.68	-1.97
	Cr	-2.33	-2.32	-2.28	-2.25	-2.29	-2.38	-2.70	-2.31	-2.39	-3.41	-2.27	-2.19	-2.22	-2.13	-2.01	-2.07	-2.16	-2.58	-2.76	-2.45
	Cu	-2.40	-2.26	-2.27	-2.24	-2.26	-2.38	-2.42	-2.41	-2.51	-1.95	-2.19	-2.01	-1.88	-2.05	-2.00	-1.99	-2.14	-2.27	-2.78	-2.46
	Pb	-2.05	-2.07	-2.14	-2.35	-2.29	-2.26	-2.51	-2.44	-2.39	-4.03	-2.63	-2.11	-1.56	-1.94	-2.11	-2.46	-2.45	-2.94	-2.93	-2.14
	Zn	-2.20	-2.23	-2.27	-2.42	-2.42	-2.65	-2.89	-2.62	-2.65	-3.77	-2.53	-2.34	-2.18	-2.42	-2.39	-2.44	-2.50	-2.94	-2.92	-2.34

Conclusion

The mineralogical content of Simbock Lake consists of Quartz, kaolinite, Illite, smectite, muscovite, goethite, rutile and traces of hematite and feldspars. This lake has high proportions of silica and alumina which increases from the center to the edge of the lake with moderate values. These proportions could justify the dominance of the quartz and the clay minerals in these samples. Similarly, the moderate titanium oxide and loss on ignition values could be justified by the presence of clay minerals. Likewise, the high zirconium contents could suggest the presence of zircon in these materials. These sediments also contain high values of barium, vanadium and chromium. The studied sediments have a high fractionation of their source rocks. Negative Eu anomaly observed suggests several stages of weathering. This weathering is confirmed by the chemical weathering indices showing that the rocks that gave birth to these sediments would be very weathered. In this study, the environmental risk assessment by heavy metals suggests absence to low contamination of the lake sediments attributed to low anthropogenic activities in the studied



*Chapter VI: Dating and
paleoenvironmental
reconstruction*

School should always aim to give its students a harmonious personality, not to train them as specialists.

-Albert Einstein-

In this chapter, a paleo-environmental reconstruction based mainly on species vegetation, hydrology and climate using the ages provided by radiocarbon dating; diatoms and pollen-algae analyses from the South and North lakes of the country are presented. To achieve this objective, the current state of the environment, the lithology of the cores, their ages and the quantification of micro-organism species will be discussed.

VI.1. Radiocarbon dating

The ages of ^{14}C obtained or inferred in this study were based on analyses of bulk samples and remnants of plant organisms from organic-rich intervals in lake sediment cores from the south and north of the country. The ages reported in this work are in radiocarbon years prior to today. When these results are used here, they have been calibrated, along with other dates, using the *INTCAL13* dataset and the *Calib 7.0.2* programs (Reimer et al., 2013, Stuiver and Reimer, 1993).

Lake sediments reflect a variety of different deposits ranging on a scale from purely allochthonous to purely autochthonous, minerogenic and/or organic material. They may contain, for example, precipitated and/or in-washed minerogenic matter, terrestrial and aquatic plant and animal remains, including algae, bacteria, fungi, as well as reworked older organic material (Figure VI.1). The organic material may also be affected by diagenesis. Although careful pre-treatments are applied to all samples before a radiocarbon measurement (e.g., Lowe and Walker, 1997), a large number of unknown factors will still influence the resulting radiocarbon age, especially if it has been obtained on the bulk sediment.

If only single dates are obtained along a sediment sequence, the likelihood and amount of contamination will, therefore, be difficult to appraise. Lake water composition is one major limiting factor for obtaining accurate radiocarbon ages on bulk sediment and aquatic plant and animal samples (Olsson, 1986).

Two cores in addition to those used in this thesis, studied by Nguetsop et al., 2000 and 2013, are included in this study. These cores are OW4 core from Lake Ossa and T2 core from Lake Tizong in the Adamaoua. The LO and AZ cores from lakes Ossa and Ngaoundaba lakes were also selected to complete this paleoenvironmental study (Figure VI.2).

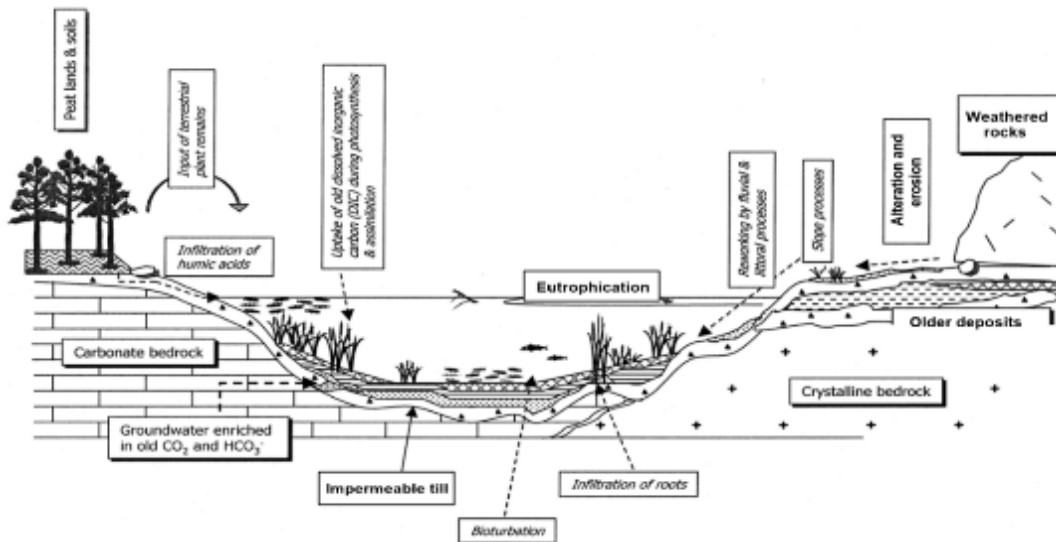


Figure VI.1. Sketch showing a variety of possible sources of errors, which can influence bulk sediment radiocarbon dates in sub-tropical lakes (adapted from Björck et al., 2002)

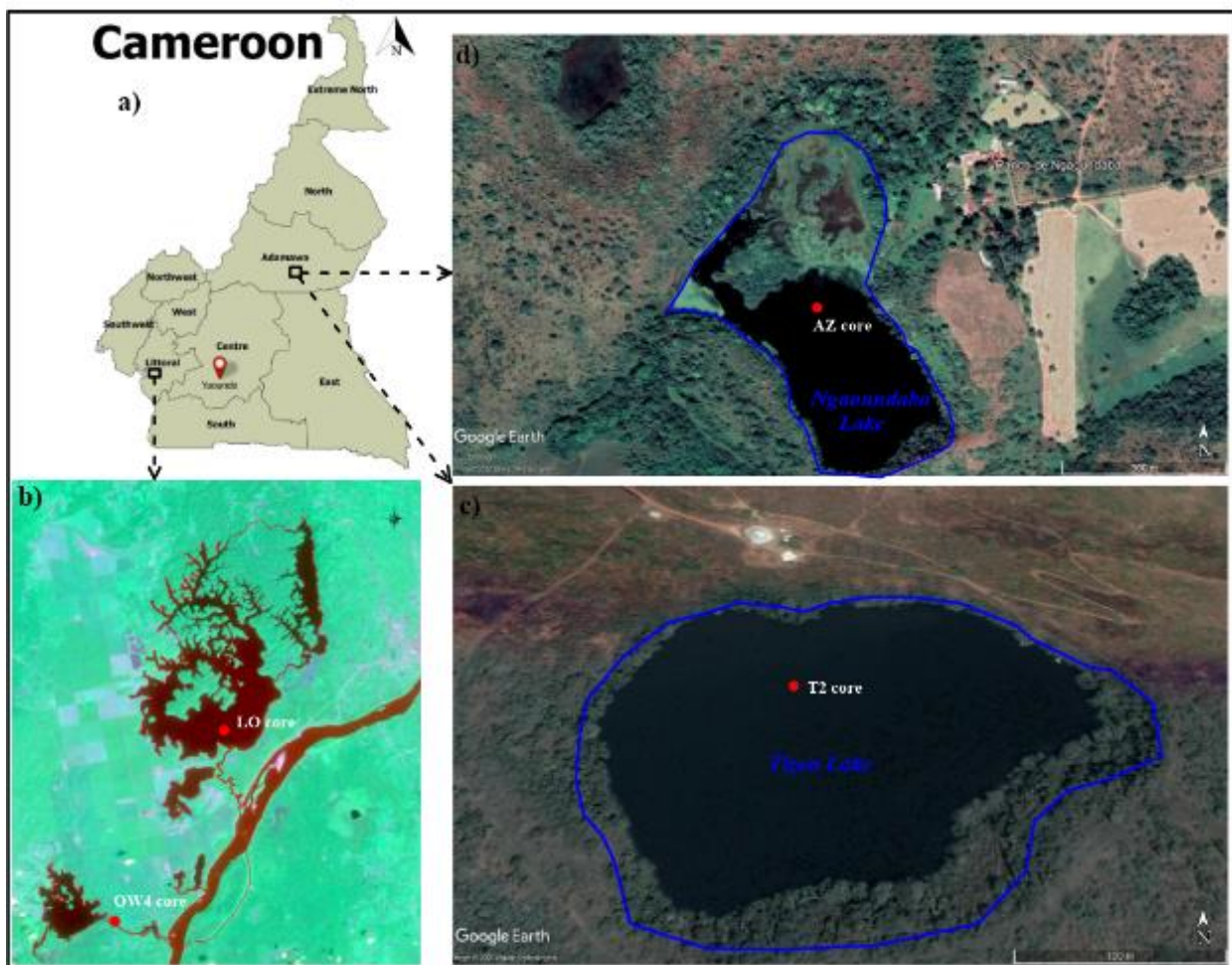


Figure VI.2. Location of the studied areas: **a)** location of the studied lakes in Cameroon; **b)** Ossa lakes Complex in Dizanguè (South-west, Cameroon); **c)** Tizon Lake and **d)** Ngaoundaba Lake both in Ngaoundéré (Adamaoua, North-Cameroon)

Table VI.1 presents data for all sites, including their location, elevation, water depth, sedimentary stratigraphy, inferred levels and ages of basin isolation, and corresponding inferred radiocarbon dates.

Table VI.1. Radiocarbon dating of organic sedimentary carbon of cores sediments

Core sediments	Depth (cm)	Description	Laboratory no.	Conventional ¹⁴ C ages (yrs BP.)
OW4*	6.8-9.0	Bulk sediment	Beta-73082	90 ± 60
OW4*	62.7-64.9	Bulk sediment	Beta-86769	740 ± 50
OW4*	122.9-125.5	Bulk sediment	Beta-73083	1890 ± 60
LO-11	10-12	Leaf	Poz-123265	230 ± 30
LO-71	70-72	Twig	Poz-122616	380 ± 30
LO-148	147-149	Wood	Poz-122828	505 ± 30
T2-22*	22	Bulk sediment	Poz-38507	485 ± 30
T2-50*	50	Bulk sediment	SacA-19776	545 ± 30
T2-90*	90	Bulk sediment	Pozan	1040 ± 30
AZ-6	5-7	Wood	Poz-123264	155 ± 30
AZ-41	41-43	Wood	Poz-122516	425 ± 30
AZ-86	85-87	Twig	Poz-122728	1030 ± 30

* indicates dates already published in Nguetsop et al. (2000, 2013)

VI.1.1. Present environment

VI.1.1.1. Ossa lake Complex (South-west, Cameroon)

Lake Ossa, 20 km west of Edéa, is located at an altitude of 8 m, its average depth being 10 feet tall. Its surface area covers about 4,500 ha for a catchment area of 190 km² (Figure VI.2b), the highest point of which is at 165 m altitude (Wirmann, 1992). The climate of this region is characterized by an average annual rainfall of about 2535.41 mm and a long rainy season from March to November, mitigated by a short dry season (June) and interrupted by a long dry season of 3 months (December to February). The annual mean temperature is around 27.2°C. Two forest formations predominate in SW Cameroon. The Biafran evergreen forest, on the one hand, is very diversified and has a high abundance of *Caesalpinaceae*. The Atlantic coastal forest, on the other hand, is poor in *Caesalpinaceae* and characterized by the abundance of *Loflhira alata* (Ochnaceae), *Sacogottis gabonensis* (Humiriaceae), *Coula edulis* (Olacaceae) and *Cynometra hankei* (Caesalpinaceae). Around Ossa Complex, in areas not degraded by the development of food crops, the Atlantic coastal forest dominates. Since the beginning of the century, a large plantation of rubber trees (*Hevea hasiliensis*) and oil palms (*Elaeis guineensis*) has gradually developed on the western shore of the lake.

VI.1.1.2. Tizon and Ngaoundaba lakes (Adamawa, North-Cameroon)

The Adamawa Plateau is located in the altitudinal tropical climate which is a transition between the Equatorial climate in the south and the Sahelian climate to the north. There are two seasons: a rainy season (April to October) and a dry season (November to March). Mean temperatures vary between 23 °C and 26 °C while mean annual precipitation varies around 1500 mm. The current precipitation reaches 1589 mm at Ngaoundéré (Olivry, 1986; Ngos and Giresse, 2011). On the vegetation map of Cameroon (Letouzey, 1985) the Adamawa is covered by Sudanese type of woody savanna characterized by two main trees: *Daniella oliveri* (Caesapiniaceae) and *Lophira lanceolata* (Orcnaceae). Northwards, the height and density of the vegetation drop, gradually giving way to herbaceous savanna. The two studied lakes are located less than 100 km to the most northerly patches of humid forest.

Lake Tizong is at an altitude of 1154 m. It is dominated westward by an ancient circular volcano topping at 1261 m. The area is about 8 ha and the maximum water depth is 48 m (Figure VI.2c). Tizong is one of the smallest crater lakes in Cameroon, with neither any drainage outlet nor active river inlet. Its watershed (about 18 ha) is asymmetric, essentially present on the western and northern sides (Kling, 1988). The vegetation is herbaceous with bouquets of wide isolated shrubs. The bathymetry describes a symmetric bowl with marked steep slopes.

Lake Ngaoundaba, 17 ha in area at 1160 m of altitude, has a maximum depth of 62 m with an average depth of 17 m (Kling, 1988). The Lake area is continuously decreasing due to eutrophication and urbanization. This fish-bearing lake, where swimming and fishing take place, is one of the attractions of the Ngaoundaba ranch, which is a place renowned for its tourist capacity. Known as a maar, this Crater lake is one of a multitude of other Crater lakes that abound in the far north of Cameroon and particularly in the Adamaoua region (Ohba et al., 2013).

VI.1.2. Lithology of cores

The sediment succession in this study includes four cores from three different lakes. The OW4 and LO cores were sampled from the Ossa Complex in the southern part of the country. The T2 core was taken from Tizon Lake while the AZ core was taken from Ngaoundaba Lake, two crater lakes from the North of the country in the Adamaoua region precisely.

VI.1.2.1. Cores from the South-Cameroon (Ossa lake Complex)

OW4 Core

The core studied, OW4, measures 140 cm (Figure VI.3) and was taken from the southern part of the lake, using a vibrating core drill. The sedimentary sequence consists of an unlaminated homogeneous clayey mud, 5Y2.5/2 wet colour (Munsell Soil Color Charts, 1975), rich in organic matter and free of signs of bioturbation. The layer was mainly composed of organic-clay mud. Three radiocarbon dates by Accelerator Mass Spectrometry (AMS) were performed on total organic matter by Beta Analytic Inc, Miami, USA (Beta). The ages obtained were corrected by reference to $\delta^{13}\text{C}$ (Table VI).

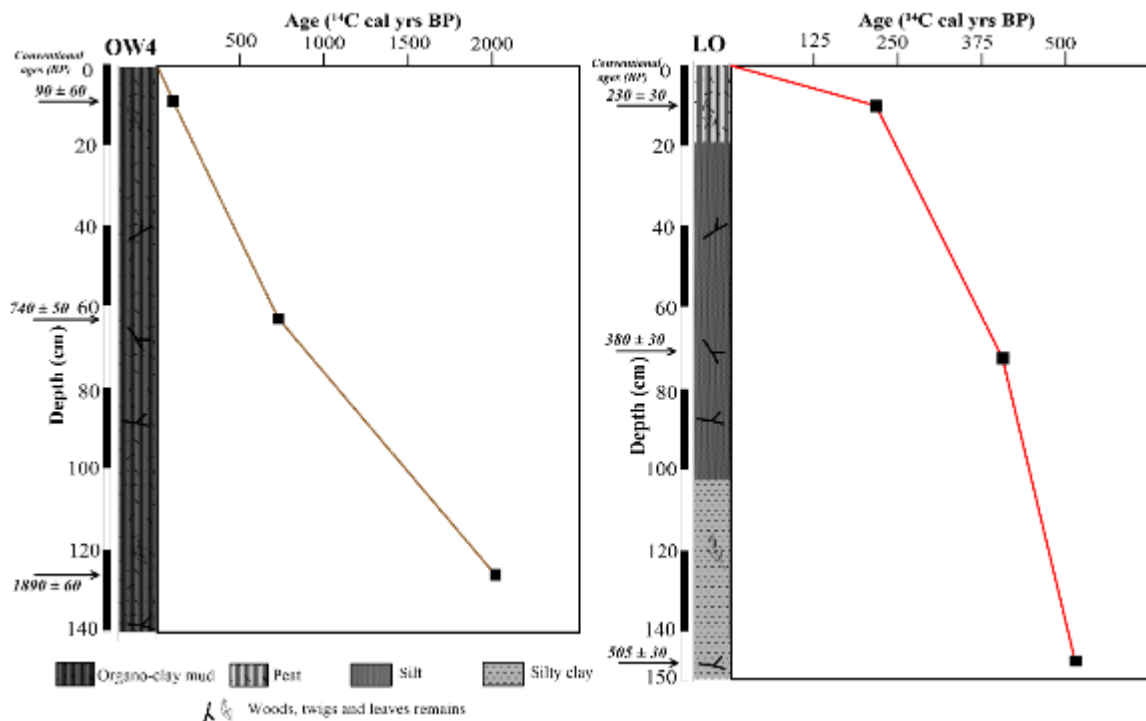


Figure VI.3. Lithology, radiocarbon ages and age models of OW4 and LO cores from Ossa lakes Complex

LO Core

The LO core was retrieved near the center of Ossa Lake, at 4.5 m water depth, it is 150 cm long. The observations show that the cores are mainly composed of fine-grayish- to brown-grained (and peat), with visible twigs and leaves. It is very humid and the grain size of the selected lake sediments is almost similar. From the bottom to the top, the layers of LO core contain organic laminates (past millimeter black organic wakes, twigs, woods and leaves). The first layer is dark grey (2.5Y 4/1) with silty clay texture, this layer is about 30 cm thick.

Secondly, the long silt texture layer of 80 cm thick is greyish brown (2.5Y 5/2). The last layer is smallest with 20 cm. It is a heavy silt layer, the color is dark greysish brown (2.5Y 4/2) (Figures IV.3). This layer has high organic debris than the others cores of the complex. Three radiocarbon dates by AMS were performed on wood, twig and leaf by the Poznan Radiocarbon Laboratory, Poland.

VI.1.2.2. Cores from the North-Cameroon (Tizon and Ngaoundaba lakes)

T2 Core

We investigated samples from core T2 that was retrieved in the central part of the Tizon Lake at a water depth of 47.1 m. The sampling was realised by the Ecofit program team using a compressed-air Mackereth corer. The 6 m long core is composed mainly of fine, dark clayey sediments (Figure VI.4). The core sediments were subdivided into two layers, a dark grey (2.5Y 4/1) silty layer and a very dark grey (2.5 Y 3/1) layer. Radiocarbon ages of three bulk sediment samples were performed in two different radiocarbon laboratories.

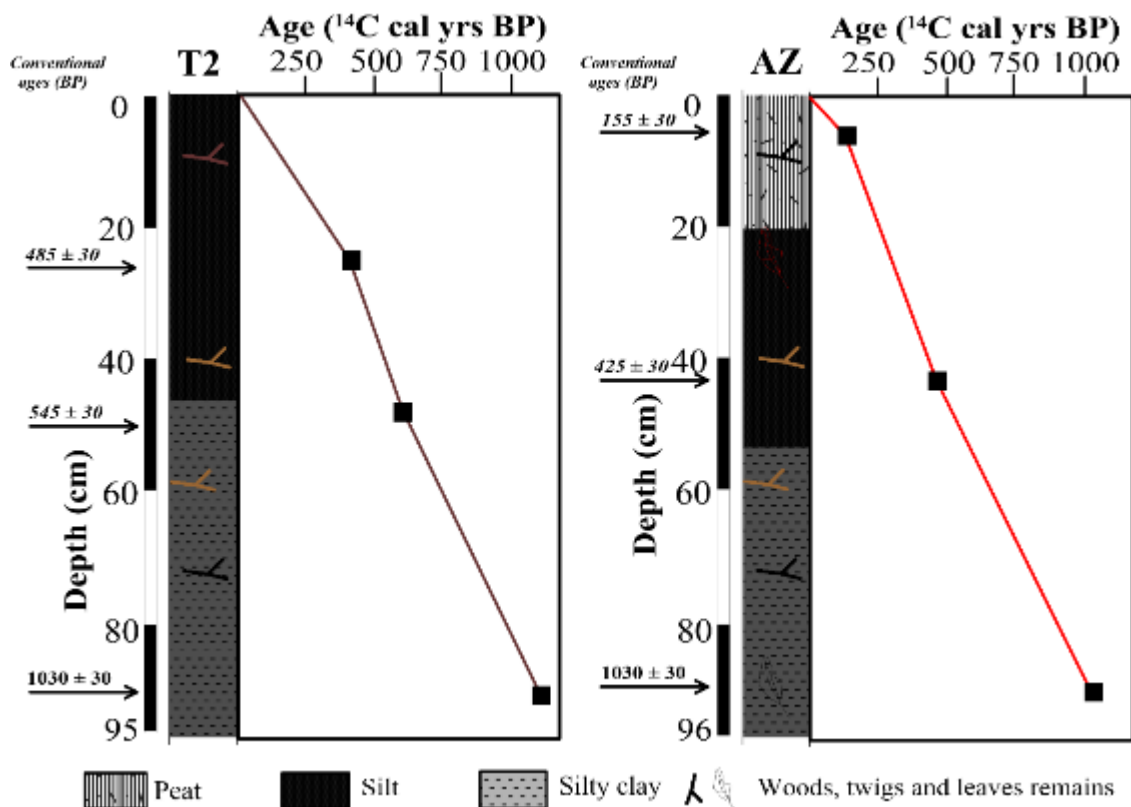


Figure VI.4. Lithology, radiocarbon ages and age models of T2 and AZ cores from Tizon and Ngaoundaba lakes

AZ Core

The central core AZ of 96 cm thick exhibits from the bottom to the top, a clayey silt texture but have different colors and thickness. This core was collected using a manual corer equipped with extension rods from a boat at 8 m depth. The core labeled AZ were collected using 50 mm diameter PVC pipes hermetically sealed. The basal layer composed is 36 cm thick and dark grey (2.5Y 4/1) in color. The second layer has a very dark grey (2.5 Y 3/1) color and it is 10 cm thick. The third layer is 30 cm thick which a black color (5Y 2.5/1) and the last layer is a dark greyish brown (2.5Y 4/2) layer of 30 cm of thickness (Figure VI.4). Likes in the others cores three samples composed of wood, and twigs were selected for radiocarbon dating in the Poznan Radiocarbon Laboratory, Poland.

VI.1.3. Radiocarbon ages and age models

The results of radiocarbon measurements are summarized in Table VI and shown in Figures VI.4 and 5. From the four sediment cores analysed, the radiocarbon ages obtained on bulk sediments are well stratigraphy but are systematically older than the radiocarbon ages obtained on plant debris (Figures VI.4 and 5). Sedimentation rate is the height of sediment deposited in a basin over a defined time interval. It is obtained from the following formula:

$$S = \frac{D2 - D1}{P2 - P1}$$

Where S represente the sedimentation rate, D1 and D2 are the ages of the sediments at P1 and P2 depth respectively, P2 > P1.

VI.1.3.1. Ossa lake Complex (South-west, Cameroon)

OW4 Core

The ages of the OW4 core were performed entirely on the bulk sediments at the top, middle and base of the sectioned core. The ages obtained are decreasing from the base to the top and respect the principle of successive deposition. The base sample is dated 1890 ± 60 cal. year BP, while the middle sample would have been dated 740 ± 50 cal. year BP. and the top sample would have been dated 90 ± 60 cal. year BP. The depositional model in this part of the lake and at this depth would be deposited in two different phases with different sedimentation rates. From 64 cm to 124 cm, this rate is about 19.2 cm/year, while from the top to 64 cm the

sediments would have been deposited at a sedimentation rate of 11.4 cm/year as shown in the curve of the depositional model of the OW4 core (Figure VI.3).

LO Core

In the LO core from the Ossa Lake, the ages were realised at the base in wood remain, at the middle in twig and at the top, in leaf remain. The wood sample (LO-148) is dated 505 ± 30 yrs BP., while the twig sample (LO-71) would have been dated 485 ± 30 yrs BP. and the leaf sample (LO-11) have been dated 230 ± 30 yrs BP. The depositional model in the central part of the Ossa lakes Complex for the first 150 cm shows three different sedimentation rates phases. From 71 to 148 cm, the sedimentation rate is about 2.21 cm/year, while from 11 to 71 cm, the rate is about 2.5 cm/year and from the top of the core sediment to around 11 cm the sediments have been deposited at a sedimentation rate of 20.9 cm/year as shown in the curve of the depositional model of the studied core (Figure VI.3). The first and second phases can be group in one phase of a sedimentation rate of 2.36 cm/year.

VI.1.3.2. Tizon and Ngaoundaba lakes (North-Cameroon)

T2 Core

The core from the center of Tizon Lake were labeled T2 core, the ages of this core were performed entirely on the bulk sediments rich in organic matter contents at the top, middle and base of the sectioned part of the core. The ages obtained are decreasing from the base to the top and respect the principle of successive deposition. The base sample is dated 1040 ± 30 cal. year BP, the middle sample of the core have been dated 545 ± 30 cal. year BP. and the top sample could have been deposit at 485 ± 30 cal. year BP. The depositional model in this part of the lake in the Adamawa plateau and at this depth would be deposited in two different phases with different sedimentation rates. The first rate of sedimentation from 22 cm to 90 cm the sediments would have been deposited at a sedimentation rate of 2.1 cm/year while from the top to 22 cm, this rate is about 4.09 cm/year. The curve of the depositional model of these sediments is shown in Figure VI.4.

AZ Core

The AZ core from the center of Ngaoundaba Lake were date for the first time in this study. The ages of this core were performed entirely on organic materials such as twigs at the base, wood at the middle and the top of the AZ core. The ages obtained are also decreasing from the base to the top with respect to the deposition principle. The base sample (AZ-86) have

been dated 1030 ± 30 yrs BP., the middle sediment of the core thru the AZ-42 sample could have been deposited after 425 ± 30 yrs BP., and the top sample (AZ-11) have been deposited at 155 ± 30 yrs BP. From this part of the Adamawa plateau, the depositional model in this part of the lake in and at these depths would be deposited in two different phases with different sedimentation rates. The curve of the depositional model of these sediments is shown in Figure VI.4. The first rate of sedimentation is from 6 to 86 cm of the sediment core is about 25.83 cm/year and the second from the top of the core to 6 cm depth were 10.94 cm/year.

VI.2. Diatom analysis

VI.2.1. Simbock sedimentary core

VI.2.1.1. Flora diversity

The diatom frustules are generally well preserved along the core, enabling good identification. A total of 70 species and varieties of diatoms distributed in 5 families and 20 genera were observed. The most abundant family is Naviculaceae (38 %), followed by Eunotiaceae (21 %), Melosiraceae (16 %). The genus with high diversity (> 10 species) is *Eunotia* (20 %, 14 species). Genera with medium diversity (5 to 9 species) are represented by *Pinnularia* (13 %, 9 species), *Aulacoseira* (10 %, 7 species), *Navicula* (9 %, 6 species), *Gomphonema* (9 %, 6 species) *Cymbella* (7 %, 5 species). Genera with relatively low diversity are *Fragilaria* (3 species), *Stephanodiscus* (3 species), *Hantzschia* (2 species), *Pleurosigma* (2 species) (Figure VI.5). The mono specific genera are *Stauroneis*, *Rhopalodia*, *Neidium*, *Frustulia*, *Denticula*, *Cyclotella*, *Cyclostephanos*, *Cocconeis* *Triceratium* and *Synedra*.

The succession of different families of diatoms along the sedimentary core bears witness to the variability of the hydroclimatic conditions that prevailed during this period.

VI.2.1.2. Dominant species and large assemblages

Figure VI.6 shows the relative abundances of the dominant species. Although *Aulacoseira distans* shows the highest abundances, the composition of the diatom flora varies significantly along the section, especially in the dominant species, allowing the identification of three typical assemblages.

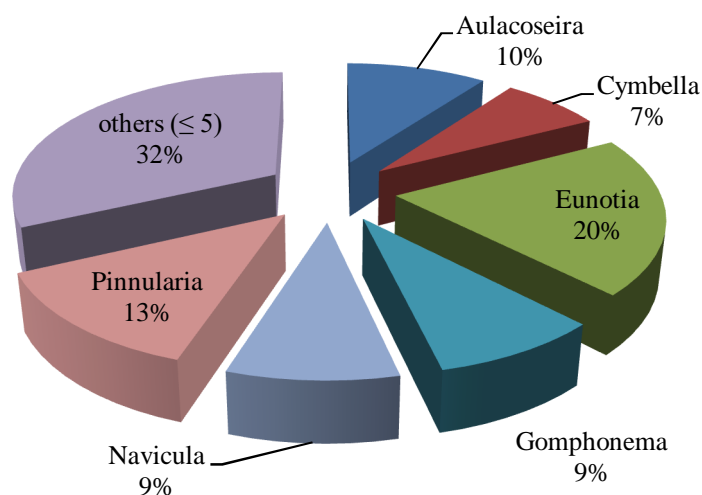


Figure VI.5. Specific diversity (in %) of the dominant genera along the Simbock sedimentary column

➤ **Assemblage at *Aulacoseira distans*, *Aulacoseira granulata* and *Synedra ulna***

Samples NR1, NR11, NR3, NR31 and NR13 with this type of assembly are located at 8, 13, 62, 81 and 101 cm. This assemblage is dominated by *Aulacoseira distans* and *Aulacoseira granulata*, two species respectively acidophilic tycho plankton and alkalophilic plankton according to Gasse (1986). The accompanying species *Synedra ulna* is characteristic of alkaline and eutrophic waters according to Denys (1991). This assemblage would be characteristic of a high-water level associated with a progressive evolution of pH and trophic levels towards increasingly basic and eutrophic conditions.

➤ **Assemblage at *Aulacoseira granulata*, *Aulacoseira distans* and *Eunotia rabenhorstii***

Observed in samples NR6, NR7, NR4, NR12 located between 27 and 34 cm then at 89 and 120 cm, this assemblage is marked by the dominance of the planktonic species *A. granulata* and the tycho planktonic species *A. distans*. The sub-dominance of *Eunotia rabenhorstii*, an aerophilic species (Husted, 1966) would indicate an episodically dry or near-border environment. Overall, this assemblage would reflect a higher lake level than in the preceding samples and marked by episodic drying up.

➤ **Assemblage in *Aulacoseira distans*, *Aulacoseira granulata* and *Eunotia incisa***

Samples NR2, NR8 and NR9 that show this type of assemblage are located between 38 and 64 cm and are marked by the dominance of tycho planktonic and planktonic species respectively *A. distans* and *A. granulata*. The accompanying species *Eunotia incisa* is acidophilic aerophilic

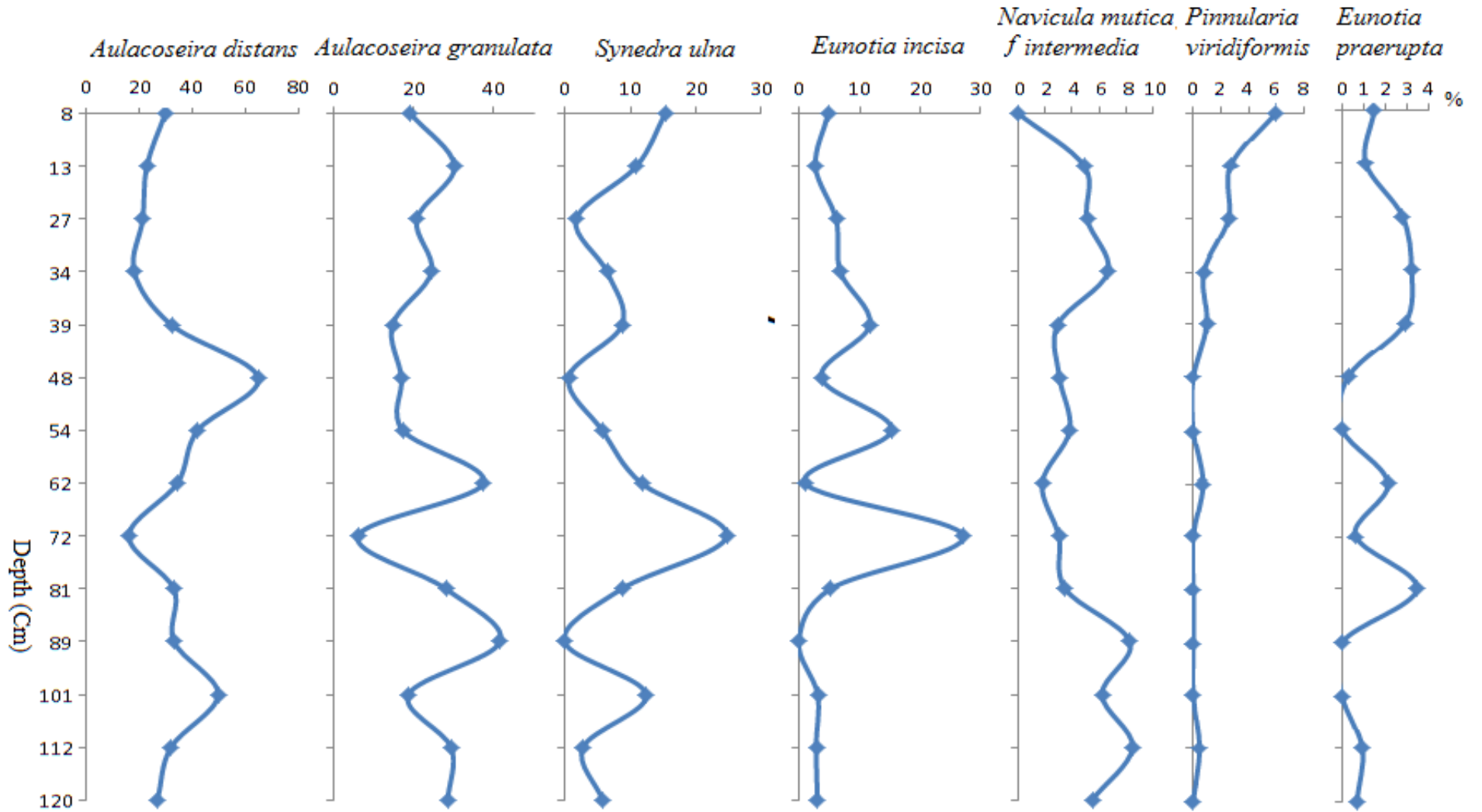


Figure VI.6. Variation in relative abundance of dominant species (> 5 % at least in one sample) as a function of depth along the Simbock sedimentary column

according to Patrick and Reimer (1966). This would reflect a transition from the previous assemblage to increasingly acidic and oligotrophic conditions associated with a slight decrease in lake levels probably due to periodic drying.

Some diatom associations have been excluded from typical assemblages because of their presence in a single sample. For example, in samples NR10 (72 cm) and NR5 (112 cm). It is difficult to interpret their ecological message. However, one might think that they reflect transitions between standard assemblages.

VI.2.1.3. Algae assemblages according to the CFA: Ecological significance

The first 6 axes of the AFC represent 83 % of the total inertia (Table VI.2). We have taken into account for our interpretations the first 3 axes (56.46 %) of the distributional variance, which contain the majority of ecological information that can highlight the environmental gradients that have governed the distribution of species.

Table VI.2. Eigenvalues, inertia and cumulative inertia of the CFA axes

Axis	Propal Values	Inertia	Cumulated inertia
1	0.21	22.47	22.47
2	0.17	17.98	40.45
3	0.15	16.01	56.46
4	0.09	10.16	66.62
5	0.08	9.27	75.90
6	0.06	7.09	83

Figure VI.7 opposite shows the representation of species and the ecological groups to which they correspond in CFA Plan 1-2. Axis 1 (22.47 % of total inertia) contrasts group 1 species with group 2 species. On the negative side, group 1 consists of tychoplanktonic (such as *Aulcoseira distans* var. *africana*-AUDA, *Fragilaria capucina*-FRCA), benthic (*Pinnularia legumen*-PILE) and aerophilic species such as *Eunotia monodon*-EUMO and *Eunotia monodon* var. *tropica*-EUMT). Group 2 on the positive side consists of a mixture of species with several habitats. We distinguish between aerophiles such as *Eunotia glacialis*-EUGL, acidophilic and oligotrophic epiphytes such as *Cymbella silesiaca*-CYSI and plankton such as *Amphiprora paludosa*-AMPA.

The opposition between these two groups shows that the depth and colonization of the environment in macrophytes are the most important factors in the distribution of species. Axis 2 contrasts the planktonic (*Fragilaria bilunaris*-FRBI) and aerophilic (*Eunotia monodon* var. *monodon*-EUMM and *Eunotia minor*-EUMI) species, which are essentially acidophilic (group 3), with the species of group 4, which are mainly alkaliphilic and eutrophic planktonic species such as *Aulacoseira granulata*-AUGR and *Achnantes inflata*-ACIN. The opposition between these two groups indicates that pH and depth would be the main factors that influenced the distribution of diatoms on this axis.

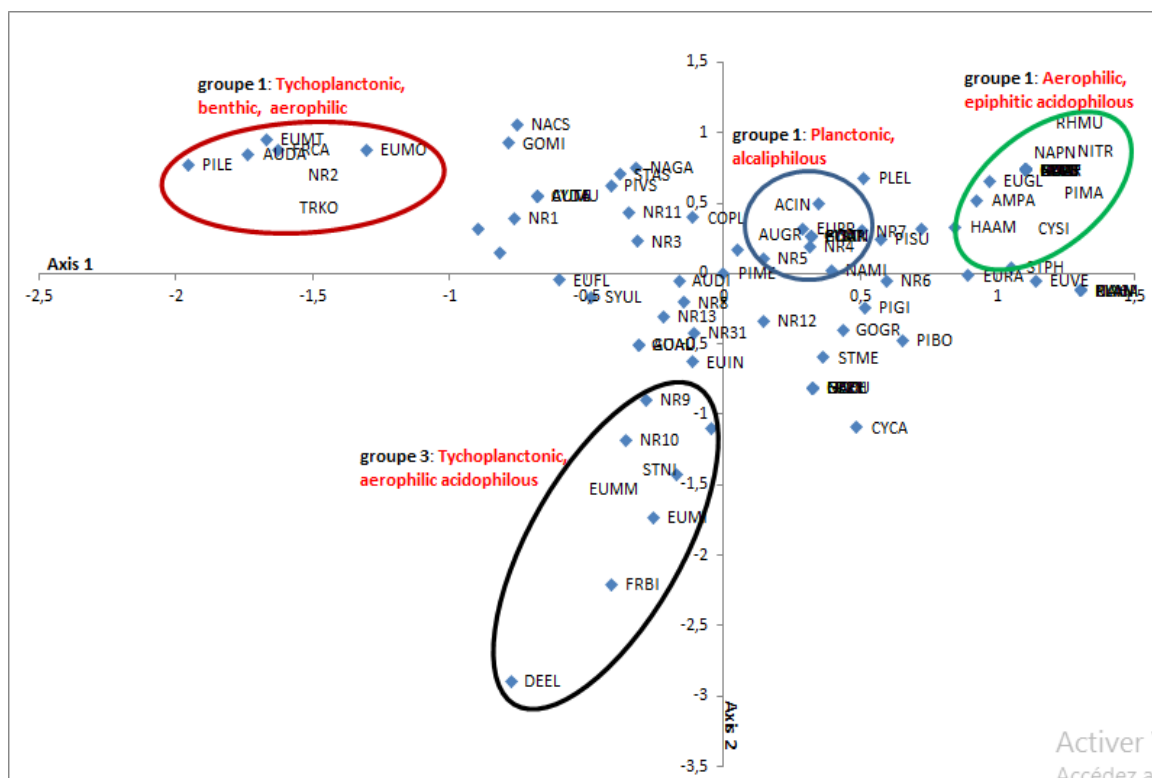


Figure VI.7. Schematic representation of the characteristic groups of axes 1 and 2 of the CFA

Identification of the environmental gradients that influenced species distribution by correspondence factor analysis (CFA) allowed the determination of the evolution of these factors in the time frame covered by the samples (Figure VI.8).

Overall, the water level in Lake Simbock has always been high (high tycho+plankton values). However, the high percentages of aerophilic species in the 72 cm, 54 cm and between 27-34 cm levels suggest a decrease in water level probably due to a decrease in the water supply in the lake by the tributaries, and/or drastic dry seasons as observed in the last decade (Simbock Lake having been formed during this period). An inversion of the pH and trophicity of the

waters (globally oligotrophic and acidic) is observed between 62 and 89 cm and between 8-27 cm which then became eutrophic and alkaliphilic. This change would be due to an enrichment of the lake water by nutrients drained from the watershed.

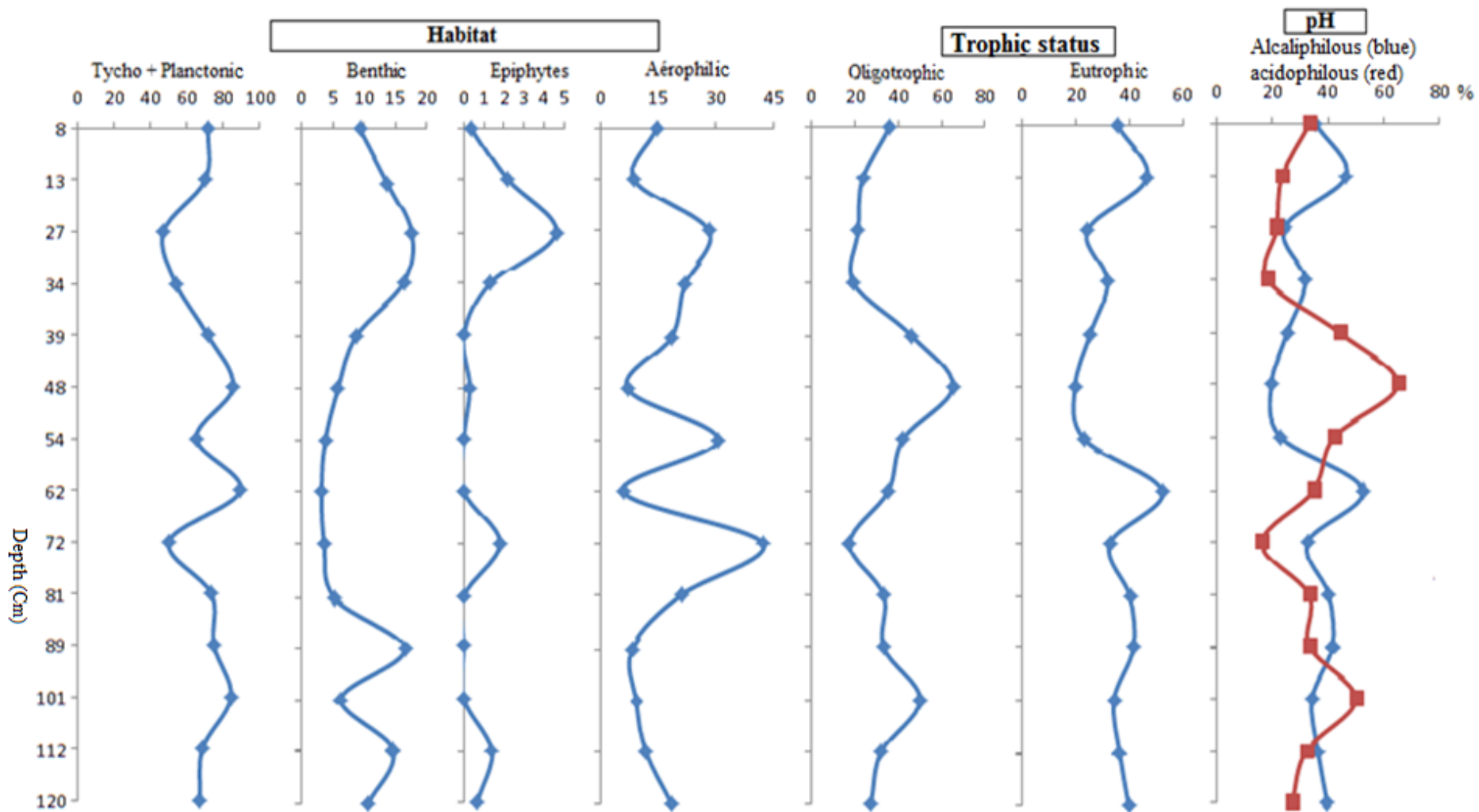


Figure VI.8. Variation in relative abundance of habitat indicator ecological groups (tycho + planktonic, benthic, epiphytic, aerophilic), trophic (eutrophic and oligotrophic) and pH (alkaliphilic, acidophilic, indifferent) along the Simbock core as a function of depth

VI.2.2. Ossa Lake sediment core

VI.2.2.1. Flora diversity

Of the 14 samples observed in the sedimentary column, 98 species belonging to 9 families and 23 genera were identified. The most abundant family is Naviculaceae (44 %), followed by Eunotiaceae (21 %) and Melosiraceae (12 %). Genera with high diversity (> 10 species) are *Eunotia* (21 %, 18 species), *Gomphonema* (14 %; 13 species) and *Navicula* (14 %; 12 species). Those with medium diversity (5 to 9 species) are *Fragilaria* (8 %; 7 species), *Cymbella* (8 %, 7 species) and *Aulacoseira* (7 %, 6 species) (Figure VI.9). Those with low diversity (≤ 5 species) are *Amphora* (4 species), *Neidium* (4 species), *Hantzschia* (2 species) and *Surirella* (2 species). The monospecific genera are *Amphiprora*, *Cocconeis*, *Frustulia*, *Stauroneis* and *Triceratium*.

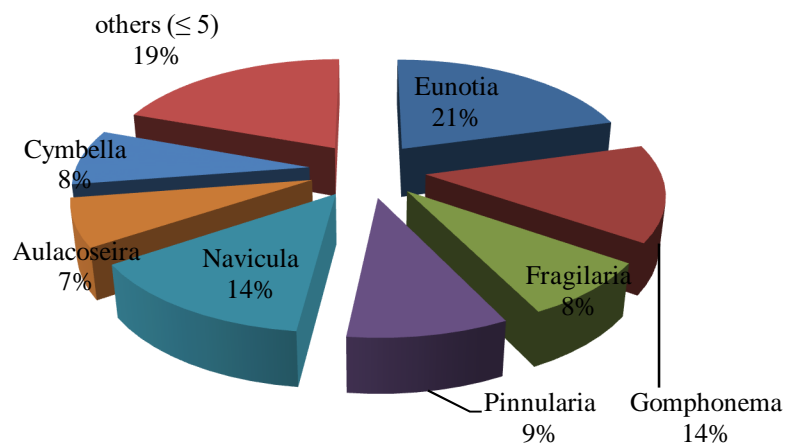


Figure VI.9. Specific diversity (in %) of the dominant genera along the Ossa sedimentary column

VI.2.2.2. Dominant species and large assemblages

The assessment of the abundance of taxa in the fossil flora has made it possible to distinguish three major groups of species; widely distributed species (Group A), moderately distributed (Group B) and weakly distributed (Group C) (Table VI.3). Only species with an abundance > 5% were considered in this distribution. Figure 9 shows the variation of dominant species along the core as a function of time.

Widespread species (Group A)

This group consists of the species present between 10 and 14 samples. The average percentages per sample are the highest (4 -77 %). The characteristic species of this group are:

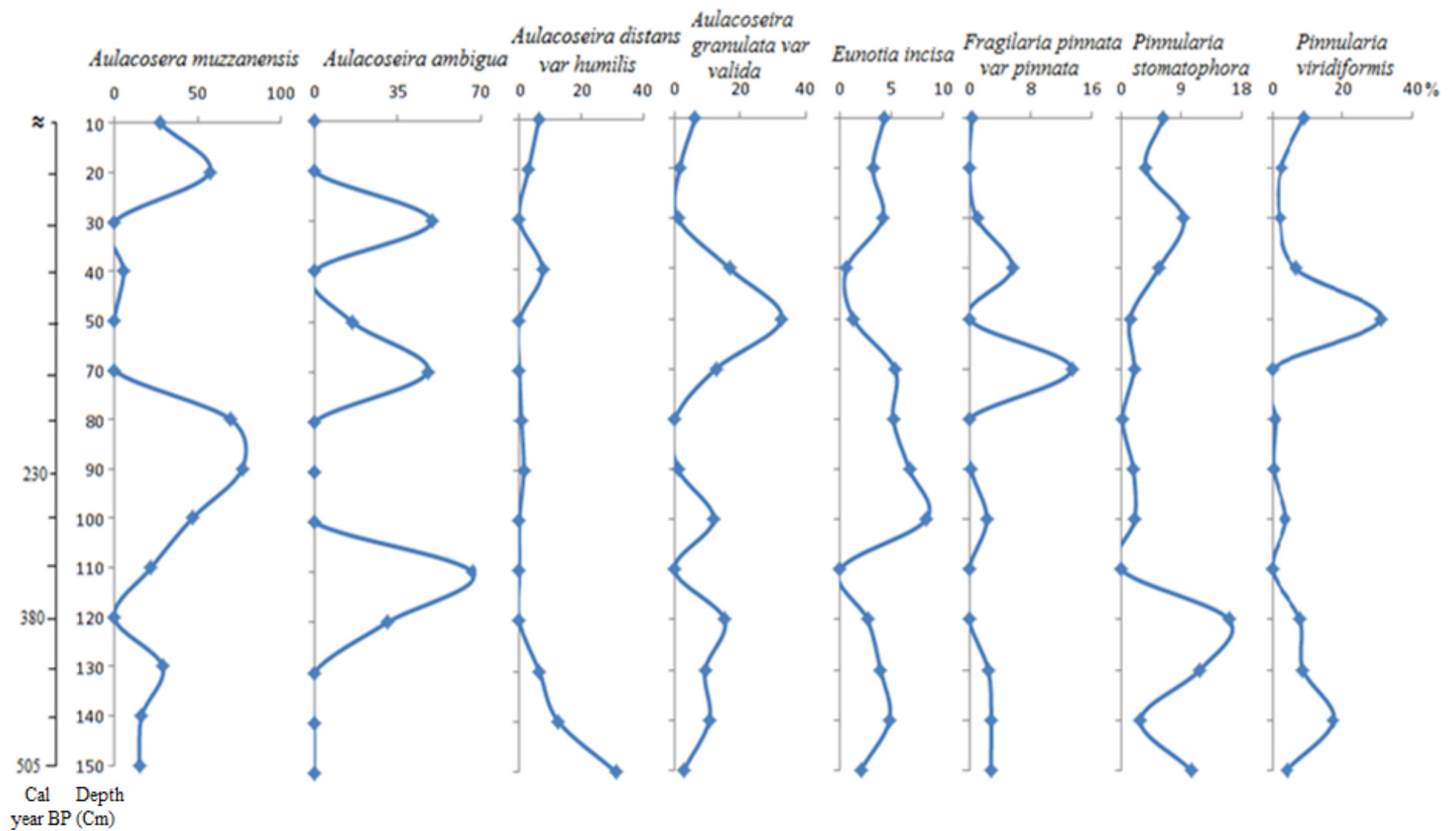


Figure VI.10. Variation in relative abundance of dominant species (> 5% at least in a sample) as a function of depth along the Ossa sedimentary column

Aulacoseira muzzanensis. The variations in abundance of this species as a function of depth (Figure VI.10) show that the highest values (> 40 %) are between 80 and 100 cm, and at 20 cm (52 – 77 %). The lowest values (< 6 %) are observed between 30 and 70 cm (0 to 5.63 %).

Aulacoseira granulata var. *valida*. This species is considered here as allochthonous with regard to the state of its frustules. The highest abundances (> 15 %) are between 40 and 50 cm, then at 120 cm (380 years cal. BP). Low abundances (less than 6 %) are observed between 10 and 30 cm, and then at 150 cm (505 yrs BP.).

Table VI.3. Spatial distribution of species along the Ossa core.

Groups	Species	Number of samples where the species is present with a percentage > 5	Percentage Min - max	Average per sample
Groupe A	<i>Aulacoseira muzzanensis</i>	10	6 - 77	26
	<i>Melosira granulata</i> var <i>valida</i>	13	2 - 22	9
	<i>Pinnularia somatophora</i>	13	2 - 16	5
	<i>Pinnularia viridiformis</i>	12	1 - 17	7
	<i>Eunotia incisa</i>	13	1 - 9	4
Groupe B	<i>Aulacoseira distans</i> var <i>humilis</i>	8	5 - 10	3
	<i>Fragilaria pinnata</i> var <i>pinnata</i>	9	1 - 13	3
	<i>Aulacoseira italica</i>	6	1 - 10	2
	<i>Gomphonema gracile</i>	2	5 - 9	1
Groupe C	<i>Cymbella perpusilla</i>	2	5 - 19	2
	<i>Cymbella gracilis</i>	1	5 - 9	1

Medium species (Group B)

The number of samples where the species in this group are present with an abundance greater than 5 % varies between 9 and 5. The average percentages per sample are low (between 3 and 5 %). This group includes:

Aulacoseira distans var. *humilis*. The relative abundances of this species as a function of depth (Figure 9) do not show great variations. Abundances are low but a slight increase at the base of the core is observed between 140 and 150 cm (13 to 31 %).

Aulacoseira italica. Abundances of this species are low (1 to 10 %), with a major peak at 80 cm (10 %).

Low abundance species (Group C)

Species in this group have abundances close to those of the previous group (5 to 11 %) but are present in less than five samples.

VI.2.2.3. Determination of assemblages by multivariate statistical processing and identification of environmental gradients*

The first 6 axes of the AFC represent 83 % of the total inertia (Table V.4). We have taken into account for our interpretations the first 2 axes that contain the majority of ecological information (52.45 % of the distributional variance) that can highlight the environmental gradients that have governed the distribution of species.

Table VI.4. Eigenvalues, inertia and cumulative inertia of the CFA axes

Axis	Propal values	Inertia	Cumulated inertia
1	0.67	33.90	33.90
2	0.37	18.57	52.45
3	0.23	11.76	64.21
4	0.15	7.49	71.70
5	0.13	6.36	78.0
6	0.09	4.68	82.74

Figure VI.11 opposite shows the representation of species and the ecological groups to which they correspond in CFA Plan 1-2. Axis 1 (33.90 % of total inertia) contrasts group 1 species with group 2 species. On the negative side, group 1 consists of a mixture of species with several habitats. One finds mainly the planktonic species *Aulacoseira ambigua*, tychoplanktonic species such as *Fragilaria capucina* f. *venter*-FRCV, *Fragilaria leptostauron*-FRLE and aerophiles such as *Eunotia rabanorstii*-EURA, *Eunotia veneris*-EUVE and *Eunotia monodon* var *monodon*-EUMM.

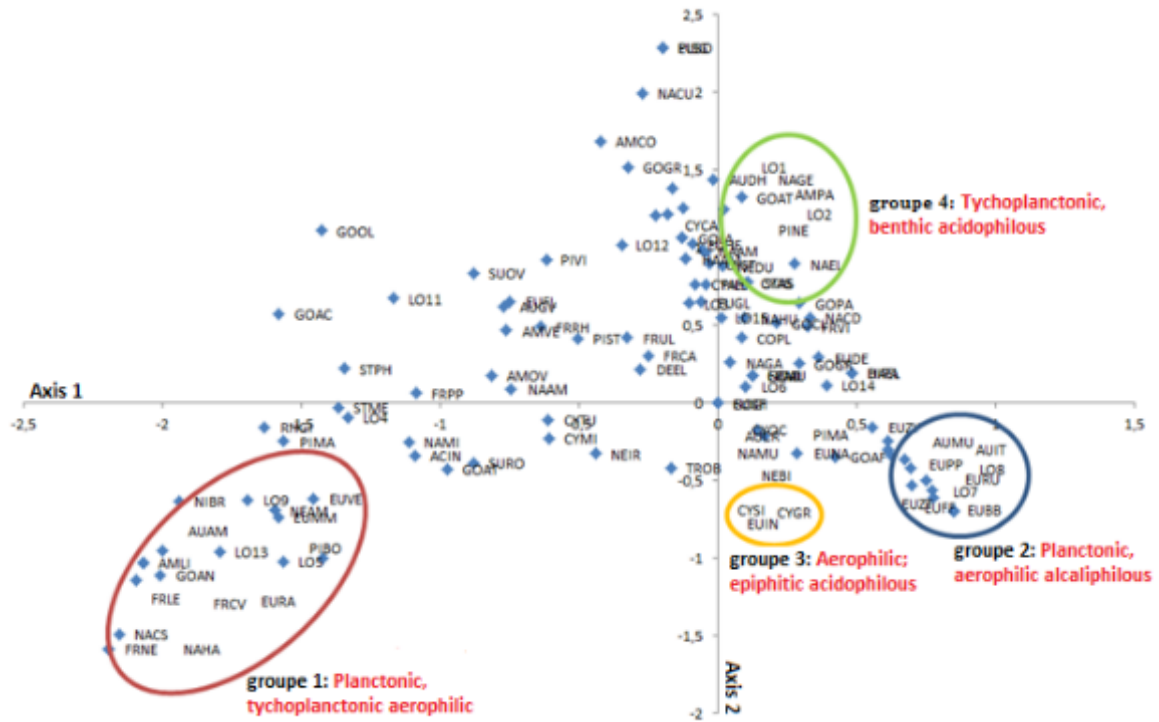


Figure VI.11. Schematic representation of the characteristic groups of axes 1 and 2 of the CFA

Group 2 on the positive side is dominated by the eutrophic planktonic species *Aulacoseira muzzanensis*-AUMU, *Aulacoseira italica*-AUIT (respectively alkaliphilic and neutrophilic) and aerophilic species such as *Eunotia bilunaris* var. *bilunaris*-EUBB, *Eunotia fallax* var. *fallax*-EUFF, *Eunotia paludosa* var. *paludosa*-EUPP. The opposition between groups 1 and 2 indicates that habitat (depth), pH and trophic would be the main factors influencing the distribution of diatoms on this axis.

Axis 2 contrasts the acidophilic aerophilic and epiphytic species located on the negative side (group 3) with group 3 species consisting of tychoplanktonic (such as *Aulacoseira distans* var. *humilis*-AUDH) and benthic (mostly acidophilic such as *Navicula geoppertiana*-NAGE, *Navicula elginensis*-NAEL, *Pinnularia neomajor*-PINE). The opposition between these two groups indicates that habitat, pH and to a lesser extent the colonization of the environment in macrophytes would be the main factors that have influenced the distribution of diatoms on this axis.

The identification of the environmental gradients that influenced the distribution of the species by correspondence factor analysis (CFA) made it possible to determine the evolution of these factors in the time frame covered by the samples (Figure VI.12).

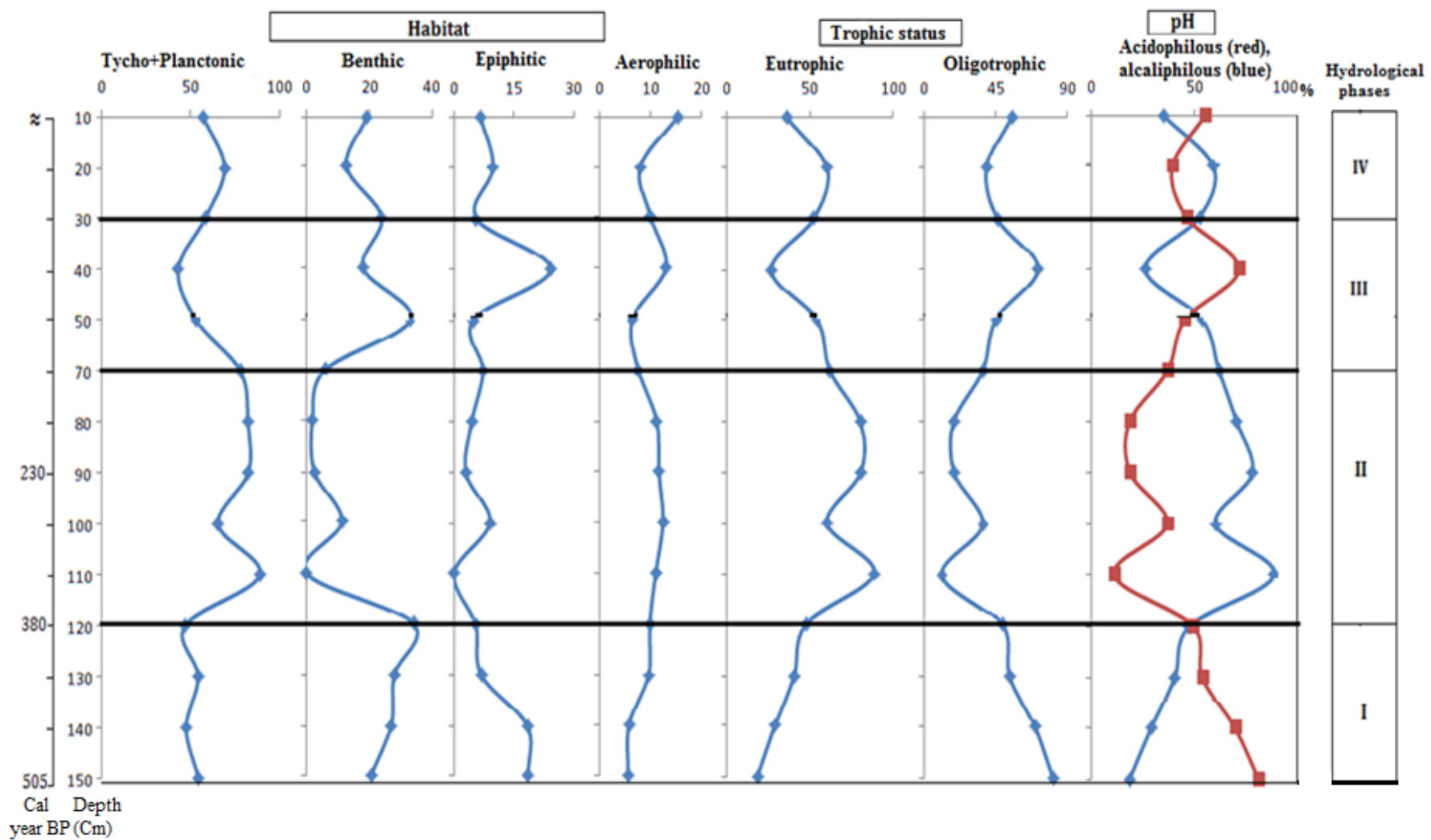


Figure VI.12. Variation in relative abundance of habitat indicator of ecological groups (tycho + planktonic, benthic, epiphytic, aerophilic), trophic (eutrophic and oligotrophic), pH (alkaliphilic, acidiphilic, indifferent) and hydrological phases along the Ossa core as a function of depth.

Figure VI.12 shows the evolution of the relative abundances of the ecological groups along the sedimentary core as a function of time (Habitat: planktonic, tychoplanktonic, epiphytic, benthic and aerophilic. Trophic status: Oligotrophic and eutrophic species. pH: Acidophilic (blue) and alkaliophilic (red) species. This evolution makes it possible to distinguish four major episodes in the paleohydrological evolution of Lake Gbali. The dominance of tychoplanktonic, especially planktonic species suggests a globally high-water level. The significant presence of benthic species and often epiphytes at the base of the core would indicate a good water transparency in a lake environment colonized by macrophytes. In any case, the low values of aerophilic species recorded indicate that the water level did not vary significantly throughout the period covered by the sediment core.

Episode 1: 150 - 120 cm (505 - 380 yrs BP.)

The diatom flora is dominated by the oligotrophic acidophilic tychoplanktonic species *Aulacoseira distans* var. *humilis*. It grows abundantly in stable and oligotrophic waters (Hustedt, 1927). The maximum abundance of this species (54 %) is reached during this episode at 150 cm (505 yrs BP.). It is associated here with the benthic species *Pinnularia stomatophora* and the epiphytic species *Gomphonema gracile*, which reach their highest abundances at this level (34 and 18 %, respectively). The decrease in pH was thus recorded by both benthic and epiphytic species. The average values in planktonic and tychoplanktonic diatoms indicate a decrease in the lake level, with a transparent water column that can allow the development of benthics. At the bottom of the lake and probably on the littoral zones, benthic diatoms (*Pinnularia Stmatophora* and *P. viridiformid*), epiphytes (*Gomphonema gracile*) and epiphytes become relatively important, indicating a drop in the lake level associated with well-marked dry seasons during which these diatoms would have developed.

Episode 2: from 120 to 70 cm

Plankton dominate and are mainly represented by *A. muzzanensis*, *A. ambigua*, and *A. italica* (Figure VI.10). The species *A. granulata* is particularly abundant during this period and reaches 77 %, it is recorded at a depth of 90 cm. These planktonic species, although observed in deep tropical lakes, can also develop in large rivers and are sometimes present in small turbid streams (Gasse, 1980). During this time period, the increase in planktonic diatoms, eutrophic alkaliphilic to the detriment of oligotrophic acidophilic tychoplanktonic species indicates a relatively high-water level, a relatively high pH and waters that are significantly more charged with organic matter compared to the previous lake episode. Benthic (0-11 %, despite a peak at

50 cm) and aerophilic (6-11 %) species become globally unimportant (between 23 and 11 cm), probably due to higher turbidity due to wind mixing or greater lake depth. These assemblages confirm a high lake level and clearly alkaline and eutrophic waters, probably more turbid, thus preventing the development of benthic species. In addition, the low abundance of *A. distans* var. *humilis* acidophilic to the benefit of *A. italica* would indicate an evolution towards facies that was first neutral and then alkaline. The water column was probably less stable compared to the previous period. This trend shows a change from an oligotrophic environment to more eutrophic conditions.

Episode 3: from 70 to 30 cm

This period is characterized by the dominance of *A. granulata* var. *valida* (12-33 %), although its abundance shows some fluctuations. In view of the degraded state of its frustules, it is thought that this species was transported from the Sahara by wind as noted by Nguetsop et al. (2010; 2011) at the same site. Benthic (*Pinnularia viridiformis* and *P. stomatophora*), epiphytic (*Cymbella silesiaca*) and aerophilic (*Eunotia incisa*, *E. glacialis*) diatoms are becoming relatively important. This would indicate a drop-in lake levels associated with well-marked dry seasons during which harmattan (dry wind from the north) would have penetrated as far as the Gulf of Guinea. The waters remained oligotrophic and acidophilic.

Episode 4: from 30 to 10 cm

This episode is similar to episode 2 and is still characterized by the dominance of diatoms of the genus *Aulacoseira*. However, the high percentages of *A. muzzanensis*, *A. ambigua* at the beginning of the phase are followed by ever-increasing values of benthic and acidophilic aerophilic species such as *P. viridiformis* and *E. glacialis* at about 10 cm. This data reflects a deeper lake environment than during the previous period with globally stable and nutrient-rich waters, which is gradually evolving towards facies with acidic and clear waters at the top of the core.

VI.2.3. Ngaoundaba sedimentary core

VI.2.3.1. Flora diversity

The diatom microflora analyzed in the 10 samples of this sedimentary column yielded 84 species belonging to 5 families and 20 genera. The most abundant family is Naviculaceae (56 %), followed by Eunotiaceae (27 %), Melosiraceae (9 %). Genera with high diversity (> 10

species) are *Pinnularia* (20 %; 16 species) and *Gomphonema* (16 %; 13 species). Those with medium diversity (5 to 9 species) are *Fragilaria* (11 %; 9 species), *Eunotia* (10 %, 8 species), *Aulacoseira* (7 %, 6 species) and *Navicula* (7 %, 6 species). Genera with low diversity (≤ 5 species) are *Cymbella* (6 %, 5 species), *Nitzschia* (4 species) and *Hantzschia* (2 species). The monospecific genera are *Amphipleura*, *Amphiprora*, *Amphora*, *Cocconeis*, *Frustulia*, *Stauroneis*, *Cocconeis*, *Triceratium* and *Synedra*.

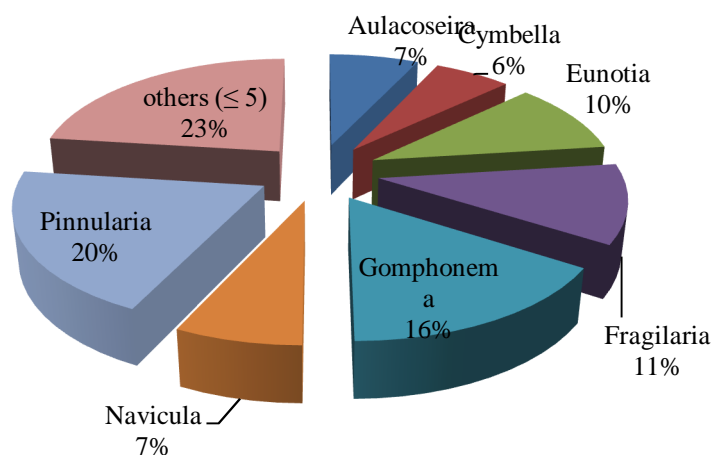


Figure VI.13. Specific diversity (%) of dominant genera along the Ngaoundaba sedimentary column

VI.2.3.2. Dominant species and large assemblages

These (widely distributed) species are important in assessing the temporal distribution of the flora. This assessment has allowed to distinguish 3 large groups of species well represented in the fossil flora (Table VI.5, Figure VI.14). Widely distributed (present in at least 8 of the 10 samples, group 1), moderately distributed (present in at least 4 and at most 7 samples, group 2) and weakly distributed (present in at most 3 samples, group 3).

Widespread species (Group 1)

The number of samples where species in this group show an abundance greater than 5 % is between 8 and 10. The average percentage is the highest (73.85 %) compared to the other species. This group consists of:

Aulacoseira distans whose abundances along the core show a wide distribution (present in 10 samples) and the highest abundance in this group (71.27 %) and even in the whole core (Figure 20);

Aulacosiera distans var. *africana* is the second dominant species in this group. It is present in 10 samples with a maximum percentage of 16.32 %;

Aulacoseira granulata and *Eunotia incisa* are two representative species of this group with maximum percentages of 10.77 and 15.91 % respectively. They are found in at least 8 samples each;

Table VI.5. Spatial distribution of species along the Ngaoundaba core

Most representative species groups	Species	Number of samples where the species is present with a number > 5 %	Percentage min - max	Average of percentages
Groupe 1	<i>Aulacoseira distans</i>	10	38.23 – 71.27	73.85
	<i>Aulacoseira distans</i> var <i>africana</i>	10	4 – 16.32	12.60
	<i>Aulacoseira granulata</i>	10	3 – 10.77	8.38
	<i>Eunotia incisa</i>	10	4.89 – 15.91	12.85
	<i>Gomphonema gracile</i>	8	3.63 – 5.94	6.66
Groupe 2	<i>Eunotia flexuosa</i>	4	2.54 – 5.12	5.10
	<i>Fragilaria biceps</i>	4	4 - 5.32	4.67
Groupe 3	<i>Surirella linearis</i> var <i>constricta</i>	3	1.5 – 7.7	4.76
	<i>Nitzschia heflaurina</i>	2	2.7 - 8	5.37

Moderately widespread species (Group 2)

This group consists of species with a medium distribution. These species consisting of *Eunotia flexuosa* and *Fragilaria biceps* have average percentages between 2 and 5.32 %. The number of samples where these species are present with a percentage higher than 5 % is 4.

Species of low prevalence (Group 3)

The number of samples where species in this group are present at a percentage greater than 5 % is 2 or 3. However, their maximum average percentage (4.76 to 5.37 %) is close to that of Group 2. *Surirella linearis* var. *constricta* and *Nitzschia heflaurina* make up the bulk of this group.

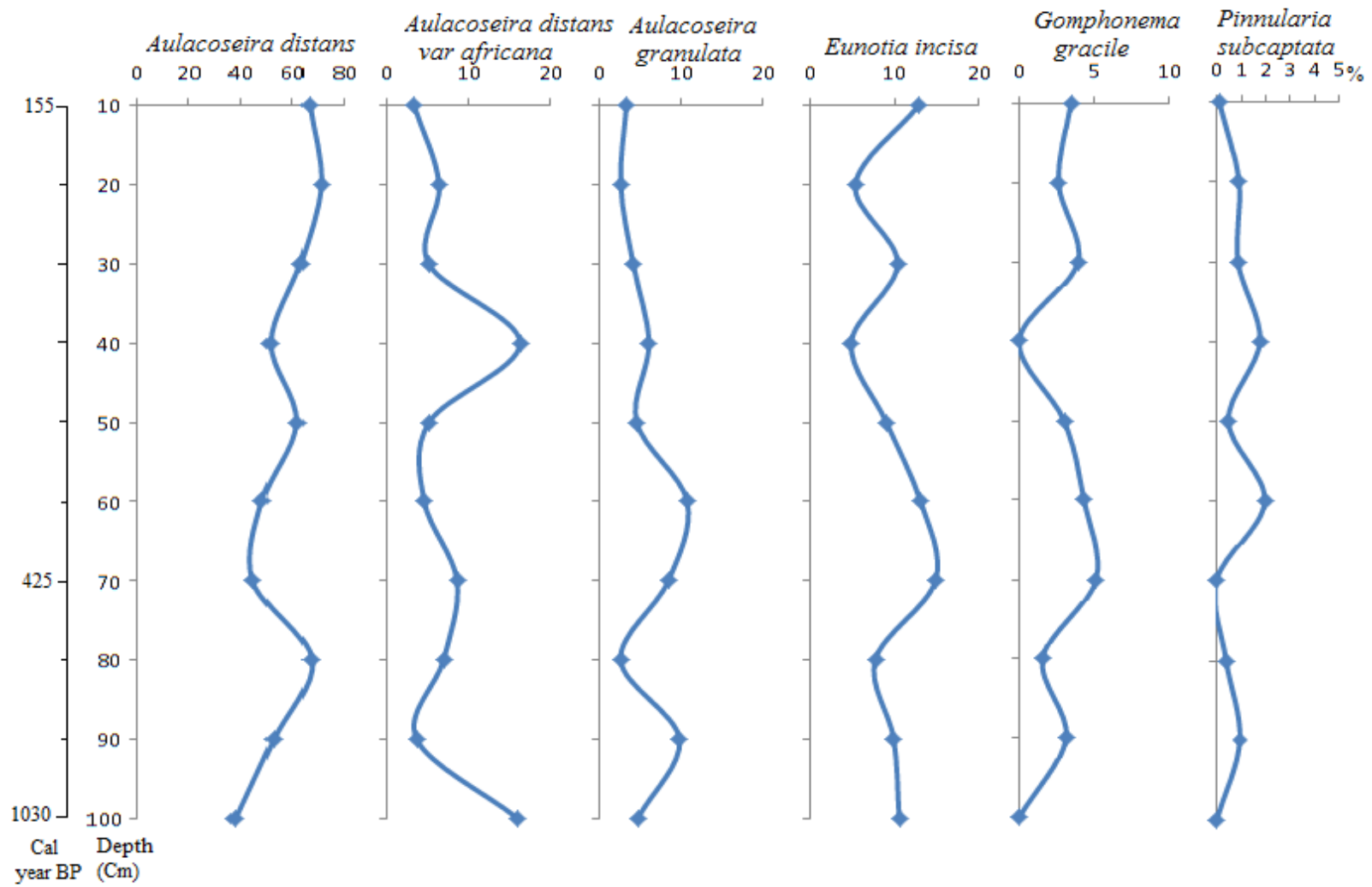


Figure VI.14. Variation in relative abundance of dominant species (> 5 % at least in one sample) as a function of depth along the Ngaoundaba sedimentary column

VI.2.3.3. Determination of the most significant species and classification of assemblages by statistical treatments

Multivariate statistical analysis (MSA) techniques are used in this section to identify large algal assemblages, as well as hypothetical environmental gradients. The first 5 axes of the MSA represent 88 % of the total inertia (Table III). We have taken into account for our interpretations the first 2 axes that contain the majority of ecological information (60.33 % of the distributional variance) that can highlight the environmental gradients that have governed the distribution of species.

Table VI.6. Eigenvalues, inertia and cumulative inertia of the CFA axes

Axis	Propal values	Inertia	Cumulated Inertia
1	0.19	43.48	43.48
2	0.07	16.85	60.33
3	0.06	13.21	73.54
4	0.03	7.59	81.12
5	0.03	7.17	88.30

Figure VI.15 shows the representation of species and the ecological groups to which they correspond in CFA Plan 1-2. Axis 1 (43.48 % of the total inertia) contrasts the species of group 1 with those of group 2. On the negative side, group 1 consists of a mixture of species with several habitats; mainly the planktonic species *Aulacoseira granulata* var. *valida*, benthic species such as *Pinnularia subgibba*-PISG, *Pinnularia sinistra*-PISI, *Pinnularia neomajor*-PINE, *Gomphonema affine*-GOAF, *Gomphonema minutum*-GOMI and epiphytes such as *Cymbella pusilla*-CYPU. Group 2 on the positive side is dominated by benthic and aerophilic species such as *Gomphonema gracile*-GOGR, *Pinnularia gibba*-PIGI, *Eunotia flexuosa*-EUFL and *Cymbella perpusilla*-CYPE. The opposition between groups 1 and 2 indicates that the habitat (depth) and the presence of macrophytes would be the main factors influencing the distribution of diatoms on this axis.

Axis 2 opposes group 3 species consisting of eutrophic plankton such as *Aulacoseira granulata*-AUGR, *Fragilaria bilunaris*-FRBI and benthic species such as *Navicula mutica* f. *intermedia*-NAMI, *Cocconeis placentula*-COPL to group 4 formed by acidophilic and oligorophilic tychoplankton such as *Aulacoseira distans*-AUDI and benthic such as *Fragilaria pinnata*-FRPI, *Pinnularia nobilis*-PINO, *Pinnularia viridis*-PIVS. The opposition between these

two groups indicates that habitat, pH and trophic were important in the distribution of species along this axis.

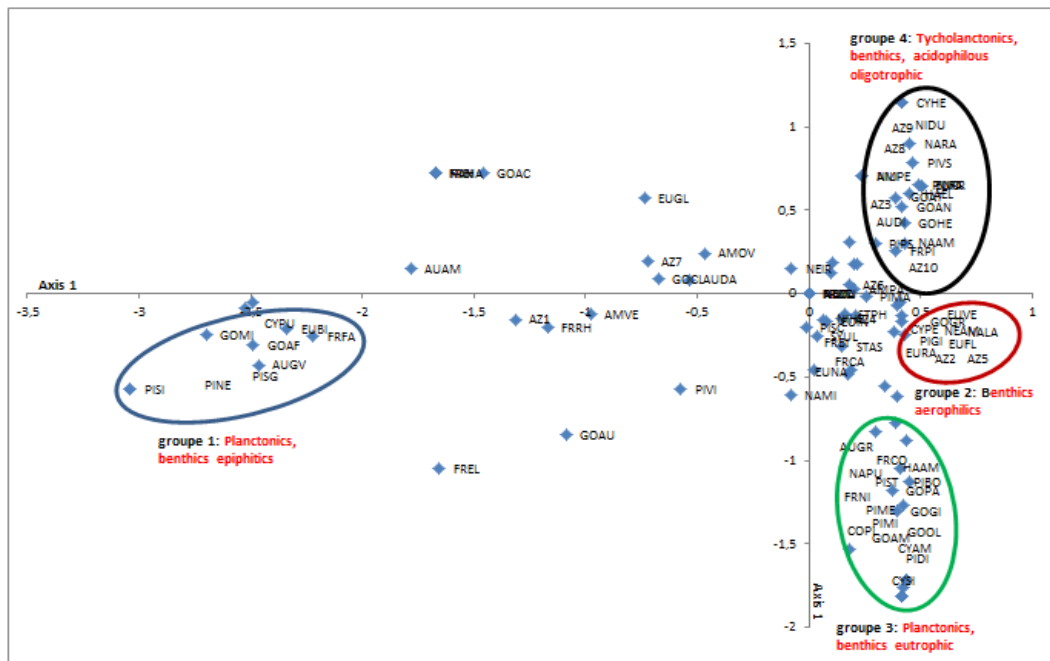


Figure VI.15. Schematic representation of the characteristic groups of axes 1 and 2 of the CFA

Identification of the environmental gradients that influenced species distribution by correspondence factor analysis (CFA) allowed the determination of the evolution of these factors in the time frame covered by the samples (Figure VI.16). This Figure VI.16 shows the evolution of the relative abundances of the ecological groups along the sedimentary core as a function of time (Habitat: planktonic, tycho planktonic, epiphytic, benthic and aerophilic). Trophic status: Oligotrophic and eutrophic species. pH: Acidophilic (blue) and alkaliophilic (red) species. This evolution makes it possible to distinguish three major episodes in the paleohydrological evolution from Lake Ngaoundaba to Ngaoundéré.

Episode 1: Between 100 and 80 cm.

The diatom flora is dominated by the oligotrophic acidophilic tycho planktonic species *Aulacoseira distans*. This species develops preferentially in tropical lakes and swamps (Gasse, 1987). Its relatively high abundance (28 %) in plankton in Adamaoua crater lakes (Kom, 2010) has been interpreted as a characteristic of more or less deep and stable waters (Nguetsop et al., 2011). The abundance of this species therefore suggests that it could be a relatively deep lake environment with a stable and oligotrophic water column.

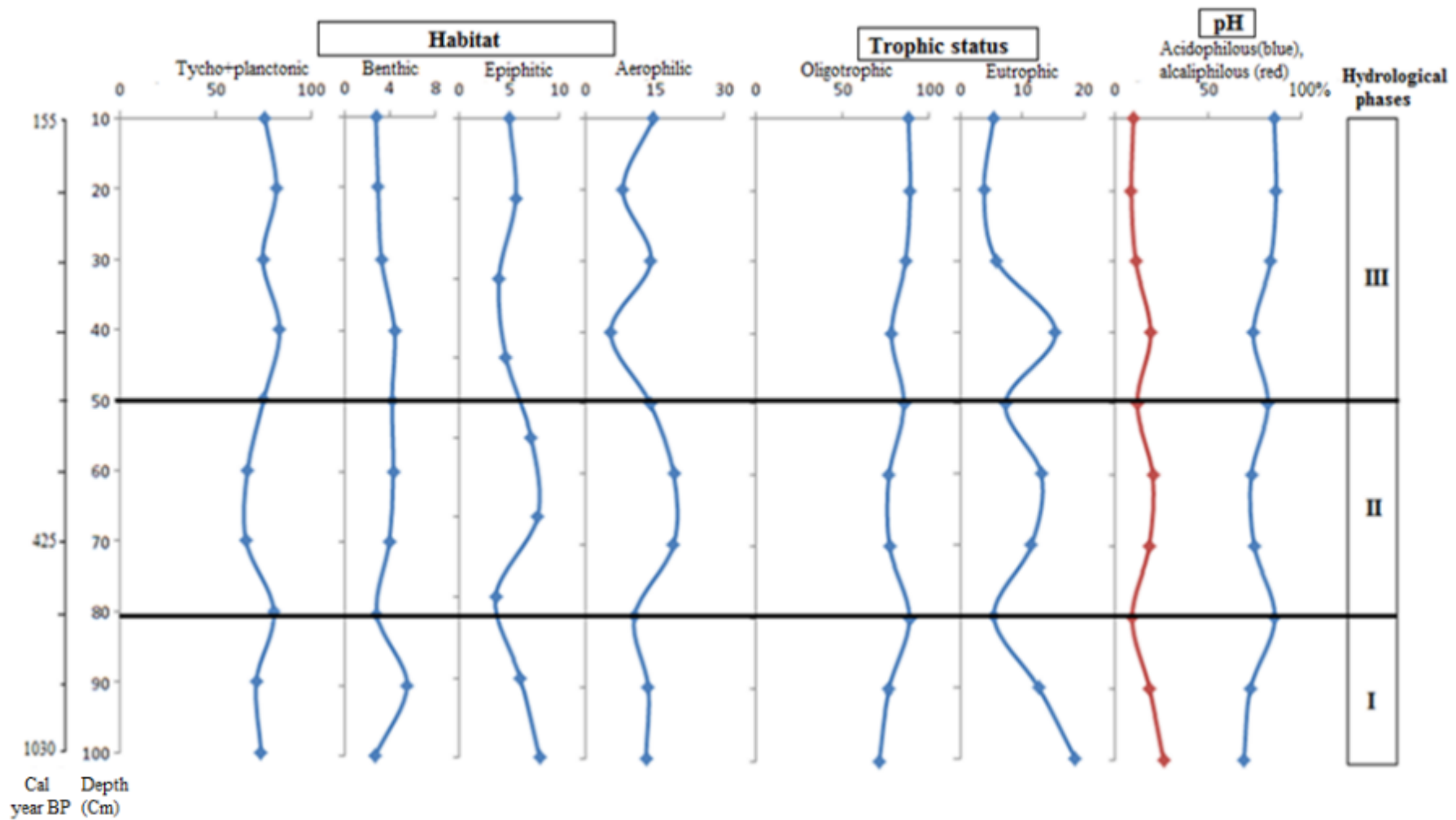


Figure VI.16. Variation in relative abundance of habitat indicator ecological groups (tycho + planktonic, benthic, epiphytic, aerophilic), trophic (eutrophic and oligotrophic) and pH (alkaliphile, acidophilic, indifferent) along the Ngaoundaba core as a function of depth

Episode 2: Between 80 and 50 cm

This period represents a transition from Episode 1 to Episode 3 and is still characterized by the dominance of *A. distans* and *A. distans* var. *Africana*. They develop abundantly in stable and oligotrophic waters (Hustedt, 1927). Nevertheless, aerophiles such as *Eunotia incisa* reach their highest abundance in this phase with a brief peak at 70 cm indicating at least episodic drying. This period showing high abundances of epiphytes (8 %) and aerophiles (20 %) would correspond to the lowest lake levels, probably due to a great variability of climate on a multiannual scale during certain years favorable to the development of such species.

Episode 3: Between 50 and 10 cm

As in Episode 1, the diatom flora is dominated by the oligotrophic acidophilic tychoplanktonic species *Aulacoseira distans*. Its maximum abundance (72 %) is reached during this episode at 20 cm. It is associated here with relatively high contents of aerophilic diatoms (up to 14 % at 30 cm) represented by *E. incisa*. Overall, the increase in tychoplanktonic species indicates a rise in the lake level compared to the previous episode, the waters being relatively more acidic. However, the plankton species remain low, indicating that this rise has remained moderate.

VI.3. Pollen and algae analysis

The pollen diagrams; presented in Figure VI.17a, b and c include only the main taxa which are abundant and consistently occurring, and therefore are considered as the most important for the palaeoenvironmental interpretation. Within the framework of this study, each lake is marked by several pollen zones which have been differentiated on the frequency fluctuations. They are described from the bottom to the top of the cores. Pollen percentages are based on a sum of at least 153 well preserved pollen grains and algae (Appendix). A temporary list of actually determined pollen taxa for varied samples of the studied cores is proposed here Ngos et al., 2003; Ngomanda et al., 2009; Maley, 1981; Maley and Brenac, 1987; Willis, 2020):

Semi-deciduous forest taxa

Bosqueia cf. *angolensis*, *Ceiba pentandra*, *Celtis*, *Chlorophora*, *Eugenia*, *Holoptelea* (*Ulmaceae*), *Moraceae undiff.*, *Myrianthus*, *Nauclea*, *Piptadenia/strum*, *Sterculia*, *Triplochiton*, *Uapaca*, *Calycobolus (Convolvulus)*, *Combretodendron*, *Hugonia* type, *Milletia* cf. *oblata*.

Pioneer forest taxa

Elaeis guineensis, *Aidia* type, *Alchornea*, *Allophylus*, *Anthocleista*, *Antidesma*, *Combretaceae*, *Macaranga*, *Mallotus*, *Milicia*, *Musanga* (big), *Musanga* type, *Phyllanthus* cf. *reticulatus*, *Phyllanthus* undiff., *Pycnanthus*, *Ricinus*, *Trema guineensis*, *Zanthoxylum* type, *Betula*, *Dicranolepis*, *Fagara* type, *Gerrardina* cf., *Plantago* cf. *palmata*, *Populus*, *Ranunculus*, *Salix*.

Evergreen and Biafrean forest taxa

Begonia, *Dialium* cf., *Ficus*, *Flacourtia* cf., *Hymenostegia*, *Irvingia-Klainedoxa*, *Martretia*, *Meliaceae*, *Mitragyna* cf. *inermis*, *Rhus* type, *Syzygium*, *Alnus*, *Chassalia* type, *Corylus*, *Quercus*, *Lawsonia*, *Maesobotrya* type, *Morus*, *Prosopis*.

Mountainous forest taxa

Podocarpus, *Phoenix* cf. *reclinata*, *Rubus* type, *Rumex*, *Polypodium* type, *Pygeum*.

Forest regrowth taxa

Bridelia, *Clausena*, *Clematis* type, *Flueggea* t. (*Phyllanthaceae*), *Stephania* cf. *abyssinica*, *Tetraploa aristata*, *Urticaceae* undiff.

Swamp forest taxa

Cleistanthus, *Cyathea*, *Lemna* type, *Uapaca*, *Phoenix* cf. *reclinata*, *Raphia* cf., *Calystegia*, *Pentodon*, *Pentodon* cf.

Savanna taxa

Acaccia, *Apiaceae*, *Asteraceae* (*Tubuliflorae*), *Bombax*, *Brassicaceae*, *Chenopodiaceae*-*Amaranthaceae*, *Cissampelos*, *Cissus*, *Commelina*, *Commelina* type, *Croton*, *Fabaceae* undiff., *Gardenia*, *Grewia* type, *Hymenocardia*, *Higrophila* (*Acanthaceae*), *Isoberlinia*, *Lamiaceae*, *Lannea* (small), *Lannea* type, *Leucas* cf., *Lophira* cf. *alata*, *Pavetta* type, *Piliostigma* (small), *Poaceae* (below 0.04 mm), *Poaceae* (above 0.04 mm), *Faurea* type, *Huperzia* cf. *ophioglossoides*, *Maclura*.

Algae

Polypodiaceae (*indusium*), *Polypodiaceae* *monoete*, *Polypodiaceae* *monoete* (*microechini*), *Polypodiaceae* *trilete*, *Pteris*, *Pteris* cf. *vittata*, *Pterocarpus*, *Adiantum*, *Arcella*, *Assulina* cf. *muscorum*, *Dryopteris* type, *Pediastrum angulosum*, *Pediastrum boryanum*, *Pediastrum integrum*, *Pediastrum tetras*, *Loxogramme*, *Scenedesmus*, *Selaginella*, *Trichomanes*, *Zygnemataceae*.

Aquatics and hygrophilous herbs taxa

Blepharis (Acanthaceae), Cyperaceae, Impatiens, Ipomea cf. aquatica, Lotus type, Nymphaea, Nymphaea basal cells, Pandanus, Typha, Utricularia hair, Crotalaria cf. axillaris, Haloragaceae, Spirogyra, Botryococcus, Tetradron. Cnetis cf.

Figure VI.17. Continued

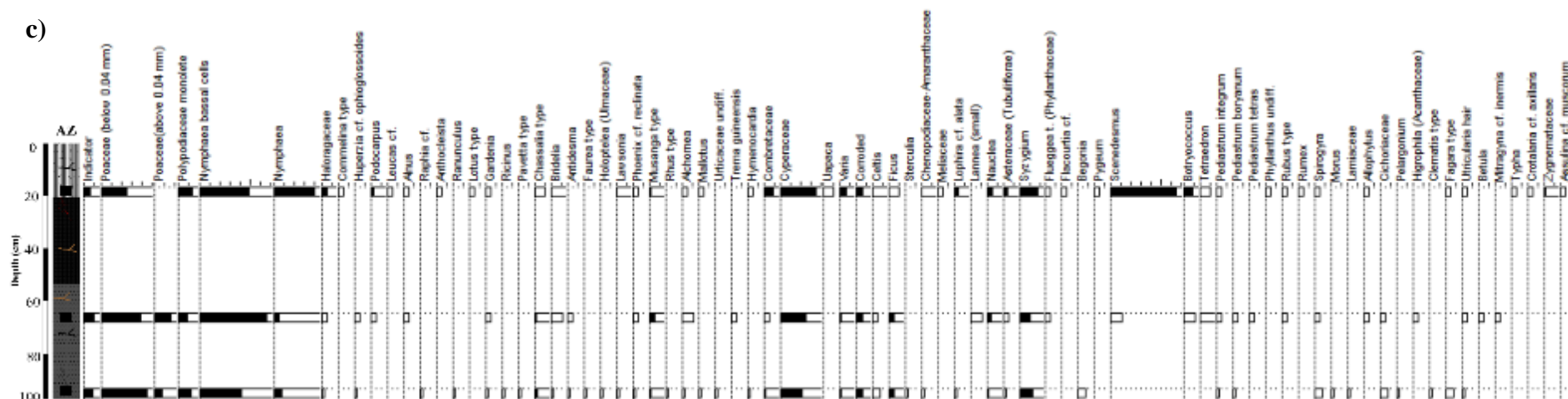


Figure VI.17. Distribution of species recorded in the sequence of : a) NR core from Simbock Lake (Yaoundé, South-Cameroon) ; b) LO core from Ossa lakes Complex (Dizangué, South-West, Cameroon) and c) AZ core from Ngaoundaba Lake (Adamawa, North-Cameroon).

Indicator is *Lycopodium* standard to assess pollen concentration it more or less reflect pollen concentration (the higher value it is the lower concentration should be) ; Varia is the variation of species for each samples and corroded is the conservation rate of species.

Cultivated taxa

Elaeis guineensis, *Cichoriaceae*, *Codiaeum*, *Paullinia pinnata*, *Pelargonium*, *Pentas*, *Plectranthus*.

VI.3.1. Simbock Lake (NR core)

For this lake, changes in the forest component and local vegetation composition represented by the pollen spectrum record, suggest a modern pollen deposition environment (Figure VI.17a). The pollen spectrum of three clay and sand samples of Lake Simbock is composed of: Pioneer forest taxa (33.57 %); Algae taxa: 27.45 %; Savanna taxa (9.09 %); Semi deciduous forest taxa (8.01 %); Evergreen and Biafrean forest taxa (6.03 %); Swamp forest taxa (5.22 %); Cultivated taxa (3.6 %); Aquatics and hygrophilous herbs taxa (3.51 %); Forest regrowth taxa (3.24 %); Mountainous forest taxa (0.27 %). They are well preserved with 7.85 % of corroded species.

This characterizes the dominance of arboreal taxa, which represent more than 55 % of the total pollen count. The most abundant ones are the *Alchornea*, *Macaranga*, *Pycnanthus*, *Combretaceae*, *Elaeis guineensis*, *Musanga type*, *Nauclea*, *Celtis* associated with some *Bosqueia angolensis*, *Trema guineensis*, *Mallotus* and *Milletia oblata*. Herbaceous, swamp and aquatic taxa are very scarce. Pteridophyta associated with some algae species represent a mean percentage of about 28 %. Pollen analysis of the local deposits, clearly show that the dynamics of the vegetation occurring on this site during the late Quaternary was characterized by extension and retreat of the local forested environment (Ngomanda et al., 2007). The low representation of herbaceous elements, which have a great local pollen production as demonstrated in modern pollen rain studies in Congo (Elenga, 1992), suggests that grassland was missing on this site. Such palaeobotanical environment would implicate a humid climatic episode with precipitation certainly higher than today. Although these data have been obtained on a single site, it can be supposed that most of the Yaoundé depressions were occupied by hydromorphous and pioneer forests. In this lake, there were more *Alchornea* in the catchment, bottom sample may have recorded a decline in the water table (increase in *Poaceae*, *Polypodiaceae monolote*) and/or more distinct deforestation.

VI.3.2. Ossa Lake (LO core)

The pollen spectrum of the three selected samples from OM core is composed of: Algae taxa (58.07 %); Aquatics and hygrophilous herbs taxa (14.59 %); Pioneer forest taxa (9.79 %);

Savanna taxa (8.82 %); Semi deciduous forest taxa (3.54 %); Evergreen and Biafrean forest taxa (1.79 %); Cultivated taxa (1.75 %); Forest regrowth taxa (0.92 %); Swamp forest taxa (0.44 %); Mountainous forest taxa (0.29 %). Based on sampling location, percentage variations and the presence of some taxa, three palynological zones were distinguished (Figure VI.17b) and described from bottom to top of the core. The species of this lake are very well preserved with 6.06 % of corrosion.

VI.3.2.1. Pollen zone LO3 (149-147 cm; 550 yrs BP.)

This zone is represented only at the bottom of the core, between 149 and 147 cm. Dated about 550 yrs BP., it is characterized by the dominance of algae taxa which represent more than 58 % of the total pollen count. At the bottom sample, there is more Botryococcus algae. It might be connected with a stronger trophy but also it might be connected with acidification (? dystrophy). This sample is characterized by the noticeable presence of tree pollen belonging to the closed canopy forest, mainly *Macaranga*, *Alchornea*, *Musanga* type and *Celtis*, associated with *Pycnanthus*, *Combretaceae*, *Elaeis guineensis* *Syzygium*, *Bosqueia angolensis*, *Nauclea*. This suggests greater woodland cover and forest taxa growing close to the forest-savanna interface, such as *Lannea* type, *Lophira alata* and climbers of the type *Cnestis*. These pollen assemblages indicate that the lake surrounding forest environment. was dominated by a mixed semi-evergreen rain forest. Its abundant pollen, associated with the presence of other forest taxa growing close to the forest-savanna interface, reflects forest expansion towards the savanna.

VI.3.2.2. Pollen zone LO2 (72-70 cm; 380 yrs BP.)

This is characterized by a progressive decrease of pioneering arboreal contemporaneous pollen with an increase of Poaceae pollen and Polypdiaceae spore percentages taxa. There is a possible decline in the water table at a depth of 72-70 cm. Because many pteridophytes today favour the well-drained soils on the lakeshore, this zone suggests significant lake-level decline. Moreover, it might have been a result of deforestation (more swampy grasslands). We infer that this reflects the regional forest canopy disturbance in response to drier conditions (Ngomanda et al., 2005) probably around 380 yrs BP., and suggest recurring seasonal lake-level fluctuations.

VI.3.2.3. Pollen zone LO1 (12-10 cm; 230 yrs BP.)

This is the most diverse zone of the whole sequence. It is located at 12-10 cm depth and date around 230 yr BP. The main pollen taxa belong to the families Caesalpiaceae, Mimosaceae and Ulmaceae (mostly represented by *Celtis*). It is also characterized by increasing forest pollen taxa (e.g., *Lophira alata*, *Cnestis*, *Fagara*), which are species living close to the forest-savanna interface, associated with a further decline in pollen from *Elaeis guineensis* and other gap-colonizer species. This pollen zone indicates a regeneration of mature forest (because of reduced canopy disturbance) and the re-expansion of forest towards the savanna. These assemblages indicate further expansion of lowland Biafran evergreen rain forest that exist today.

VI.3.3. Ngaoundaba Lake (NL core)

A total of 74 terrestrial pollen and algae taxa were identified in the 3 samples from core NL, with changes in the relative pollen abundance clearly reflecting the vegetation dynamics (Figure VI.17c). Based on floristic changes of the forest component, three pollen zones characterizing the main successive stages have been visually defined. The pollen spectrum of the selected sample of Lake Ngaoundaba is composed of: Aquatics and hygrophilous herbs taxa (52.14 %); algae taxa (20.85 %); Savanna taxa (14.4 %); Evergreen and Biafran forest taxa (6.4 %); Pioneer forest taxa (3.03 %); Semi deciduous forest taxa (1.64 %); Cultivated taxa (0.19 %); Swamp forest taxa (0.19 %); Mountainous forest taxa (0.67 %); Forest regrowth taxa (0.48 %). Almost all the species are preserved, only 2.23 % of species are corroded.

VI.3.3.1. Pollen zone NL3 (87-85 cm; 1030 yrs BP.)

In zone NL3 (1030 yrs BP.; 87–85 cm) pioneer forest pollen taxa (e.g., *Macaranga*, *Alchornea*, *Musanga* type and *Elaeis guineensis*) are scarce or absent. However, arboreal pollen taxa from the mosaic forest-savanna (e.g., *Lophira alata* and *Lannea* type) are the dominant trees; these species are today actively involved in savanna colonization in the absence of fire (White et al., 2000). Mature forest trees, mainly Mimosaceae and *Celtis* are also well-represented in the pollen assemblage, indicating that the rainforest was being progressively reconstructed. In addition, pollen from aquatic taxa (> 52 % of the total pollen sum) are mostly present, associated with the marked of *Uapaca* and *Raphia* pollen most probably from the swamp trees present today. In addition to the importance of swampy environments around Lake

Ngaoundaba like Lake Maridor in Gabon, the high abundance of Cyperaceae pollen and pteridophyte algae suggest a mosaic of marshy-swampy vegetation (Ngomanda et al., 2009).

VI.3.3.2. Pollen zone NL2 (43-41 cm; 425 yrs BP.)

This pollen zone between 43-41 cm and dated of about 425 yrs BP., shows a progressive decrease in the major closed savanna-forest taxa such as *Lannea type*, *Lophira alata* and *Poaceae*. There is also a possible decline in the water table because many pteridophytes today favour the well-drained soils on the lakeshore and suggests significant lake-level decline. Contrary to the decrease of the savanna taxa, the apparition and increase of some forest tree taxa like *Syzygium*, *Ficus*, *Alnus*, *Lophira alata* and *Mallotus* are observed. These taxa are classified as components of Biafran and evergreen forests.

VI.3.3.3. Pollen zone NL1 (7-5 cm; 155 yrs BP.)

At 155 yrs BP. (pollen zone NL1: 7–5 cm), eutrophic water body was overgrown by *nymphheids*; at the top decrease in water table and increase in trophy (see a strong increase in *Scenedesmus*), appearance of peat patches (presence of *testate amoeba-Assulina muscorum*), suggesting a potentially more acidic condition. In local woodlands, *Syzygium* was also more frequent (in comparison to the previous zones), suggesting drier climatic conditions than before.

Conclusion

This chapter reconstructs the history of tropical forests in North and South Cameroon in particular, but also in Central Africa, based on the radiocarbon dating and palynological analysis of Quaternary sedimentary sequences taken from three lakes in Cameroon. The analysis of the high-resolution microflora of the sedimentary deposits of lakes Simbock, Ossa and Ngaoundaba has made it possible to highlight the impact of past climatic variations on the dynamics of forest ecosystems of Cameroon. Within the framework of this study, each lake is marked by several palynological zones which have been differentiated on the frequency fluctuations and sediment deposition periods.

The data collected show that 1000 yrs BP., the tropical forests of Cameroon suffered significant destruction of their floristic and structural compositions, characterized by the formation of savannas in the northern region of the country and by the expansion of pioneer and secondary forests, to the detriment of evergreen primary forests. This opening up of the



Part three: Discussions

The third part concerns the discussions of obtained results in selected lakes. It is composed of a chapter which deals with the synthesis and discussion based on the part two chapters.



Chapter VII: Synthesis and discussion

Theory is when you know everything and nothing works. Practice is when everything works and no one knows why. Here we have brought theory and practice together: Nothing works... and nobody knows why!

-Albert Einstein-

The sedimentological, petrological and paleoenvironmental studies of the sediments from the studied lakes have been used to reconstruct the sequence of sedimentary deposits in the different lakes and their sedimentogenesis. They included classification; maturity and recycling; provenance and tectonic setting; paleoweathering of the source rocks, and the paleoclimates of South and North Cameroon since the last 2000 cal. years BP. It is important to notify that some calculations for the diagrams are shown in tables from part two.

VII.1. Classification of sediments

VII.1.1. Simbock Lake

The sediments of Simbock Lake are mainly composed sand and clay size particules with a clayey to sandy-clayey texture. These grain sizes favoured the formation of quartz and clay minerals. Based on the $\log (\text{Na}_2\text{O}/\text{K}_2\text{O})$ vs. $\text{Log} (\text{SiO}_2/\text{Al}_2\text{O}_3)$ following Pettijohn et al. (1972) most of samples occupy the arkosic field and some the subarkose field (Figure VII.1a). In the binary plot $\log (\text{Fe}_2\text{O}_3/\text{K}_2\text{O})$ vs. $\text{Log} (\text{SiO}_2/\text{Al}_2\text{O}_3)$ following Herron (1988), sediment plots into lithic arenite, iron-sand and iron-shale fields (Figure VII.1b). Samples plotting in the pettijohn arkose field generally correspond to the iron-sand and iron-shale in the Herron diagram. Then, the subarkose would belong to the lithic arenite field. The arkosic character of these sediments would be linked to the presence of feldspars. These sediments have the same characteristics as sandstones which suggests that in the future, these sediments could give birth to sandstones if conditions change and the grains consolidate. From another angle, the sediments in the subarkose field show that some of the sediments would not have finished their weathering processes. Hence, the lithic fragment marks in localized sediments much further down the lake bottom. This signature could also be explained by the remains of rocks left when the lake was created less than 30 years ago. They could have been altered over time at the bottom of the lake and produced these lithic arenite signature.

VII.1.2. Ossa lakes Complex

The grain size fraction of the Ossa Complex sediments is heterogenous with a dominance of clay. The texture of this is heavy-sandy to clay texture. The sandy character is mostly represented in the river supplying the lakes. According to the binary plot of Pettijohn et al. (1972), the sediments deposited under these bodies of water would be considered as arkose (Figure VII.1a). The same sediments after the Herron (1988), are classified as shales and iron-shales (Figure VII.1b). The iron-shales are mostly present in the river supplying the lakes. In

this context, arkotic sediments could be related to primary minerals such as feldspars that would have resisted to weathering. On the other hand, the clayey sediments are just the result of the dominant clayey texture of the sediments which at the end of diagenesis could give rise to schists and perhaps later on after a first metamorphism to gneisses and if conditions change again to a second metamorphism to granites. rocks found in the study area. The fine to medium grains from the Ossa lakes Complex can be link to leaching of the surrounding gneisses rocks and also the granitoids from the Sanaga River during 1890 ± 60 cal. year BP.

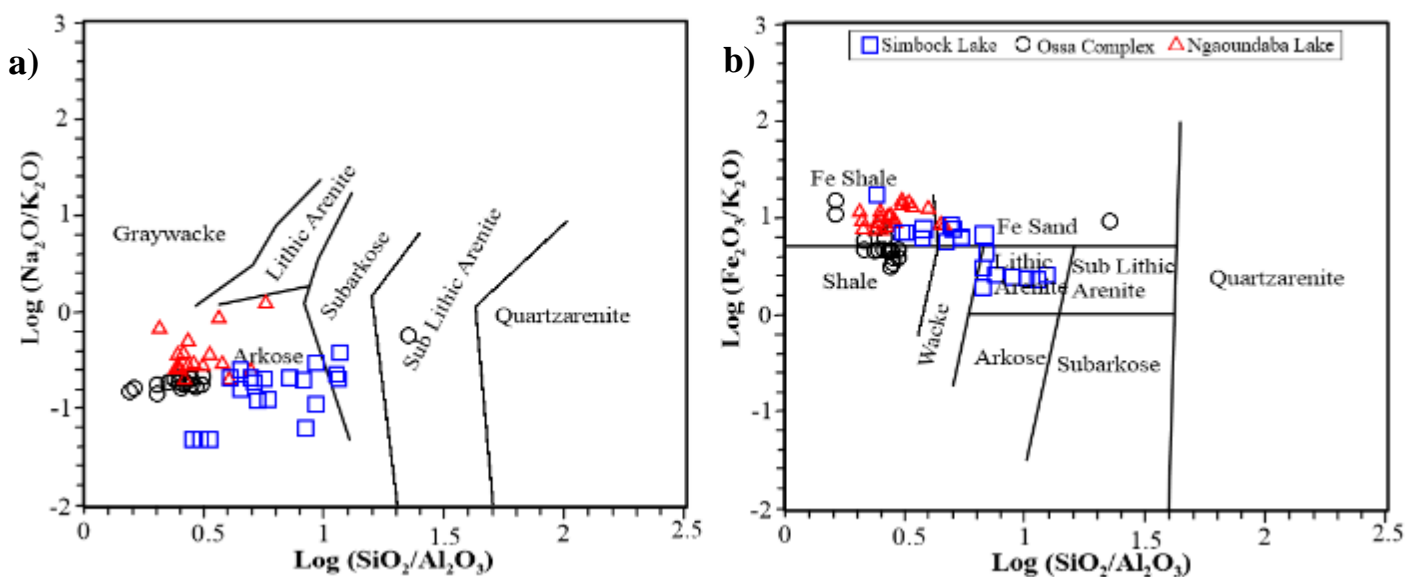


Figure VII.1. Geochemical classification of lacustrine sediments based on: **a)** log ($\text{SiO}_2/\text{Al}_2\text{O}_3$) versus log ($\text{Na}_2\text{O}/\text{K}_2\text{O}$) diagram (Pettijohn et al., 1972) and **b)** log ($\text{SiO}_2/\text{Al}_2\text{O}_3$) versus log ($\text{Fe}_2\text{O}_3/\text{K}_2\text{O}$) diagram (after Herron, 1988)

VII.1.3. Ngaoundaba Lake

The predominance of the fine fraction (mud) consisting of clay and silt in the lake sediments is due to the low and/or absence of drainage flow towards the lake. Textural class of sample sediment was found to be mostly silty with few samples from the base cores showing clayey silty texture for the bottom core of the lake. The base texture of border part of the lake is sandy silt. Water content, water depth and grain size showed a clear association in the samples taken from the lake. It was found that the fine fraction is dominant along the bottom core due to the depth and the anthropogenic activity sites while few sands was found to be associated with the lower water column close to the lake border. The abundance of fine grain sizes in the lacustrine sediments from Ngaoundaba area reflecting the weathering from basement rocks consisting of pre-Pan-African granitoids and metamorphic formations and also from the eolian

source of quartz grains. These textures and grain size distribution is confirmed by the geochemical diagrams of Pettijohn et al. (1972) and Herron (1988), where almost all sediments fall into arkose from the Pettijohn and into Fe-shale field in majority (Figure VII.1). The iron characteristics associated with grain size can be link to the high proportion of hematite and the presence of ilmenite.

VII.2. Maturity and recycling

The maturity can be ascertained by calculating the index compositional variation (ICV) introduced by Cox et al. (1995). In general, the degree of chemical weathering increases when alumina content is enriched, and detrital ferromagnesian minerals decrease and can often reflect the compositional maturity of sediments. According to Cox et al. (1995), $ICV > 1$ have abundant unweathered detrital minerals (e.g., pyroxene and olivine) and are compositionally immature while, $ICV < 1$ usually derived from weathered minerals (e.g., clay minerals) and denoted for compositionally mature sediments. The textural maturity of clastic sediments can be inferred through ratios like SiO_2/Al_2O_3 , Al_2O_3/Na_2O , and K_2O/Na_2O , where high values (> 6 , > 5 , and > 1) represent compositionally matured sediments (Armstrong-Altrin et al., 2016). The binary diagram ICV vs. CIA also infer the maturity of sediments (Figure VI.2).

VII.2.1. Simbock Lake

From the Simbock Lake in Yaoundé, the SiO_2/Al_2O_3 ratio values vary from 2.5 to 12.5. These ratios are higher than the average PAAS (3.3), indicating a high textural maturity. However, except few samples, all the lake samples exhibit Al_2O_3/Na_2O and K_2O/Na_2O ratios < 5 and < 1 , respectively, whereas those ratios are noticeably high, varying from 52.3 to 521.3 and 4.1 to 16, respectively, in Simbock Lake samples. This suggests that the textural maturity is very high in these sediments. Furthermore, the ICV (Cox et al., 1995; Cullers, 2000), which has been successfully used by many authors to measure the compositional maturity, is consistent with this result. The range ICV values of the studied sediments varying from 0.2 to 0.6 indicating a compositionally mature (Figure VII.2a) or recycled sediment. This recycled effect is also reflected in the Zr and Hf contents, which are high field strength element present in zircon. The Zr contents in these materials are from 114 to 553 ppm. Similarly, the average Hf contents in the Simbock Lake is high (6.1 to 14.5 ppm). Zircon, and thus Zr enrichment during sorting, can also be evaluated when the Zr/Sc ratio is plotted against the Th/Sc ratio (McLennan et al., 1993). In this diagram, which indicates a chemical differentiation, the Zr/Sc

ratios increase more rapidly than Th/Sc for the studied sediments, suggesting recycling and sorting of the sediment studied (Figure VII.2b). The fact that the Simbock Lake samples are compositionally mature, is coherent with the sediment characteristics and the mineralogy of this basin. For example, sediment samples from this area shows abundance of detrital clay minerals and many rock forming minerals. This result suggests that these sediments were derived and deposited close to their source, due to the tectonic activity linked to the rift environment. This interpretation is based on the fact that the sediment is fringed by reactivated fault-bounded gneissic source rocks (Eyong et al., 2013). Furthermore, the adjacent highlands surrounding the town of Yaoundé (“*ville aux sept collines*”) may have acted as the nearby source rocks.

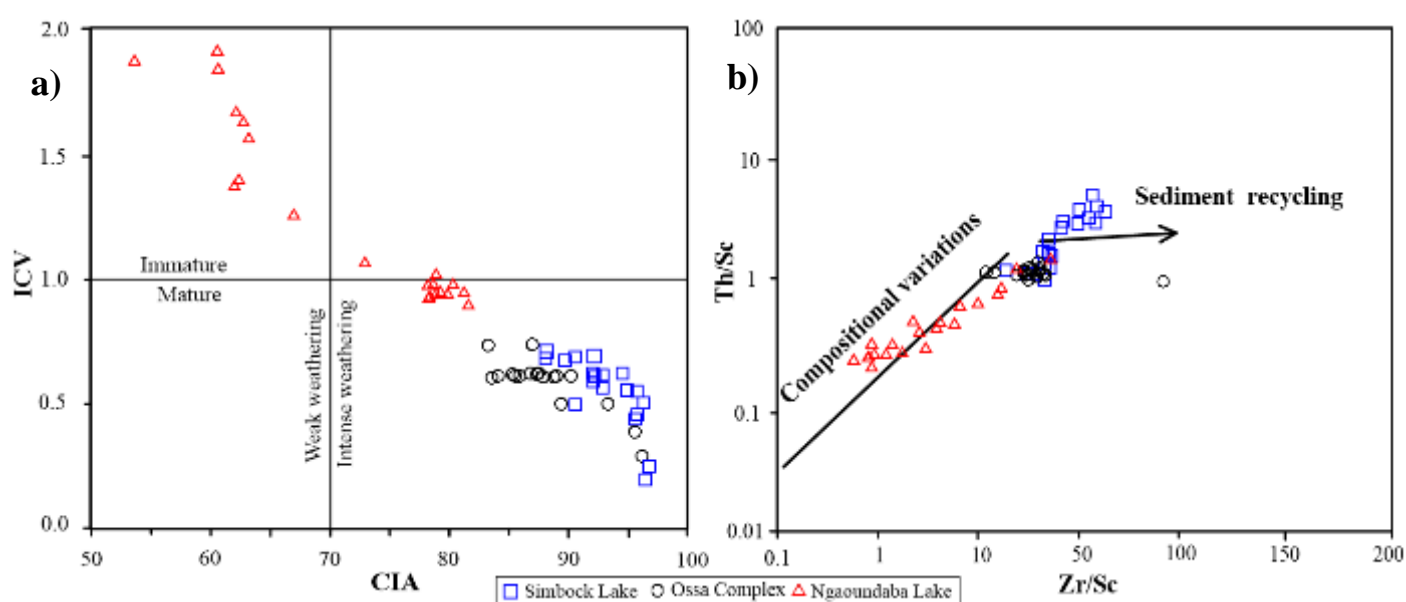


Figure VII.2. a) ICV versus CIA diagram (Nesbitt and Young, 1984; Cox et al. 1995) showing maturity of sediments and b) Th/Sc vs. Zr/Sc bivariate plot (after McLennan et al., 1993) for samples from studied lakes showing possible sorting effects and recycling sediments

VII.2.2. Ossa lakes Complex

The ICV values of investigated sediments in the Ossa lakes Complex range from 0.31 to 0.67, thus inferring compositionally mature sediments deposited in a tectonically active environment. The K_2O/Na_2O ratio for the core sediments vary from 4.8 to 7.7, which also suggests maturity of sediments. The SiO_2/Al_2O_3 and Al_2O_3/Na_2O ratios are used generally to infer the textural maturity of sediments, which varies from 1.7 to 2.7 and 52.3 to 521.3 respectively indicating high compositional maturity, probably due to the alteration of feldspars (Nesbitt and Young, 1984). The binary diagram ICV vs. CIA (Figure VII.2a) confirms the high

maturity of sediments or a slightly recycled sediment. The slightly recycled effect can also be reflected in the high Zr and low Hf contents, which vary from 114 to 468 ppm and 2.9 to 11.7 ppm respectively. Zircon, and thus Zr enrichment during sorting, can also be evaluated when the Zr/Sc ratio is plotted against the Th/Sc ratio. From this binary diagram, which indicates a chemical differentiation, the Zr/Sc ratios increase more rapidly than Th/Sc for the studied sediments, suggesting low recycling and sorting of the sediment studied (Figure VII.2b). The maturity of sediments from the studied lakes en river is coherent with the petrography of the bulk sediments and the selected sand grains of this watershed. These samples also show abundance of detrital clay minerals and secondary minerals. This suggests that the sediments from this complex may have derived and deposited close to their source, due to the tectonic activity linked to the rift environment. This interpretation is based on the fact that these sediments are fringed by reactivated fault-bounded granito-gneissic rocks (Eyong et al., 2013; Nguetchoua et al., 2019). On the other hand, the recycled input of the Ossa Complex could reflect distal facies, with an increase of silica content, deposited under low regular topographic relief through the Sanaga River. This inference suggests a less intense tectonic activity during the post-rift stage and a relative long transport of terrigenous materials.

VII.2.3. Ngaoundaba Lake

The $\text{SiO}_2/\text{Al}_2\text{O}_3$ and $\text{Al}_2\text{O}_3/\text{Na}_2\text{O}$ are prerequisite chemical indices to assess the maturity of sedimentary rocks (e.g., Chen et al., 2014). These ratios vary from 2.4 to 4.8 and 11.8 to 96.8 respectively for the sediments from the center of the lake and from 2.2 to 2.8 and 19.5 to 32.1 respectively for the sediment from the border. This suggested textural maturity for the source rocks from the center of the lake and immature for the border. The $\text{K}_2\text{O}/\text{Na}_2\text{O}$ ratio which also suggests maturity of source rocks, they vary from 0.9 to 5.5 and 1.5 to 2.2 respectively for the center and the border lake sediments reflecting the immature nature of the border sources and mature nature of the center source rocks. In addition, ICV is another important indicator to judge the maturity of the sedimentary rocks (Cox et al., 1995). From the ICV calculation and the ICV versus CIA diagram (Figure VII.2a), sediments from the bottom of the lake have immature source materials. Whereas, sediment from the border have generally mature nature of source rocks. This could also be demonstrated by the preservation of feldspars. Feldspars in the sediments of Ngaoundaba Lake would be altered in-situ, suggesting that they would not be recycled. This lack of recycling is also observed in Figure VII.2b (Th/Sc vs. Zr/Sc diagram) where the Zr/Sc ratio values indicate no significant recycling and no zircon enrichment (McLennan et al., 1993). Both compositionally maturity and immaturity in the Ngaoundaba

Lake, is coherent with the morphology and the mineralogy of this crater lake. Sediment from this area shows abundance of clay minerals and many rock forming minerals in the center sediments lake. This result suggests that these sediments were derived and deposited close to their source, due to wind transport around the environment. Whereas, the subrounded shape of grain in the border sediments suggest the nearby source rocks.

VII.3. Paleoweathering

The above mentioned ICV results also demonstrate that sediments can derived from a low to a high intense weathered source area. In the present study, numerous weathering indices have been calculated to determinate the source area weathering degree including CIA; CIW; WIP and some ratios. For the values of CIA, PIA and CIW, values < 50 indicates very low weathering, 50 – 80 low to moderate weathering, and > 80 indicates high intensity of weathering, with complete conversion of feldspars to aluminous clay minerals (Fedo et al., 1995). However, the CIA and CIW formula use total aluminium (Al) without correction for Al in K- feldspar. The PIA index is therefore used in the current study for evaluating K- metasomatism effects. Parker's WIP index is used to evaluate the intensity of the weathering of silicate rocks, based upon the proportion of alkali and alkaline earth elements in the products of weathering. High Al_2O_3/Na_2O and Rb/Sr ratios are other indicators of intense degree of weathering (McLennan et al., 1993), since the latter leads to accumulate Al^{3+} (residual constituent) and Rb (often fixed in weathered profiles) relative to Na^+ (labile cation) and Sr (easily removed from weathered profiles), respectively. Condie (1993) reported that the number of elements which are lost is proportional to the extent of weathering.

VII.3.1. Simbock Lake

In the Simbock Lake, the values for the sample sediments, of CIA are between 90 and 96.7, PIA vary from 96.6 to 99.1 %, and CIW from 97.4 to 98.8 % indicate, overall, very intense weathered source area (Table V). The studied samples sediments exhibit very high Al_2O_3/Na_2O and Rb/Sr ratios varying from 52.3 to 521.3 and from 0.4 to 0.7 respectively, suggesting that the rock which give the present sediment were highly weathered. The weathering intensity of sediments and their source areas can be quantified by considering major element contents, despite the probable interplay of diagenetic processes. To investigate effects of post-depositional metasomatic modifications on the major elements of the Simbock Lake, their compositions were plotted within A-CN-K (Al_2O_3 , $CaO^* + Na_2O$, K_2O) compositional space.

On this diagram, the studied samples offset at the end the weathering trend for Upper Archean crust which is predicted by Nesbitt and Young (1984) from kinetic leach rates (Figure VII.3). This A-enrichment is due by the presence in high proportion and the conversion of aluminous clay minerals to illite. It is characterized, in the A-CN-K diagram, by a path toward the A apex (Figure VII.3). This result is consistent with the XRD data which consistently shows the presence of clay minerals in high proportion. This result indicates an intense to very intense degree of weathering. This interpretation is further confirming by binary plot ICV versus CIA (Figure VII.2a) suggesting an intense weathering of source rocks.

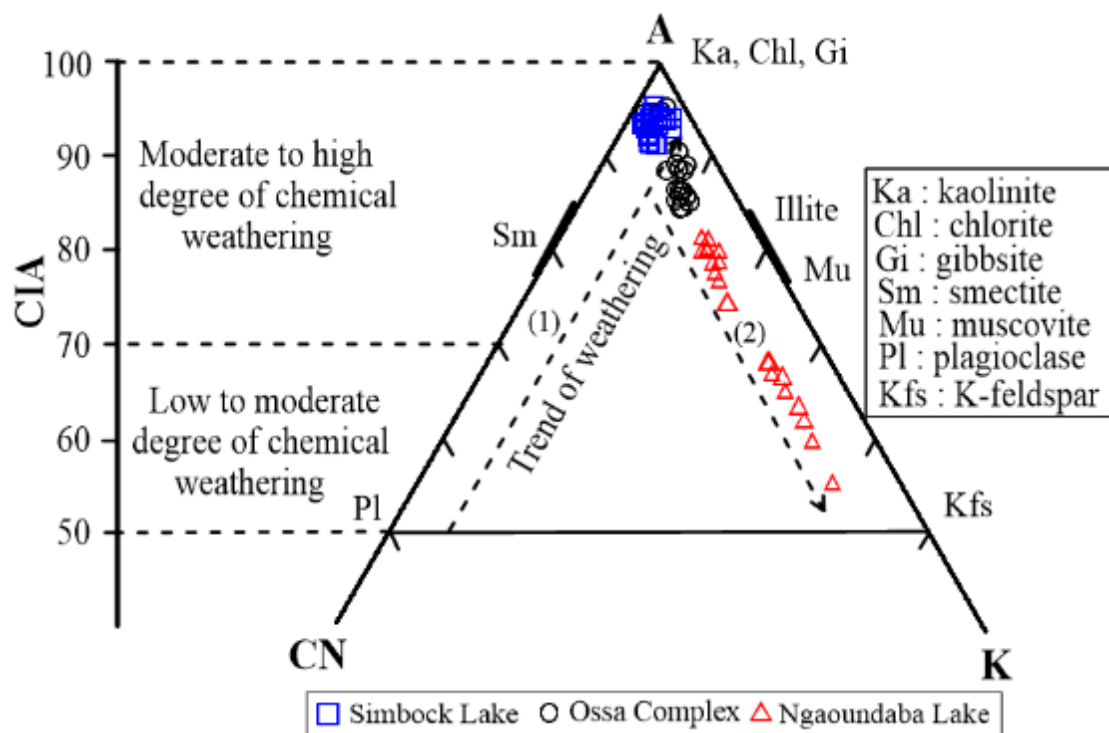


Figure VII.3. Ternary diagram A-CN-K (Nesbitt and Young, 1982, 1984) to infer the intensity of weathering for the samples from Simbock, Ossa Complex and Ngaoundaba lakes. Oxides A (Al_2O_3), CN ($\text{CaO} + \text{Na}_2\text{O}$), and K (K_2O) are plotted as molar proportions; (1) weathering trend for Upper Archean crust; (2) K-metasomatism

VII.3.2. Ossa Lake Complex

In this lake sediments, subrounded grains are link to long transport but moderate weathered of source rocks. Surface microtextures embedded in grains can be relate to some mechanical and chemical processes, whereas others may follow the principle of equifinality due to geological processes. The mechanical action of lacustrine sediments including fresh surfaces, abrasive surfaces, striations, conchoidal fractures, straight step and V-shaped pits that affect the surface texture of minerals. The effects of abrasion in abrasive surfaces and straight step are clearly engraved in the surface of the grains in these grains, that reflect sustained high shear stress and conchoidal fractures on the subrounded edges. In the selected grains, these conchoidal fractures are mostly weathered. The latter coated by amorphous silica and clay minerals, it is clear a significant population of samples are reworked, possibly sourced from a warmer and more humid palaeoclimate and possibly involving fluvial transport. Fluvial action produced collisions between two grains resulting in V-shaped pit which are interpreted to a deposition in high energetic subaqueous environments like the watershed of Sanaga River.

The CIA values of sediment samples from Ossa lake range from 84.4 to 96.1 %, indicating intense-degree of chemical weathering of the source rocks. This high chemical weathering is also confirmed by high PIA (av. = ~ 94.7%) and CIW (av. = ~ 95.2%) values (Tables V). Mineralogical data also revealed dominance of clay minerals and high content of iron oxide coatings, which may result from diagenetic alteration or from intense weathering in the source area. The presence of illite and kaolinite suggests chemical weathering of feldspars and mica which are mineral phases from the gneissic source area. Hence, the A-CN-K diagram shows that all the samples plot well above the feldspar line near the illite and kaolinite, chlorite, gibbsite field following the weathering trend of A-CN join towards the A-apex (Figure VII.3), suggesting gneisses as main source rocks and also reflects relatively steady-state weathering conditions. The variation in the values of chemical indices in sediments is attributed to the variation in the source rocks composition. This inference suggests that sediments from Ossa lake, deposited during the drift stage in 1890 ± 60 cal. year BP, likely experienced high tectonic activities. The binary diagram ICV vs. CIA confirms the intense weathering of sediments (Figure VII.2a). Hence, the degree of chemical weathering is mainly a function of climate and erosion in the source area.

VII.3.3. Ngaoundaba Lake

To better understand paleoweathering, SEM of sand grains was helpful. The mechanical action of sediments from Ngaoundaba Lake including fresh surfaces, abrasive surfaces, striations, conchoidal fractures, straight step and V-shaped pits that affect the surface texture of minerals. The effects of abrasion in abrasive surfaces and straight step are clearly engraved in the surface of the grains in this lake sediments, that reflect sustained high shear stress and conchoidal fractures on the subrounded edges. Straight step is generally characteristic of a tectonic origin and can be related to fault systems (Mahaney, 2002), whereas conchoidal fractures are known on aeolian sands. In this study, these conchoidal fractures are both fresh and weathered. The latter coated by amorphous silica and clay minerals, it is clear a significant population of samples are reworked, possibly sourced from a humid and warmer palaeoclimate and possibly involving aeolian transport. Fluvial action produced collisions between two grains resulting in V-shaped pit which are interpreted to a deposition in high energetic subaqueous environments like the hillside of the Ngaoundaba Crater (e.g., Mahaney et al., 1988). Quartz grain presents: solution pits, vesicular shards, weathered surfaces, scaling and dissolution pit, which are chemical weathering products of source rock during contact with external factors, probably present at the time when source rock was exposed to the atmosphere. Among the chemical weathering microtextures on some grains relative to fresh surfaces indicates a pre-weathering history, followed by local fluvial transport to the lake.

Shape of grains, mineralogy, geochemical indices and elemental ratios, are some of the parameters which can help for determination of weathering conditions. In this part on the country, subrounded grain are link to eolian transport but moderate weathered of source rock. However, subangular and angular grain are characteristic of moderate weathering. Higher Ca/Al ratio is related to sands, and higher Fe/Al and Mg/Al values are linked to fine particles. This may be due to the comminution of mineral particles during transportation by fluvial or eolian. The recycling of aeolian sediments thus leads to increase in feldspars. In addition, Iron is sensitive to redox in aquatic environments. Redox conditions lead to the release and recycling of iron in the limnological ecosystem, which could lead to a distribution of lake sediments according to the particle size fractions of the Ngaoundaba Crater sediments. (Naehar et al., 2013). Mineralogy from this crater lake also revealed presence of clay minerals and high content of iron oxide coatings, which may result from diagenetic processes or from intense weathering in the source area. The presence of kaolinite and illite suggests chemical weathering of feldspars which is mineral phase from the granitic and gneissic source area.

Moreover, chemical indices such as CIA and WIP values are well correlate in the bottom core and quite well in the border core sediments, exhibiting moderate and greater CIA and smaller WIP values respectively for AZ and NL cores (Tables V). The above correlations suggest that these indices of weathering, despite their different methods of assessing the degree of weathering of lake sediments, can be significantly influenced by the size of the sediment grains (Sun et al., 2018). From the ICV calculation and the ICV versus CIA diagram sediments from the bottom of the lake are immature and the moderate weathering character of these sediments is confirmed. Whereas, sediments from the border are generally mature with intense weathering (Figure VII.2a).

The weathering intensity of sediments and their source areas can be quantified by considering major element contents, despite the probable interplay of diagenetic processes. To investigate effects of post-depositional metasomatic modifications on the major elements of the center and the border sediments of this lake. Their compositions were plotted within A-CN-K compositional space. On this diagram, the studied samples offset from the weathering trend for Upper Archean crust (trend 1), which is predicted by Nesbitt and Young (1984) from kinetic leach rates (Figure VII.3). This deviation (trend 2) is probably attributable to differential dissolution of labile minerals, since plagioclase is more easily dissolved than K-feldspar. It can also be interpreted as an addition of K_2O to aluminous clay during diagenesis. This K-enrichment is caused by the conversion of aluminous clay minerals to illite. It is characterized, in the A-CN-K diagram, by a path toward the K apex (Figure VII.3). This result is consistent with the XRD and SEM-EDS data which consistently shows the presence of K-feldspar. An estimate of this enrichment can be made by drawing a line from K_2O apex through individual data point. The intersection point of this line with the weathering path gives the pre-metasomatised CIA value. The difference between the premetasomatised and the current CIA values allows quantitative estimation of K-enrichment in the rock (Fedó et al., 1995; Armstrong-Altrin et al., 2016).

VII.4. Provenance and tectonic setting

Provenance and tectonic setting can be determined by sedimentological and petrological parameters. The provenance and tectonic setting of the lacustrines sediments were determined using elemental ratios and discriminant functions (Roser and Korsch 1986; Verma and Armstrong-Altrin, 2013; Ramos-Vázquez et al., 2018; Armstrong-Altrin et al., 2019; Ngueutchoua et al., 2019). Hayashi et al. (1997) established Al_2O_3/TiO_2 ratios to infer the

provenance of clastic sediments, where a value greater than 21 indicates a felsic parent rock (Armstrong Altrin et al., 2015; Vosoughi Moradi et al., 2016). This ratio, varying between 8 and 21, is suggestive of an intermediate source rocks, whereas it is less than 8 for mafic source rocks. Geochemical compositions of sedimentary materials have been widely used to disclose their tectonic settings signature (Verma and Armstrong-Altrin, 2016; Armstrong-Altrin, 2014; McLennan et al., 1990; Armstrong-Altrin, 2015). The new major and trace element-based discrimination diagram of tectonic setting (active and passive margins) recently proposed by Verma and Armstrong-Altrin, 2016, where ten major elements (SiO_2 to P_2O_5) and six trace elements (Cr, Nb, Ni, V, Y, and Zr) were selected for the combined major and trace element-based function. All these 16 elements were adjusted to sum to 100 % (SiO_2MT to ZrMT) and then transformed to 15 isometric log-ratios (ilr1TiMT to ilr15ZrMT) which is calculated after Egozcue et al. (2003). The major element-based discrimination diagrams which present three main tectonic settings (island or continental arc, continental rift, and collision) proposed by Verma and Armstrong-Altrin (2013) consist of a diagram created for the tectonic discrimination of silica, (high and/or low). In the case of this study sediments have low-silica [$(\text{SiO}_2)_{\text{adj}} = 35\% - 63\%$] and high-silica [$(\text{SiO}_2)_{\text{adj}} = 63\% - 95\%$]. The major-element contents were recalculated to an anhydrous (LOI-free) basis and adjusted to 100 % before interpretation.

In the present study we have used REE to show the chemical composition of the source rocks. After Graf (1984) high LREE/HREE ratios and negative Eu anomalies is linked to felsic rocks, whereas low LREE/HREE ratios with no Eu anomalies indicate mafic rocks.

VII.4.1. Simbock Lake

The provenance of clastic sedimentary rocks can be determined by using grain sizes and mineralogy (Young, 1976; Mack and Rasmussen, 1984). The dominance of quartz and sand grain size suggests derivation of sediments from a granitic source and also suggests that the quartz grains of the Sanaga watershed are of plutonic, and middle and upper metamorphic sources. The greater abundance of alkali feldspar suggests a granitic or gneissic source for the sediments of the Ossa Complex (Trevena and Nash, 1981). The geochemical composition of clastic sedimentary rocks is also employed to deduce provenance in this lake by various diagrams. The Zr and TiO_2 plot (Hayashi et al., 1997) suggests that the source rock for the sediments of the studied lake are mafic to intermediate igneous rock (Figure VII.4a). The major element discriminant diagram proposed by Roser and Korsch (1986) is widely used to decipher provenance. The Simbock Lake samples fall mainly in mafic and intermediate igneous

provenances (Figure VII.4b), suggesting their derivation from the cratonic interior. The low to moderate $\text{Al}_2\text{O}_3/\text{TiO}_2$ ratios of the sediments from Simbock Lake (3.4 to 13.2) suggest a mafic source to an intermediate source.

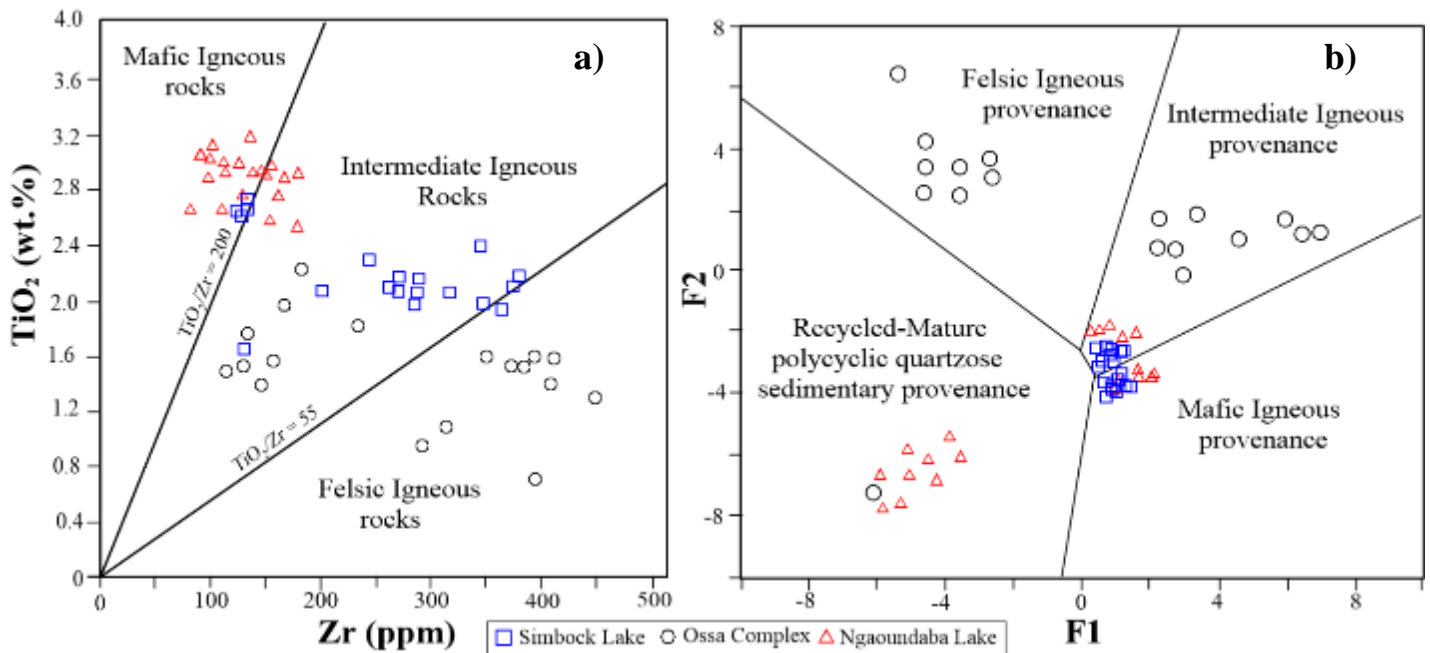


Figure VII.4. Major and trace element provenance diagrams: **a)** TiO_2 versus Zr diagram (Hayashi et al., 1997); **b)** Discriminant function (F) diagram after Roser and Korsch (1986) where $F1 = (-1.773 \times \text{TiO}_2) + (0.607 \times \text{Al}_2\text{O}_3) + (0.76 \times \text{Fe}_2\text{O}_3) + (-1.5 \times \text{MgO}) + (0.616 \times \text{CaO}) + (0.509 \times \text{Na}_2\text{O}) + (-1.22 \times \text{K}_2\text{O}) + (-9.09)$. $F2 = (0.445 \times \text{TiO}_2) + (0.07 \times \text{Al}_2\text{O}_3) + (-0.25 \times \text{Fe}_2\text{O}_3) + (-1.142 \times \text{MgO}) + (0.438 \times \text{CaO}) + (1.475 \times \text{Na}_2\text{O}) + (1.426 \times \text{K}_2\text{O}) + (-6.861)$

Recently, Verma and Armstrong-Altrin (2013) recommended two new discriminant function diagrams for the tectonic discrimination of siliciclastic sediments from three tectonic settings; island or continental arc, continental rift and collision, which are constructed for tectonic discrimination of high silica (SiO_2)_{adj} = 63–95% and low silica (SiO_2)_{adj} = 35–63%. In these diagrams (high silica and low silica; Figures VII.5a-b), the sediments samples mostly plot in the collision field with few samples in the arc field. The active and passive margin incorporates continental margin and is developed along the edges of continents (Bhatia, 1983). This also suggests that rocks are derived from both stable continental blocks and has the signature of a collision of a continental and an oceanic margin. They have been deposited in various types of basins including collision basins. The integration of grain size, mineralogy and geochemical signature strongly suggests that the sediment from the Simbock Lake were derived from stable continental areas and deposited in a basin like the studied lake.

VII.4.2. Ossa lakes Complex

The provenance and tectonic setting of the Ossa lakes Complex were determined using elemental ratios and discriminant functions. Hayashi et al. (1997) established Al_2O_3/TiO_2 ratios to distinguish mafic Al_2O_3/TiO_2 (< 14) and felsic (Al_2O_3/TiO_2 from 19 to 28) source rocks which could be gneisses, granitoids and amphibolite in Sanaga watershed. This ratio is high in lake sediments (12.3 to 22), suggesting a felsic source, with little contribution from an intermediate source.

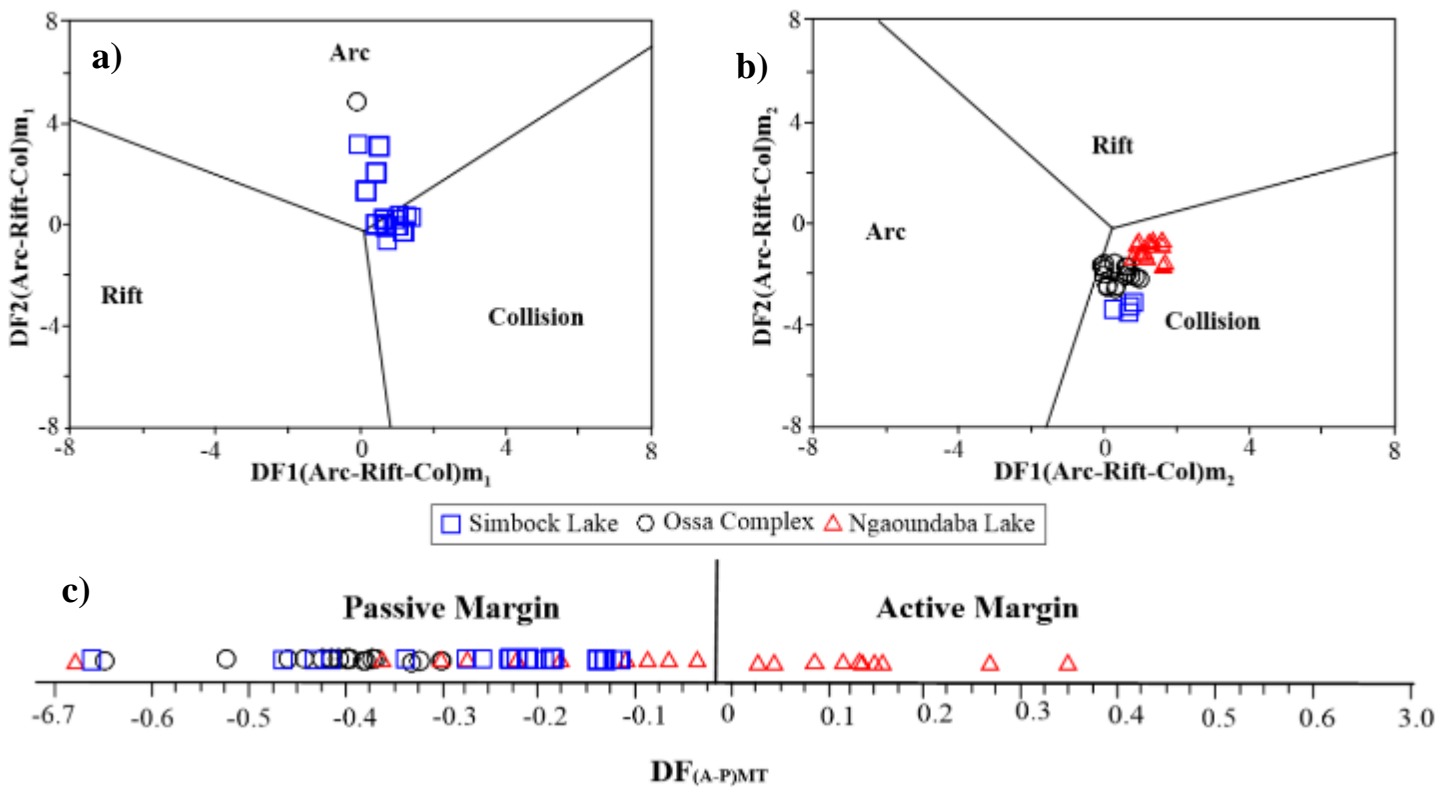


Figure VII.5. Tectonic diagrams for the samples from Simbock, Ossa Complex and Ngaoundaba lakes):
a) Discriminant-function multi-dimensional diagram for high-silica clastic sediments (Verma and Armstrong-Altrin, 2013). The subscript m₁ in DF1 and DF2 represents the high-silica diagram based on loge-ratios of major-elements. The discriminant function equation are: $DF1 (Arc-Rift Col)m_1 = (-0.263 \times \ln(TiO_2/SiO_2)_{adj}) + (0.604 \times \ln(Al_2O_3/SiO_2)_{adj}) + (-1.725 \times \ln(Fe_2O_3t/SiO_2)_{adj}) + (0.660 \times \ln(MnO/SiO_2)_{adj}) + (2.191 \times \ln(MgO/SiO_2)_{adj}) + (0.144 \times \ln(CaO/SiO_2)_{adj}) + (-1.304 \times \ln(Na_2O/SiO_2)_{adj}) + (0.054 \times \ln(K_2O/SiO_2)_{adj}) + (-0.330 \times \ln(P_2O_5/SiO_2)_{adj}) + 1.588$. $DF2 (Arc-Rift-Col)m_1 = (-1.196 \times \ln(TiO_2/SiO_2)_{adj}) + (1.604 \times \ln(Al_2O_3/SiO_2)_{adj}) + (-0.303 \times \ln(Fe_2O_3t/SiO_2)_{adj}) + (0.436 \times \ln(MnO/SiO_2)_{adj}) + (0.838 \times \ln(MgO/SiO_2)_{adj}) + (-0.407 \times \ln(CaO/SiO_2)_{adj}) + (1.021 \times \ln(Na_2O/SiO_2)_{adj}) + (-1.706 \times \ln(K_2O/SiO_2)_{adj}) + (-0.126 \times \ln(P_2O_5/SiO_2)_{adj}) - 1.068$; **b)** Discriminant-function multi-dimensional diagram for low-silica clastic sediments (Verma and Armstrong-Altrin, 2013). The subscript m₂ in DF1 and DF2 represents the low-silica diagram based on

loge-ratios of major-elements. The discriminant function equation are: DF1 (Arc-Rift-Col)m2 = $(0.608 \times \ln(\text{TiO}_2/\text{SiO}_2)_{\text{adj}}) + (-1.854 \times \ln(\text{Al}_2\text{O}_3/\text{SiO}_2)_{\text{adj}}) + (0.299 \times \ln(\text{Fe}_2\text{O}_3/\text{SiO}_2)_{\text{adj}}) + (-0.550 \times \ln(\text{MnO}/\text{SiO}_2)_{\text{adj}}) + (0.1120 \times \ln(\text{MgO}/\text{SiO}_2)_{\text{adj}}) + (0.194 \times \ln(\text{CaO}/\text{SiO}_2)_{\text{adj}}) + (-1.510 \times \ln(\text{Na}_2\text{O}/\text{SiO}_2)_{\text{adj}}) + (1.941 \times \ln(\text{K}_2\text{O}/\text{SiO}_2)_{\text{adj}}) + (0.003 \times \ln(\text{P}_2\text{O}_5/\text{SiO}_2)_{\text{adj}}) - 0.294$. DF2 (Arc-Rift-Col)m2 = $(-0.554 \times \ln(\text{TiO}_2/\text{SiO}_2)_{\text{adj}}) + (-0.995 \times \ln(\text{Al}_2\text{O}_3/\text{SiO}_2)_{\text{adj}}) + (1.765 \times \ln(\text{Fe}_2\text{O}_3/\text{SiO}_2)_{\text{adj}}) + (1.391 \times \ln(\text{MnO}/\text{SiO}_2)_{\text{adj}}) + (1.034 \times \ln(\text{MgO}/\text{SiO}_2)_{\text{adj}}) + (0.225 \times \ln(\text{CaO}/\text{SiO}_2)_{\text{adj}}) + (0.713 \times \ln(\text{Na}_2\text{O}/\text{SiO}_2)_{\text{adj}}) + (0.330 \times \ln(\text{K}_2\text{O}/\text{SiO}_2)_{\text{adj}}) + (0.637 \times \ln(\text{P}_2\text{O}_5/\text{SiO}_2)_{\text{adj}}) - 3.631$ and c) Multidimensional discriminant function diagram discriminating the active (A) and Passive (P) margin settings (Verma and Armstrong-Altrin, 2016), where $DF_{(A-P)MT} = (3.2683 \times \text{Ilr}_{1\text{TiO}_2\text{MT}}) + (5.3873 \times \text{Ilr}_{2\text{Al}_2\text{O}_3\text{MT}}) + (1.5546 \times \text{Ilr}_{3\text{Fe}_2\text{O}_3\text{MT}}) + (3.2166 \times \text{Ilr}_{4\text{MnOMT}}) + (4.7542 \times \text{Ilr}_{5\text{MgOMT}}) + (2.0390 \times \text{Ilr}_{6\text{CaOMT}}) + (4.0490 \times \text{Ilr}_{7\text{Na}_2\text{OMT}}) + (3.1505 \times \text{Ilr}_{8\text{K}_2\text{OMT}}) + (2.3688 \times \text{Ilr}_{9\text{P}_2\text{O}_5\text{MT}}) + (2.8354 \times \text{Ilr}_{10\text{CrMT}}) + (0.9011 \times \text{Ilr}_{11\text{NbMT}}) + (1.9128 \times \text{Ilr}_{12\text{NiMT}}) + (2.9094 \times \text{Ilr}_{13\text{VMT}}) + (4.1507 \times \text{Ilr}_{14\text{YMT}}) + (3.4871 \times \text{Ilr}_{15\text{ZrMT}}) - 3.2088$.

The $\text{K}_2\text{O}/\text{Na}_2\text{O}$ ratio from Potter (1978) is also considered as a provenance indicator in clastic sediments; low ratio suggests a mafic source rather than felsic. In this study, samples from Ossa lake indicate their derivation from a felsic and intermediate source with $\text{K}_2\text{O}/\text{Na}_2\text{O}$ ratios ranging from 4.8 to 6.7, also confirmed by the presence of illite and illite-smectite. The zircon content can also specify the provenance of sediments (Hayashi et al. 1997). A binary plot of Zr versus TiO_2 suggests that the source rocks for the Ossa lake sediments are felsic to intermediate igneous rocks that derived from the craton (Figure VII.4a). This felsic igneous provenance is also confirmed by the major element discriminant diagram proposed by Roser and Korsch (1986), where samples fall mostly in felsic provenance, except one sample, which plots in the intermediate igneous provenance (Figure VII.4b). The felsic provenance may be linked to gneisses, whereas the intermediate provenance is attributed to the mixture of gneisses located near to the study area, or to the amphibolite, granitic and magmatic gneisses in the Sanaga watershed.

The presence of high LREE/HREE ratios and negative Eu anomalies is linked to felsic rocks such as gneisses and gneissoids (McLennan et al., 1993).

The discrimination diagrams were proposed for the tectonic discrimination of low-silica [$(\text{SiO}_2)_{\text{adj}} = 35\text{--}63\%$ (m2)] sediments (Verma and Armstrong-Altrin, 2013). All samples, were plotted in the collision field (Figure VII.5b). Collision setting for the lake sediments is further confirmed by the new discriminant diagram. On this plot, almost samples plotted in the active margin setting (Figure VII.5c). According to the geological background and geochemical characteristics of the Paleocene to Holocene deposits of the Ossa Complex volcanic, metamorphic and sedimentary rocks, the volcanic and metamorphic rocks which derive the

sediments were formed in both collision and rift setting (passive margin) and marked the onset of the Paleocene to Holocene deposit of the Ossa lake Complex which is a part of Douala sub-basin. This interpretation is consistent with the geological background of the Ossa lake Complex (Giresse et al. 2005; Kossoni and Giresse, 2010, Ngueutchoua et al. 2019).

VII.4.3. Ngaoundaba Lake

Alteration minerals including clays, rutile, calcite and ferromagnesian were most probably precipitated in the parental rock, either by weathering or diagenesis processes. Although distance between edges of the Crater and Ngaoundaba Lake is minimal link to the subangular to angular sharp of the border sands. Hence, the source of sediment samples of the Crater lake can only be inferred. In addition, the presence minerals such as hematite and zircon; the presence of rounded grain quartz revealed that the sediments of the Ngaoundaba Lake may have been derived from variety of source rocks (mixed provenance). The presence of illite in core sediments suggests that the lake sediments are derived from the weathering of volcanic rocks exposed in the source area.

The major and trace elements from sediments can also be related to that of their source area and is extensively used to investigate the source and provenance of the sediments using discrimination diagrams (Roser and Korsch 1986). Based on this provenance diagram the lake bottom sediments fall in the fields of quartzose sedimentary provenance. However, sample sediments from the border of the lake plot towards mafic igneous and intermediate igneous provenance (Figure VII.4a-b). The mafic provenance may be linked to basalt, whereas the intermediate provenance is attributed to the metamorphic formations (gneisses and amphibolite) recovering the Oligocene to Pleistocene mafic lavas surrounding the Crater lake. The quartzose sedimentary provenance of bottom sediments from the Ngaoundaba Crater Lake suggest a sedimentary strata and subordinate volcanic rocks, in part metamorphosed. It is exposed to erosion by the orogenic uplift of the Adamawa and Djerem-Mbéré faults from the surrounding area. These sediments were deposited by longitudinal transport parallel to the orogenic grain prior to final crustal collision along the Adamawa and Djerem-Mbéré faults in a passive margin. The longitudinal transport in this study is due to the shape of the grain and from the course of the grain around the Crater for short distances (created by winds) or far for distant sources.

The tectonic setting is distinguishing in this lake by low-silica [$(\text{SiO}_2)_{\text{adj}} = 35\text{--}63\%$ (m²)] sediments. Almost all samples, were plotted in the collision field (Figure VII.5b). Collision

setting for this lake sediments is further confirmed by the new discriminant diagram. On this plot, almost samples plotted in both active and passive margin setting (Figure VII.5c). According to the geological background and geochemical characteristics of the Holocene deposits of the Adamawa plateau, the volcanic and metamorphic rocks which derive the sediments were formed in a collision setting (active and passive margin).

The absence of Eu anomalies in the sediment contents indicates that they originated from undifferentiated to slightly differentiated mafic provenance such as basalt and their products (McLennan et al., 1993).

VII.5. Paleoclimate and Depositional environment

Grain size, microtexture, mineralogy, weathering indices (CIA and PIA), some major and trace elements and their ratio (Sr, Cu, Rb Sr/Ba, Rb/Sr, Sr/Cu and $\text{Na}_2\text{O}/\text{Al}_2\text{O}_3$), and palynology can be considered as reliable tools to address the paleoenvironment of the source area (Cao et al., 2012; Hernández-Hinojosa et al., 2018). Rb/Sr and Sr/Cu ratios have been used in several studies to decipher the paleoclimatic conditions under which the lacustrine environment was produced (Cao et al., 2012; Ngueutchoua et al., 2019). Low Rb/Sr and Sr/Cu ratios reflect a warm and humid condition. As Sr contents are higher in seawater, Sr/Ba ratios can be used to discriminate freshwater (Sr/Ba: < 1) and marine sediments (Sr/Ba: > 1) (Sun et al., 1997). Sr/Ba ratios between 1.0 and 0.5 may indicate brackishwater. In lacustrine environments, a Sr/Ba ratio above 1.0 may indicate saline lake water under arid climate (Shi et al., 2003; Meng et al., 2012). This is also confirmed by the binary plot of Ga/Rb and Sr/Cu showing paleoclimatic conditions. Paleoenvironmental conditions in the depositional milieu of sediments can be inferred through elemental ratios like U/Th, V/Cr and Ni/Co (Jones and Manning, 1994; Madhavaraju and Lee, 2009). It is proposed that Ni/Co ratios of < 5 indicate oxic environments, while a ratio of > 5 proposes suboxic and anoxic environments. Typical anoxic environments have U/Th ratios > 1.25 , whereas low values < 0.75 suggest an oxic environment (Jones and Manning, 1994). Similarly, a V/Cr ratio with high value (> 4.5) indicates an anoxic environment, while low values (< 2) are associated with oxic conditions (Jones and Manning, 1994). Owing to the preferential removal of Ce^{4+} from the deep-sea water, leading to a negative Ce anomaly ($\text{Ce}/\text{Ce}^* < 1$), this element can provide information about the paleo-redox conditions of a depositional milieu (Toyoda et al., 1990). Based mainly on the ecology of the diatom associations noted in the sites, a reconstruction of the major climate trends and of certain factors such as paleobathymetry, water stability, water chemistry can be

proposed. Variations in paleobathymetry can be evaluated by studying the specific content of each sample and especially the distribution of diatoms according to their ecological affinity. Figures VII.6 and 7 show the distribution, along the sedimentary columns, of the palynological groupings that can help in understanding the oscillations of water bodies.

In the South four major fluctuations have been identified

a drop in the water level is observed at the beginning of the phase between 150 and 120 cm (505 yrs BP.).

an increase in the water level between 120 and 70 cm (505 - 380 yrs BP.).

a drop in the water level is recorded between 70 and 30 cm (380 – 250 yrs BP.)

a rise in water level is recorded between 30 and 10 cm and is marked by the dominance of plankton (250 yrs BP. to present days).

The almost similar evolution of the hydrological levels of these two ecosystems from 500 years BP. would probably be due to the synchronous response of these sites to the displacement of ITCZs in space and time.

Three major fluctuations have been individualized In the Ngaoundaba Lake (North):

- a high lake level recorded between 96 and 80 cm (1050 -1000 yrs BP.);
- a low lake level recorded between 80 and 50 cm (1000 - 420 yrs BP.);
- a high lake level is observed from 50 and 10 cm (420 - 155 yrs BP.).

The lake level has evolved according to water inflows and outflows, themselves controlled by climatic parameters such as precipitation, evaporation or evapotranspiration. Major trends in climate evolution and comparisons with other paleodata from some regional reference sites was done principally in two main areas, the South (Simbock and Ossa lakes) and the North (Ngaoundaba Lake) Cameroon.

VII.5.1. South, Cameroon (Simbock and Ossa Lakes)

The palynological assemblages along the Simbock and Ossa core show significant variations and can therefore be used to reconstruct the hydrological and climatic history of this area over the last 500 years. Figure VII.6 shows the variations in water level from planktonic + tycho planktonic diatoms, harmattan intensity and rainfall at Ossa. The evolution of the water level and vegetation in Paurosa, the evolution of vegetation in Barombi Mbo (Maley and Brenac, 1998) and Bambili (Lézine et al., 2012) are also presented. The dominance of

tychoplanktonic and planktonic diatoms along the Ossa core shows that the level of this lake remained significant overall.

At the base of the Ossa core (500 - 380 yrs BP.), the oligotrophic acidophilic tychoplanktonic dominance associated here with the high percentages of benthic and epiphytic diatoms suggests a drop in the lake level, with a transparent, stable and nutrient-poor water column. At the same site, analyses of sediments and diatom assemblages from Lake Ossa during this period indicate a low lake level marked by low percentages of tychoplanktonic + planktonic diatoms associated with a diatom peak brought by the wind (Nguetsop et al., 1998). Most lake sites around the Gulf of Guinea show low water levels from 400 years cal. BP. In Cameroon, for example, palynological data indicate the presence of herbaceous savannas at Barombi Mbo Nyabessan (Elenga et al., 1996; Reynaud-Farrera et al., 1996; Maley and Brenac., 1998; Ngomanda et al., 2009) and a forest opening in Gabon (Ngomanda et al., 2009). Bambili's pollen spectrum from this period reveals a seriously impoverished forest environment where *Podocarpus* percentages fall, except for a small peak at 4 % in the middle of the period, and where *Schefflera* experiences a continuous decline of 30 % to 1 % in tree pollen (Lezine et al., 2012). In Sinnda, on the other hand, around 500 cal. BP, forest taxa almost completely disappear in favour of Gramineae, Cyperaceae and Pteridophyte spores (Vincens et al., 1998), attesting to a significant opening of the environment.

Considering the low temporal and sampling resolution observed at the Ossa site, this phase of low-level malaria would be contemporary to a lacustrine episode brought to light in a few sites such as Nguéné and Kamalété in Gabon under the name "Petit Age de Glace" (Little Ice Age). The temporal shift may be due to chronological uncertainties inherent in the age patterns between sites (Anchukaitis and Tierney, 2013) or to other site-specific parameters (shape, area, type of relief or water supply mode) that may influence the recording of hydrological fluctuations and the responses of palynological assemblages.

From 380 yrs BP., diatom assemblages dominated by planktonic, eutrophic and alkaliphilic species become preponderant, indicating a significant change in the lake environment compared to the previous episode. These assemblages indicate a deep environment, a turbid and probably more turbid water column. These conditions globally reflect a relatively high balance, eutrophic conditions may be associated with more erosive rains (abundance of alkaliphilic diatoms) which have led to the leaching of soils and the transport of organic matter to the lake basin. In the South-Cameroon, between approximately 380-550 yr BP., an hydromorphous forest occupied a large area in both Dizangué and Yaoundé localities. The low representation of herbaceous elements, particularly Gramineae which have a great

local pollen production as demonstrated in modern pollen rain studies in Cameroon and Congo (Elenga, 1992; Ngomanda et al., 2009), suggests that grassland was missing at this area. Such palaeobotanical environment would implicate humid climatic episode with precipitation certainly higher than today. Although these data have been obtained on two lakes, but the same information can be shown in the western part of Cameroon in Barombi-Mbo Lake (Maley and Brenac, 1987; Giresse et al., 1994). It can be supposed that at 550 yr BP., most of the depressions of the southern and western parts of Cameroon as well as the Northern part of Gabon were occupied by hydromorphous forests close to the forest-savanna interface. At this period, it is suggesting a significant lake-level decline which might have been a result of deforestation.

In Simbock and Ossa Lakes, like other nearby paleoecological sites (Gabon, Cameroon, Congo), this humid trend has been characterized by forest recolonization. For example, in Bambili (West Cameroon), the abundance of taxa characteristic of montane and sub-montane forests such as *Scheffera* sp, *Ilex* sp, *Macaranga* sp, increases by up to 40 % (Lezine et al., 2012). In low-latitude sites in Gabon (Lake Nguéné, Kamalété and Maridor) and Congo (Lake Kitina, Mopo Mbai depression), increasingly higher percentages of dense forest taxa are recorded after 500 cal. BP. in pollen diagrams (Elenga et al., 1996; Ngomanda et al., 2009; Sutra, 2013).

However, between 70 and 30 cm, the diatom assemblages dominated by non-native species, combined with the high percentages of benthic and aerophilic diatoms, reflect a decrease in the water level in the environment. These data indicate much drier climatic conditions suggesting a significant change in seasonality, probably with well-marked dry seasons in relation to a southward shift in the mean position of the Intertropical Convergence Zone (ITCZ) and consequently, changes in precipitation rate and/or distribution of precipitation over the year. This phase could be contemporaneous with the dry phase recorded by Nguetsop et al. (2004), dated around 250 cal. BP in the same area. However, in most of the sites in Central Africa, this period is characterized by forest recolonization which indicates climatic conditions, and notably rainfall favorable to forest expansion. For example, pollen diagrams from Mopo-Bai (North-Congo Brazzaville) and Bambili (West, Cameroon) show the dominance of tree species such as *Alchornea* sp over the *Poaceae*. These records demonstrate the heterogeneity and complexity of the response of terrestrial and aquatic ecosystems in the intertropical zones, despite the forcing which is a priori comparable. Between 380 yr BP. to actual, pollen data show the retreat of the arboreal strata and the regeneration of mature forest on the Dizangué and Yaoundé sites giving way to hygrophytic and expansion of lowland Biafran evergreen rain

forest that exist today, rich in *Xyris*, *Nymphaea* and some other herbaceous components which were particularly well developed before 230 yr BP. During this period, the vegetation could be interpreted as mosaic of swampy grasslands with free and open water indicated by local patches of forests, suggesting more drier climatic conditions than before. Such reconstruction is consistent with the modern distribution of the aquatic plants identified in the fossil spectra. Indeed, *Nymphaea totus* can be develop in temporary pools flooded only during four months by year. So, it is possible that between 230 and 380 yr B.P., a rainfall decreasing coincided with a more contrasting seasonal distribution of precipitation. During this long dry season, the drop of the surface water level could have permitted the development of *Xyris* on the emerged sandy banks of the sites. At the same time, the forest, rather open as confirmed by the presence of numerous climbers, could have remained in the lowest zones of the depression where water would have been present. Such water occurrence in the Dizangué lakes during a period interpreted as dry can be explained by the fact that these low zones would have taken advantage of the flow of underground water. These dry and humid phases was recently described in a pollen sequence from lakes Kamlaté and Nguené, Gabon (Ngomanda et al., 2007).

During the Holocene, changes in the characteristics and intensity of the monsoon flow thus imposed wet or dry phases in tropical Africa (Itambi et al., 2010; Shanahan et al., 2012). However, it is likely that factors such as basin topography and distance from the sea have influenced the hydrological functioning of the lakes.

Likewise, clay minerals can reflect climatic changes in a source area (Meng et al., 2012). Kaolinite is generally formed under subtropical humid climate by intense weathering of feldspars, whereas illite is usually formed under humid climate with low precipitation. The high CIA and PIA values suggest that an overall subtropical warm and humid climate prevailed during deposition of the sediments. The Rb/Sr ratios range from 0.31 to 0.51 and Sr/Cu ratios vary from 1.1 to 4.57, reflect a negligible variation over time. This indicates that the sediments from the South, Cameroon belong to the Holocene to Quaternary stratigraphic division which did not experience markedly paleoclimatic variations. Paleoenvironmental conditions in the lacustrine environments can be inferred through the contents of Al_2O_3 , P_2O_5 and V (Mortazavi et al., 2014; Anaya-Gregorio et al., 2018). The binary diagrams of paleoenvironmental reconstructions (Figure VII.8a-b) show that sediments were deposited in shallow marine and fluvial environments as confirm in V vs. Al_2O_3 plot (Figure VII.8a). The interpretation emphasizes the importance of clay minerals in these lacustrine sediments. The moderate P content and the high Al_2O_3 values plotted in binary diagram of Al_2O_3 versus P_2O_5 show the increase of depositional environments water depth (Figure VII.8b) which can be linked to the

presence of organic matter. In Figure VII.8c, the values of Ga/Rb and Sr/Cu ratios in sediment samples vary from 0.4 to 2.5 reflect that the Sanaga watershed including the Ossa watershed was characterized by warm-humid climatic conditions during the Holocene period. The shallow marine and fluvial depositional environments of sediments took place in an oxic environment as suggested by U/Th and Ni/Co ratios, which vary from 0.19 to 0.28 and 1.62 to 4.21, respectively. However, Ni/Co ratio < 5 in these lakes indicates an oxic environment (Jones and Manning, 1994).

VII.5.2. North, Cameroon (Ngaoundaba Lake)

The palynological assemblages along the studied sequence (AZ) show important variations and can thus be used to reconstruct the hydrological past. The crossing of these different data can thus make it possible to retrace the climatic history of North Cameroon over the last 1000 years. Figure VII.7 presents the variations in water level from planktonic + tychoplanktonic diatoms, stability at Ngaoundaba, the evolution of the lake level and vegetation at Gbali (Sutra, 2013) and at Mbalang (Nguetsop et al., 2011), the evolution of the water level in Lake Chad (Maley, 2001). Changes in the characteristics and intensity of monsoon flow during the Holocene imposed wet or dry phases in tropical Africa (Itambi et al., 2010; Shanahan et al., 2012). These changes have played an important role on water budgets in tropical regions (Nguetsop et al., 2004). The dominance of tychoplanktonic and planktonic diatoms along the Ngaoundaba core shows globally that the level of this lake remained significant except for the phase centered between 500-700 yrs BP.

In the Northern part of Cameroon, savannah-forest was developed according to climate since 1030 to 700 yrs BP. But, as seen before, the lacustrine domain is actually contracting. This is due to accumulation of sediments, probably combined with a recent tendency of high precipitation. However, the presence of intraclasts as mud at the 90 cm depth of Ngaoundaba Lake allow an observation of the vegetal cover during this period. The dominance of acidophilic and oligotrophic tychoplanktonic diatoms represented by *Aulacoseira distans* and *Aulacoseira distans* var. *humilis* suggests a relatively high, stable and low turbidity water level. These wet conditions can be explained by a more intense monsoon flow during this period, linked to the northward shift of the mean position of the ITCZ inducing an increase in fine precipitation at the expense of erosive precipitation.

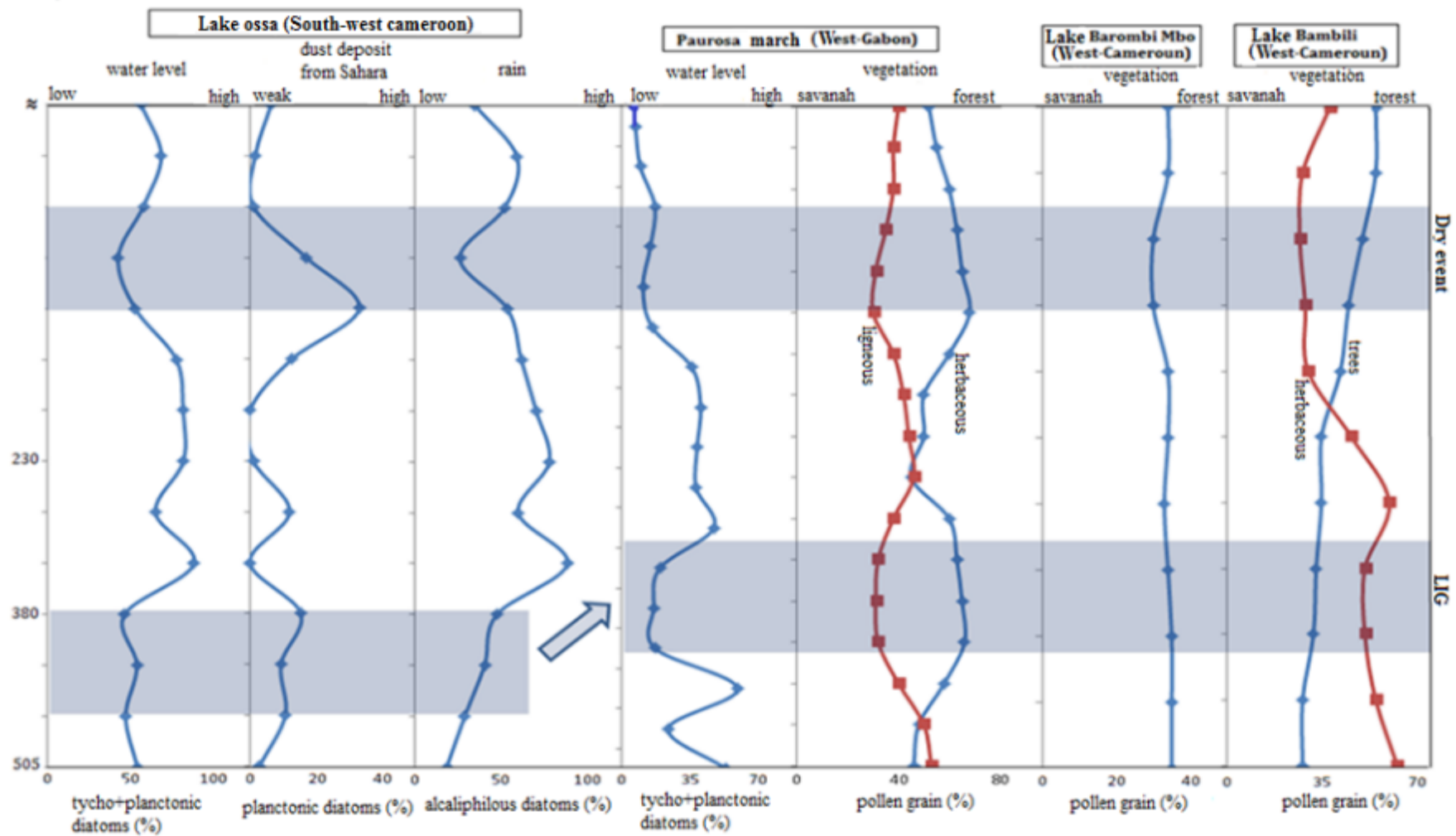


Figure VII.6. Comparison between Lake Ossa (South-West Cameroon), Paurosa Marsh (West Gabo), Lake Barombi Mbo (West Cameroon) and Bambili (West Cameroon): regional synthesis

Between 700-500 yrs BP., the percentages of planktonic and tychoplanktonic diatoms become relatively low compared to the previous period, with high abundances of benthic and aerophilic diatoms indicating a drop in lake levels and probably good water transparency. Multivariate analyses clearly individualize the diatom assemblages of this time slice, and show the ecological particularity (lower water level) of the lake conditions of this time slice. The abundance of aerophilic diatoms would also indicate a strengthening of the dry season, or dewatering on multi-year scales during which the reduction in lake area has allowed the development of these species in the edge areas. This time period, which is very marked by the drop in lake level, would correspond to the "Medieval Warming" recorded at several sites in Africa. For example, the sudden drop in water levels in Lake Chad (Maley, 2004), Lake Mbalang (Nguetsop et al., 2011) and the Paurosa Marsh (Kom et al., 2018) is recorded. At other sites in central Africa, palynological data indicate the presence of herbaceous savannahs at Mbalang and Gbali (Nguetsop et al., 2011; Sutra, 2013) or forest opening in Gabon (Ngomanda et al., 2009). In the regional climatic context, one can think of a shift in the average position of the ITCZ towards the south, and consequently a drop in average rainfall and a marked dry season around Lake Ngaoundaba. The decrease in Marine Surface Temperatures (MST) would be at the origin of the decrease in monsoon flow in the regions closer to the Gulf of Guinea during this period (Fontaine et al., 1998).

From 500 yrs BP., high abundances of acidophilic and oligotrophic tychoplankton + plankton are observed, sometimes associated with high values of epiphytic species (60 - 70 cm). At the same time, there is a mixing of the waters (probably by the winds) translated by considerable percentages of planktonic species. These data reflect a resumption of wet conditions and a higher and globally stable water column compared to the previous episode. This period of relative humidity was marked in other surrounding paleoecological sites (Gabon, Cameroon) by forest recolonisation. For example, in Mbalang (North Cameroon), the isotopic signature of $\delta^{13}\text{C}$ is mainly composed of trees ($\delta^{13}\text{C}$ between -30 ‰ and -21 ‰). At low-latitude sites in Gabon (Lakes Nguéné and Kamalété), Central African Republic (Lake Gbali) and Congo (Lakes Kitina, Mopo Mbai depression), increasingly higher percentages of dense forest taxa are recorded after 600 cal. BP in pollen diagrams (Elenga et al., 1996; Ngomanda et al., 2009; Sutra, 2013).

Around 400 yrs BP., diatoms record a low lake level associated with a decrease in water stability. At nearby sites (Gbali, Paurosa, Mbalang), this downward trend in water levels has also been recorded by several authors (Nguetsop et al., 2011; Kom et al., 2018).

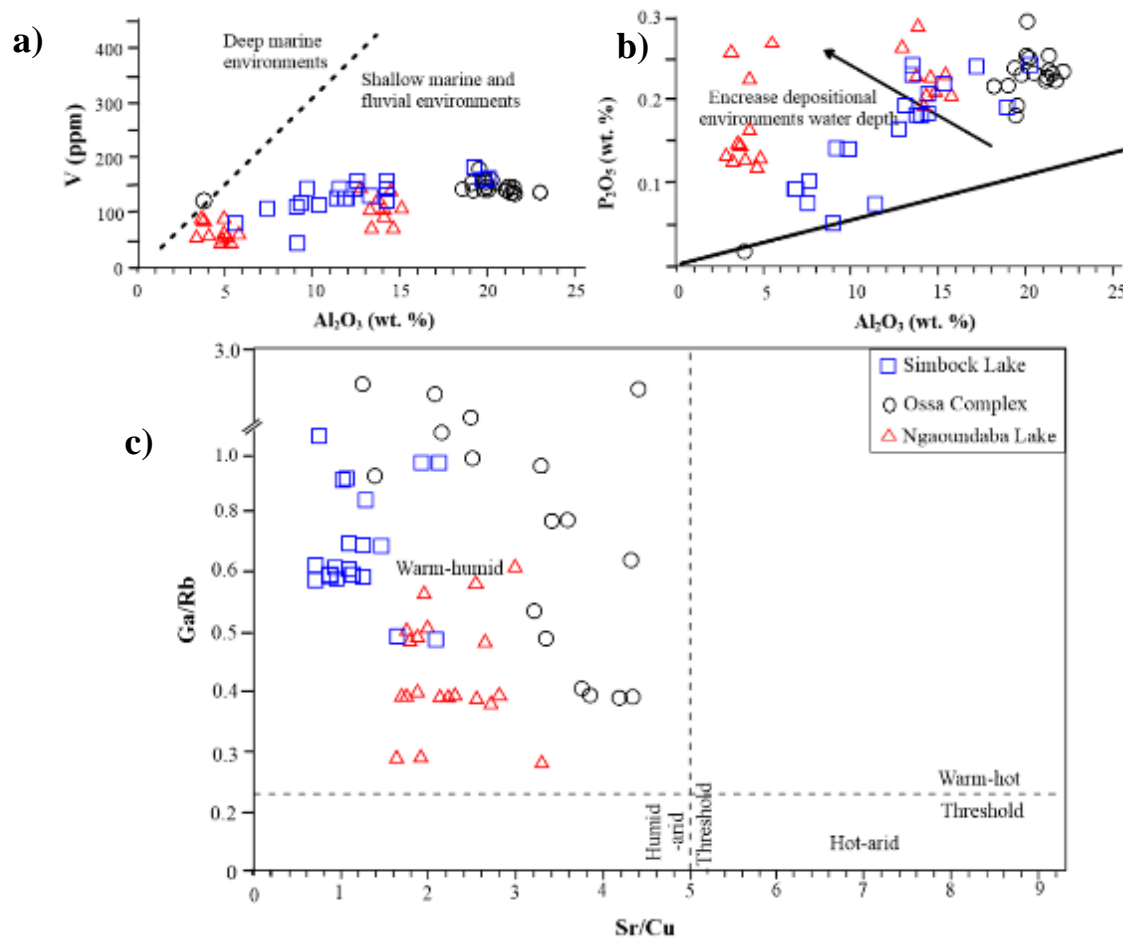


Figure VII.7. Plots of: **a)** V versus Al_2O_3 ; **b)** P_2O_5 versus Al_2O_3 and **c)** Sr/Cu versus Ga/Rb ratios in the studied lakes for paleoenvironmental reconstructions

In addition, pollen digrams indicate an increase in aquatic herbaceous pollens to the detriment of forest taxa in Nguéné and Kamalété (Ngomanda et al., 2009). From 155 yr BP., eutrophic water body was overgrown at the top the decrease in water increase in trophy associated which the appearance of peat patches in potentially more acidic condition. In this zone woodlands and *Syzygium* was also more frequent suggesting drier climatic conditions. The same information was recently described in a pollen sequence from Lake Assom (Ngos et al., 2003) and Lake Fonjak (N'anga et al., 2019) in the Adamaoua Plateau, North-Cameroon. These data reflect a relatively low water balance, which may be associated with climate degradation that has favored a decrease in the water slice. A decrease in the length of rainy seasons and harsh dry seasons (high evaporation) and/or a reduction in rainfall rates could be at the origin of the very low lake level observed in this time frame. However, the magnitude of the decrease in water level was not the same from one site to another. This phase of low lake level would be contemporary to a lacustrine episode highlighted in some sites such as Nguéné and Kamalété in Gabon under the name "Petit Age de Glace" (Little Ice Age).

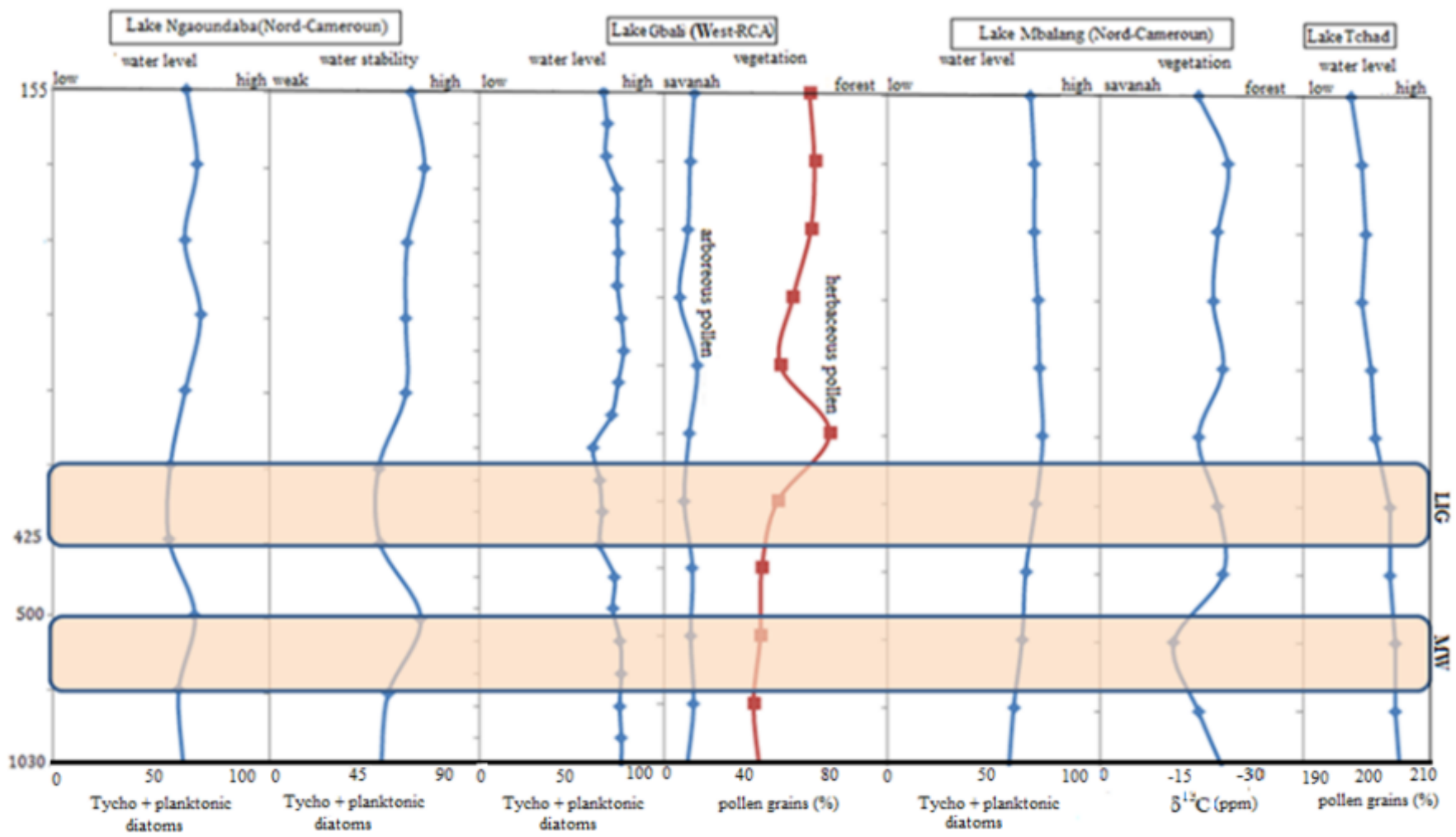


Figure VII.8. Comparison between Lake Ngaoundaba (North Cameroon), Lake Gbali (West-Central Africa), Lake Mbalang (North Cameroon) and Lake Chad: Regional Synthesis

Conclusion

The studied sediments from these areas have similar characteristics for some lakes and different characteristics for others. All the studied sediments have an arkosic signature, they are classified as litharenite, Fe-sands and Fe-shales. Most of the sediment samples studied have mature rock sources and intensely weathered rocks. The results interpretations showed that the studied sediments have diverse origins. They illustrate a mafic, a felsic and an intermediate signature. Almost all the studied sediments have been formed in a collision environment, these sediments have been formed in a passive margin. However, it should be noted that according to radiocarbon dating, the studied sediments are dated to the Holocene. They have been deposited in a shallow marine and fluvial depositional environments with an increase in depositional environments water depth environmental conditions are oxic with low salinity. When these sediments are deposited, the climate would be warm and humid.



*Conclusions and suggestions
for further studies*

My suffering may be the reason a person laughs but my laughter should never be the reason a person suffers.

-Albert Einstein-

This thesis focuses on a paleoenvironmental reconstruction over the last 1000 yrs BP. in three regions of Cameroon (Yaoundé, Dizanguè and Ngaoundéré) using a multiproxy approach including sedimentology, mineralogy, geochemistry. This was achieved by combining field work with a detailed description of lake sediments without neglecting the environmental status of some lakes. This thesis allowed us to refine our knowledge on the sedimentological and petrographic characteristics and recent history of sediments and tropical forests of Central Africa while coupling several disciplines of geosciences. Using lake sediments as tracers, it demonstrates that the dynamics of Cameroon's forest ecosystems have always been influenced by natural climatic variability. It corroborates and supports (in more detail) the climatic interpretations of geochemical and palynological data from other sites in this region and demonstrates that the current landscapes (e.g., the forest/savanna mosaic of the coastal region) of Cameroon are indeed the result of climate change over the last millennium.

The sediments from studied lakes of South and North of Cameroon has characteristics which vary from a lake to another but they are almost similar for some features. The artificial Simbock Lake at Yaoundé is shallow with 1.5 mean depth. The pile sediment is low in the center and low at the edge. The sediments from this lake are moderately humid with light brown to dark brown color. Grain sizes from the this shows high content of sands and clay which confer to the sediment a clayey sand texture. The sediment samples from this lake would have undergone a long fluvial transport with high content of organic matter. However, the Subduction lakes Complex Ossa at Dizangué are deep and goes over 10 m with a very large pile of sediments. These sediments are mixed with some organic matter and are quite humid. The color of these sediments varies generally from dark brown to dark with high proportion of silts and clays. The quartz grains shapes which are generally sub-rounded would have undergone a long fluvial transport and sometimes less confirming a physical and chemical alteration of the surrounding rocks and quite far away. Likewise, the Ngaoundaba Crater Lake located near the town of Ngaoundéré is deep, with up to 17 m in the middle with a large pile of very wet sediment. These sediments have a very high proportion of plant debris and the layer after the water is an herbaceous peat which favours a large percentage of organic matter. The overall dark pile of sediment consists of a high proportion of silt and moderate clay gives the sediment a clayey silt texture. The sand grains of this lake have sub-rounded shapes in the center of the lake and mainly subangular the edge. They are the result of aeolian and low turbulent transports.

The mineralogical content of studied lakes generally consists of quartz, kaolinite, Illite, feldspars, goethite, hematite and rutile with additional smectite and muscovite in Simbock Lake; smectite, zircon, gibbsite and some vivianite in Ossa sediments and calcite with traces of ilmenite in the Ngaoundaba Crater Lake. These lakes have moderate to high proportions of silica and alumina, this justifies the dominance of the quartz and the clay minerals in these samples. Similarly, the moderate titanium oxide and loss on ignition values could be justified by the presence of clay minerals. The presence of iron oxide is related to the presence of hematite and ilmenite while the rutile would be close to the fairly high titanium oxide values. Likewise, the high zirconium contents could suggest the presence of zircon in these materials. These sediments also contain high values of barium, vanadium and chromium. The studied sediments have a high fractionation of their source rocks. Negative Eu anomaly observed suggests several stages of weathering, these materials would therefore have undergone a remobilization and an intense weathering according to the chemical weathering indices. Furthermore, sediments from the selected lakes have low to moderate pollution.

All studied sediments have an arkosic signature however those from Simbock Lake are classified as litharenite, Fe-sands and Fe-shales while those from the Ossa Complex and Lake Ngaoundaba are shales and Fe-shales. Most of the sediment samples studied are mature with intensely weathered rocks from the surrounding catchments or along the supply's rivers, except those from central part of the Ngaoundaba Lake, which would be weakly to moderately weathered. However, sediments from Simbock Lake, Ossa Complex and some from Ngaoundaba Lake would be recycled, while most of the sediments from Ngaoundaba Lake would be derived from a compositional variation of basalts and granitoids. The Simbock Lake sediments illustrate a mafic to intermediate signature due to gneissic bedrock and probably a mafic protolith. The Ossa lakes Complex presents a felsic and intermediate source that are in agreement with the granito-gneissic bedrock without, neglecting the contribution of amphibolites. On the other hand, Ngaoundaba Lake at its western edge shows a mafic to intermediate signature confirmed by the geology of the study area consisting of granitoids and basalts with its products. However, the sediments from the center of the lake would be recycled and transported by the wind.

Palynological data from Lakes Simbock, Ossa and Ngaoundaba in Cameroon show that major hydrological changes have occurred over the last 1000 years, mainly characterized by strong fluctuations in wet and dry conditions during the "Medieval Warm Period" (1100-800 yrs BP.) and dry conditions during the "Little Ice Age" (500-300 yrs BP.). These hydrological

changes have controlled the dynamics of tropical rainforests in this part of Central Africa, resulting in expansion of tropical rainforest during periods of heavy rainfall and contraction during periods of reduced rainfall.

However, this thesis has led to undeniable progress on two levels. The first is that it clearly shows that tropical forests are also sensitive to short-lived climate changes, of the order of a decade to a century, and therefore defeats the idea that these ecosystems, because of the complexity of their tropical chains, have only reacted in the course of their history to climatic upheavals of great amplitude and intensity. This study therefore justifies the use of pollen data from tropical regions to reconstruct past climatic variations and to test the sensitivity of ecosystems with a view to future climate change.

The quantitative reconstruction of the evolution of the water balance over the last millennium shows that the inter-decadal variability of hydrological conditions plays a fundamental role in the functioning of ecosystems. High levels of rainfall with high inter-decadal variability act on the internal dynamics of dense humid forests by modifying the rate of renewal (sylvigenesis) of the forest cover, whereas a regular decrease in rainfall causes a change in the floristic composition.

It demonstrates, using lake sediments as tracers, that the dynamics of Cameroon's forest ecosystems have always been influenced by natural climatic variability. It corroborates and supports (in more detail) the climatic interpretations of geochemical and palynological data from other sites in this region and demonstrates that the current landscapes (e.g., the forest/savanna mosaic of the coastal region) of Cameroon are indeed the result of climate change over the last millennium.

The objective of this study was to carry out a paleoenvironmental reconstruction during the last 1000 yrs BP. in three regions of Cameroon (Yaoundé, Dizanguè and Ngaoundéré) using a multiproxy approach including sedimentology, geochemistry and mineralogy. This in other to retrace and compare their respective depositional environment and diagenetic processes. This objective has been attained but a further study of the lacustrine sediments from other lakes have to be done to have general information about the paleoenvironment in other to better understand the present and prevent further geological events. For further research, it is recommended that the study be extended to a longer time scale and a great number of lakes and core sediments.



References



Everybody knew it was impossible, until some idiot who didn't know it showed up and did it.

-Albert Einstein-

Abu, M., and Sunkari, E.D. (2020). Geochemistry and petrography of beach sands along the western coast of Ghana: implications for provenance and tectonic settings. *Turkish Journal of Earth Sciences*, 29(2), 363-380.

Adatte, T., Stinnesbeck, W., Keller, G., Ryder, G., Fastovsky, D., and Gartner, S. (1996). Lithostratigraphic and mineralogic correlations of near K/T boundary clastic sediments in northeastern Mexico: implications for origin and nature of deposition. *Geological Society of America. Special Paper*, 307, 211-226.

Adatte, T., Keller, G., and Stinnesbeck, W. (2002). Late Cretaceous to early Paleocene climate and sea-level fluctuations: the Tunisian record. *Palaeogeography, Palaeoclimatology, Palaeoecology*, 178(3-4), 165-196.

Ajeegah, G.A., Abanda, W.V.B., and Nkeng, G.E. (2017). An application of a water assessment and simulation model in the remediation of the eutrophication capacity of a tropical water system: Case study the Lake Obili in Yaounde (Cameroon). *Journal of Water and Land Development*, 33(1), 11-22.

Anaya-Gregorio, A., Armstrong-Altrin, J.S., Machain-Castillo, M.L., Montiel-García, P.C., and Ramos-Vázquez, M.A. (2018). Textural and geochemical characteristics of late Pleistocene to Holocene fine-grained deep-sea sediment cores (GM6 and GM7), recovered from southwestern Gulf of Mexico. *Journal of Palaeogeography*, 7(1), 3.

Armstrong-Altrin, J.S., Lee, Y.I., Verma, S.P., and Ramasamy, S. (2004). Geochemistry of sandstones from the Upper Miocene Kudankulam Formation, southern India: implications for provenance, weathering, and tectonic setting. *Journal of Sedimentology Research*, 74, 285–297.

Armstrong-Altrin, J.S., Nagarajan, R., Balaram, V., and Natalhy-Pineda, O. (2015). Petrography and geochemistry of sands from the Chachalacas and Veracruz beach areas, western Gulf of Mexico, Mexico: constraints on provenance and tectonic setting. *Journal of South American Earth Sciences*, 64, 199-216.

Armstrong-Altrin, J.S., and Machain-Castillo, M.L. (2016). Mineralogy, geochemistry, and radiocarbon ages of deep sea sediments from the Gulf of Mexico, Mexico. *Journal of South American Earth Science*, 71, 182–200.

Armstrong-Altrin, J.S., Lee, Y.I., Kasper-Zubillaga, J.J., and Trejo-Ramírez, E. (2017). Mineralogy and geochemistry of sands along the Manzanillo and El Carrizal beach areas southern Mexico: implications for palaeoweathering, provenance and tectonic setting. *Geological Journal*, 52, 559–582.

Armstrong-Altrin, J.S., Ramos-Vázquez, M.A., Zavala-León, A.C., and Montiel-García, P.C. (2018). Provenance discrimination between Atasta and Alvarado beach sands, western Gulf of Mexico, Mexico: Constraints from detrital zircon chemistry and U–Pb geochronology. *Geological Journal*, 53, 2824–2848.

Armstrong-Altrin, J.S., Botello, A. V., Villanueva, S.F., and Soto, L.A. (2019). Geochemistry of surface sediments from the northwestern Gulf of Mexico: implications for provenance and heavy metal contamination. *Geological Quarterly*, 63(3), 522-538.

- Asaah, A.N., Yokoyama, T., Aka, F.T., Usui, T., Kuritani, T., Wirmvem, M.J., and Ohba, T. (2015). Geochemistry of lavas from maar-bearing volcanoes in the Oku Volcanic Group of the Cameroon Volcanic Line. *Chemical Geology*, 406, 55-69.
- Assi-Kaudjhis, C., Lézine, A.M., and Roche, E. (2008). Dynamique de la végétation d'altitude en Afrique centrale atlantique depuis 17000 ans BP. Analyses préliminaires de la carotte de Bambili (Nord-Ouest du Cameroun). *Geo-Eco-Trop*, 32, 131-143.
- Bachelier, G., and Laplante, A. (1953). On the origin and the formation of so-called lateritic breastplates in Adamawa (North Cameroon). *Comptes Rendus de l'Académie des Sciences*, 237(20), 1277-1279.
- Bagnouls F., and Gaussen, H. (1957). Biological climates and their classification. *American Geography*. XXVI, 193-220.
- Bahanak, D.N.D., Nack, J., Pariselle, A., and Bilong Bilong, C.F. (2016). Description of three new species of *Quadriacanthus* (Monogenea: Ancyrocephalidae) gill parasites of *Clarias submarginatus* (Siluriformes: Clariidae) from Lake Ossa (Littoral region, Cameroon). *Zoologia*, 33(4).
- Bal Akkoca, D., Eriş, K.K., Çağatay, M.N., and Biltekin, D. (2019). The mineralogical and geochemical composition of Holocene sediments from Lake Hazar, Elazığ, Eastern Turkey: implications for weathering, paleoclimate, redox conditions, provenance, and tectonic setting. *Turkish Journal of Earth Sciences*, 28(5).
- Bayly, I.A.E., and Williams, W.D. (1973). *Inland waters and their ecology*. Longman Publishing Group.
- Beaudoin, A. (2014). *Paleoenvironmental reconstruction of the Nettilling Lake region, (Nunavut): a multi-proxy analysis (Doctoral dissertation, Université Laval)*.
- Benayad, S., Park, Y.S., Chaouchi, R., and Kherfi, N. (2013) Parameters controlling the quality of the Hamra Quartzite reservoir, southern Hassi Messaoud, Algeria: insights from a petrographic, geochemical, and provenance study. *Arabian Journal of Geosciences*.
- Benkhelil, J., Giresse, P., Poumot, C., and Nguetchoua, G. (2002). Lithostratigraphic, geophysical and morpho-tectonic studies of the South Cameroon shelf. *Marine and Petroleum Geology*, 19(4), 499-517.
- Berthois, L., 1975. *Les roches sédimentaires*. Paris, 1 : étude sédimentologique des roches meubles (techniques et méthodes), 278 p.
- Bessoles, B. (1969). Simplified synthesis of knowledge on the Geology of Cameroon. *Bulletin de la Direction des Mines et de la Géologie*, (5).
- Bhatia, M. R. (1983). Plate tectonics and geochemical composition of sandstones. *The Journal of Geology*, 91(6), 611-627.
- Bhuiyan, M.A., Rahman, J.J., Dampare, S.B., and Suzuki, S. (2011). Provenance, tectonics and source weathering of modern fluvial sediments of the Baahmaputra-Jamuna River, Bangladesh: inference from geochemistry. *Journal of Geochemical Exploration*, 111, 113–137.

- Björck, S., and Wohlfarth, B. (2002). 14 C chronostratigraphic techniques in paleolimnology. In *Tracking environmental change using lake sediments*. Springer, Dordrecht, 205-245.
- Boutrais, J. (1998). Bulls in western Cameroon. Bulls and men, eds. C. Seignobos and E. Thys, 313-326. Paris: Orstom.
- Brindley, G.W., and Brown, G. (1980). Quantitative X-ray mineral analysis of clays. Crystal structures of clay minerals and their X-ray identification, 5, 411-438.
- Burnham, O.M., and Schweyer, J. (2004). Trace element analysis of geological samples by ICP-MS at the Geoscience Laboratories: Revised capabilities due to improvements to instrumentation. Summary of field work and other activities, 54-71.
- Calmano, W., Forstner, U., and Hong, J. (1994). Mobilization and scavenging of heavy metals following resuspension of anoxic sediments from the Elbe River, American Chemical Society; Washington D.C. ACS Symposium Series, 550, 298-321.
- Calmano, W., Hong, J., and Förstner, U. (1993). Binding and mobilization of heavy-metals in contaminated sediments affected by pH and redox potential. *Water Science and Technology* 28, 223-235.
- Cao, L., Bala, G., and Caldeira, K. (2012). Climate response to changes in atmospheric carbon dioxide and solar irradiance on the time scale of days to weeks. *Environmental Research Letters*, 7(3), 034015.
- Chairi, R. (2005). Study of the sedimentary filling of a hypersaline system from eastern Tunisia during the recent quaternary: the Moknine sebkha. *Quaternary. Journal of the French Association for the Study of the Quaternary*, 16 (2), 107-117.
- Chairi, R. (2005). Study of the sedimentary filling of a hypersaline system from eastern Tunisia during the recent quaternary: the Moknine sebkha. *Quaternary. Journal of the French Association for the Study of the Quaternary*, 16 (2), 107-117.
- Chamley H. (2000). *Bases de sédimentologie (2ème Edition)*. Ed. Dunod, Paris, pp. 178 CNR. (2005). *Analyse de l'impact des dragages du Rhône au regard de la qualité physico-chimique des sédiments. Rapport Technique*, CNR, 102 p.
- Chen, M., Sun, M., Cai, K., Buslov, M.M., Zhao, G., and Rubanova, E.S. (2014). Geochemical study of the Cambrian-Ordovician meta-sedimentary rocks from the northern Altai-Mongolian terrane, northwestern Central Asian Orogenic Belt: Implications on the provenance and tectonic setting. *Journal of Asian Earth Sciences*, 96, 69-83.
- Cohen, A.S., Lezzar, K.E., Cole, J., Dettman, D., Ellis, G.S., Gonneea, M.E., and Zilifi, D. (2006). Late Holocene linkages between decade-century scale climate variability and productivity at Lake Tanganyika, Africa. *Journal of Paleolimnology*, 36(2), 189-209.
- Cojan, I., and Renard, M. (2013). *Sedimentology-3rd edition*. Dunod.
- Condie, K.C. (1993). Chemical composition and evolution of the upper continental crust: contrasting results from surface samples and shales. *Chemical Geology*, 104(1-4), 1-37.

Cox, R., Lowe, D.R., and Cullers, R.L. (1995). The influence of sediment recycling and basement composition on evolution of mudrock chemistry in the southwestern United States. *Geochimica et Cosmochimica Acta*, 59(14), 2919-2940.

Cullers, R.L. (2000). The geochemistry of shales, siltstones and sandstones of Pennsylvanian–Permian age, Colorado, USA: implications for provenance and metamorphic studies. *Lithos*, 51(3), 181-203.

Das, B.K., Al-Mikihlafi, A.S., and Kaur, P. (2006). Geochemistry of Mansar lake sediments, Jammu, India: implication for source-area weathering, provenance, and tectonic setting. *J. Asian Earth Sci.* 26, 640–668.

De Martonne E. (1942). New world map of aridity. *Annal of Géography*, 241-250.

Debret, B., Koga, K.T., Nicollet, C., Andreani, M., and Schwartz, S. (2014). F, Cl and S input via serpentinite in subduction zones: implications for the nature of the fluid released at depth. *Terra Nova*, 26(2), 96-101.

Delachet, A. (1960). *Logarithms*. University press in France.

Demanou, J., and Brummett, R.E. (2003). Heavy metal and faecal bacterial contamination of urban lakes in Yaoundé, Cameroon. *Food Africa*, 5-9.

Dimon, F., Dovonou, F., Adjahossou, N., Chouti, W., Mama, D., Alassane, A., and Boukari, M. (2014). Physico-chemical characterization of Lake Ahémé (South Benin) and highlighting of sediment pollution by lead, zinc and arsenic. *Journal of Society of West-African Chemistry*, 37, 36-42.

Djoufack V. (2011) Multi-scale rainfall and vegetation cover study in Cameroon: Spatial analyses, temporal trends, climatic and anthropogenic factors of NDVI variability, *Université de Bourgogne*, 322 p.

Donfack, P., Moukouri-Kuoh, H., Mainam, F., Seyni-Boukar, L., Abega, R., Ayangma, A. and Carré, P. (1988). Use and conservation of soil and water resources (North Cameroon): final report.

Dongmo, J. L. (1981). *The Bamileke dynamism*. 2 vol. Cameroon: University of Yaounde.

Egozcue, J. J., Pawlowsky-Glahn, V., Mateu-Figueras, G., and Barcelo-Vidal, C. (2003). Isometric logratio transformations for compositional data analysis. *Mathematical Geology*, 35(3), 279-300.

Ekengele, L. N., Blaise, A., and Jung, M.C. (2017). Accumulation of heavy metals in surface sediments of Lere Lake, Chad. *Geosciences Journal*, 21(2), 305-315.

Ekengele, L.N., Baussand, P., and Ekodeck, E.G. (2012). Heavy Metals accumulation in sediment cores of the Municipal Lake of Yaounde, Cameroon. *Global Journal of Environmental Research* 6(3), 100–110.

Ekoka Bessa, A.Z., Nguetchoua, G., and Ndjigui, P.D., 2018, Mineralogy and geochemistry of sediments from Simbock Lake, Yaoundé area (southern Cameroon): Provenance and environmental implications. *Arabian Journal of Geosciences*, 11, 710.

- Elenga, H., and Vincens, A. (1990). Recent quaternary paleoenvironments of the Batéké plateaus (Congo): palynological study of the deposits of the Bilanko wood depression. In *Quaternary Landscapes of Atlantic Central Africa*, 271-282.
- Eno Belinga, S.M. (1984). *Geology of Cameroon: introduction to external Geodynamic, historical geology, petroleum geology; for the use of undergraduate students*. University library.
- Eyong, J.T., Wignall, P., Fantong, W.Y., Best, J., and Hell, J.V. (2013). Paragenetic sequences of carbonate and sulphide minerals of the Mamfe Basin (Cameroon): Indicators of palaeo-fluids, palaeo-oxygen levels and diagenetic zones. *Journal of African Earth Sciences*, 86, 25-44.
- Fadil-Djenabou, S., Ndjigui, P.D., Mbey, J.A. (2015). Mineralogical and physicochemical characterization of Ngaye alluvial clays (Northern Cameroon) and assessment of its suitability in ceramic production. *Journal of Asian Ceramic Societies* 3(1), 50–58.
- Fedo, C.M., Wayne Nesbitt, H., and Young, G.M. (1995). Unraveling the effects of potassium metasomatism in sedimentary rocks and paleosols, with implications for paleoweathering conditions and provenance. *Geology*, 23(10), 921-924.
- Fedo, C.M., Young, G.M., Nesbitt, H.W., Hanchar, J.M. (1997). Potassic and sodic metasomatism in the Southern Province of the Canadian Shield: evidence from the Paleoproterozoic Serpent Formation Huronian Supergroup, Canada. *Precambrian Res.* 84, 17–36.
- Fezeu, W.M.L., Ngassoum, M.B., Montarges-Pelletier, E., Echevarria, G., and Mbofung, C.M.F. (2009). Physicochemical characteristics of Lake IRAD, an artificial lake in Wakwa region, Cameroon. *Lakes and Reservoirs: Research and Management*, 14(3), 259-268.
- Folk, R.L. (1980). *Petrology of sedimentary rocks*, Hemphills, Austin, 182 p.
- Food and Agriculture Organization of the United Nations, and Diekmann, M. (1995). *FAO/IPGRI technical guidelines for the safe movement of germplasm*. FAO.
- Forel, F.A. (1892). *Limnological monography*. F. Rouge, Lausanne, 3 vol., T.1, 543 p.
- Fotsing, J.M. (1995). *Land competition and land use strategies in Bamileke country (Cameroon)*. Land, terroir, land tensions. Paris: Orstom éditions.
- Foucault, A., and Raoult, J.F. (1995). *Geology Dictionary*.
- Freeth, S.J. (1990). Lake Bambuluwe: Could it be the source for a third gas disaster in western Cameroon?. *Journal of volcanology and geothermal research*, 42, 393-395.
- Frost, B.R., Barnes, C.G., Collins, W.J., Arculus, R.J., Ellis, D.J., and Frost, C.D. (2001). A geochemical classification for granitic rocks. *Journal of petrology*, 42(11), 2033-2048.
- Giguet-Covex, C. (2010). *Contribution of laminated lake sediments to the study of environmental changes Holocene: high resolution sedimentological / geochemical coupled approach: application to two northern alpine lakes (Doctoral dissertation, Chambéry)*.
- Giresse, P., Maley, J., and Kossoni, A. (2005). Sedimentary environmental changes and millennial climatic variability in a tropical shallow lake (Lake Ossa, Cameroon) during the Holocene. *Palaeogeography, Palaeoclimatology, Palaeoecology*, 218(3-4), 257-285.

- Giresse, P., Ngos, S., and Pourchet, M. (1994). Secular sedimentary processes and geochronology at 210 Pb of the main lakes of the Cameroon ridge. *Bulletin of the Geological Society of France*, 165 (4), 363-380.
- Graf Jr, J.L. (1984). Effects of Mississippi Valley-type mineralization on REE patterns of carbonate rocks and minerals, Viburnum Trend, southeast Missouri. *The Journal of Geology*, 92(3), 307-324.
- Green, J. (1972). Ecological studies on crater lakes in West Cameroon zooplankton of Barombi Mbo, Mboandong, Lake Kotto and Lake Soden. *Journal of Zoology*, 166(3), 283-301.
- Gufler, H.J. (2009). Reenactment of a Myth. The Fon of Oku Visits Lake Mawes (Cameroon). *Anthropos*, 347-357.
- Harnois, L. (1988). The CIW index: a new chemical index of weathering. *Sedimentary geology*, 55, 319-322.
- Hayashi, K.I., Fujisawa, H., Holland, H.D., and Ohmoto, H. (1997). Geochemistry of ~ 1.9 Ga sedimentary rocks from northeastern Labrador, Canada. *Geochimica and Cosmochimica Acta*, 61(19), 4115-4137.
- Hedges, J.I., and Oades, J.M. (1997). Comparative organic geochemistries of soils and marine sediments. *Organic geochemistry*, 27(7-8), 319-361.
- Hernández-Hinojosa, V., Montiel-García, P.C., Armstrong-Altrin, J.S., Nagarajan, R., and Kasper-Zubillaga, J.J. (2018). Textural and geochemical characteristics of beach sands along the western Gulf of Mexico, Mexico. *Carpathian Journal of Earth Environment Science*, 13(1), 161-174.
- Herron, M.M. (1988). Geochemical classification of terrigenous sands and shales from core or log data. *Journal of Sedimentary Research*, 58(5), 820-829.
- Hofmann, A., 2005. The geochemistry of sedimentary rocks from the Fig Tree Group, Barberton green stone belt: implications for tectonic, hydrothermal and surface processes during mid-Archaean times. *Precambrian Research*, 143, 23-49.
- Ineris (2006) Toxicological and environmental data sheet for chemical substances, Nickel and its inorganic derivatives. National Institute for the Industrial Environment and Risks, Paris. 14 p. Jamagne J., 1967. Base et techniques d'une cartographie des sols. *Annal of Agronomy* 18, 142 p.
- Iwuoha, G.N., and Osuji, L.C. (2012). Changes in Surface Water Physico-Chemical Parameters following the Dredging of Otamiri and Nworie Rivers, Imo State of Nigeria. *Research Journal of Chemical Sciences*, ISSN, 2231, 606X.
- Jacob, J. (2003). Recording of paleoenvironmental variations for 20,000 years in the North East of Brazil (Lake Caço) by triterpenes and other organic markers (Doctoral dissertation).
- Joly, R., and Assako, A. (2001). Formulation et validation d'une hypothèse de pollution de l'eau de surface: Le cas du lac municipal de Yaoundé. *Déchets sciences and techniques*, (23), 35-38.

- Jones, B., and Manning, D.A. (1994). Comparison of geochemical indices used for the interpretation of palaeoredox conditions in ancient mudstones. *Chemical geology*, 111(1-4), 111-129.
- Jouve, S., Bouya, B., Amaghaz, M., and Meslough, S. (2015). *Maroccosuchus zennaroi* (Crocodylia: Tomistominae) from the Eocene of Morocco: phylogenetic and palaeobiogeographical implications of the basalmost tomistomine. *Journal of Systematic Palaeontology*, 13(5), 421-445.
- Kamtchueng, B.T., Fantong, W.Y., Wirmvem, M.J., Tiodjio, R.E., Takounjou, A.F., Ngoupayou, J.R.N., and Hell, J.V. (2016). Hydrogeochemistry and quality of surface water and groundwater in the vicinity of Lake Monoun, West Cameroon: approach from multivariate statistical analysis and stable isotopic characterization. *Environmental monitoring and assessment*, 188(9), 524.
- Kaotekwar, A. B., Ahmad, S. M., Satyanarayanan, M., and Krishna, A. K. (2019). Geochemical investigations in bulk and clay size fractions from lower Krishna river sediments, southern India: implications of elemental fractionation during weathering, transportation and deposition. *Geosciences Journal*, 1-10.
- Kasanzu, C., Maboko, M.A., and Manya, S. (2008). Geochemistry of fine-grained clastic sedimentary rocks of the Neoproterozoic Ikorongo Group, NE Tanzania: Implications for provenance and source rock weathering. *Precambrian Research*, 164(3-4), 201-213.
- Kling, G.W. (1988). Comparative transparency, depth of mixing, and stability of stratification in lakes of Cameroon, West Africa 1. *Limnology and Oceanography*, 33(1), 27-40.
- Korte, N.E., Skopp, J., Fuller, W.H., Niebla, E.E., and Alesii, B.A. (1976). Trace element movement in soils: influence of soil physical and chemical properties. *Soil Science*, 122(6), 350-359.
- Kossoni, A. (2003). Sedimentary processes of Lake Ossa (Dizangué, South West Cameroon) and holocene paleoclimatic evolution. These of Doctorate, University of Perpignan, Perpignan, France.
- Kossoni, A. (2003). Sedimentary processes of Lake Ossa (Dizangué, southwest Cameroon) and holocene paleoclimatic evolution for 9,000 years BP (Doctoral dissertation, Doctoral thesis, University of Perpignan, France, 221 p.
- Kossoni, A., and Giresse, P. (2010). Interaction of Holocene infilling processes between a tropical shallow lake system (Lake Ossa) and a nearby river system (Sanaga River)(South Cameroon). *Journal of African Earth Sciences*, 56(1), 1-14.
- Kuete, M. (1990). The quaternary paleoforms of southern Cameroon forest. Lanfranchi and Schwartz éd. : The quaternary landscapes of Atlantic central Africa. Didactiques ORSTOM, Paris, 161-166.
- Kusakabe, M., Ohba, T., Yoshida, Y., Satake, H., Ohizumi, T., Evans, W.C., and Kling, G.W. (2008). Evolution of CO₂ in Lakes Monoun and Nyos, Cameroon, before and during controlled degassing. *Geochemical Journal*, 42(1), 93-118.

- Kusakabe, M., Ohsumi, T., and Aramaki, S. (1989). The Lake Nyos gas disaster: chemical and isotopic evidence in waters and dissolved gases from three Cameroonian crater lakes, Nyos, Monoun and Wum. *Journal of volcanology and geothermal research*, 39(2-3), 167-185.
- Kuscu, M., Cengiz, O., and Kahya, A. (2018). Mineralogy and Geochemistry of Sedimentary Huntite Deposits in the Egirdir-Hoyran Lake Basin of Southern Turkey. *Journal of the Geological Society of India*, 91(4), 496-504.
- Lambert, P. (1997). Sedimentation in Lake Neuchâtel (Switzerland) (Doctoral dissertation, University of Neuchâtel).
- Lebamba, J., Vincens, A., and Maley, J. (2010). Pollen, biomes, forest successions and climate at Lake Barombi Mbo (Cameroon) during the last ca. 33 000 cal yr BP--a numerical approach. *Climate of the Past Discussions*, 6(6).
- Lebamba, J., Vincens, A., and Maley, J. (2012). Pollen, vegetation change and climate at Lake Barombi Mbo (Cameroon) during the last ca. 33 000 cal yr BP: a numerical approach. *Climate of the Past*, 8(1), 59.
- Lebamba, J., Vincens, A., Buchet, G., and Lézine, A.M. (2012). Vegetation dynamics during the last 4000 years in the Adamawa plateau (central Cameroon): a high-resolution pollen record from Lake Tizong.
- Lebamba, J., Vincens, A., Lézine, A.M., Marchant, R., and Buchet, G. (2016). Forest-savannah dynamics on the Adamawa plateau (Central Cameroon) during the “African humid period” termination: A new high-resolution pollen record from Lake Tizong. *Review of Palaeobotany and Palynology*, 235, 129-139.
- Lesven, L. (2008). Becoming trace metallic elements within the sediment: a key compartment of the aquatic environment (Doctoral dissertation, Lille 1).
- Letouzey, R. (1985). A record of the phytogeographical map of Cameroon at 1:500 000. Domain of the evergreen dense rainforest. *Institut de la Carte Internationale de la Végétation, Toulouse*, 63-142.
- Lévêque, C. (1996). Aquatic ecosystems.
- Liéno, G., Mahé, G., Olivry, J.C., Naah, E., Paturel J.E, Servat, E., Lubès-Niel H., Sighomnou, D., Ekodeck, G.E., Dezetter A. (2005) Changement des régimes hydrologiques des rivières du sud-Cameroun : un impact de la variabilité climatique en zone équatoriale. In : *Regional Hydrological impacts of Climatic Change–Hydroclimatic Variability. Proceedings of symposium S6 held during the Seventh IAHS Scientific Assembly at Foz do Iguaçu, Brazil, April 2005* (ed. by : Franks S., Wagener T., Bøgh E., Gupta H.V., Bastidas L. and Nobre C. and Oliveira Galvão C.), 158-168, IAHS publication, 296.
- Lisk, D.J. (1972). Trace metals in soils, plants, and animals. In *Advances in Agronomy* (Vol. 24, pp. 267-325). Academic Press.
- Lone, A., Babeesh, C., Achyuthan, H., Chandra, R. (2017). Evaluation of environmental status and geochemical assessment of sediments, Manasbal Lake, Kashmir, India. *Arabian Journal of Geosciences* 10(4), 92–110.

- Loska, K., Cebula, J., Pelczar, J., Wiechula, D., and Kwapuliński, J. (1997). Use of enrichment, and contamination factors together with geoaccumulation indexes to evaluate the content of Cd, Cu, and Ni in the Rybnik water reservoir in Poland. *Water, Air, and Soil Pollution*, 93(1-4), 347-365.
- Lowe, J.J., and Walker, M.J.C. (1997). Temperature variations in NW Europe during the last glacial-interglacial transition (14-9 ¹⁴C ka BP) based upon the analysis of coleopteran assemblages-the contribution of Professor GR Coope. In *Quaternary Proceedings*, 165-176.
- Mack, G.H., and Rasmussen, K.A. (1984). Alluvial-fan sedimentation of the Cutler Formation (Permo-Pennsylvanian) near Gateway, Colorado. *Geological Society of America Bulletin*, 95(1), 109-116.
- Madhavaraju, J., and Lee, Y. I. (2009). Geochemistry of the Dalmiapuram Formation of the Uttatur Group (Early Cretaceous), Cauvery basin, southeastern India: Implications on provenance and paleo-redox conditions. *Revista Mexicana de Ciencias Geológicas*, 26(2), 380-394.
- Madhavaraju, J., Saucedo-Samaniego, J.C., Löser, H., Espinoza-Maldonado, I.G., Solari, L., Monreal, R., and Jaques-Ayala, C. (2019). Detrital zircon record of Mesozoic volcanic arcs in the Lower Cretaceous Mural Limestone, northwestern Mexico. *Geological Journal*, 54(4), 2621-2645.
- Mahaney, W.C., Vortisch, W., and Julig, P.J. (1988). Relative differences between glacially crushed quartz transported by mountain and continental ice; some examples from North America and East Africa. *American Journal of Science*, 288(8), 810-826.
- Mahaney, W.C. (2002). *Atlas of sand grain surface textures and applications*. Oxford University Press, USA.
- Mahop, F., Van Ranst, E., and Boukar, S. (1995). Influence of land use on the effectiveness of rains in North Cameroon. *Study. Soils Gestion*, 2 (2), 105-117.
- Marques, R., Prudêncio, I.M., Rocha, F. (2011). Patterns of rare earth and other trace elements in different size fractions of clays of Campanian-Maastrichtian deposits from the Portuguese western margin (Aveiro and Taveiro formations). *Chemie der Erde-Geochemistry*, 71, 337-347.
- Martin, C.H. (2012). Weak disruptive selection and incomplete phenotypic divergence in two classic examples of sympatric speciation: Cameroon crater lake cichlids. *The American Naturalist*, 180(4), E90-E109.
- Martin, C.H., Cutler, J.S., Friel, J. P., Denning Touokong, C., Coop, G., and Wainwright, P.C. (2015). Complex histories of repeated gene flow in Cameroon crater lake cichlids cast doubt on one of the clearest examples of sympatric speciation. *Evolution*, 69(6), 1406-1422.
- Martin, D. (1961). *Soil Map of North Cameroon at 1/100.00 th Mora leaf*. ORSTOM-IRCAM, Yaoundé, Cameroon.
- Mbey, J. A., Thomas, F., Sabouang, C.N., and Njopwouo, D. (2013). An insight on the weakening of the interlayer bonds in a Cameroonian kaolinite through DMSO intercalation. *Applied clay science*, 83, 327-335.

- McDonough, W.F., and Sun, S.S. (1995). The composition of the Earth. *Chemical geology*, 120(3-4), 223-253.
- McLennan, S.M. (1989). Rare earth elements in sedimentary rocks: influence of provenance and sedimentary processes. In: Lipin, B.R., McKay, G.A. (Eds.), *Geochemistry and Mineralogy of Rare Earth Elements*. Mineral Society of America. 21, 169–200.
- McLennan, S.M., Taylor, S.R., McCulloch, M.T., and Maynard, J.B. (1990). Geochemical and Nd/Sr isotopic composition of deep-sea turbidites: crustal evolution and plate tectonic associations. *Geochimica et Cosmochimica Acta*, 54(7), 2015-2050.
- McLennan, S.M., Hemming, S., McDaniel, D.K., Nanson, G.N. (1993). Geochemical approaches to sedimentation, provenance, and tectonics. In: Johnsson, M.J., Basu, A. (Eds.), *Processes Controlling the Composition of Clastic Sediments*: Boulder, Colorado. Geological Society of America, Special Publications 284, 21–40.
- Meng, Q.T., Liu, Z.J., Hu, F., Sun, P.C., Zhou, R.J. and Zhen, Z. (2012). Productivity of Eocene ancient lake and enrichment mechanism of organic matter in Huadian Basin. *Journal of China University of Petroleum*, 36/5, 38-44.
- Michaels, C.J., Tapley, B., Harding, L., Bryant, Z., Grant, S., Sunter, G., and Doherty-Bone, T. (2015). Breeding and rearing the critically endangered lake Oku clawed frog (*Xenopus longipes* Loumont and Kobel 1991). *Amphibian and Reptile Conservation*, 9(2), 100-110.
- Michaels, C.J., Tapley, B., Harding, L., Bryant, Z., Grant, S., Sunter, G., and Doherty-Bone, T. (2015). Breeding and rearing the critically endangered lake Oku clawed frog (*Xenopus longipes* Loumont and Kobel 1991). *Amphibian and Reptile Conservation*, 9(2), 100-110.
- Mimpfoundi, R., and Ndassa, A. (2006). Morphological studies on *Bulinus* sp. (Gastropoda: Planorbidae) from Nchout Monoun, Cameroon *African Zoology*, 41(2), 210-214.
- Anonymous. (2010). *Growth and Employment Strategy Paper*, Yaounde: Anonymous.
- Moore, D.M., and Reynolds Jr, R. C. (1989). *X-ray Diffraction and the Identification and Analysis of Clay Minerals*. Oxford University Press (OUP).
- Moradi, A.V., Sari, A., and Akkaya, P. (2016). Geochemistry of the Miocene oil shale (Hançili Formation) in the Çankırı-Çorum Basin, Central Turkey: Implications for Paleoclimate conditions, source–area weathering, provenance and tectonic setting. *Sedimentary Geology*, 341, 289-303.
- Morin, S. (1981). The current evolution of natural environments in central and western Cameroon. *Works of the Reims Geographic Institute Reims*, (45-46), 117-139.
- Mortazavi, M., Moussavi-Harami, R., Mahboubi, A., and Nadjafi, M. (2014). Geochemistry of the Late Jurassic–Early Cretaceous shales (Shurijeh Formation) in the intracontinental Kopet Dagh Basin, northeastern Iran: implication for provenance, source weathering, and paleoenvironments. *Arabian Journal of geosciences*, 7(12), 5353-5366.
- Müller G. (1969). Index of geoaccumulation in sediments of the rhine River, *Geojournal*, 2, 109-118.

Munsell Color, (2000) Munsell Soil Color Charts. U.S. Department of Agriculture Handbook 18-Soil Survey Manual.

Munsell. (1975). Soil color charts. Munsell color.

Musilová, Z., Indermaur, A., Nyom, A.R.B., Tropek, R., Martin, C., and Schliewen, U.K. (2014). Persistence of *Stomatepia mongo*, an endemic cichlid fish of the Barombi Mbo crater lake, southwestern Cameroon, with notes on its life history and behavior. *Copeia*, 2014(3), 556-560.

N'anga A., Simon III, N., and Gabriel, N. (2019). The late Pleistocene–Holocene paleoclimate reconstruction in the Adamawa plateau (Central Cameroon) inferred from the geochemistry and mineralogy of the Lake Fonjak sediments. *Journal of African Earth Sciences*, 150, 23-36.

Naah, M. (2013). Impact of the urban development of the Mingoa river watershed on the municipal lake of Yaoundé (Cameroon) (Doctoral dissertation).

Nack, J., Nyom, A.B., Pariselle, A., and Bilong, C.B. (2016). New evidence of a lateral transfer of monogenean parasite between distant fish hosts in Lake Ossa, South Cameroon: the case of *Quadriacanthus euzeti* n. sp. *Journal of helminthology*, 90(4), 455-459.

Naeher, S., Gilli, A., North, R.P., Hamann, Y., and Schubert, C.J. (2013). Tracing bottom water oxygenation with sedimentary Mn/Fe ratios in Lake Zurich, Switzerland. *Chemical Geology*, 352, 125-133.

Ndjama, J., Ajeegah, G.A., Nkoue, N.G.R., Jude, W.M., Birama, N.E.B., Eyong, G.E.T., and Hell, J.V. (2017). Physico-Chemical and Biological Characteristics of the Nklobisson Artificial Lake in Yaounde, Cameroon. *Journal of Water Resource and Protection*, 9(12), 1547-1563.

Ndjigui, P.-D., Badinane, M.F.B., Nyeck, B., Nandjip, H.P.K., Bilong, P. (2013). Mineralogical and geochemical features of the coarse saprolite developed on orthogneiss in the SW of Yaoundé, South Cameroon. *Journal of African Earth Science*, 79, 125–142.

Ndjigui P.D., Fadil-Djenabou S., Beauvais A., Ambrosi J.P. (2014). Origin and evolution of Ngaye River alluvial sediments, Northern Cameroon: Geochemical constraints. *Journal of African Earth Science*, 100, 164-178.

Nesbitt, H.W., and Young, G.M. (1982) Early Proterozoic climates and plate motions inferred from major element chemistry of lutites. *Nature* 299:715–717.

Nesbitt, H.W., and Young, G.M. (1984). Prediction of some weathering trends of plutonic and volcanic rocks based on thermodynamic and kinetic considerations. *Geochimica et Cosmochimica Acta*, 48(7), 1523-1534.

Neumann, D., Stiassny, M.L., and Schliewen, U.K. (2011). Two new sympatric *Sarotherodon* species (Pisces: Cichlidae) endemic to Lake Ejagham, Cameroon, west-central Africa, with comments on the *Sarotherodon galilaeus* species complex. *Zootaxa*, 2765(1), 1-20.

Ngon Ngon, G.F. (2007). Morphological, mineralogical, geochemical and crystallographic study of lateritic clays and hydromorphic clays of the Yaoundé region (Cameroon) (Doctoral dissertation, Doctoral thesis / Ph.D. University of Yaoundé I, Cameroon).

- Ngon Ngon, G.F., Yongue–Fouateu, R., Bitom, D.L., and Bilong, P. (2009). A geological study of clayey laterite and clayey hydromorphic material of the region of Yaoundé (Cameroon): a prerequisite for local material promotion. *Journal of African Earth Sciences*, 55(1-2), 69-78.
- Ngon Ngon G.F., Bayiga E., Ntamack-Nida M.J., Etamé J., Noa Tang S. (2012). Trace elements geochemistry of clay deposits of Missole II from the Douala sub basin in Cameroon (Central Africa): a provenance study. *Sciences, Technologie and Développement* 13, (1), 20-35.
- Ngos III, S., Giresse, P., and Maley, J. (2003). Palaeoenvironments of Lake Assom near Tibati (south Adamawa, Cameroon). What happened in Tibati around 1700 years bp?. *Journal of African Earth Sciences*, 37(1-2), 35-45.
- Ngos III, S., and Giresse, P. (2005) pyroclastic accumulations of two crater lakes (Mbalang, Tizong) of. *The Holocene*, 22, 1-15.
- Ngos III, S., and Giresse, P. (2011). The Holocene sedimentary environments and the pyroclastic accumulations of two crater lakes (Mbalang, Tisong) of the volcanic plateau of Adamawa (Cameroon). *Holocene*.
- Ngounouno, I., Déruelle, B., and Demaiffe, D. (2000). Petrology of the bimodal Cenozoic volcanism of the Kapsiki plateau (northernmost Cameroon, Central Africa). *Journal of Volcanology and Geothermal Research*, 102(1-2), 21-44.
- Nguetsop, F., Servant Vildary, S., Roux, M., Reynaud-Farrera, I., Servant, M., and Wirrmann, D. (2000). Lac Ossa, Cameroun: relations statistiques diatomées/milieus aquatiques, application à l'estimation des paléo-niveaux lacustres durant les 5000 dernières années: comparaisons avec les changements de la végétation.
- Nguetsop, V.F., Servant-Vildary, S., Servant, M., and Roux, M. (2010). Long and short-time scale climatic variability in the last 5500 years in Africa according to modern and fossil diatoms from Lake Ossa (Western Cameroon). *Global and Planetary Change*, 72(4), 356-367.
- Nguetsop, V.F., Bentaleb, I., Favier, C., Bietrix, S., Martin, C., Servant-Vildary, S., and Servant, M. (2013). A late Holocene palaeoenvironmental record from Lake Tizong, northern Cameroon using diatom and carbon stable isotope analyses. *Quaternary Science Reviews*, 72, 49-62.
- Ngueutchoua, G., Ekoa Bessa, A.Z., Eyong, J.T., Zandjio, D.D., Djaoro, H.B., and Nfada, L.T. (2019). Geochemistry of cretaceous fine-grained siliciclastic rocks from Upper Mundeck and Logbadjeck Formations, Douala sub-basin, SW Cameroon: Implications for weathering intensity, provenance, paleoclimate, redox condition, and tectonic setting. *Journal of African Earth Sciences*, 152, 215-236.
- Njike Ngaha, P.R. (1984). Contribution to the geological, stratigraphic and structural study of the edge of the Atlantic basin of Cameroon. Doctorate thesis 3rd cycle, University of Yaoundé.
- Nkoumbou, C., Barbey, P., Yonta-Ngouné, C., Paquette, J.L., and Villiéras, F. (2014). Pre-collisional geodynamic context of the southern margin of the Pan-African fold belt in Cameroon. *Journal of African Earth Sciences*, 99, 245-260.

- Noumi, B.G., Marie, S.J., Fidèle, F., and Jean-Marie, D.D. (2015). Speciation of phosphorus in Lake Dang of Ngaoundere-Cameroon. *Environmental Science and Pollution Research*, 22(4), 3098-3106.
- Nuttin, L., Francus, P., Preda, M., Ghaleb, B., and Hillaire-Marcel, C. (2013). Authigenic, detrital and diagenetic minerals in the Laguna Potrok Aike sediment sequence. *Quaternary Science Reviews*, 71, 109-118.
- Nzenti, J.P., Barbey, P., Bertrand, J.M., and Macaudière, J. (1994). The pan-African chain in Cameroon: let's look for suture and model. Abstracts 15eme RST, Nancy, Société Géologique France, édition Paris, 99.
- Nziéleu, T.G.J., Hubert, Z.T.S., Samuel, F.M., Thomas, N., and Pinel-Alloul, B. (2016). Baseline Information on the Metallic Pollution of Sediments of the Lakes of the Ossa Complex, Dizangue, Cameroon. *Current Journal of Applied Science and Technology*, 1-14.
- Ohba, T., Fantong, W., Fouepe, A., Tchamabe, B.C., Yoshida, Y., Kusakabe, M., Sigha, N., Tsunogai, U., Oginuma, Y., and Tanyileke, G. (2013). Contribution of methane to total gas pressure in deep waters at lakes Nyos and Monoun (Cameroon, West Africa). *Geochemical Journal*, 47(3), 349-362.
- Olivry, J.-C. (1986). Rivers of Cameroon. *Hydrological Monographs, Mesres/Orstom* 9, 733 p.
- Olsson, K. (1986). The influence of genotype on the effects of impact damage on the accumulation of glycoalkaloids in potato tubers. *Potato research*, 29(1), 1-12.
- Ongboye, P.R.B., Sababa, E., Bidzang, F.N., and Ndjigui, P.D. (2019). Geochemical characterization of surface sediments from Tongo Gandima (Eastern Cameroon): implications for gold exploration. *Arabian Journal of Geosciences*, 12(18), 598.
- Onguene Mala, (1993). Pedological differentiation in the Yaoundé region (Cameroon). Transformation of a red ferralitic soil into a yellow horizon soil and relationship with the evolution of the model. (Doctorate Dissertation), Paris VI University, 253 p.
- Oumar, B., Ekengele, N.L., and Balla, O.A.D. (2014). Assessment of the level of pollution by heavy metals from Bini and Dang lakes, Adamawa region, Cameroon. *Afrique Science: International Journal of Science and Technology*, 10 (2), 184-198.
- Owona, S., Mvondo Ondo, J., Essono, J., Tjomb, B., and Enama Mengong, M. (2003). Géomorphologie et cartographie de deux faciès paradérivés et un orthodérivé de la région de Yaoundé. *Journal Science Technologie et Développement* 10 (1), 81–91.
- Parker, G.A. (1970). Sperm competition and its evolutionary consequences in the insects. *Biological reviews*, 45(4), 525-567.
- Pettijohn, F.J., Potter, P.E., and Siever, R. (1972). Diagenesis. In *Sand and sandstone* (pp. 383-437). Springer, New York, NY.
- Potter, P.E. (1978). Petrology and chemistry of modern big river sands. *The Journal of Geology*, 86(4), 423-449.
- Ramade F. (2002). Dictionnaire encyclopédique de l'écologie et des sciences de l'environnement (2èmeEdition). Ed. Dunod, Paris, 1075 p.

- Ramade, F. (2005). Element of ecology. Applied ecology (6th Edition). Ed. Dunod, pp.846 (125-128, 309-311, 314).
- Ramaroson, J. (2008). Calcination of contaminated dredged sediments. Physico-chemical properties studies (Doctoral dissertation, Thèse, Institut National des Sciences Appliquées de Lyon).
- Ramos-Vázquez, M.A., and Armstrong-Altrin, J.S. (2019). Sediment chemistry and detrital zircon record in the Bosque and Paseo del Mar coastal areas from the southwestern Gulf of Mexico. *Marine and Petroleum Geology*, 110, 650–675.
- Reimer, P.J., Bard, E., Bayliss, A., Beck, J.W., Blackwell, P.G., Ramsey, C.B., and Grootes, P.M. (2013). IntCal13 and Marine13 radiocarbon age calibration curves 0–50,000 years cal BP. *Radiocarbon*, 55(4), 1869-1887.
- Reneick., H.E et Sing. I.B, 1980. Depositional sedimentary environment. Springer-Verlag, Berlin, 549 p.
- Reyre, D. (1966). Geological history of the Douala basin (Cameroon). *Sedimentary basins of the African coast*, 143-161.
- Roser, B.P., and Korsch, R.J. (1986). Determination of tectonic setting of sandstone-mudstone suites using SiO₂ content and K₂O/Na₂O ratio. *The Journal of Geology*, 94(5), 635-650.
- Santoir C., and Bopda A. (1995). South Cameroon Regional Atlas. Ed. ORSTOM, 53 p. + 21 plates.
- Sawyer, E.W. (1986). The influence of source rock type, chemical weathering and sorting on the geochemistry of clastic sediments from the Quetico metasedimentary belt, Superior Province, Canada. *Chemistry Geology*, 55, 77–95.
- Schliewen, U., Rassmann, K., Markmann, M., Markert, J., Kocher, T., and Tautz, D. (2001). Genetic and ecological divergence of a monophyletic cichlid species pair under fully sympatric conditions in Lake Ejagham, Cameroon. *Molecular Ecology*, 10(6), 1471-1488.
- Ségalen P. (1967). Soils and geomorphology of Cameroon. *Cah. ORSTOM, ser. Pedol.*, V, 2, 137-
- Ségalen, P. (1994). Ferrallitic soils: formation factors and ferrallitic soils in America. Volume 3. Ferrallitic soils in Africa and the Far East, Australia and Oceania: general conclusions.
- Sharma, A., Sensarma, S., Kumar, K., Khanna, P.P., and Saini, N.K. (2013). Mineralogy and geochemistry of the Mahi River sediments in tectonically active western India: Implications for Deccan large igneous province source, weathering and mobility of elements in a semi-arid climate. *Geochimica and Cosmochimica Acta*, 104, 63-83.
- Shepard, F.P. (1954). Nomenclature based on sand-silt-clay ratios. *Journal of Sedimentary Petrology*, 24: 151–158.
- Shi, J.A., Guo, X.L., Wang, Q., Yan, N.Z. and Wang, J.X. (2003). Geochemistry of REE in QH1 Sediments of Qinghai Lake since Late Holocene and Its Paleoclimatic Significance. *Journal of Lake Sciences*, 15/1, 28-33.

- Singh, P. (2009). Major, trace and REE geochemistry of the Ganga River sediments: influence of provenance and sedimentary processes. *Chemical Geology*, 266(3-4), 242-255.
- Singh, H., Pandey, R., Singh, S.K., and Shukla, D.N. (2017). Assessment of heavy metal contamination in the sediment of the River Ghaghara, a major tributary of the River Ganga in Northern India. *Applied Water Science*, 7(7), 4133-4149.
- Šmuc, N.R., Serafimovski, T., Dolenc, T., Dolenc, M., Vrhovnik, P., Vrabec, M., Komar, D. (2015). Mineralogical and geochemical study of Lake Dojran sediments (Republic of Macedonia). *Journal of Geochemical Exploration*, 150, 73–83.
- Sone, B.N., Rosseland, B.O., and Teien, H.C. (2017). Determination of water quality, and trace metals in endemic *Sarotherodon linellii*, *Pungu maclareni* and *Clarias maclareni*, in crater Lake Barombi Mbo, Cameroon. *African journal of aquatic science*, 42(2), 161-169.
- Stager, J.C., Alton, K., Martin, C.H., King, D.T., Petruny, L.W., Wiltse, B., and Livingstone, D. A. (2018). On the age and origin of Lake Ejagham, Cameroon, and its endemic fishes. *Quaternary Research*, 89(1), 21-32.
- Strand, K., Passchier, S., and Näsi, J. (2003). Implications of quartz grain microtextures for onset Eocene/Oligocene glaciation in Prydz Bay, ODP Site 1166, Antarctica. *Palaeogeography, Palaeoclimatology, Palaeoecology*, 198(1-2), 101-111.
- Stuiver, M., and Reimer, P.J. (1993). Extended ^{14}C data base and revised CALIB 3.0 ^{14}C age calibration program. *Radiocarbon*, 35(1), 215-230.
- Suchel, J.B. (1987). *Climates of Cameroon*. State thesis. University of Bordeaux III, 2 volumes, 1186 p.
- Suchel, F.G. (1988). The climatic regions of Cameroon. *The climates of Cameroon*. Works of Tropical Geography, 5, 1-288.
- Sun, Z.C., Yang, F., Zhang, Z.H., Li, S.J., Li, D.M., Peng, L.C., Zeng, X.L., Xu, Y.L., Mao, S.Z. and Wang, Q. (1997). *Seolmentirry Enuironments and Hydrocarbon Generation of Cenoaoic Salified Lakes in China*. Petroleum Industry Press, Beijing, China, 35-120.
- Sun, H., Xiao, Y., Gao, Y., Zhang, G., Casey, J.F., and Shen, Y. (2018). Rapid enhancement of chemical weathering recorded by extremely light seawater lithium isotopes at the Permian–Triassic boundary. *Proceedings of the National Academy of Sciences*, 115(15), 3782-3787.
- Tabi, E.B., Oben, P.M., and Oben, B.O. (2015). Diversity and dynamics of potentially toxic cyanobacteria and their public health significance in lake Koto Barombi, Cameroon. *Tropical Freshwater Biology*, 24, 89.
- Tamungang, S.A., Awa II, T., and Luchuo, N.G. (2016). Avian species richness and diversity at the Dschang Municipal Lake, Cameroon: Implications of site management for conservation and ecotourism. *Journal of Ecology and the Natural Environment*, 8(11), 192-200.
- Tatsadjieu, N.L., Maïworé, J., Hadjia, M.B., Loiseau, G., Montet, D., and Mbofung, C.M.F. (2010). Study of the microbial diversity of *Oreochromis niloticus* of three lakes of Cameroon by PCR-DGGE: Application to the determination of the geographical origin. *Food Control*, 21(5), 673-678.

- Tawfik, H.A., Salah, M.K., Maejima, W., Armstrong-Altrin, J. S., Abdel-Hameed, A.M.T., and El Ghandour, M. M. (2018). Petrography and geochemistry of the lower Miocene Moghra sandstones, Qattara depression, north Western Desert, Egypt. *Geological Journal*, 53(5), 1938-1953.
- Taylor, S.R., and McLennan, S.M. (1985). *The continental crust: its composition and evolution*.
- Tchawa, P. (1991). *Landscape dynamics on the southern fallout of the Hauts Plateaux of West Cameroon (Doctoral dissertation, Bordeaux 3)*.
- Temdjim, R. (1986). *The volcanism of the Ngaoundéré region (Adamaoua-Cameroon): volcanological and petrological study (Doctoral dissertation)*.
- Temdjim, (2005) *Contribution to the growth of the upper mantle of Cameroon through the study of the ultra-basic and basic enclaves raised by the volcanoes of Youkou (Adamaoua and Nyos (Line of Cameroon), State doctoral thesis, University de Yaoundé I, 339 p.*
- Tenyang, N., Ponka, R., Tiencheu, B., Womeni, H.M., and Djikeng, F.T. (2016). Proximate Composition, Fatty Acid and Mineral. *American Journal of Food Science and Technology*, 4(3), 64-69.
- Tombi, J., Box, O., Miriane, T.J., and Francis, A.J. (1897). *Microecology of Monogenean Gill Parasites of Tilapia Rendalli Boulenger, 1897 From Bamendjing Lake, Cameroon*.
- Toteu S. F. Van Schmus W. R. Penaye J., Nyobe J.B., 1994. U-Pb and Sm-Nd evidence for erburnian and panafrican high grade metamorphism in cratonic rock of southern Cameroon. *Precambrian Res.* 67, 321-347.
- Toteu, S.F., Penaye, J., Deloule, E., Van Schmus, W.R., and Tchameni, R. (2006). Diachronous evolution of volcano-sedimentary basins north of the Congo craton: insights from U–Pb ion microprobe dating of zircons from the Poli, Lom and Yaoundé Groups (Cameroon). *Journal of African Earth Sciences*, 44(4-5), 428-442.
- Touchart, L. (2000). *Geography: The lakes; Origin and morphology*. Editions L'Harmattan.
- Toyoda, K., Nakamura, Y., and Masuda, A. (1990). Rare earth elements of Pacific pelagic sediments. *Geochimica and Cosmochimica Acta*, 54(4), 1093-1103.
- Traczyk, A., and Woronko, B. (2010). Historia zlodowacenia doliny Łomnicy w Karkonoszach w zapisie mikromorfologii powierzchni ziarn kwarcu. *Przegląd Geologiczny*, 58(12), 1182-1191.
- Trevena, A.S., and Nash, W.P. (1981). An electron microprobe study of detrital feldspar. *Journal of Sedimentary Research*, 51(1), 137-150.
- Trewin, N. (1988). Use of the scanning electron microscope in sedimentology. *Techniques in sedimentology*, 229-273.
- Tsamo, C., Abba, P., and Tize, D. (2017). Investigating the pollution of Lake Mofole (Cameroon) using field studies, it's water, sediments, fish content and nearby well water. *American-Eurasian Journal of Agriculture and Environmental Science*, 17(1), 22-29.
- Turekian K., and Wedepohl K. (1961). Distribution of the elements in some major units of the earth's crust. *American Geological Society. Bulletin*, 72, 175–182.

- Ufer, K., Stanjek, H., Roth, G., Dohrmann, R., Kleeberg, R., and Kaufhold, S. (2008). Quantitative phase analysis of bentonites by the Rietveld method. *Clays and Clay Minerals*, 56(2), 272-282.
- Valet, S. (1980). Hypsometric and climatic map of West Cameroon-1970.
- Verma, S.P., and Armstrong-Altrin, J.S. (2013). New multi-dimensional diagrams for tectonic discrimination of siliciclastic sediments and their application to Precambrian basins. *Chemical Geology*, 355, 117–133.
- Verma, S.P., and Armstrong-Altrin, J.S. (2016). Geochemical discrimination of siliciclastic sediments from active and passive margin settings. *Sedimentary Geology*, 332, 1-12.
- Villiers, J.F., and Santoir C. (1995). Regional Atlas of South Cameroon. Vol. Végétation, ORSTOM éd., pp. 10–11.
- Vincens, A., Buchet, G., and Servant, M. (2010). Vegetation response to the " African Humid Period" termination in central Cameroon (7 N)-new pollen insight from Lake Mbalang. *Climate of the Past*, 6(3), 281.
- Vos, K., Vandenberghe, N., and Elsen, J. (2014). Surface textural analysis of quartz grains by scanning electron microscopy (SEM): From sample preparation to environmental interpretation. *Earth-Science Reviews*, 128, 93-104.
- Walkley, A., and Black, I.A. (1934). An examination of the Degtjareff method for determining soil organic matter, and a proposed modification of the chromic acid titration method. *Soil science*, 37(1), 29-38.
- Wedepohl, K.H. (1971). Environmental influences on the chemical composition of shales and clays. *Physics and Chemistry of the Earth*, 8, 307-333.
- Wedepohl K.H. (1995). The composition of the continental crust. *Geochemica and Cosmochimica Acta*, 59, 1217-1232.
- Wentworth C.K. (1922). A scale of grade and class terms for clastic sediments: *Journal of Geology*, 30, 377-392.
- Whalley, W.B., and Krinsley, D.H. (1974). A scanning electron microscope study of surface textures of quartz grains from glacial environments. *Sedimentology*, 21(1), 87-105.
- Wirrmann, D., 1992. Lake Ossa: a preliminary monograph, *Revue de Géographie du Cameroun*, XI, 1, 27-38.
- Woronko, B. (2012). Micromorphology of quartz grains as a tool in the reconstruction of periglacial environment: P. *Contemporary issues in Polish geography*, 111-131.
- Xiao, Y., Liu, H., Chen, Y., and Jiang, J. (2014). Bounding surface plasticity model incorporating the state pressure index for rockfill materials. *Journal of Engineering Mechanics*, 140(11), 04014087.
- Yong Ngondjeb, D., Dia Kamgnia, B., Nje, P., and Havard, M. (2014). The Economic Assessment of Investment in Soil Conservation: The Case of Anti-Erosion Development in the Lagdo Lake Watershed in Cameroon. *Canadian Journal of Agricultural Economics / Revue canadienne d'agroeconomie*, 62 (3), 393-410.

- Yongue, R. (1986). Contribution to the petrological study of the alteration and the ferruginous armor plating of migmatic gneiss in the Yaoundé region, 214 p.
- Yoshida, Y., Kusakabe, M., Ohba, T., Tanyileke, G., and Hell, J.V. (2017). Decreasing capability of the degassing systems at lakes Nyos and Monoun (Cameroon): a new gas removal system applied to Lake Monoun to prevent a future limnic eruption. Geological Society, London, Special Publications, 437(1), 205-212.
- Young, S.M., Amarasooriya, P., Hiroaki, I. (2012). Geochemical characteristics of stream sediments, sediment fractions, soils, and basemen trocks from the Mahaweli River and its catchment, Sri Lanka. *Chemie Erde-Geochemistry*, 25230, 1-15.
- Young, S.W. (1976). Petrographic textures of detrital polycrystalline quartz as an aid to interpreting crystalline source rocks. *Journal of Sedimentary Research*, 46(3), 595-603.
- Yu, L., Zou, S., Cai, J., Xu, D., Zou, F., Wang, Z., Wu, C., Liu, M. (2016). Geochemical and Nd isotopic constraints on provenance and depositional setting of the Shihuiding Formation in the Shilu Fe-Co-Cu ore district, Hainan Province, south China. *Journal of Asian Earth Science*, 119, 100–117.
- Zhang, Y., Chu, C., Li, T., Xu, S., Liu, L., Ju, M. (2017). A water quality management strategy for regionally protected water through health risk assessment and spatial distribution of heavy metal pollution in 3 marine reserves. *Science of the Total Environment*, 599, 721–731.
- Berglund, B.E., Ralska-Jasiewiczowa, M. (1986). Pollen analysis and pollen diagrams. *Handbook of Holocene palaeoecology and palaeohydrology*, 455, 484-486.
- Maley, J. (1970). Contributions a l'etude du Bassin tchadien Atlas de pollens du Tchad. *Bulletin du Jardin botanique national de Belgique/Bulletin van de Nationale Plantentuin van België*, 29-48.
- Maley, J., Brenac, P. (1998). Vegetation dynamics, palaeoenvironments and climatic changes in the forests of western Cameroon during the last 28,000 years B.P. *Review of Palaeobotany and Palynology* 99: 157–187.
- Sowunmi, M.A. (1973). Pollen Grains of Nigerian Plants. *Grana*, 13(3) 145–186.
- Sowunmi, M.A. (1995). Pollen of Nigerian Plants. *Grana*, 34(2), 120–141
- Schüler, L., Hemp, A. (2016). Atlas of pollen and spores and their parent taxa of Mt Kilimanjaro and tropical East Africa. *Quaternary International* 425, 301–386.
- Willis, K.J. (2020). African Pollen Reference Collection (Version 5). Digitised Palynological Reference Collection accessed via globalpollenproject.org on 11/29/2020 11:45:19
- Anchukaitis, K.J., Tierney, J.E. (2013). Identifying coherent spatiotemporal modes in uncertain proxy paleoclimate records. *Climate dynamics*, 41(5-6), 1291-1306.
- Battarbee, R.W. (1986). Diatom analysis. In: *Handbook of Holocene. Palaeoecology and Palaeohydrology and Palaeohydrology*. B.E. Berglund, John Wiley and Sons, 527- 578.
- Brncic, T.M., Willis, K.J., Telfer, M.W., Bailey, R.M. (2009). Fire and climate change impacts on lowland forest composition in northern Congo during the last 2580 years from palaeoecological analyses of a seasonally flooded swamp. *The Holocene* 19, 79-89.

- De Menocal, P., Ortiz, J., Guilderson, T., Sarin, M. (2000). Coherent high and low latitude climate variability during the Holocene warm period. *Science* 288, 2198-2202.
- Gasse, F. (1986). East African diatoms, taxonomy, ecological distribution. *Bibliotheca Diatomologica*, edited by Cramer, J. In: der Gebrüder Borntraeger Vertragsbuchhandlung, Berlin-Stuttgart, 201p.
- Germain, H. (1981). Flore des diatomées. Diatomophycées. Eaux douces et saumâtres du massif Américain et des contrées voisines d'Europe occidentale. 444 p.
- Husted, F. (1927-1966). Die Kieselalgen, in: L. Rabenhorst's Kryptogamen, floravon Deutschland, Österreich und der Schweiz. Akademische Verlagsgesellschaft Leipzig. 1 (1927-30), 920 pp., 2 (1931-59), 845pp 3 (1961-66), 816 p.
- Krammer, K., Lange-Bertalot, H. 1991-2000. Süßwasserflora von Mitteleuropa. Bacillariophyceae. 1 Teil: Naviculaceae. 598pp. 1991a; 1 Teil: Centrales, Fragilariaceae, Eunotiaceae. 576 pp. 1991b; 2 Teil: Bacillariophyceae, Epithemiaceae, Surirellaceae. 610pp. 1999; Teil 3: Centrales, Fragilariaceae, Eunotiaceae. 598pp. 2000. Süßwasserflora von Mitteleuropa. *Bibliotheca Diatomologica* 2. Editions, Cramer, J. Berlin- Stuttgart
- Lange-Bertalot, H., Krammer, K. (1986). Süßwasserflora von Mitteleuropa. Bacillariophyceae. Teil 1: Naviculaceae. VEB Gustav Fischer Verlag, Jena, 876 p.
- Lange-Bertalot, H. (1993). 85 Neue taxa und über 100 weitere neue definierte Taxa ergänzend zur Süßwasserflora von Mitteleuropa. VEB Gustav Fischer Verlag, Jena, 610 p.
- Lezine, A-M., Cazet, J-P. (2007). High-resolution pollen record from core KW31, Gulf of Guinea, documents the history of the lowland forests of West Equatorial Africa since 40,000 yr ago. *Quaternary Research* 64 (3), 432-443.
- Maley, J., Brenac, P. (1998). Vegetation dynamics, paleoenvironments and climatic changes in the forests of western Cameroon during the last 28,000 years BP. *Review of Palaeobotany and Palynology* 99 (2), 157-187.
- Maley, J. (2000). Last Glacial Maximum lacustrine and fluvial formations in the Tibesti and other Saharan Mountains, and largescale climatic teleconnections linked to the activity of the Subtropical Jet Stream. *Global and Planetary Change* 26, 121-136.
- Ngomanda, A., Chepstow-Lusty, A., Makaya, M., Schevin, P., Maley, J., Fontugne, M., Oslisly, R., Rabenkogo, N., Jolly, D. (2007). Vegetation changes during the past 1300 years in western equatorial Africa: a high-resolution pollen record from Lake Kamaléké, Lopé reserve, Central Gabon. *The Holocene* 15, 1021-1031.
- Ngomanda, A., Chepstow-Lusty, A., Makaya, M., Favier, C., Schevin, F., Maky, J., Fontugne, M., Oslisly, R., Jolly, D. (2009). Western equatorial African forest-savanna mosaics: a legacy of late Holocene climatic change? *Climate of the Past* 5, 647-659.
- Nguetsop, V.F., Servant, M., Servant-Vildary, S. (1998). Paléolimnologie et paléoclimatologie de l'ouest-Cameroun au cours des 5000 dernières années, à partir de l'étude des diatomées du lac Ossa. *Comptes Rendus de l'Académie de Science – Series II A- Earth and Planetary Science* 327, 39-45.

- Nguetsop, V.F., Servant-Vildary, S., Servant, M. (2004). Late Holocene climatic changes in West Africa, a high-resolution diatom record from equatorial Cameroon. *Quaternary Sciences Review* 23, 591-609.
- Shanahan, T.M., Overpeck, J.T., Wheeler, J.W., Beck, J., Pigati, W. J. S., Talbot, M. R., Sholz, C. A., Peck, J., King, J. W. (2006). Paleoclimatic variations in West Africa from a record of late Pleistocene and Holocene lake level stands of Lake Bosumtwi, Ghana. *Palaeogeography, Palaeoclimatology, Palaeoecology* 242, 287-312.
- Simonsen, R. 1987. Atlas and Catalogue of the diatom types of Friedrich Hustedt. Editions, J. Cramer, 1, 525 pp., 2, 597 pp., 3, 619 p.
- Sutra, J. (2013). Reconstruction paléo-environnementale de la composition et la structure de la végétation en République Centrafricaine sur les 3000 dernières années. Thèse de master, Université de Montpellier, France. 46 p.
- Vincens, A., Schwartz, D., Bertaux, J., Elenga, H., de Namur, C. 1998. Late holocene climatic changes in Western Equatorial Africa inferred from pollen from lake Sinnda, Southern Congo. *Quaternary Research* 50, 34-45.
- Kom, M. F., Nguetsop, V. F., Bremond, L., Fonkou, T., Noumsi, B., Sebag, D., Tsalefac, M. (2018). Evolution paléohydrologique du marais Paurosa au centre du Gabon au cours des deux derniers millénaires: Contribution des diatomées. *Cameroon Journal of Experimental Biology*, 12(1), 65-78.

Table of contents

DEDICACE	
Acknowledgements	<i>i</i>
List of Figures	<i>iv</i>
List of Table	<i>viii</i>
List of abbreviations	<i>ix</i>
Abstract	<i>x</i>
Résumé	<i>xii</i>
General introduction	<i>1</i>
Part one: Background	<i>6</i>
Chapter I: Natural setting	<i>7</i>
I.1. Location.....	<i>8</i>
I.2. Climate	<i>10</i>
I.3. Hydrography	<i>14</i>
I.4. Vegetation	<i>18</i>
I.5. Orography.....	<i>23</i>
I.6. Soils.....	<i>28</i>
I.7. Geology	<i>31</i>
Chapter II: Litterature review	<i>38</i>
II.1. Concepts and definitions	<i>39</i>
II.1.1. Sediments	<i>39</i>
II.1.2. Lake sediments	<i>39</i>
II.1.3. Sediment granulometry.....	<i>40</i>
II.1.4. Origin of sediments.....	<i>40</i>
II.1.5. Sedimentation and water decontamination	<i>40</i>
II.1.6. Impact of lake sediments in pollution.....	<i>42</i>
II.1.7. Lakes	<i>42</i>
II.1.8. Origin and typology of lakes.....	<i>43</i>
II.1.9. Evolution of a lake.....	<i>44</i>
II.1.10. Some methodologies of lake sediment sampling	<i>45</i>
II.1.11. Pollution	<i>46</i>
II.1.12. Characteristic parameters of pollution.....	<i>47</i>
II.2. Previous work on sedimentological characterization of lake sediments	<i>48</i>

II.3. Previous work on the mineralogical characterization of sediments.....	50
II.4. Previous work on the geochemical characterization of sediments.....	52
II.5. Previous work on sediment pollution.....	53
II.6. Some studies of lakes in Cameroon	55
II.6.1- Yaoundé.....	55
II.6.2- Dizangué (Ossa Lakes Complex).....	55
II.6.3- Ngaoundere	56
II.6.4- Work on other lakes	56
Chapter III: Material and methods.....	58
III.1. Field work.....	59
III.2. Laboratory analyses.....	61
III.2.1. Sedimentological analysis.....	62
III.2.1.1. Grain size analyses	62
III.2.1.2. Residual humidity.....	62
III.2.1.3. Total Organic Carbon (TOC) and Organic Matter (OM).....	63
III.2.1.4. Scanning electron microscopic (SEM) observations of quartz grains	63
III.2.2. Mineralogical analysis	63
III.2.2.1. X-ray diffraction for bulk sediments	64
III.2.2.2. Scanning electron microscopic equipped with energy dispersive spectrometer (SEM-EDS)	64
III.2.2.3. Fourier transform infrared (FT-IR) spectroscopy	64
III.2.2.4. X-ray diffraction of the finest grain-sized	65
III.2.3. Geochemical analysis	65
III.2.3.1. Major elements geochemistry	65
III.2.3.2. Trace elements and rare earth elements (REE) geochemistry	66
III.2.4. Heavy metals analysis	66
III.2.5. Radiocarbon dating (¹⁴ C).....	67
III.2.6. Analysis of diatoms	67
III.2.7. Palynological analyses	68
Chapter IV: Sedimentological characteristics of lake deposits	70
Part two: Results and interpretations.....	70
Chapter IV: Sedimentological characteristics of lake deposits	71
IV.1. Physical characteristics of sediments.....	72
IV.1.1. Simbock Lake (Yaoundé).....	72

IV.1.2. Ossa lake Complex (Dizanguè)	76
IV.1.3. Ngaoundaba crater Lake (Ngaoundéré)	79
IV.2. Quartz grain microtextures	81
IV.2.1. Ossa lake Complex.....	82
IV.2.2. Ngaoundaba Lake	83
IV.3. Total Organic Carbon (TOC) and influence on organic matter accumulation.....	85
IV.3.1. Simbock Lake	85
IV.3.2. Ossa lake Complex.....	86
IV.3.3. Ngaoundaba Lake	87
Chapter V: Petrological and environmental aspects of lake sediments	90
V.1. Mineralogy of lacustrine sediments	91
V.1.1. Simbock Lake.....	91
V.1.2. Ossa Lake Complex.....	96
V.1.3. Ngaoundaba Lake.....	99
V.2. Geochemistry of lacustrine sediments.....	102
V.2.1. Simbock Lake.....	102
V.2.1.1. Major elements.....	102
V.2.1.2. Trace elements	104
V.2.1.3. Rare earth elements (REE).....	106
V.2.2. Ossa lake Complex	108
V.2.2.1. Major elements.....	108
V.2.2.2. Trace elements	109
V.2.2.3. Rare earth elements (REE).....	109
V.2.3. Ngaoundaba Lake.....	114
V.2.3.1. Major elements.....	114
V.2.3.2. Trace elements	116
V.2.3.3. Rare earth elements (REE).....	117
V.3. Environmental statut of lakes.....	121
V.3.1. Simbock Lake.....	121
V.3.2. Ossa lake Complex	122
V.3.3. Ngaoundaba Lake.....	123
Chapter VI: Dating and paleoenvironmental reconstruction	128
VI.1. Radiocarbon dating	129
VI.1.1. Present environment.....	131

VI.1.1.1. Ossa lake Complex (South-west, Cameroon).....	131
VI.1.1.2. Tizon and Ngaoundaba lakes (Adamawa, North-Cameroon).....	132
VI.1.2. Lithology of cores	132
VI.1.2.1. Cores from the South-Cameroon (Ossa lake Complex).....	133
VI.1.2.2. Cores from the North-Cameroon (Tizon and Ngaoundaba lakes)	134
VI.1.3. Radiocarbon ages and age models	135
VI.1.3.1. Ossa lake Complex (South-west, Cameroon).....	135
VI.1.3.2. Tizon and Ngaoundaba lakes (North-Cameroon)	136
VI.2. Diatom analysis.....	137
VI.2.1. Simbock sedimentary core.....	137
VI.2.1.1. Flora diversity	137
VI.2.1.2. Dominant species and large assemblages.....	137
VI.2.1.3. Algae assemblages according to the CFA: Ecological significance	140
VI.2.2. Ossa Lake sediment core	144
VI.2.2.1. Flora diversity	144
VI.2.2.2. Dominant species and large assemblages.....	144
Widespread species (Group A).....	144
VI.2.2.3. Determination of assemblages by multivariate statistical processing and identification of environmental gradients*	147
VI.2.3. Ngaoundaba sedimentary core.....	151
VI.2.3.1. Flora diversity	151
VI.2.3.2. Dominant species and large assemblages	152
VI.2.3.3. Determination of the most significant species and classification of assemblages by statistical treatments.....	155
VI.3. Pollen and algae analysis.....	158
VI.3.1. Simbock Lake (NR core).....	163
VI.3.2. Ossa Lake (LO core)	163
VI.3.2.1. Pollen zone LO3 (149-147 cm; 550 yrs BP.)	164
VI.3.2.2. Pollen zone LO2 (72-70 cm; 380 yrs BP.)	164
VI.3.2.3. Pollen zone LO1 (12-10 cm; 230 yrs BP.)	165
VI.3.3. Ngaoundaba Lake (NL core).....	165
VI.3.3.1. Pollen zone NL3 (87-85 cm; 1030 yrs BP.)	165
VI.3.3.2. Pollen zone NL2 (43-41 cm; 425 yrs BP.)	166
VI.3.3.3. Pollen zone NL1 (7-5 cm; 155 yrs BP.)	166

<i>Part three: Discussions</i>	167
<i>Chapter VII: Synthesis and discussion</i>	168
VII.1. Classification of sediments.....	169
VII.1.1. Simbock Lake.....	169
VII.1.2. Ossa lakes Complex.....	169
VII.1.3. Ngaoundaba Lake.....	170
VII.2. Maturity and recycling.....	171
VII.2.1. Simbock Lake.....	171
VII.2.2. Ossa lakes Complex.....	172
VII.2.3. Ngaoundaba Lake.....	173
VII.3. Paleoweathering.....	174
VII.3.1. Simbock Lake.....	174
VII.3.2. Ossa Lake Complex.....	176
VII.3.3. Ngaoundaba Lake.....	177
VII.4. Provenance and tectonic setting.....	178
VII.4.1. Simbock Lake.....	179
VII.4.2. Ossa lakes Complex.....	181
VII.4.3. Ngaoundaba Lake.....	183
VII.5. Paleoclimate and Depositional environment.....	184
VII.5.1. South, Cameroon (Simbock and Ossa Lakes).....	185
VII.5.2. North, Cameroon (Ngaoundaba Lake).....	189
<i>Conclusions and suggestions for further studies</i>	195
<i>References</i>	199
<i>Table of contents</i>	220